Title
Development of novel and selective thyroid hormone receptor antagonists to understand hormone signaling

Author
Nguyễn, Ngọc Hà

Publication Date
2005

Peer reviewed|Thesis/dissertation

Development of Novel and Selective Thyroid Hormone Receptor Antagonists to Understand Hormone Signaling

by

Ngoc-Ha Nguyen

DISSERTATION

Submitted in partial satisfaction of the requirements for the degree of

DOCTOR OF PHILOSOPHY

in

Chemistry and Chemical Biology

in the

GRADUATE DIVISION

of the

UNIVERSITY OF CALIFORNIA, SAN FRANCISCO

[redacted]

Date University Librarian

Degree Conferred:.....

This dissertation is dedicated

To my parents, Sang Ly and Mui Nguyen, for their love and sacrifices;

To my sister, An, for her 'bosom' in good times and bad;

To my brother, Lee, for his comic support

That have made my educational achievements possible.

Acknowledgments

First and foremost, I would like to thank Tom Scanlan for his guidance, support, and indulgence in my scientific exploration. When experiments went awry, I could always go to Tom for advice and inevitably leave his office inspired with new and better ideas on how to tackle the science. Tom's relaxed approach to life has counter-balanced the stress and anxiety of being a graduate student allowing me to enjoy the challenging experience of graduate school.

This project grew from the initial groundbreaking work by Grazia Chiellini and Hikari Yoshihara, who developed the first generation of TR agonists and antagonists. It was an honor and pleasure to begin my graduate career with these two exceptional chemists. Grazia was an excellent mentor and friend who took me under her wing when I first started in the lab and shared my adventures once my training wheels came off.

I would like to thank all past and present Scanlanites for their collegial support and for providing such a fun environment in which to do science. I am especially grateful to Nicola Clegg, Nilesh Shah, and Matthew Hart for their friendship in and out of the lab. They have reinforced my appreciation for life and the company of friends.

UCSF's friendly atmosphere has been conducive to establishing collaborations, many of which have evolved into enduring friendships. I have been fortunate to work with scientists who have made immeasurable contributions to the success of this project. I would like to thank John Baxter's lab for providing expertise and resources. In particular, Jim Apriletti has been an invaluable resource in conducting the TR binding assays. Suzana Cunha Lima, Marie Togashi, and Paul Webb have been instrumental in the biochemical characterization of lead compounds. I greatly appreciate their patience in teaching me techniques for two-hybrid assays and gel-shift experiments. I would also

like to thank members of Kip Guy's lab, namely Jamie Moore, Andrea McReynolds, and Sarah Galicia for their work on TR-coregulator interactions and members of Robert Fletterick's lab for their efforts in obtaining X-ray crystal structures of the TR•NH-3 complex.

Wayland Lim, Ha Yung Yang, and J. David Furlow (UC Davis) provided expertise and performed *in vivo* tadpole studies with NH-3. The greatest thrill for me as an organic chemist is to see the utility of small molecules validated in animal models with the hope that they will eventually display therapeutic value. The initial successful use of NH-3 in tadpoles has made the effort necessary for overcoming the challenges in developing TR antagonists worthwhile.

My orals and thesis committee members Kip Guy, Holly Ingraham, Kevan Shokat and Robert Fletterick have offered valuable suggestions and insights into the project, for which I am grateful. They asked tough questions and taught me to think on my feet and out of the box.

I would like to give a big thank you and hug to Chris Olson, our Graduate Program Coordinator and "CCB Mom", for always having her door open to talk about life and lending an ear (and Kleenex) as needed.

My fond memories of UCSF also include wonderful classmates and friends who have been inspirational and supportive throughout the years. In particular, I'd like to thank the "Girls"—Chung-Fei, Chandreyee, Nicola, Alina, Anne, and Feixia. Special thanks go to Chandreyee and Nicola for always bringing a smile to my face with their joyful spirits and big hearts. I have grown to appreciate Charles and Kevin, who have been true friends (and golf buddies) and provided comic relief under almost any circumstance.

Most of all, I would like to thank my immediate and extended family for their unconditional love and support. My parents have provided me with the opportunity to

gain a good education and have encouraged me to pursue my passions in life. They have taught me the importance of respect, the value of life-long relationships, and the virtue of working hard—all of which have been invaluable lessons. My sister and brother have rallied by my side during every successful step forward as well as every stumble backwards.

Many people beyond those I have been able to specifically acknowledge above have contributed to my professional and personal development throughout my graduate journey. I would like to share this accomplishment with everyone who has supported me along the way; this would not have been possible without them.

— Ha ☺

Chapter 2 is adapted from and reproduced in part with permission from:

J. Steroid Biochem. & Mol. Biol. Vol. 83. Webb, P., Nguyen, N.H., Chiellini, G., Yoshihara, H.A.I., et al. Design of thyroid hormone receptor antagonists from first principles, p. 59-73. ©2002 Elsevier. I provided compound NH-3 and contributed Figures 1, 3, and 4.

Methods in Enzymology Vol. 364. Yoshihara, H.A.I., Nguyen, N.H., Scanlan, T.S. Design and synthesis of receptor ligands, p. 71-91. ©2003 Elsevier. I authored text and figures related to compound NH-3.

Chapter 3 is adapted from and reproduced in part with permission from:

Bioorganic Med. Chem. Lett. Vol. 10. Chiellini, G., Nguyen, N.H., Yoshihara, H.A.I. & Scanlan, T.S. Improved synthesis of the iodine-free thyromimetic GC-1, p. 2607-2611. ©2000 Elsevier. I helped to develop the synthetic route and synthesized compound GC-1.

J. Med. Chem. Vol. 45. Nguyen, N.H., Apriletti, J.W., Cunha Lima, S.T., Webb, P., Baxter, J.D. & Scanlan, T.S. Rational design and synthesis of a novel thyroid hormone antagonist that blocks coactivator recruitment, p. 3310-20. ©2002 American Chemical Society. I synthesized the compounds described therein and performed the transactivation assays.

J. Biol. Chem. Vol. 277. Lim, W., Nguyen, N.H., Yang, H.Y., Scanlan, T.S. & Furlow, J.D. A thyroid hormone antagonist that blocks thyroid hormone action *in vivo*, p. 35664-35670. ©2002 American Society for Biochemistry and Molecular Biology. I performed the *in vitro* transactivation and mammalian two-hybrid assays for the Xenopus TR.

J. Biol. Chem. Vol. 279. Moore, J.M.R., Galicia, S.J., McReynolds, A.C., Nguyen, N.H., Scanlan, T.S., Guy, R.K. Quantitative proteomics of the thyroid hormone receptor coregulator interactions, p. 27584-90. ©2004 American Society for Biochemistry and Molecular Biology. I provided compound NH-3.

Chapter 4 is adapted from and reproduced in part with permission from:

J. Amer. Chem. Soc., Submitted for publication. Nguyen, N.H., Apriletti, J.W., Baxter, J.D., Scanlan, T.S. Hammett analysis of selective thyroid hormone modulators reveals structural and electronic requirements for hormone antagonists. *Unpublished work* ©2004 American Chemical Society. I synthesized the compounds described therein and performed the transactivation and mammalian two-hybrid assays.

Methods in Enzymology Vol. 364. Yoshihara, H.A.I., Nguyen, N.H., Scanlan, T.S. Design and synthesis of receptor ligands, p. 71-91. ©2003 Elsevier. I authored text and figures related to compound NH-3.

Abstract

Development of Novel and Selective Thyroid Hormone Receptor Antagonists to Understand Hormone Signaling

Ngoc-Ha Nguyen

Compounds that selectively modulate the thyroid hormone receptor (TR) activity have therapeutic utility and are important pharmacological probes to understand the physiological roles of the receptors in mediating thyroid hormone signaling. Only a few TRβ-selective antagonists have been reported to date with poor efficacy and potency, thus limiting their usefulness for *in vivo* studies. The focus of this thesis has been to develop improved TR antagonists that have potent *in vitro* and *in vivo* activity. A secondary effort has been to understand the structural and chemical requirements for such antagonists.

Crystallographic data for TR and structure-activity relationship data for thyroid mimetics reveal the 5'-position of the thyronine scaffold is an effective site to attach extension groups to prevent TR from adopting an active conformation. Such compounds should be TR antagonists. The synthetic route used to produce **GC-1** was adapted to synthesize 5'-phenylethynyl **GC-1** derivatives. The compound **NH-3**, which emerged from these studies, is a potent TRβ-selective antagonist *in vitro* and *in vivo*. One mechanism of antagonism appears to be the inability of **NH-3** to induce coactivator recruitment to TR, while still allowing corepressor release. **NH-3** is chemically similar to **GC-14**, a previously reported mixed agonist/antagonist. Both compounds contain a *para*-nitroaryl moiety. Rigidly extending the nitroaryl group by two carbon atoms was

sufficient to shift the mixed agonist/antagonist activity of **GC-14** to the full antagonist activity of **NH-3**.

The contribution of the *para*-nitroaryl moiety of **NH-3** to its antagonistic activity was also explored by synthesizing a characterizing a series of 5'-derivatives with variable structural and electronic properties. Results indicate the nitro group is not required for antagonism, although its presence confers maximal antagonistic potency. Analogues bearing an electron-deficient 5'-phenylethynyl extension generally exhibit antagonist activity by preventing coactivator recruitment to TR. Furthermore, a psuedo-Hammett correlation is observed where increased electronic deficiency correlates with increased antagonistic potency, with no correlation to binding affinity. These results suggest the structural and chemical changes are predominantly affecting the compounds' functional modulation of TR. Thus, electron-deficient 5'-phenylethynyl extensions may be interacting with receptor residues possibly through π-interactions to favor the inactive conformation of the receptor.

Table of Contents

List of Figures and Schemes

List of Tables

Chapter 1

Introduction: Thyroid Hormone Biosynthesis, Endocrinology, and Molecular Biology

Thyroid hormones, of which 3,5,3'-L-triiodothyronine (T_3) is the major active form, regulate a multitude of physiologic effects ranging from embryonic development to maintenance of homeostasis in adults. Aberrant thyroid hormone production and signaling have been implicated in several diseases including Grave's disease, cardiovascular disease, atherosclerosis, cancer, and mental retardation. Their actions are primarily mediated by the thyroid hormone nuclear receptor (TR), a member of a superfamily of proteins that regulate gene transcription. In addition, recent evidence suggests the hormones and their metabolites also have rapid, non-genomic effects through cell surface signaling. This chapter provides an introduction and summary of our current understanding in thyroid hormone physiology and mechanisms of action.

1.1 Biosynthesis and Metabolism of Thyroid Hormone

Thyroid hormones, 3,5,3'-L-triiodothyronine (T_3) and 3,5,3',5'-tetraiodo-L-thyronine (T_4, thyroxine), are synthesized and secreted from the thyroid gland as shown in Figure 1-1.[2,3] Hormone biosynthesis begins with iodide (I^-) transport and uptake primarily from dietary sources of iodide into thyroid follicular cells. The iodide is then oxidized by thyroidal peroxidase to molecular iodine (I_2) that rapidly iodinates specific tyrosine residues within the thyroglobulin proteins to form monoiodotyrosine (MIT) and diiodotyrosine (DIT). Enzymatic coupling of MIT and DIT by thyroidal peroxidase gives covalently caged T_3 and T_4, which are released upon proteolysis of the thyroglobulin. MIT and DIT are also released, but are deiodinated within the gland to recycle the iodine source. In normal adults, approximately 5 μg of T_3 and 75 μg of T_4 are released from the thyroid gland per day into circulating blood. While T_4 is the major form released by the gland, T_3 appears to be the active form of the hormone. The bulk of T_3 is produced in peripheral tissues by mono-deiodination of T_4 by the type I or type II deiodinases.

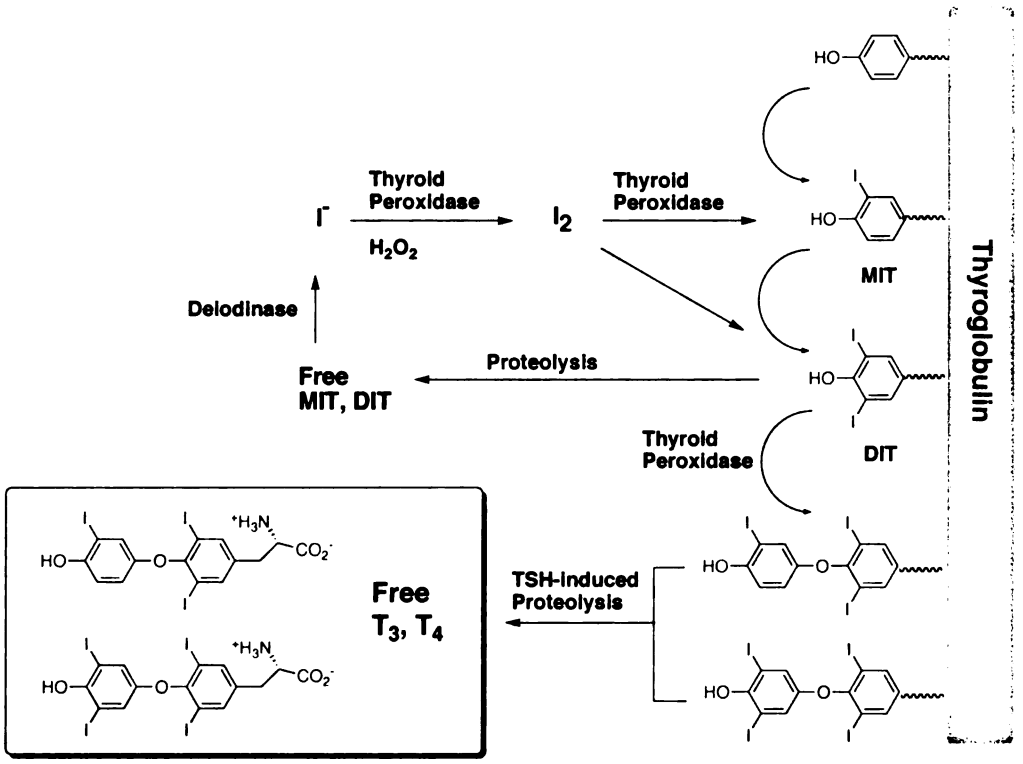

Figure 1-1. Biosynthesis of thyroid hormones. T_4 is the major form released by the thyroid gland. The bulk of T_3 is produced in peripheral tissues by mono-deiodination of T_4.

Once T_3 is localized to target tissues, its activity can be regulated by metabolic degradation.[4] Further deiodination of T_3 by type I,II deiodinase leads to the deactivated 3,5-diiodothryonine (T_2) (Figure 1-2). Deiodination of T_4 by type III deiodinase results in reverse-T_3 (rT_3), which is also inactive. To a lesser extent, thyroid hormones can be inactivated by deamination, decarboxylation, or conjugation and excretion as a glucuronides or sulfates.[2] It is important to note that some T_3 metabolites, such as Triac, still retain partial thyromimetic activity.[5-7]

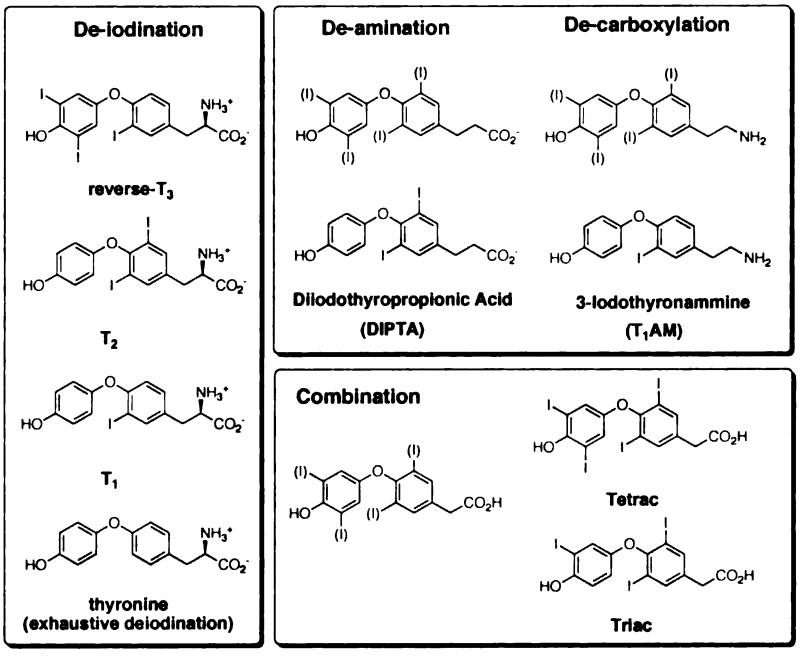

Figure 1-2. Examples of thyroid hormone metabolites.

1.2 Thyroid Hormone Transport and Uptake

Thyroid hormones circulate in the blood predominantly bound to the plasma protein thyroxine-binding globulin (TBG).[8,9] Other plasma proteins that bind thyroid hormone, albeit with weaker affinity, include transthyretin (TTR) and albumin.[8] Plasma binding increases hormone half-life and assures that an even distribution of hormone reaches the target tissues and cells. Over 99% of T_4 and T_3 are reversibly bound, with a turnover rate of approximately 10% and 75% per day, respectively.[10] Thus, T_3 has a much shorter half-life and therefore its concentration responds much more rapidly to changes in production or replacement. Having T_4 as the dominant supplier of T_3 to the peripheral tissues shields the hormone from fast metabolic clearance and buffers active tissue uptake.

The exchange characteristics between plasma and cellular pools of T_3 and T_4 dictate the peripheral distribution of the hormones and vary from tissue to tissue. Factors that determine the fractional T_3 exchange rate include the strength of plasma

and intracellular tissue binding as well as the permeability of the endothelial structure.[11] For example, the rate of T_3 exchange between plasma and muscle cells is slow mainly due to the low permeability to protein of the vascular endothelium in muscle. In contrast, rapid exchange is observed in the liver as a result of the relatively large gaps in the endothelial lining that allow virtually direct contact between plasma protein and the plasma membrane of the hepatocytes.

It was traditionally believed that thyroid hormones, like steroid hormones, entered and exited cells by passive diffusion through the membrane.[4] However studies in the past decade suggest active transport across the plasma membrane as a mechanism to regulate cellular levels of thyroid hormone and its activity.[12] A variety of facilitated transport mechanisms have been identified, including transporters shared with certain amino acids or organic anions, namely the system L or T amino acid transporters and the NCTP or OATP family of transporters, respectively.[13,14] Factors that influence plasma membrane transport include energy charge, in particular cellular ATP concentrations, number and type of transporter per cell, and Na^+ gradient over the plasma membrane. Additionally, plasma membrane transporters in different organs may have different thyroid hormone affinity thereby providing an additional level of regulating thyroid hormone tissue-specific bioavailability.[14]

1.3 Regulation of Thyroid Hormone Production

Normal thyroid hormone production and thyroid function require a finely tuned signaling network along the hypothalamic-pituitary-thyroid axis (HPT, Figure 1-3).[2] Hypothalamic cells secrete thyrotropin-releasing hormone (TRH) in response to stimulating factors such as acute psychosis and prolonged exposure to cold. TRH is secreted into capillaries of the pituitary venous system and triggers the synthesis and secretion of thyroid-stimulating hormone (TSH) in the pituitary gland. TSH in turn

stimulates an adenylyl cyclase mechanism in the thyroid cell to increase the synthesis and release of T_4 and T_3. To prevent overproduction of thyroid hormones, T_4 and T_3 can block TSH and TRH synthesis and release in a negative feedback loop.

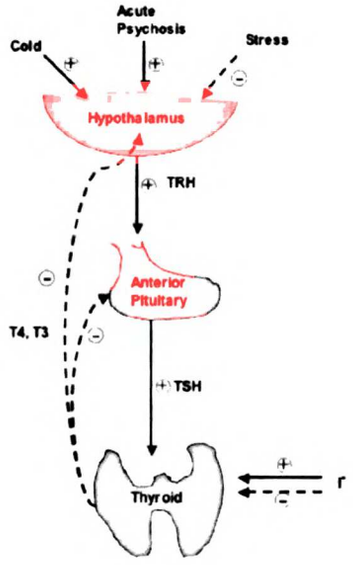

Figure 1-3. Negative feedback regulation of thyroid hormone production via the hypothalamic-pituitary-thyroid (HPT) axis. Iodide can also effect negative regulation of hormone production. Small amounts of iodide are necessary for hormone production, but large amounts inhibit T_4 and T_3 synthesis and release. ***Adapted from Basic & Clinical Pharmacology, 6th Edition ©1998, Ed. B.G. Katzung; Appleton & Lange: Norwalk, Conn.***

1.4 Physiological Effects of Thyroid Hormone

Thyroid hormones are essential for normal development, cellular differentiation, and metabolic balance.[2,10] The clinical conditions of hypo- and hyper-thyroidism provide insight into the consequences of abnormal levels of thyroid hormone.[15] Under-production of thyroid hormone results in severe impairment of mental development and growth in childhood. In the adult, hypothyroidism leads to a slow metabolism, decreased body temperature and heart rate, weight gain, and elevated cholesterol levels. By contrast, abnormalities in an excess state of thyroid hormone include weight loss, muscle wasting, tachycardia, bone loss, decreased cholesterol levels, and nervousness. This section highlights the physiological effects of thyroid hormone in major target tissues of brain, bone, adipose tissues, skeletal muscle, heart, and liver as summarized in Table 1-1. Also included is a brief discussion of the current practices for clinical treatment of hypo- and hyper-thyroidism.

Table 1-1. Examples of genes regulated thyroid hormone in target tissues.

Tissue	Gene	Function	Ref.
Brain	Cyclin D2	Apoptosis and proliferation—development of cerebellum	[18]
CNS growth and differentiation	c-Myc	Cell cycle arrest—blocks proliferation and induced differentiation of neuroblastoma cells	[18]
	Myelin	Oligodendrocyte maturation	[19]
	Neutrophins	Synaptic excitation	[20,21]
	Mitochondrial genes	Axon count and dendritic branching	[20,21]
Bone	Alkaline phosphatase, Osteocalcin, Collagen, IGF/IGFBP	Osteoblast protein activities	[30-35]
bone formation and resorption			
Adipose tissues	Acetyl CoA carboxylase, malic enzyme, FA synthase, spot 14	Fatty acid synthesis—lipogenic pathway (WAT)	[18,22,29]
Development and function of brown/white adipose tissue (BAT/WAT), theromogenesis	SREBP 1c	Fatty acid metabolism—lipolytic pathway (WAT)	[18]
	Na^+/K^+ ATPase	Transmembrane ion gradients in obligatory themogenesis (BAT)	[36]
	Mitochondrial uncoupling proteins (UCP1,UCP2, UCP3), PGC-1	Cellular ATP utilization in adaptive thermogenesis (BAT)	[22,36,38]
Skeletal muscle	SERCA	Intracellular Ca^{2+} cycling in muscle relaxation	[40,41]
Muscle contraction, metabolism and thermogenesis	Na^+/K^+ ATPase	Transmembrane ion gradients for restoration of membrane potential	[40]
	UCP3	Cellular ATP utilization in adaptive thermogenesis	[42]
Heart	α-MHC, β-MHC	Cardiac contraction	[39,46,47]
Cardiac output, thermogenesis	SERCA	Intracellular Ca^{2+} cycling in muscle relaxation	[18,22]
	K^+ ion channels, HCN2, HCN4	Pace-making functions	[18,48]
Liver	Lipogenic enzymes, malic enzyme, FA synthase, glucose-6-phosphate dehydro-genase, spot 14	Fatty acid synthesis and metabolism—lipogenic and lipolytic pathways	[22,50]
Lipid and cholesterol homeostasis	HMG CoA reductase	Cholesterol biosynthesis	[51]
	Cyp7α	Cholesterol metabolism to bile acids	[52]
	LDL receptor	Cholesterol transport and clearance	[52]

1.1.1 Brain

Thyroid hormones play a critical role in early growth and development of most organs, especially that of the brain which occurs during pre- and post-natal life. They

regulate expression of various genes involved in the central nervous system growth and differentiation.[16,17] For example, T_3 has been shown in animal models to control cyclin D2 expression, a key regulator of apoptosis and proliferation in external granular layer cells for normal postnatal development of the cerebellum.[18] T_3 also blocks proliferation and induces differentiation of neuroblastoma cells, possibly through regulation of the c-myc gene involved in cell cycle arrest.[18] Other T_3-regulated genes encode proteins of myelin for oligodendrocyte maturation,[19] mitochondria that affect axon count and dendritic branching, neurotrophins for synaptic excitation,[20,21] and several proteins important for neuronal migration.[22]

While thyroid hormone levels are important throughout gestation, there is increasing evidence that these hormones are already needed for orderly development during the first trimester when the fetus is entirely dependent on the maternal transfer of T_4.[23,24] The clinical consequences of hormone deficiency during this period have been extensively studied, including mental retardation/cretinism[25] and neuromotor dysfunction.[26] Early T_4 treatment of congenital hypothyroidism can prevent intellectual impairment. By contrast, clinical manifestation of excess thyroid hormone during early development is largely unexplored. Recent evidence suggests that fetal hyperthyroidism can also cause permanent detrimental effects to the nervous system by early interruption of neuron proliferation.[20]

1.4.2 Bone

Normal bone growth and development also depends on thyroid hormone regulation.[27,28] Hypothyroidism in children can lead to stunted growth while hyperthyroidism in adults increases risk of osteoporosis and bone fractures due to increase in porosity and decrease in cortical bone thickness.[29] However, little is known about the direct effects of thyroid hormone on osteoblast (bone formation) and

osteoclast (bone resorption) activities. A number of osteoblast proteins are directly or indirectly stimulated by T_3, including alkaline phosphatase,[30,31] osteocalcin[32], and collagen.[33] Thyroid hormone also stimulates IGF and IGFBPs, suggesting it may be involved in osteoblast differentiation and proliferation by regulating growth factor synthesis and action.[34,35] In osteoclasts, no T_3-regulated target genes have been described to date.

1.1.3 Adipose Tissues

The biologic hallmark of abnormal thyroid function is a change in the basal metabolic rate that affects thermogenesis, oxygen consumption, and fat stores maintained by lipogenesis and lipolysis.[36-38] To the latter effect, thyroid hormones play important roles in the development and function of brown and white adipose tissues (BAT, WAT). In differentiating WAT, T_3 induces enzymes of the lipogenic pathway to modulate fatty acid (FA) synthesis, including acetyl CoA carboxylase, malic enzyme, spot 14, and fatty acid synthase.[18,22,39] In the lipolytic pathway, T_3 modifies the response to catecholamines and insulin, and regulates expression of genes involved in lipid metabolism (eg. SREBP 1c) in mature adipocytes.[18]

Maintenance of trans-membrane ionic gradients is important for obligatory thermogenesis to provide energy for the transport of substances. The thermogenic effect of T_3 involves activation of the Na^+/K^+ ATPase and intracellular Ca^{2+} cycling, as well as accelerating mitochondria respiration.[36] Adaptive or facultative thermogenesis predominantly occurs in BAT in response to cold exposure or overeating. BAT thermogenesis depends on T_3-induced synthesis of the mitochondrial uncoupling proteins (UCP1, UCP2, UCP3) and PGC-1 protein, and T_3 stimulation of the norepinephrine-signaling pathway.[22,36,38] UCP-1 and PGC-1 are fundamental in mediating effects of cellular ATP utilization. Moreover, BAT contains type II deiodinase

activity that is stimulated by norepinephrine to provide high concentrations of T_3, allowing for T_3 auto-regulation of thermogenesis in BAT.[18]

1.4.4 Skeletal Muscle

Given that skeletal muscle represents up to 40% of the total body weight and has significant energy capacity, recent studies have focused on the contribution of skeletal muscle to metabolism and thermogenesis. Skeletal muscle contraction relies on thyroid hormone regulation of the sarcoplasmic/endoplasmic reticulum calcium ATPase (SERCA) for intracellular Ca^{2+} removal in muscle relaxation and the Na^{+}/K^{+} ATPase activity for restoration of the membrane potential after excitation.[40] T_3 induces the fast-muscle isoform SERCA1 activity with concomitant down-regulation of the slow-muscle isoform SERCA2a in slow muscle fibers. Consequently, the average level of contractile activity of the slow fibers is high and provides an increase in the overall metabolic rate.[41] Furthermore, skeletal muscles express high levels of mitochondrial UCP3 mRNA upon stimulation with T_3 suggesting thermogenesis may also occur via mitochondrial uncoupling in skeletal muscles.[42]

1.4.5 Heart

The net effect of increased thyroid hormone-induced metabolic rate is an increase in resting cardiac output for the control of energy and heat dissipation.[37,43] Hyperthyroid patients generally suffer from atrial arrhythmias, limitations in exercise tolerance, and congestive heart failure.[15] Thyroid hormones regulate heart rate and rhythm through regulation of cardiac specific genes and induction of hemodynamic changes.[44,45] The contractile properties of the heart depend on the relative amounts of the myosin heavy chain (MHC) α and β isoforms, which are inversely regulated by T_3.[39,46,47] Up-regulation of α-MHC, which has higher ATPase activity and increased

velocity of fiber shortening, with concurrent down-regulation of β-MHC enhances cardiac contractility.

As in skeletal muscle, thyroid hormones also control the rate of diastolic relaxation of the heart mediated by the intracellular Ca^{2+} concentration and the activity of Ca^{2+} ATPase (SERCA2).[18,22] Unlike skeletal muscle, however, SERCA2 expression and activity are upregulated by T_3 for faster relaxation of cardiac muscles. T_3 also regulates expression of several ion channels responsible for pace-making function in the heart such as the K^+ channels (KV4.2 and minK) and hyperpolarization-activated cyclic nucleotide-gated channels (HCN2 and HCN4).[18,48] Additionally, thyroid hormones can enhance β-adrenergic receptor sensitivity to catecholamines that also control cardiac output.[22,45]

1.4.6 Liver

Several forms of liver disease are clinically associated with thyroid hormones and thyroid dysfunction.[49] Comprehensive microarray analysis of liver gene expression revealed approximately 200 genes regulated (directly or indirectly) by T_3, many of which are responsible for lipogenesis, lipolysis, lipid mobilization, and oxidative processes.[50] Among these genes, the lipogenic enzymes, malic enzyme, glucose-6-phosphate dehydrogenase, fatty acid synthase and spot 14 have been extensively studied.[22] In some cases, T_3 regulation of these enzymes can be affected by carbohydrate intake, insulin and cAMP levels.

Thyroid hormones also regulate expression of important proteins and enzymes involved in cholesterol metabolism and synthesis in the liver. For example, T_3 down-regulation of the HMG CoA reductase, a key enzyme for cholesterol biosynthesis,[51] in balance with induction of the hepatic cholesterol 7α-hydroxylase (Cyp7α) for conversion of cholesterol to bile acids and of the low density lipoprotein (LDL) receptor for

cholesterol clearance is important for cholesterol homeostasis.[52] Interestingly, T_3 may also affect post-translational editing of the apolipoprotein B gene that is important for assembly and secretion of lipoproteins.[51,53] This may be the molecular basis for hypercholesterolemia with elevated serum LDL cholesterol concentrations observed in hypothyroid patients.

1.4.7 Treatment of Hypo- and Hyperthyroidism

There are currently no methods available for management of hypo- or hyper-thyroidism that do not induce detrimental side effects.[2,15] The current recommended treatment for hypothyroidism involves hormone replacement therapy with synthetic T_4 preparation levothyroxine, which is stable, inexpensive, and has a relatively long seven day half-life in serum. However, levothyroxine has a narrow therapeutic range, large absorption variability, and significant drug-drug interactions. Liothyronine, a synthetic T_3 preparation, can also be used although it is not recommended for routine replacement therapy despite its greater hormone activity. Liothyronine has a short one day serum half-life, thus requiring multiple daily doses that can lead to greater risk of cardiotoxicity.

For hyperthyroidism, anti-thyroid drug therapies, including methimazole and propylthiouracil, are prescribed to block thyroid hormone release from the gland or peripheral conversion of T_4 to T_3.[2,15] Complications with these methods include acute thyroid toxicosis and heart failure. Under these circumstances, β-adrenergic blockers such as propranolol can be used in adjunct to ameliorate symptoms of tachycardia and hypertension. Alternatively, radioactive ablation of the thyroid gland followed by life-long hormone replacement therapy can be pursued.

1.5 Molecular Biology of Thyroid Hormone Action

1.5.1 Transcriptional Regulation Through Thyroid Hormone Receptor (TR)

The effects of thyroid hormone (T_3) are primarily mediated by the thyroid hormone receptor (TR), a member of the nuclear receptor (NR) superfamily of ligand-modulated transcription factors. Genes responsive to thyroid hormone contain a *cis*-acting regulatory DNA sequence, thyroid hormone response element (TRE), upstream of the promoter region. A simple model of TR-mediated thyroid hormone signaling describes unliganded TR localized in the nucleus and bound to the TRE as a monomer, homodimer, or heterodimer with retinoid X receptor (RXR) (Figure 1-4). On genes positively regulated by thyroid hormone, the TR is associated with a group of corepressor proteins to repress formation of the transcription machinery complex. The TR undergoes a conformational change, most dramatically in the C-terminal helix 12 (H12) of the ligand binding domain (LBD), upon binding of T_3 that allows release of corepressors and subsequent recruitment of coactivator proteins to activate expression of T_3-responsive genes.[12,22,54]

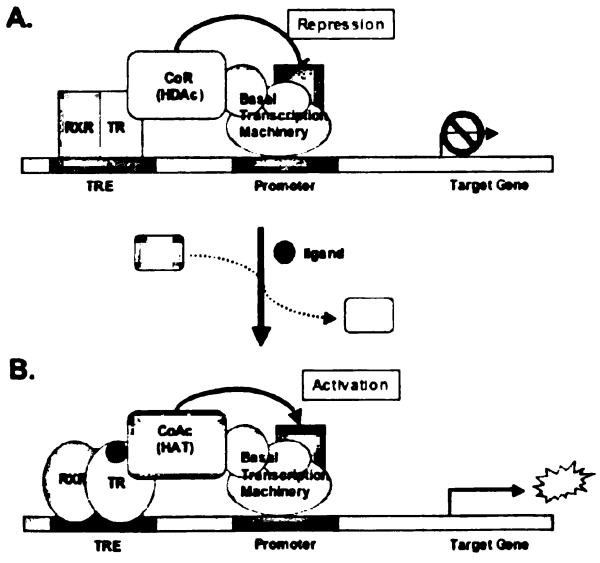

Figure 1-4. Mechanism of TR action. (A) TR occupies TRE binding sites on DNA in the absence of ligand, typically as a heterodimer with RXR, and represses transcription of nearby target gene by recruiting corepressors (CoR) and their associated histone deacetylases (HDAc). HDAc increases chromatin packing and inhibit gene expression. (B) Ligand promotes a conformational change in TR that leads to release of CoR and recruitment of coactivators (CoAc). CoAc and their associated histone acetyltransferases (HAT) loosen chromatin packing and promote binding of the basal transcription machinery for increased gene expression.

While it has long been recognized that thyroid hormones can also have negative transcriptional effects, the nature of the response elements and the mechanism of ligand-dependent repression remain poorly defined. Genes negatively regulated by T_3, including the TRH and TSH involved in the negative feedback control of T_3 production, are stimulated in the absence of T_3 and repressed upon addition of T_3. Recent evidence suggests that the roles of corepressors and coactivators are reversed on a negative TRE where corepressor recruitment by liganded TR is associated with transcriptional stimulation.[55,56] This paradoxical situation has been rationalized by differences in TR topology, allosterically induced by different response elements that can dictate whether a cofactor will function as a coactivator or corepressor in its interaction with the basal transcription machinery.[57,58]

1.5.1.1 TR Genes and Expression

Two different thyroid hormone receptor subtypes, TRα and TRβ, mediate the wide range of physiological effects of T_3. The TRs were originally cloned and identified from embryonal chicken and human placental cDNA libraries.[59,60] In humans, the TRα and TRβ subtypes are encoded on separate genes of chromosomes 17 and 3, respectively. Alternative splicing of the initial RNA transcripts gives rise to at least four additional isoforms (TRα_1, TRα_2, TRβ_1, and TRβ_2)[61] as shown in Figure 1-5. TRα_1, TRβ_1 and TRβ_2 all bind thyroid hormone with high affinity and specificity. Only TRα_2 is unresponsive to T_3 and can antagonize actions of other TR isoforms by competing for binding to TREs. Additional splice variants—TRα_3, TRβ_3, and TR$\Delta\beta_3$—have been identified in the rat.[61,62] TRα_3 and TR$\Delta\beta_3$ display dominant negative antagonism of TR-mediated action *in vitro*, although their roles *in vivo* are unclear.

All TR isoforms, except TRβ_2, are expressed in virtually all tissues, although they have distinct patterns of developmental and tissue-specific expression.[22,61,63] Knowledge

of these expression patterns has provided insight into the specific biological roles of each TR isoform. Studies in rodent models show TRα_1 is most abundant in skeletal muscle and BAT while TRα_2 is predominant in the brain, specifically the olfactory bulb, hippocampus, and cerebral cortex granular layer. TRα_2 was also found with lower abundance in skeletal muscle and BAT, in addition to heart and kidney. TRβ_1 is more homogeneously distributed, but high in brain, liver, and kidney. TRβ_2 is unique in that it is almost exclusively expressed in the anterior pituitary gland, hypothalamus, developing brain and retina, and inner ear. These studies suggest TRα likely exerts significant functions in the CNS, heart, and skeletal muscle. In contrast, the TRβ form may play a prominent role in mediating actions of T_3 in the liver, kidney, and the negative feedback regulation of the HPT axis. Furthermore, ontogeny of the TR subtypes in animal models reveal the TRα is expressed at higher levels than TRβ in early development, even before the thyroid gland is formed. TRβ expression subsequently increases disproportionately as development proceeds.[22,61,64]

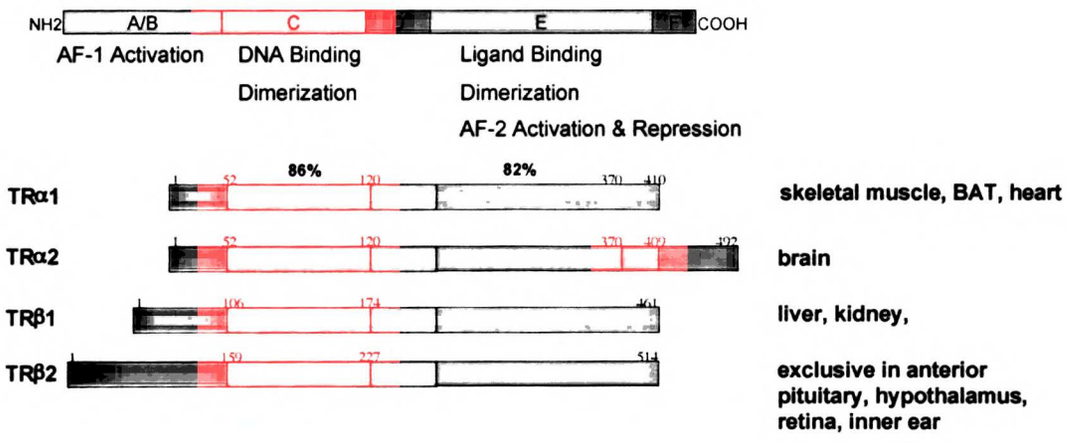

Figure 1-5. TR functional domains and isoforms. TRα and TRβ are encoded on separate genes and produce four major isoforms due to differential splicing. Additional splice variants have been identified but their *in vivo* roles are unclear. TRα_2 is the only isoform unresponsive to hormone due to its extended LBD. All isoforms, except TRβ_2, are co-expressed in different ratios in various tissues. The predominant tissue expression for each isoform is shown.

1.5.1.2 TR Functional Domains

The TR isoforms are highly homologous with respect to their amino acid sequences in various vertebrate species and share similar domain organization as that found in the NR superfamily. In general, NRs contain a highly variable N-terminal domain, a central DNA-binding domain (DBD) containing two zinc fingers important for specific DNA recognition, a hinge region containing the nuclear localization signal (NLS), and a C-terminal ligand-binding domain (LBD) (Figure 1-5).[65,66]

Like other NRs, the TR DBD contains cysteine-rich regions that form two zinc fingers for coordination of zinc ions.[67] These regions are important in sequence-specific recognition of the TRE through specific contacts with nucleic acids and phosphates within the major and minor grooves. The DBD zinc fingers and proximal regions are also sites for dimerization contacts with the TR heterodimeric partner RXR to stabilize the DNA binding and determine the spacing between TRE half sites. TRα and TRβ DBD regions are highly conserved, sharing 87% sequence homology.[61]

The LBD, as the name implies, is necessary for thyroid hormone binding and ligand-regulated transactivation.[61,68] The TRα and TRβ LBDs are less well conserved (82% homology) compared to the DBDs, however both subtypes bind T_3 with comparable affinities. The LBD plays a dominant role in interacting with auxillary proteins such as coactivator and corepressor proteins to mediate transcriptional activation and repression in response to hormone. The region located in the LBD C-terminus, dubbed as the activation function-2 (AF-2) domain, has high sequence homology among the NR superfamily members.[12] Mutations in this region result in loss of transcriptional activation without affecting DNA and hormone binding. The LBD also provides dimerization interfaces critical for homo- and hetero-dimerization.[68]

The hinge region links the DBD and LBD and contains a highly conserved lysine-rich nuclear localization sequence.[69] TRs are likely imported into the nucleus shortly after synthesis, as they are predominantly found in the nucleus, and can bind DNA even in the absence of hormone. Unlike some steroid hormone receptors, TRs do not associate with cytoplasmic heat shock proteins. The hinge region is also involved in TR corepressor interactions either by direct contact or allosteric effects.[70] Moreover, the crystal structure of the TR DBD reveals the hinge structure forms an extension of the DNA-binding surface and acts as a molecular ruler that directly measures the half-site spacing of the TRE by steric exclusion.[71]

The N-terminal domains are highly variable in length and amino acid sequence among the TR isoforms. Their role in TR function is poorly understood. While evidence suggests the N-terminus has no effect on T_3-dependent transcriptional activation, it may still be important for transcriptional activation and interactions with the general transcription factors including TFIIB.[12,54] In addition, the N-terminal domain can modulate ligand-independent interaction, also referred to as activation function-1 (AF-1), with corepressors and influence the conformation of the DBD and the repertoire of TREs to which it can bind.[72]

1.5.1.3 TR Response Elements

The nuclear hormone response elements are composed of two hexameric half sites with variable spacing.[67] The half sites can be arranged in symmetrical palindromic (Pal) or inverted palindromic (IP) orientation, or asymmetrical direct repeat (DR) orientation. TRs can bind to TREs as monomers, homodimers, and heterodimers with the RXR in which the half-sites are arranged as Pal, IP, or DR.[12,73] The optimal half-site spacings for TR binding are zero, six, and four nucleotides, respectively (TREpal0, IP6, DR4). Most of the naturally occurring TREs are of the DR4 type.[12] Mutational analyses

and sequence comparison of known TREs suggest a putative consensus hexamer half-site sequence of (G/A)GGT(C/G)A.

For TR-RXR heterodimers, Pal and IP TREs are symmetric and thus do not dictate a particular heterodimer orientation. On the other hand, DR-type TREs have a 5' to 3' polarity and thereby specify heterodimer orientation by requiring one receptor DBD to twist 180 degrees with respect to its LBD.[73] On a DR4 element, biochemical and crystallographic studies have confirmed that the RXR occupies the upstream half-site and the TR the downstream half-site.[74,75] The polarity of the TR/RXR complex may be important in protein-protein interactions with coactivators and corepressors that link the heterodimer with the transcriptional machinery. For example, it has been shown that the TRE sequence can dictate the preference for corepressor recruitment and affect corepressor release from TR in the presence of ligand.[76,77]

1.5.1.4 TR-RXR Dimer

The RXR has traditionally been characterized as a silent partner in the TR-RXR heterodimer where it is believed that the allosteric control by TR somehow prevents RXR from engaging in ligand binding, in part due to the TR-RXR polarity on TREs.[12] However, recent functional studies suggest that the RXR is not a silent partner and RXR can bind its natural ligand 9-*cis* retinoic acid in cells.[78] Although ligand binding by RXR does not directly elicit transcriptional response at the TRE, it promotes dissociation of corepressors from unliganded TR and may attenuate the transrepression function of TR on a positive TRE. The transcriptional activation function of liganded TR may also be affected by ligand binding by its RXR partner.

1.5.1.5 Dimerization Interface

Mutational and deletion studies of the DBD identified the zinc finger regions contribute to the dimerization interface,[79] which was later confirmed by crystallographic data of the isolated TR-RXR DBD heterodimer on the DR4 element.[71] Residues from the second zinc finger module of the upstream RXR DBD form stabilizing interactions with residues from the first zinc module and hinge region of the downstream TR. No data is currently available for the TR DBD homodimer interface, however crystallographic data from the isolated glucocorticoid receptor (GR) DBD homodimer suggest residues form the second zinc module of each dimeric partner interact to form a head-to-head symmetric dimer.[74]

In the LBD, a series of heptad repeats scattered throughout the LBD were initially identified by mutational studies to be involved in dimerization, with differential contribution of each heptad region.[80] In particular, the ninth heptad encompassed by helix 10 and 11 (H10, H11) was implicated to be critical for TR dimerization, which was supported by subsequent crystallographic evidence.[81,82] Moreover, the TRs use similar LBD surfaces for homo- and heterodimerization, although there may be differences in specific contacts made within the overlapping surfaces. These LBD surfaces account for approximately 75% of the dimer interface and allow for formation of dimers in solution before DNA targeting.

It has been proposed that the dimers bind TREs by initial formation of the LBD-LBD interface in solution, which leads to the formation of the DBD-DBD interface involving the zinc finger regions upon DNA binding. Recent functional evidence supports this biphasic dimerization model where DBD dimerization further stabilizes the heterodimers on the DR4 element.[82] However, such stabilization is not observed for heterodimers on IP6 or homodimers on DR4. These DBD-DBD interactions are very

weak and appear to have no functional significance.[82] Thus, the relative contribution to dimerization of the LBD and DBD may depend on the receptor dimer and response element.

1.5.1.6 Structure of TR Ligand Binding Domain

The crystal structures of the ligand-bound TR LBD of both TRα1 and TRβ1 have been solved and share a common fold with other NR members (Figure 1-6).[83-86] The LBD is composed of twelve α-helices and two β-turns arranged as an antiparallel helical sandwich in a three layer structure. The ligand is completely buried and plays a structural role in contributing to the hydrophobic core of the LBD.[85] Polar contacts are made from the receptor to the carboxylate and phenol substructures located on either end of the hormone. The majority of the contacts between receptor and ligand are hydrophobic. Although there is 82% homology in the LBD between TRα and TRβ subtypes, there is only one residue difference lining the ligand-binding pocket (Ser277 in TRα, Asn331 in TRβ) situated at the carboxylate end of the hormone.

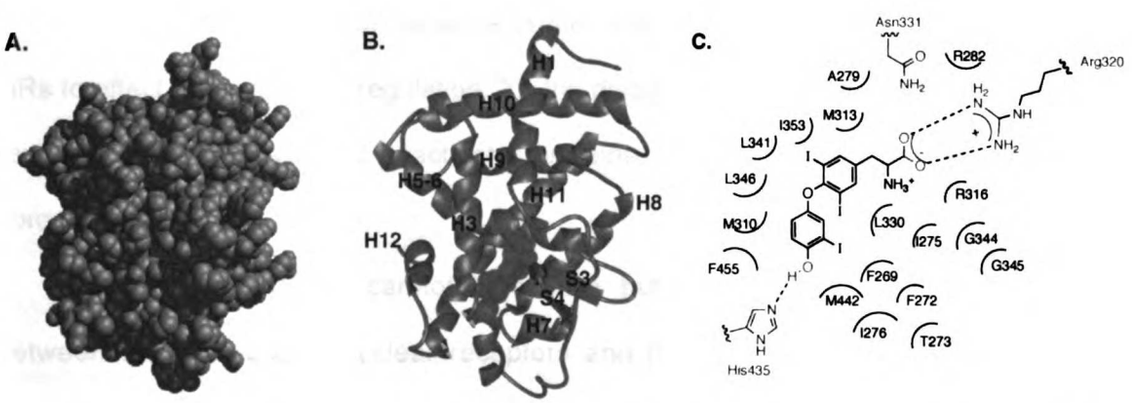

Figure 1-6. Crystal structure of T_3•TRβ LBD complex. (A) Space-filling representation that shows T_3 is completely buried within the hydrophobic core of the LBD. (B) Ribbon diagram showing α-helices (H) and β-strands (S) secondary structural elements. (C) Schematic diagram showing hormone-LBD interactions within the binding cavity.

Liganded LBD structures of other NRs (ER, PR, RAR, PPARγ) as well as unliganded structures (RXR, PPARγ) have been solved.[68,83] Comparison of these structures with the TR LBD reveals a common mousetrap mode for ligand binding and transactivation. Binding of ligand induces a conformational change in the overall NR structure, most dramatically in the C-terminal portion of the LBD corresponding to helix 12 (H12) and the AF-2 domain. Helix 12 appears to act as a molecular "lid" that packs against the body of the receptor upon ligand binding to close the binding pocket and further stabilize the NR structure by contributing to additional ligand-protein interactions.[68,87] In this conformation, H12 induces release of corepressor proteins and completes formation of a putative hydrophobic cleft accessible to coactivator proteins for transcriptional activation on a positive TRE.[88] Although there are other subtle structural differences in proximal and distal regions that may contribute to allosteric control of NR function,[89,90] rearrangement of H12 appears to be the prominent mechanism for ligand-induced gene regulation.[91]

1.5.1.7 TR Interactions with Coregulators

Given the plethora of literature in the field of coregulators that interact with the NRs to effect transcriptional regulation,[54,92] the discussions to follow will focus on general features of corepressor and coactivator proteins, and the specific interactions of the coregulators with TR.

Coregulators alone cannot bind DNA but instead mediate the interactions between the DNA-bound nuclear receptors and the transcription machinery through regulation of chromatin structure.[93] Histone acetyltransferase (HAT) and histone deacetylase (HDAc) activities are functionally associated with coactivators and corepressors, respectively. Hyperacetylation of chromatin loosens the DNA packing on chromatin structures and facilitates assembly of the basal transcription machinery. In

contrast, histone deacetylation condenses the chromatin structure and blocks entry of transcription machinery leading to target gene repression.

The LXXLL (L = leucine, X = any amino acid; NR box) motifs, which are amphipathic α-helical structures, located in the nuclear interacting domains (NIDs) of coactivators have been shown to be necessary and sufficient to mediate the ligand-dependent interactions with nuclear receptors.[86,94] Residues immediately adjacent to the motif modulate the affinity of the interaction and confer NR binding specificity.[86,95,96] In the crystal structure of TR bound to the coactivator GRIP-1,[86] the LXXLL binds into a surface hydrophobic groove formed by helices H3, H4, H5, and H12 of the LBD.[88] The floor of the groove is lined with hydrophobic residues that contact the leucine residues of the coactivator LXXLL motif, with charged residues lining the rim. These charged residues are highly conserved among the NRs and create capping interactions that may be important for selective coactivator recognition and binding by restricting the length of the interacting α-helix.

Parallel to the coactivator NR box, corepressors contain CoRNR ('corner') boxes with an extended consensus sequence of LXX(I/H)IXXX(I/L) (L = leucine, I = isoleucine, H = histidine, X = any amino acid).[97,98] The CoRNR box also binds NRs as an α-helical structure[93] and interacts with specific residues in H3-H5 that overlap the receptor pocket for coactivator binding.[98,99] The ligand-dependent formation of the charge clamp through rearrangement of H12 that stabilizes the NR box binding can also serve as a molecular switch to sterically inhibit interaction with the extended corepressor CoRNR box helix. However, H12 is not the only feature that regulates corepressor binding and release. Structure-guided mutational analyses revealed a novel corepressor interaction site required for optimal corepressor binding. This site encompasses residues buried underneath the usual position of H12 in the liganded TR (rather than including residues of H12), residues along H1, and residues above H11.[99]

Based on the TR interaction surfaces with corepressors and coactivators with respect to H12, a proposed mechanism for ligand-regulated NR activity describes H12 located in an unspecified position that exposes the corepressor binding site in the absence of ligand (Figure 1-7).[100] Repositioning of H12 over the lower part of the hydrophobic cleft in response to ligand binding simultaneously occludes the corepressor binding sites and reveals the coactivator binding surface. Thus, the hormone can dictate the position of a mobile H12 and shift co-regulator recruitment to alter the equilibrium between inactive and active states.[101]

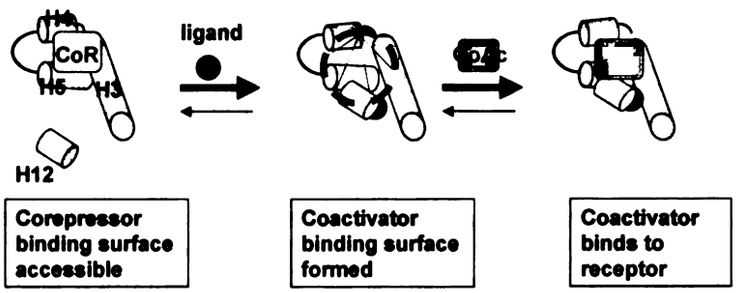

Figure 1-7. Model of ligand effects on TR cofactor binding. In the absence of hormone, H12 is displaced exposing the entire co-repressor binding surface. Ligand promotes packing of H12 over the lower part of the corepressor binding surface, simultaneously promoting corepressor release and formation of the coactivator binding surface.

1.5.2 Rapid Nongenomic Effects

Thyroid hormone actions independent of nuclear receptors have been reported to occur at the plasma membrane, at the cytoskeleton, in cytoplasm, and in various cell organelles.[102-105] Rapid onset of hormone action, on the scale of seconds to minutes, distinguishes nongenomic from nuclear effects, which manifest over hours to days. These nongenomic effects are diverse and include alterations in cellular (mitochondrial) respiration, cell morphology and surface presentation of proteins, vascular tone of arterial smooth muscle cells, and ion homeostasis through regulation of Ca^{2+} pumps and

Na^+ ion channels. The magnitude of the nongenomic effects is generally smaller than, but can potentiate, the nuclear actions. For example, thyroid hormones can activate the mitogen-activated protein (MAP) kinase-signaling cascade through cell surface receptors to promote phosphorylation of the TR and in turn activate TR transcriptional activity.[67,103] The molecular mechanisms of the nongenomic activities are not well understood and research in this area is still in the beginning stages. Recently, high-affinity specific binding sites for thyroid hormone have been detected in cell membranes and on intact cells in various tissues from humans and other species.[14,106] The nature and identity of these binding sites have yet to be elucidated.

Although the nongenomic and genomic effects of thyroid hormone can overlap, the hormone structure-activity relationships of these effects are distinct.[102] T_3 is predominantly active in eliciting nuclear action; however, all iodothyronines (T_4, T_3, rT_3, T_2) have been reported to have nongenomic activity. Recent studies also implicate metabolites of thyroid hormones, specifically 3-iodothyronamine (T_1AM, Figure 1-2), to have rapid nongenomic effects through the G-protein coupled trace amine receptor TAR1.[107]

1.6 Conclusions

Thyroid hormones play critical roles in differentiation, growth, and metabolism in virtually all tissues. Early studies showing their involvement in transcriptional regulation followed by the molecular cloning of TRs resulted in an explosion of information on the molecular mechanisms of hormone action. We have learned that there are multiple TR isoforms that bind to TREs with variable orientation, spacing, and sequences for TRE half-sites. TRs are also involved in complex ligand-modulated signaling networks through protein-protein interactions with corepressors and coactivators to effect transcriptional regulation. The solution of the crystal structures of the TR LBD and other

NR LBDs have provided insight into some of these complex interactions at the molecular level. Apart from TR-mediated effects, recent studies on the rapid effects of thyroid hormone have identified possible cell surface sites of hormone signaling.

In light of the information available, our understanding of thyroid hormone action is still incomplete. Pieces of the puzzle that are missing include understanding the different roles of the TR isoforms in thyroid hormone-mediated processes in specific tissues, in resistance to thyroid hormone, and in disease states associated with aberrant hormone signaling. While profiling the expression patterns of the TR isoforms has provided some information on their physiological roles, the molecular and structural events underlying their transcriptional activity remain elusive. The following chapters will describe current approaches and novel chemical tools used to address this issue and advance our understanding of thyroid hormone action.

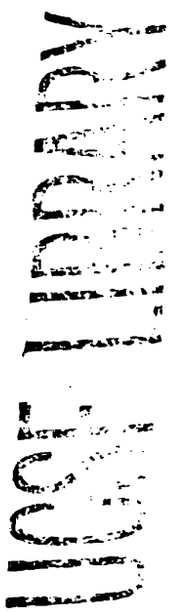

1.7 References

(1) Scanlan, T. S.; Yoshihara, H. A.; Nguyen, N. H.; Chiellini, G. Selective thyromimetics: tissue-selective thyroid hormone analogs. *Curr Opin Drug Discov Devel* **2001**, *4*, 614-622.

(2) Greenspan, F. S. The Thyroid Gland. *Basic & Clinical Endocrinology*; 5th Ed. ed.; Appleton & Lange: Stamford, 1997; pp 192-262.

(3) Degroot, L. J.; Niepomniszcze, H. Biosynthesis of thyroid hormone: basic and clinical aspects. *Metabolism* **1977**, *26*, 665-718.

(4) Utiger, L. E. B.; Utiger, R. D. *The Thyroid: a Fundamental and Clinical Text*; Lippencott: Philadelphia, 1991.

(5) Messier, N.; Laflamme, L.; Hamann, G.; Langlois, M. F. In vitro effect of Triac on resistance to thyroid hormone receptor mutants: potential basis for therapy. *Mol Cell Endocrinol* **2001**, *174*, 59-69.

(6) Sherman, S. I.; Ladenson, P. W. Organ-specific effects of tiratricol: a thyroid hormone analog with hepatic, not pituitary, superagonist effects. *J Clin Endocrinol Metab* **1992**, *75*, 901-905.

(7) Takeda, T.; Suzuki, S.; Liu, R. T.; DeGroot, L. J. Triiodothyroacetic acid has unique potential for therapy of resistance to thyroid hormone. *J Clin Endocrinol Metab* **1995**, *80*, 2033-2040.

(8) Schussler, G. C. The thyroxine-binding proteins. *Thyroid* **2000**, *10*, 141-149.

(9) Power, D. M.; Elias, N. P.; Richardson, S. J.; Mendes, J.; Soares, C. M. et al. Evolution of the thyroid hormone-binding protein, transthyretin. *Gen Comp Endocrinol* **2000**, *119*, 241-255.

(10) Utiger, R. D. The thyroid: physiology, thyrotoxicosis, hypothyroidism, and the painful thyroid. *Endocrinology and Metabolism*; McGraw-Hill: New York, 1995; pp 435-519.

(11) Oppenheimer, J.; Samuels, H.; Apriletti, J. W. *Molecular basis of thyroid hormone action*; Academic Press: New York, 1983; xv, 498 p.

(12) Ribeiro, R. C.; Apriletti, J. W.; Wagner, R. L.; West, B. L.; Feng, W. et al. Mechanisms of thyroid hormone action: insights from X-ray crystallographic and functional studies. *Recent Prog. Horm. Res.* **1998**, *53*, 351-392.

(13) Ritchie, J. W.; Shi, Y. B.; Hayashi, Y.; Baird, F. E.; Muchekehu, R. W. et al. A role for thyroid hormone transporters in transcriptional regulation by thyroid hormone receptors. *Mol Endocrinol* **2003**, *17*, 653-661.

(14) Hennemann, G.; Docter, R.; Friesema, E. C.; de Jong, M.; Krenning, E. P. et al. Plasma membrane transport of thyroid hormones and its role in thyroid hormone metabolism and bioavailability. *Endocr Rev* **2001**, *22*, 451-476.

(15) American Association of Clinical Endocrinologists medical guidelines for clinical practice for the evaluation and treatment of hyperthyroidism and hypothyroidism. *Endocr Pract* **2002**, *8*, 457-469.

(16) Delange, F. The role of iodine in brain development. *Proc Nutr Soc* **2000**, *59*, 75-79.

(17) van Tuyl, M.; Blommaart, P. E.; de Boer, P. A.; Wert, S. E.; Ruijter, J. M. et al. Prenatal exposure to thyroid hormone is necessary for normal postnatal development of murine heart and lungs. *Dev Biol* **2004**, *272*, 104-117.

(18) Viguerie, N.; Langin, D. Effect of thyroid hormone on gene expression. *Curr Opin Clin Nutr Metab Care* **2003**, *6*, 377-381.

(19) Rodriguez-Pena, A. Oligodendrocyte development and thyroid hormone. *J Neurobiol* **1999**, *40*, 497-512.

(20) Mussa, G. C.; Mussa, F.; Bretto, R.; Zambelli, M. C.; Silvestro, L. Influence of thryoid in nervous system growth. *Minerva Pediatr.* **2001**, *53*, 325-353.

(21) Bernal, J.; Guadano-Ferraz, A. Analysis of thyroid hormone-dependent genes in the brain by in situ hybridization. *Methods Mol Biol* **2002**, *202*, 71-90.

(22) Yen, P. M. Physiological and molecular basis of thyroid hormone action. *Physiol Rev* **2001**, *81*, 1097-1142.

(23) Hume, R.; Simpson, J.; Delahunty, C.; van Toor, H.; Wu, S. Y. et al. Human fetal and cord serum thyroid hormones: developmental trends and interrelationships. *J Clin Endocrinol Metab* **2004**, *89*, 4097-4103.

(24) Morreale de Escobar, G. The role of thyroid hormone in fetal neurodevelopment. *J Pediatr Endocrinol Metab* **2001**, *14 Suppl 6*, 1453-1462.

(25) Bernal, J. Action of thyroid hormone in brain. *J Endocrinol Invest* **2002**, *25*, 268-288.

(26) Delange, F. Iodine deficiency as a cause of brain damage. *Postgrad Med J* **2001**, *77*, 217-220.

(27) Allain, T. J.; McGregor, A. M. Thyroid hormones and bone. *J Endocrinol* **1993**, *139*, 9-18.

(28) Klaushofer, K.; Varga, F.; Glantschnig, H.; Fratzl-Zelman, N.; Czerwenka, E. et al. The regulatory role of thyroid hormones in bone cell growth and differentiation. *J Nutr* **1995**, *125*, 1996S-2003S.

(29) Pantazi, H.; Papapetrou, P. D. Changes in parameters of bone and mineral metabolism during therapy for hyperthyroidism. *J Clin Endocrinol Metab* **2000**, *85*, 1099-1106.

(30) Banovac, K.; Koren, E. Triiodothyronine stimulates the release of membrane-bound alkaline phosphatase in osteoblastic cells. *Calcif Tissue Int* **2000**, *67*, 460-465.

(31) Kozawa, O.; Hatakeyama, D.; Yoshida, M.; Kamiya, Y.; Kondo, C. et al. Activation of p44/p42 mitogen-activated protein kinase limits triiodothyronine-stimulated alkaline phosphatase activity in osteoblasts. *Biochem Biophys Res Commun* **2001**, *286*, 1140-1143.

(32) Gouveia, C. H.; Schultz, J. J.; Bianco, A. C.; Brent, G. A. Thyroid hormone stimulation of osteocalcin gene expression in ROS 17/2.8 cells is mediated by transcriptional and post-transcriptional mechanisms. *J Endocrinol* **2001**, *170*, 667-675.

(33) Pereira, R. C.; Jorgetti, V.; Canalis, E. Triiodothyronine induces collagenase-3 and gelatinase B expression in murine osteoblasts. *Am J Physiol* **1999**, *277*, E496-504.

(34) Lakatos, P.; Foldes, J.; Nagy, Z.; Takacs, I.; Speer, G. et al. Serum insulin-like growth factor-I, insulin-like growth factor binding proteins, and bone mineral content in hyperthyroidism. *Thyroid* **2000**, *10*, 417-423.

(35) Milne, M.; Kang, M. I.; Quail, J. M.; Baran, D. T. Thyroid hormone excess increases insulin-like growth factor I transcripts in bone marrow cell cultures: divergent effects on vertebral and femoral cell cultures. *Endocrinology* **1998**, *139*, 2527-2534.

(36) Silva, J. E. Thyroid hormone control of thermogenesis and energy balance. *Thyroid* **1995**, *5*, 481-492.

(37) Silva, J. E. The multiple contributions of thyroid hormone to heat production. *J Clin Invest* **2001**, *108*, 35-37.

(38) Lowell, B. B.; Spiegelman, B. M. Towards a molecular understanding of adaptive thermogenesis. *Nature* **2000**, *404*, 652-660.

(39) Brent, G. A. The molecular basis of thyroid hormone action. *N Engl J Med* **1994**, *331*, 847-853.

(40) Everts, M. E. Effects of thyroid hormones on contractility and cation transport in skeletal muscle. *Acta Physiol Scand* **1996**, *156*, 325-333.

(41) Simonides, W. S.; Thelen, M. H.; van der Linden, C. G.; Muller, A.; van Hardeveld, C. Mechanism of thyroid-hormone regulated expression of the SERCA genes in skeletal muscle: implications for thermogenesis. *Biosci Rep* **2001**, *21*, 139-154.

(42) Lanni, A.; Moreno, M.; Lombardi, A.; Goglia, F. Thyroid hormone and uncoupling proteins. *FEBS Lett* **2003**, *543*, 5-10.

(43) Klein, I. Clinical, metabolic, and organ-specific indices of thyroid function. *Endocrinol Metab Clin North Am* **2001**, *30*, 415-427, ix.

(44) Klein, I.; Ojamaa, K. Thyroid hormone: targeting the vascular smooth muscle cell. *Circ Res* **2001**, *88*, 260-261.

(45) Klein, I.; Ojamaa, K. Thyroid hormone and the cardiovascular system. *N Engl J Med* **2001**, *344*, 501-509.

(46) Ojamaa, K.; Klemperer, J. D.; MacGilvray, S. S.; Klein, I.; Samarel, A. Thyroid hormone and hemodynamic regulation of beta-myosin heavy chain promoter in the heart. *Endocrinology* **1996**, *137*, 802-808.

(47) Ojamaa, K.; Klemperer, J. D.; Klein, I. Acute effects of thyroid hormone on vascular smooth muscle. *Thyroid* **1996**, *6*, 505-512.

(48) Sun, Z. Q.; Ojamaa, K.; Nakamura, T. Y.; Artman, M.; Klein, I. et al. Thyroid hormone increases pacemaker activity in rat neonatal atrial myocytes. *J Mol Cell Cardiol* **2001**, *33*, 811-824.

(49) Malik, R.; Hodgson, H. The relationship between the thyroid gland and the liver. *Qjm* **2002**, *95*, 559-569.

(50) Flores-Morales, A.; Gullberg, H.; Fernandez, L.; Stahlberg, N.; Lee, N. H. et al. Patterns of liver gene expression governed by TRbeta. *Mol Endocrinol* **2002**, *16*, 1257-1268.

(51) Ness, G. C.; Lopez, D.; Chambers, C. M.; Newsome, W. P.; Cornelius, P. et al. Effects of L-triiodothyronine and the thyromimetic L-94901 on serum lipoprotein levels and hepatic low-density lipoprotein receptor, 3-hydroxy-3-methylglutaryl coenzyme A reductase, and apo A-I gene expression. *Biochem Pharmacol* **1998**, *56*, 121-129.

(52) Ness, G. C.; Lopez, D. Transcriptional regulation of rat hepatic low-density lipoprotein receptor and cholesterol 7 alpha hydroxylase by thyroid hormone. *Arch Biochem Biophys* **1995**, *323*, 404-408.

(53) Davidson, N. O.; Carlos, R. C.; Lukaszewicz, A. M. Apolipoprotein B mRNA editing is modulated by thyroid hormone analogs but not growth hormone administration in the rat. *Mol Endocrinol* **1990**, *4*, 779-785.

(54) Zhang, J.; Lazar, M. A. The mechanism of action of thyroid hormones. *Annu Rev Physiol* **2000**, *62*, 439-466.

(55) Tagami, T.; Madison, L. D.; Nagaya, T.; Jameson, J. L. Nuclear receptor corepressors activate rather than suppress basal transcription of genes that are negatively regulated by thyroid hormone. *Mol Cell Biol* **1997**, *17*, 2642-2648.

(56) Tagami, T.; Park, Y.; Jameson, J. L. Mechanisms that mediate negative regulation of the thyroid-stimulating hormone alpha gene by the thyroid hormone receptor. *J Biol Chem* **1999**, *274*, 22345-22353.

(57) Lefstin, J. A.; Yamamoto, K. R. Allosteric effects of DNA on transcriptional regulators. *Nature* **1998**, *392*, 885-888.

(58) Berghagen, H.; Ragnhildstveit, E.; Krogsrud, K.; Thuestad, G.; Apriletti, J. et al. Corepressor SMRT functions as a coactivator for thyroid hormone receptor

T3Ralpha from a negative hormone response element. *J Biol Chem* **2002**, *277*, 49517-49522.

(59) Sap, J.; Munoz, A.; Damm, K.; Goldberg, Y.; Ghysdael, J. et al. The c-erb-A protein is a high-affinity receptor for thyroid hormone. *Nature* **1986**, *324*, 635-640.

(60) Weinberger, C.; Thompson, C. C.; Ong, E. S.; Lebo, R.; Gruol, D. J. et al. The c-erb-A gene encodes a thyroid hormone receptor. *Nature* **1986**, *324*, 641-646.

(61) Lazar, M. A. Thyroid hormone receptors: multiple forms, multiple possibilities. *Endocr Rev* **1993**, *14*, 184-193.

(62) Williams, G. R. Cloning and characterization of two novel thyroid hormone receptor beta isoforms. *Mol Cell Biol* **2000**, *20*, 8329-8342.

(63) Glass, C. K.; Holloway, J. M. Regulation of gene expression by the thyroid hormone receptor. *Biochim Biophys Acta* **1990**, *1032*, 157-176.

(64) Oppenheimer, J. H.; Schwartz, H. L.; Strait, K. A. Thyroid hormone action 1994: the plot thickens. *Eur J Endocrinol* **1994**, *130*, 15-24.

(65) Evans, R. M. The steroid and thyroid hormone receptor superfamily. *Science* **1988**, *240*, 889-895.

(66) Ribeiro, R. C.; Kushner, P. J.; Baxter, J. D. The nuclear hormone receptor gene superfamily. *Annu Rev Med* **1995**, *46*, 443-453.

(67) Tsai, M. J.; O'Malley, B. W. Molecular mechanisms of action of steroid/thyroid receptor superfamily members. *Annu Rev Biochem* **1994**, *63*, 451-486.

(68) Moras, D.; Gronemeyer, H. The nuclear receptor ligand-binding domain: structure and function. *Curr Opin Cell Biol* **1998**, *10*, 384-391.

(69) Zhu, X. G.; Hanover, J. A.; Hager, G. L.; Cheng, S. Y. Hormone-induced translocation of thyroid hormone receptors in living cells visualized using a receptor green fluorescent protein chimera. *J Biol Chem* **1998**, *273*, 27058-27063.

(70) Safer, J. D.; Cohen, R. N.; Hollenberg, A. N.; Wondisford, F. E. Defective release of corepressor by hinge mutants of the thyroid hormone receptor found in patients with resistance to thyroid hormone. *J Biol Chem* **1998**, *273*, 30175-30182.

(71) Rastinejad, F.; Perlmann, T.; Evans, R. M.; Sigler, P. B. Structural determinants of nuclear receptor assembly on DNA direct repeats. *Nature* **1995**, *375*, 203-211.

(72) Hadzic, E.; Habeos, I.; Raaka, B. M.; Samuels, H. H. A novel multifunctional motif in the amino-terminal A/B domain of T3Ralpha modulates DNA binding and receptor dimerization. *J Biol Chem* **1998**, *273*, 10270-10278.

(73) Glass, C. K. Some new twists in the regulation of gene expression by thyroid hormone and retinoic acid receptors. *J Endocrinol* **1996**, *150*, 349-357.

(74) Rastinejad, F. Structure and function of the steroid and nuclear receptor DNA binding domain. *Molecular Biology of Steroid and Nuclear Hormone Receptors*; Birkhauser: Boston, 1998; pp 105-131.

(75) Glass, C. K. Differential recognition of target genes by nuclear receptor monomers, dimers, and heterodimers. *Endocr Rev* **1994**, *15*, 391-407.

(76) Cohen, R. N.; Putney, A.; Wondisford, F. E.; Hollenberg, A. N. The nuclear corepressors recognize distinct nuclear receptor complexes. *Mol Endocrinol* **2000**, *14*, 900-914.

(77) Olson, D. P.; Sun, B.; Koenig, R. J. Thyroid hormone response element architecture affects corepressor release from thyroid hormone receptor dimers. *J Biol Chem* **1998**, *273*, 3375-3380.

(78) Li, D.; Yamada, T.; Wang, F.; Vulin, A. I.; Samuels, H. H. Novel roles of retinoid X receptor (RXR) and RXR ligand in dynamically modulating the activity of the thyroid hormone receptor/RXR heterodimer. *J Biol Chem* **2004**, *279*, 7427-7437.

(79) Umesono, K.; Evans, R. M. Determinants of target gene specificity for steroid/thyroid hormone receptors. *Cell* **1989**, *57*, 1139-1146.

(80) Simons Jr., S. S. Structure and function of the steroid and nuclear receptor ligand-binding domain. *Molecular Biology of Steroid and Nuclear Hormone Receptors*; Birkhauser: Boston, 1998; pp 35-104.

(81) Zhang, J.; Zamir, I.; Lazar, M. A. Differential recognition of liganded and unliganded thyroid hormone receptor by retinoid X receptor regulates transcriptional repression. *Mol Cell Biol* **1997**, *17*, 6887-6897.

(82) Ribeiro, R. C.; Feng, W.; Wagner, R. L.; Costa, C. H.; Pereira, A. C. et al. Definition of the surface in the thyroid hormone receptor ligand binding domain for association as homodimers and heterodimers with retinoid X receptor. *J Biol Chem* **2001**, *276*, 14987-14995.

(83) Weatherman, R. V.; Fletterick, R. J.; Scanlan, T. S. Nuclear-receptor ligands and ligand-binding domains. *Annu Rev Biochem* **1999**, *68*, 559-581.

(84) Wagner, R. L.; Huber, B. R.; Shiau, A. K.; Kelly, A.; Cunha Lima, S. T. et al. Hormone selectivity in thyroid hormone receptors. *Mol Endocrinol* **2001**, *15*, 398-410.

(85) Wagner, R. L.; Apriletti, J. W.; McGrath, M. E.; West, B. L.; Baxter, J. D. et al. A structural role for hormone in the thyroid hormone receptor. *Nature* **1995**, *378*, 690-697.

(86) Darimont, B. D.; Wagner, R. L.; Apriletti, J. W.; Stallcup, M. R.; Kushner, P. J. et al. Structure and specificity of nuclear receptor-coactivator interactions. *Genes Dev* **1998**, *12*, 3343-3356.

(87) Apriletti, J. W.; Ribeiro, R. C.; Wagner, R. L.; Feng, W.; Webb, P. et al. Molecular and structural biology of thyroid hormone receptors. *Clin Exp Pharmacol Physiol Suppl* **1998**, *25*, S2-11.

(88) Feng, W.; Ribeiro, R. C.; Wagner, R. L.; Nguyen, H.; Apriletti, J. W. et al. Hormone-dependent coactivator binding to a hydrophobic cleft on nuclear receptors. *Science* **1998**, *280*, 1747-1749.

(89) Bendik, I.; Pfahl, M. Similar ligand-induced conformational changes of thyroid hormone receptors regulate homo- and heterodimeric functions. *J Biol Chem* **1995**, *270*, 3107-3114.

(90) Nettles, K. W.; Sun, J.; Radek, J. T.; Sheng, S.; Rodriguez, A. L. et al. Allosteric control of ligand selectivity between estrogen receptors alpha and beta: implications for other nuclear receptors. *Mol Cell* **2004**, *13*, 317-327.

(91) Lin, B. C.; Hong, S. H.; Krig, S.; Yoh, S. M.; Privalsky, M. L. A conformational switch in nuclear hormone receptors is involved in coupling hormone binding to corepressor release. *Mol Cell Biol* **1997**, *17*, 6131-6138.

(92) McKenna, N. J.; Lanz, R. B.; O'Malley, B. W. Nuclear receptor coregulators: cellular and molecular biology. *Endocr Rev* **1999**, *20*, 321-344.

(93) Xu, L.; Glass, C. K.; Rosenfeld, M. G. Coactivator and corepressor complexes in nuclear receptor function. *Curr Opin Genet Dev* **1999**, *9*, 140-147.

(94) Heery, D. M.; Kalkhoven, E.; Hoare, S.; Parker, M. G. A signature motif in transcriptional co-activators mediates binding to nuclear receptors. *Nature* **1997**, *387*, 733-736.

(95) Geistlinger, T. R.; Guy, R. K. Novel selective inhibitors of the interaction of individual nuclear hormone receptors with a mutually shared steroid receptor coactivator 2. *J Am Chem Soc* **2003**, *125*, 6852-6853.

(96) Geistlinger, T. R.; Guy, R. K. Steroid receptor coactivator peptidomimetics. *Methods Enzymol* **2003**, *364*, 223-246.

(97) Hu, X.; Lazar, M. A. The CoRNR motif controls the recruitment of corepressors by nuclear hormone receptors. *Nature* **1999**, *402*, 93-96.

(98) Perissi, V.; Staszewski, L. M.; McInerney, E. M.; Kurokawa, R.; Krones, A. et al. Molecular determinants of nuclear receptor-corepressor interaction. *Genes Dev* **1999**, *13*, 3198-3208.

(99) Marimuthu, A.; Feng, W.; Tagami, T.; Nguyen, H.; Jameson, J. L. et al. TR surfaces and conformations required to bind nuclear receptor corepressor. *Mol Endocrinol* **2002**, *16*, 271-286.

(100) Webb, P.; Nguyen, N. H.; Chiellini, G.; Yoshihara, H. A.; Cunha Lima, S. T. et al. Design of thyroid hormone receptor antagonists from first principles. *J Steroid Biochem Mol Biol* **2002**, *83*, 59-73.

(101) Schulman, I. G.; Juguilon, H.; Evans, R. M. Activation and repression by nuclear hormone receptors: hormone modulates an equilibrium between active and repressive states. *Mol Cell Biol* **1996**, *16*, 3807-3813.

(102) Davis, P. J.; Davis, F. B. Nongenomic actions of thyroid hormone. *Thyroid* **1996**, *6*, 497-504.

(103) Davis, P. J.; Tillmann, H. C.; Davis, F. B.; Wehling, M. Comparison of the mechanisms of nongenomic actions of thyroid hormone and steroid hormones. *J Endocrinol Invest* **2002**, *25*, 377-388.

(104) Davis, P. J.; Davis, F. B. Nongenomic actions of thyroid hormone on the heart. *Thyroid* **2002**, *12*, 459-466.

(105) Falkenstein, E.; Tillmann, H. C.; Christ, M.; Feuring, M.; Wehling, M. Multiple actions of steroid hormones--a focus on rapid, nongenomic effects. *Pharmacol Rev* **2000**, *52*, 513-556.

(106) Schmidt, B. M.; Gerdes, D.; Feuring, M.; Falkenstein, E.; Christ, M. et al. Rapid, nongenomic steroid actions: A new age? *Front Neuroendocrinol* **2000**, *21*, 57-94.

(107) Scanlan, T. S.; Suchland, K. L.; Hart, M. E.; Chiellini, G.; Huang, Y. et al. 3-Iodothyronamine is an endogenous and rapid-acting derivative of thyroid hormone. *Nat Med* **2004**, 10, 638-642.

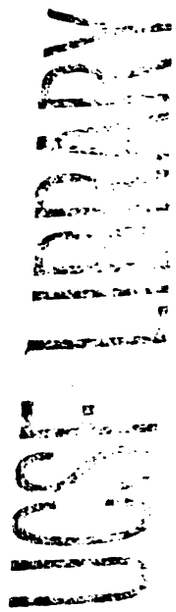

Chapter 2

Delineating the Physiological Roles of the TR Subtypes

Much effort has focused on delineating the physiological roles of the TR isoforms ($TR\alpha_1$, $TR\alpha_2$, $TR\beta_1$, $TR\beta_2$) in specific tissues to better define thyroid hormone receptor function. While expression profiling of the TR isoforms has provided clues to their function, the overlap in their expression begs the question of whether they have redundant transcriptional activity and can compensate for each other in regulating most target genes. Progress in our understanding of thyroid hormone action *in vivo* has principally relied on observations made of TR knock-out and knock-in transgenic mouse models. Unfortunately, the results have been ambiguous due to the complex signaling pathways related to TR, as well as the spatial and temporal difference in TR function in vertebrate development and homeostasis. Recent success in developing selective TR modulators (STRMs) has provided valuable chemical tools to improve our understanding of the roles of the TR subtypes in hormone signaling. STRMS are TR subtype-selective ligands capable of activating or inactivating thyroid hormone-regulated responses. Furthermore, STRMs may be therapeutically useful in the treatment of diseases associated with thyroid hormone.

2.1 Transgenic Mouse Models of TR Function

To date, thirteen TR knock-out mice strains and four mutant TR knock-in mice strains have been generated to assess the roles of TRα and TRβ *in vivo.*[1-3] The mutant knock-out mice include mice that lack TRα ($TR\alpha^{0/0}$),[4-6] $TR\alpha_1$ ($TR\alpha_1^{-/-}$),[7,8] $TR\alpha_2$ ($TR\alpha_2^{-/-}$),[9] TRβ ($TR\beta^{-/-}$),[6,10-14] $TR\beta_2$ ($TR\beta_2^{-/-}$),[12] both $TR\alpha_1$ and TRβ ($TR\alpha_1^{-/-}$, $TR\beta^{-/-}$),[6,10] and the completely TR-deficient mice ($TR\alpha^{0/0}$, $TR\beta^{-/-}$).[6,15,16] These transgenic mice display distinct phenotypes, as outlined in Table 2-1, that indicate the TRα and TRβ isoforms have non-overlapping, tissue-selective functions. In general, TRβ knock-out mice are viable and show a subset of the abnormalities found in patients with autosomal dominant

resistance to thyroid hormone (RTH), where dysregulation of the HPT axis is observed with elevated serum TSH and T_4 levels. $TR\beta_1$ mainly controls inner ear development and liver cholesterol metabolism while $TR\beta_2$ controls retina development and T_3-mediated suppression of TSH in the HPT axis. Both $TR\beta_1$ and $TR\beta_2$ can also mediate hormone-induced increases in heart rate.

Mice deficient in one or more forms of TRα have phenotypes distinct from TRβ. TRα knock out mice become progressively hypothyroid after birth, have stunted development and growth, and generally have low survival rates. In contrast, disruption of either $TR\alpha_1$ or $TR\alpha_2$ alone results in mice that are viable, indicating both $TR\alpha_1$ and $TR\alpha_2$ are required for postnatal development and normal survival. $TR\alpha_1$ plays a major role in regulating baseline cardiac function, core body temperature, and maturation of the small intestine. The role of $TR\alpha_2$ is still unclear due to the concomitant over-expression of $TR\alpha_1$ in $TR\alpha_2$-deficient mice. These mice display a mixed hypothyroid and hyperthyroid phenotype, where they have low levels of circulating T_4, inappropriately normal levels of TSH, and increased heart rate and body temperature.

Interestingly, mice lacking both $TR\alpha_1$ and TRβ or completely devoid of all TR isoforms exhibit mild congenital hypothyroidism and are viable with less deleterious effects than ones that have the TRs present during hypothyroidism. These results suggest an important role for the repressive effects of unliganded TR, which is further underscored by the phenotypes observed in TR knock in mice. Various TR transgenic mice models have been developed to reproduce the dominant negative mutations found in generalized RTH.[17,18] Some mutations introduced in TR altered the ability of TR to *bind* ligand and/or interact with coregulators, including deletion of residue ΔT337 in the TRβ-LBD, R383H mutation in the TRβ-LBD, and PV frameshift mutation in TRα and TRβ.[1,2] For example, TRβ–deficient mice have normal brain development while mice

with the TRβ ΔT337 mutation have severe abnormalities in cerebellar development and learning disabilities.[19] The ΔT337 mutation resulted in constitutive unliganded TR interaction with corepressors to block gene expression, suggesting abnormal transrepression of target genes by unliganded TRs can have detrimental effects. Thus, relieving TR transrepression may have therapeutic significance.[20]

Table 2-1. Summary of TR knockout phenotypes.

Tissue	$TR\alpha^{0/0}$ [4-6]	$TR\alpha_1^{-/-}$ [7,8]	$TR\alpha_2^{-/-}$ [9]	$TR\beta^{-/-}$ [6,10-14]	$TR\beta_2^{-/-}$ [12]	$TR\alpha_1^{-/-}$, $TR\beta^{-/-}$ [6,10]	$TR\alpha^{0/0}$, $TR\beta^{-/-}$ [6,15,16]
Thyroid	Hypoplastic	Normal	Reduced size	Hyperplastic	Hyperplastic	Enlarged	Enlarged
Serum T_4	Low	Low	Low	Increased	Increased	High	High
Serum TSH	Reduced	Reduced	Normal	Elevated	Elevated	High	High
Survival	Neonatal lethal 4-6 wk	Normal	Normal	Normal	Normal	Low, 9 months	Neonatal lethal 4-6 wk
Bone	Demineral-ized	Normal	Growth retardation	Normal	Normal	Demineral-ized, growth retardation	Demineral-ized, growth retardation
Brain	Normal	Normal	Normal	Normal	Normal	Normal	Normal
Heart	Reduced	Reduced	Elevated	Elevated, unresponsive to T_3	Normal	Reduced	Reduced
Other	Arrested maturation of small intestine	Lowered body temp.	Elevated body temp.	Cochlear defect, decreased liver metabolism	Normal auditory function, defective retina development	Arrested maturation of small intestine, lowered body temp.	Arrested maturation of small intestine, retina degeneration, lowered body temp.

2.2 Synthetic Ligands as Chemical Probes to Study TR Function

Since the natural hormone T_3 does not discriminate between the TRα and TRβ subtypes, development of synthetic thyroid hormone analogues that selectively bind to either TRα or TRβ and have tissue-selective actions has been a burgeoning field to delineate the roles of the TR isoforms. Structural characterization of the TR LBD has

facilitated the design and synthesis of selective TR modulators (STRMs). The term STRM, derived from selective estrogen receptor modulators (SERMs), has been coined to describe the spectrum of agonist and antagonist actions that stem from selective binding to receptor subtypes, which function at particular response elements and effect differential coactivator and corepressor recruitment.[21] Several STRMs have been successfully developed through the combined use of extensive structure-activity relationship (SAR) data and the X-ray crystal structures of liganded TR complexes.

2.2.1 Thyroid Hormone Pharmacophore

The field of thyroid hormone medicinal chemistry has been in existence for approximately 50 years and has provided extensive SAR data for the development of thyroid hormone analogues.[22,23] These studies reveal the minimal requirements for a high-affinity TR ligand, as summarized in Figure 2-1: (1) the 4'-hydroxyl and carboxylic acid-containing side chain at the 1-position are essential for tight TR binding and thyromimetic activity and (2) halogen or hydrocarbon substitution at the 3, 5, 3'-positions is required. **DIMIT** (Figure 2-2) is an example of a thyromimetic that satisfies the SAR requirements, although **DIMIT** binds TRα/TRβ approximately 100-fold less tightly than T_3. This crude picture of the thyromimetic pharmacophore is further supported by the co-crystal structure of **DIMIT** and TRβ,[24] which shows the 4'- and 1-positions of the thyronine structure are involved in hydrogen bonding and electrostatic contacts, respectively, with residues in the binding pocket. The 3, 5, and 3'-substituents of T_3 reside in small hydrophobic pockets, and the ligand occupies almost 90% of the volume of the binding pocket. SAR data further reveal substituents significantly larger than iodine atoms hinder ligand binding and activity, presumably due to size limitations in the binding pocket of the receptor. However, recent biochemical and structural evidence shows that substitution at the 3'-position with a larger benzyl group can still be

accommodated in the TR binding pocket and allows full thyromimetic activity.[25] Combined, these results provide important criteria required for developing high-affinity T_3 analogues.

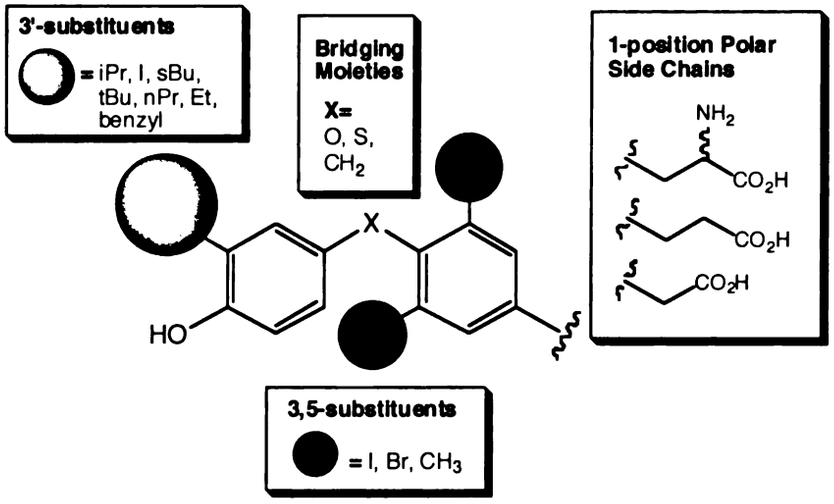

Figure 2-1. SAR profile of compounds with thyromimetic activity.

2.2.2 Selective TR Modulators: Agonists

Early work on developing thyroid hormone analogues have focused on tissue and/or TR-subtype specific thyroid hormone agonists to obtain the beneficial effects of T_3 (reduction of weight or cholesterol levels) without inducing the deleterious effects (tachycardia, osteoporosis, and muscle wasting). Since TRβ plays a predominant role in the liver to regulate lipid homeostasis, TRβ-selective thyroid hormone analogues would be useful in the treatment of metabolic diseases such as obesity and hyperlipidemia. Similarly, TRα-selective thyromimetics could be used to treat bradycardia and hypothermia, indications where TRα has a critical role in regulating hormone response. While there has been significant progress and success in the development of TRβ-selective thyromimetics, no TRα-selective compounds have been reported to date.

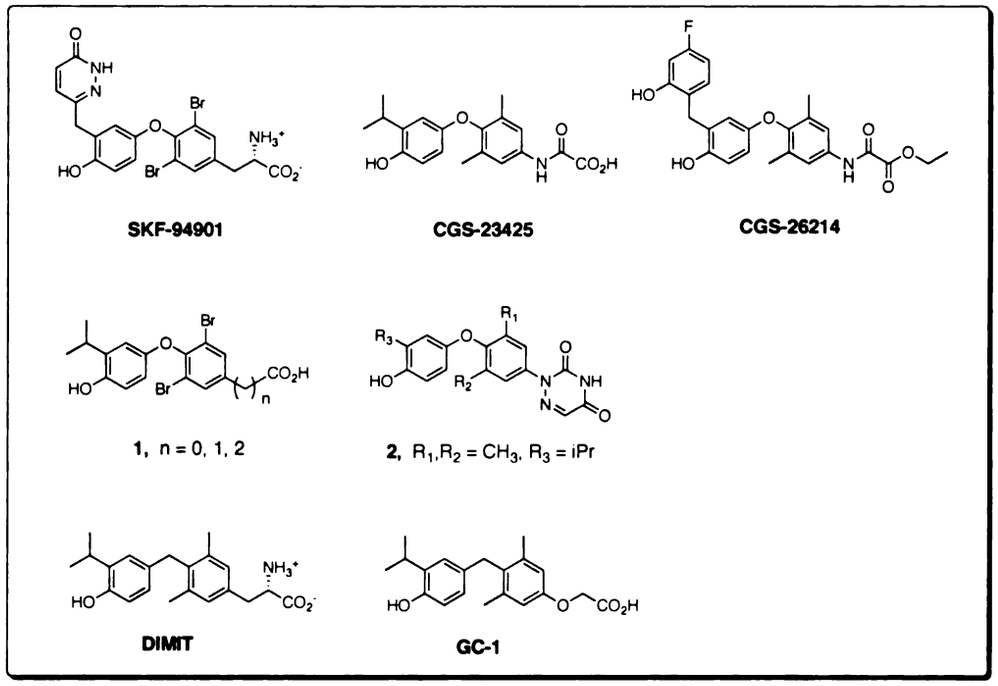

Figure 2-2. Structures of reported TR-β selective thyromimetics.

2.2.2.1 SKF-94901, CGS-23425 & CGS-26214

SKF-94901, a lead compound developed by Smith, Kline & French, is a 3,5-dibromo-L-thyronine analogue (Figure 2-2).[26] In rats, this compound decreases plasma cholesterol concentrations, increases oxygen consumption, and decreases plasma TSH and T_3/T_4. Unlike T_3, **SKF-94901** does not significantly increase heart rate. Such liver-selective and cardiac-sparing properties of **SKF-94901** are due to selective tissue uptake in the liver rather than TR-subtype selective binding and activation. Direct receptor binding assays show **SKF-94901** binds to TRα and TRβ with equal affinity, but has 500-fold weaker affinity relative to T_3. Furthermore, cell uptake experiments show reduced affinity of the drug for heart cytoplasmic binding proteins and efficacy of nuclear transport.

Ciba-Geigy (now Novartis) developed a novel series of halogen-free selective thyromimetics derived from **DIMIT** that contain an oxamic acid side chain at the 1-

position.[26] Of this series, **CGS-26214** and **CGS-23425** were reported to be potent cholesterol-lowering agents devoid of cardiotoxic effects (Figure 2-2). While direct binding data were not obtained for these compounds, **CGS-23425** exhibited $TR\beta_1$-selective activity in transactivation assays of the liver ApoA1 gene. However, the observed liver selectivity of **CGS-26214** is questionable due to conflicting results from tissue-uptake experiments. Novartis recently expanded the oxamic acid series of compounds to include sulfur-bridged and additional 3'-alkyl and aryl derivatives, some of which also have cholesterol-lowering and cardiac-sparing properties.[27]

2.2.2.2 Phenylacetic Acid and 6-Azauracil Derivatives

Karo Bio recently developed thyromimetic compounds with variable carboxylic acid chain lengths at the 1-position.[28] Their results show that TR affinity increased in the order of formic, acetic, and proprionic acid, with the acetic acid 1-position side chain conferring greatest TRβ-selectivity. The lead compound (**1**, n=1) is approximately 10-fold TRβ-selective and exhibited cholesterol-lowering properties with minimal effects on the heart in rats.

Pfizer reported the 6-azauracil thyromimetic **2** that has equal binding affinity relative to T_3 at TRβ and exhibit 8-fold TRβ-selectivity in both binding and transactivation.[29] Co-crystallization of **2** with human $TR\beta_1$ LBD revealed the ionized imide functionality of the 6-azauracil mimics the 1-position amino acid side chain of T_3 to participate in a hydrogen-bond network with receptor residues. Derivatizing the 3'-position of **2** with carboxamido- and sulfonamido-based substituents resulted in thyromimetics with up to 100-fold TRβ-selectivity for binding and functional activation. The biological and therapeutic significance of these compounds remain to be determined.

2.2.2.3 *GC-1*

The Scanlan lab at UCSF designed and synthesized **GC-1**, a halogen-free thyromimetic containing an oxyacetic acid side chain at the 1-position and a methylene bridge linking the aryl rings of the thyronine scaffold.[30,31] The design of **GC-1** was motivated by SAR data and synthetic considerations that would provide an efficient route readily adaptable to a wide variety of **GC-1** analogues.[31-33] **GC-1** is selective for TRβ over TRα in both binding (7-fold) and transactivation potency (20-fold) relative to T_3. Moreover, the **GC-1** binding affinity for TRβ is equivalent to the binding affinity of T_3 in direct binding assays. In cell-based transactivation experiments using a synthetic DR4-containing TRE-driven reporter gene, **GC-1** is a full agonist at TRβ with approximately 5-fold reduced potency compared to that of T_3.

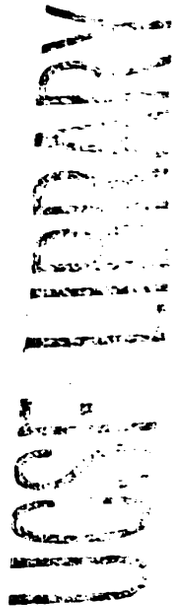

GC-1 has been tested in various animal models to determine its *in vivo* activity. Tadpole metamorphosis is highly dependent on thyroid hormone action through TRα and TRβ, each of which play different roles during the development process in different tissues. TRα mediates limb formation in early stage metamorphosis while TRβ mediates tail and gills resorption at the climax of metamorphosis. Tadpoles treated with **GC-1** displayed little or no limb development but show significant resorption of tail and gills, which correlate with the TRβ selective action of the compound.[34] In hypothyroid mice and hypercholesterolemic rats, **GC-1** had no significant effects on heart rate but effectively lowered serum cholesterol levels and suppressed TSH levels, also consistent with **GC-1** behaving as a TRβ-selective thyromimetic.[35,36] Similarly, cynomolgus monkeys treated with **GC-1** showed significant reduction in body weight and reduction in cholesterol and lipoprotein (a) levels, without induction of tachycardia.[35] Comparison of T_3 and **GC-1** treatment in hypothyroid mice and rats suffering from defective cerebellar development shows differential effects. Defective cerebellar development is

characterized by stunted dendritic branching of Purkinje cells and reduced migration of granule cells. While T_3 affects both processes to promote cerebellar development, **GC-1** partially restores Purkinje cell dendrite density but does not affect granule cell migration, suggesting a role for TRα in the latter process.[7] A study on the effect of **GC-1** on adaptive thermogenesis showed **GC-1** is able to activate the UCP1, but not the β-adrenergic, pathway for thermogenesis, suggesting that the two pathways are mediated by TRβ and TRα, respectively.[37]

The X-ray crystal structure of **GC-1** bound to the TRβ-LBD has been solved and provides clues to the TRβ selectivity of the compound. **GC-1** binds TR in much the same way as T_3 and Triac (Figure 1-2).[38] However, the hydrogen-bond network of charged and polar residues around the 1-position oxyacetic acid side chain is more extensive from that observed in TRα and TRβ complexes with other ligands. Asparagine 331 of TRβ (corresponding to serine 277 in TRα), the single amino acid difference in the ligand binding pocket between the receptor subtypes, participates in this hydrogen-bonding network and provides a structural rationale for **GC-1**'s selectivity. In fact, swapping the residues between TRα and TRβ (mutant TRβ-N331S and mutant TRα-S277N) leads to a reversal of activity towards **GC-1** where **GC-1** selectively binds and activates the mutant TRα–S277N receptor.[21] Analysis of the chemical features of **GC-1** further confirms that the oxyacetic acid side chain confers selective binding to TRβ.[39]

2.2.3 Selective TR Modulators: Antagonists

In addition to being useful pharmacological probes for studying thyroid hormone signaling, selective T_3 antagonists may have clinical utility in the treatment of hyperthyroid patients or atrial fibrillations in normal patients.[40] As mentioned previously, current therapies for hyperthyroidism usually require weeks before symptoms are relieved or provide only partial relief. Direct blockade of T_3 action with T_3 antagonists at

the receptor level would bypass such complications and provide a more effective treatment of hyperthyroidism.

The active metabolite (desethylamiodarone, Figure 2-3) of the cardiac anti-arrhythmic agent amiodarone has been reported to have antithyroid effects *in vitro*, but has not been shown to be a true T_3 antagonist in cell culture or in animals.[41-45] Both amiodarone and desethylamiodarone have low affinity for TR and a slow onset of action with serious liver toxicity;[46] therefore, these compounds are not ideal drug therapies. The recently reported dronerarone, a halogen-free derivative of amiodarone, acts as a TRα-selective inhibitor of *in vitro* T_3 binding via its metabolite debutyldronedarone.[47] Dronerarone has selective effects on lengthening QTc intervals in rat hearts without significant effects on cholesterol and LDL levels. However, its utility in the clinics is yet to be determined.

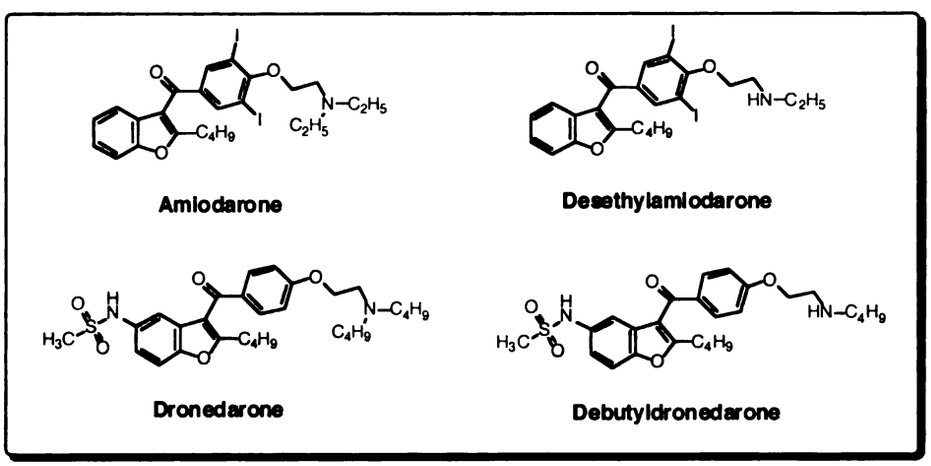

Figure 2-3. Structures of anti-arrhythmic agents with anti-thyroid effects.

2.2.3.1 Antagonist Design: "Extension Hypothesis"

The development of T_3 antagonists is in its infancy with only a handful of antagonists having moderate to weak potency reported to date. The general strategy for designing NR antagonists has been based on the "extension hypothesis", as illustrated in Figure 2-4.[40,48] Comparison of crystal structures of various liganded NR LBDs show

that the ligand plays a structural role in completing the hydrophobic core of the active NR conformer. Residues from H3, H5, and H12 comprise the coactivator binding surface, where H12 is relatively mobile in the absence of ligand. Upon ligand binding, H12 undergoes rearrangement and is locked into an active conformation to reveal the coactivator binding surface. Based on this mode of ligand-regulated activation, the extension hypothesis suggests antagonists could be generally obtained by mimicking an agonist scaffold for high-affinity binding, but also contain bulky extension groups at key positions to effectively perturb proper folding of H12 and disrupt formation of the coactivator binding surface. The validity of the extension hypothesis was also reinforced by the observation that antagonists for several classes of nuclear receptors had "extensions" relative to comparable agonists.

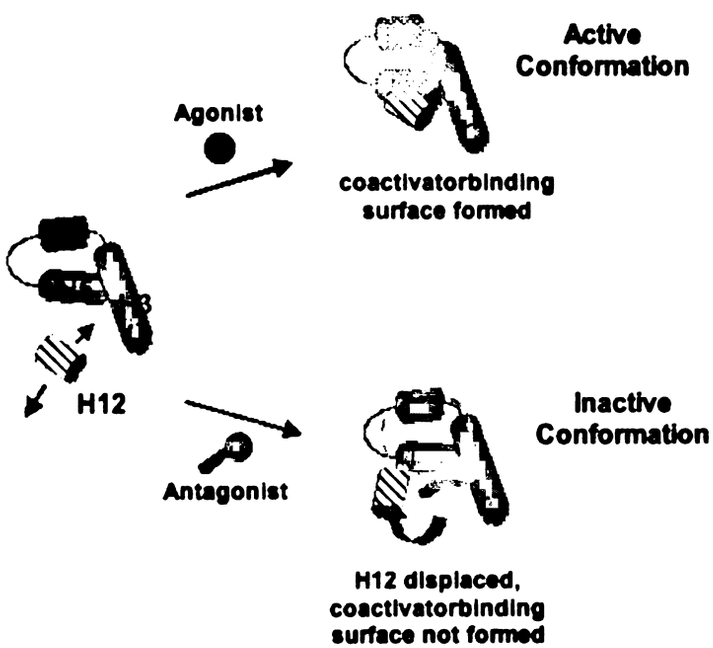

Figure 2-4. The "Extension Hypothesis". T_3 promotes packing of H12 in the agonist conformation where the coactivator binding surface is revealed. By contrast, a T_3-like ligand with a large extension that protrudes toward H12 should prevent appropriate H12 packing and inhibit formation of the coactivator binding surface.

The first generation TR antagonists **DIBRT**, **HY-4** and **GC-14** (Figure 2-5) were designed based on first principles applying the "extension hypothesis". **DIBRT** was derived from the agonist **MIBRT** (3,5-dibromo-4-(3'-isopropyl-4'-hydroxyphenoxy) benzoic acid), while **HY-4** and **GC-14** were based on the TRβ-selective **GC-1** agonist. Recent efforts towards rational discovery of antagonists utilized computer models of TR structures and virtual screening of compound libraries to identify a number of lead compounds, such as **1-850** (Figure 2-5), that also satisfy the "extension" requirement.

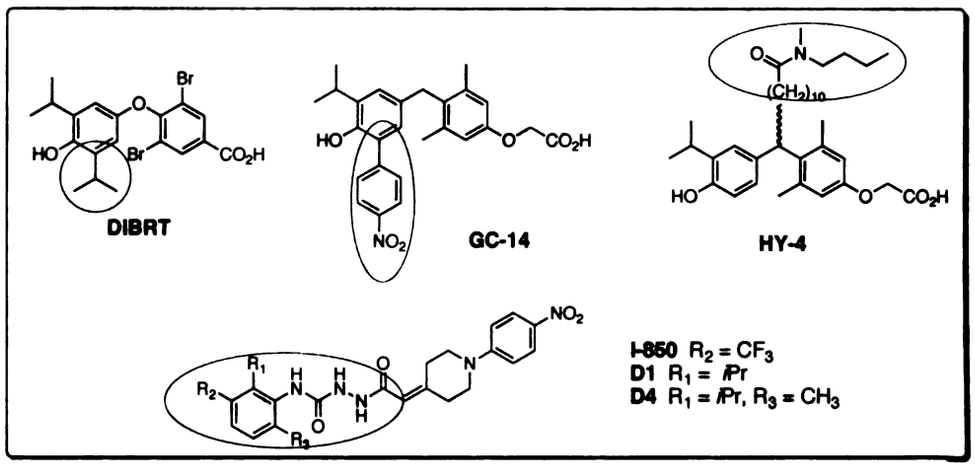

Figure 2-5. Structures of reported thyroid hormone antagonists. The portions circled in red are the "extension" groups protruding from the agonist scaffold.

2.2.3.2 1-850

In silico modeling of the antagonist-bound conformation of TRβ-LBD[49,50] was built by homology to the raloxifene-bound ERα-LBD where the C-terminal helix H12 is docked in the coactivator recruitment site.[51,52] The model was used to screen a library of >250,000 commercially available compounds and successfully identified fourteen compounds that antagonized the effect of T_3 on TR with IC_{50} values ranging from 1.5 μM to 30 μM. Of these, compound **1-850** and its derivatives **D1** and **D4** (Figure 2-5) have the greatest binding affinity and antagonistic efficacy.[50] For example, 20 μM of **1-850** blocked 90% of 6 nM T_3-induced transactivation of an IP-driven reporter gene while 5

μM of **D4** resulted in 84% inhibition. Despite the lack of structural and chemical similarity between **1-850** and T_3, the compound superimposes well with the crystal structure of bound T_3. However, **1-850** also presents an additional extension that would clash with the active conformation of H12. Consequently these compounds failed to recruit coactivator and blocked T_3-induced coactivator recruitment in GST-pulldown assays.

2.2.3.3 HY-4

The antagonist **HY-4** contains the **GC-1** agonist core structure bearing a long alkylamide extension analogous to the pure estrogen receptor (ER) antagonist ICI-164384 (ICI) at the bridging methylene position of **GC-1** (Figure 2-5).[53] Modeling of ICI based on the ERα LBD structure bound to estradiol (E_2)[51] suggested the ICI extension would project out towards helix H8 and the beta sheets, opposite of the raloxifene extension towards H12.[54] Superposition of the ICI-ER modeled structure to that of the liganded TR LBD[24] revealed substitution at the bridging atom of T_3 would allow the extension to point in a direction analogous to the antagonistic side chain of ICI. Subsequent solution of the ERβ-LBD co-crystallized with ICI[55] showed that the E_2 core of ICI adopted a flipped orientation and the antagonist side chain displaces H12 in the same manner as other antagonist extensions. Despite this faulty design of **HY-4** to perturb H12 folding for antagonism, the compound was able to inhibit 300 pM T_3-induced transactivation in DR4-driven reporter gene assays with IC_{50} of approximately 2 μM. Alone, **HY-4** failed to activate TR-mediated transcription even at 10 μM concentration. **HY-4** showed little TR-subtype selectivity, with >1000-fold weaker binding affinity relative to T_3.

2.2.3.4 DIBRT & GC-14

Crystallographic analysis of agonist-bound TR suggests the 5'-position points towards a loop between helices H11 and H12 of the LBD. Thus, an extension at this position may impair folding of H12 and prevent formation of the coactivator-binding surface. Antagonists **DIBRT** and **GC-14** contain extensions at the 5'-position with the aim of displacing of H12. **DIBRT** (Figure 2-5) is a T_3 antagonist based on **MIBRT**, a thyromimetic with a carboxylic acid group at the 1-position.[56] **DIBRT** contains an additional hydrophobic isopropyl appendage at the 5'-position. It has comparable micromolar affinities for both TRα and TRβ and is able to antagonize T_3-regulated responses at both positive (DR4-type) and negative (TSHβ promoter) TREs. In addition, T_3-induced association between TR and coactivator GRIP-1 is inhibited by **DIBRT** in GST-pulldown assays.

The antagonist **GC-14** is based on the agonist **GC-1** and bears a 4-nitrophenyl extension group at the 5'-position (Figure 2-5).[32] Similar to **GC-1**, **GC-14** is selective for TRβ in binding affinity and antagonist potency. It has K_D values of 220±60 nM and 35±12 nM for TRα and TRβ, respectively. In transactivation assays using a DR4-driven reporter, **GC-14** shows maximal activation of 35% compared to saturating T_3 for TRα and 18% for TRβ. In competition assays, 10 μM **GC-14** was able to inhibit transactivation induced by 1 nM T_3 down to the level of **GC-14** alone. Thus, **GC-14** has a mixed agonist/antagonist profile. Structure-activity relationship (SAR) data for a series of 5'-phenyl **GC-1** derivatives underscore the significance of the *para*-nitro substitution on the aryl ring for conferring antagonistic activity; other analogs in this series displayed partial or full agonist activities.[32]

2.3 Conclusions

The phenotypes observed from TR transgenic models provide an indirect measure of the physiological roles of the TR isoforms, which are generally consistent with their roles contemplated from tissue expression profiling. Interpretation of the transgenic phenotypes to delineate TR function is limited by the possibility of a redundant system in which the intact TRα or TRβ can partially compensate for the inactivated gene.

Recent progress in the development of selective thyroid hormone agonists and antagonists has provided a chemical handle for modulating hormone signaling and understanding TR function. The most extensively studied TRβ subtype-selective thyromimetic **GC-1** has been useful to identify tissue-specific activities of TRβ in various animal models that lend further support to the activities identified in the transgenic models. These results validate the usefulness of selective analogues as pharmacological probes to delineate the roles of the TR isoforms. The weak potencies of reported T_3 antagonists **I-850**, **DIBRT**, **HY-4**, and **GC-14** have limited their usefulness and characterization *in vivo*. Further research to develop potent TR-subtype selective T_3 antagonists will be instrumental in our understanding of thyroid hormone action and reveal new therapeutic opportunities for treatment of thyroid-hormone related diseases.

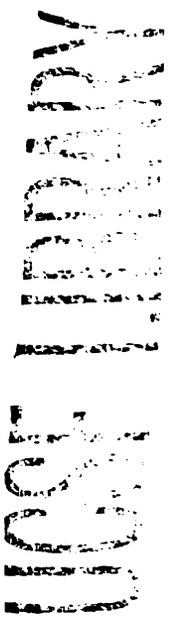

2.4 References

(1) Brent, G. A. Tissue-specific actions of thyroid hormone: insights from animal models. *Rev Endocr Metab Disord* **2000**, *1*, 27-33.

(2) Flamant, F.; Samarut, J. Thyroid hormone receptors: lessons from knockout and knock-in mutant mice. *Trends Endocrinol Metab* **2003**, *14*, 85-90.

(3) Hsu, J. H.; Brent, G. A. Thyroid hormone receptor gene knockouts. *TEM* **1998**, *9*, 103-112.

(4) Fraichard, A.; Chassande, O.; Plateroti, M.; Roux, J. P.; Trouillas, J. et al. The T3R alpha gene encoding a thyroid hormone receptor is essential for post-natal development and thyroid hormone production. *Embo J* **1997**, *16*, 4412-4420.

(5) Macchia, P. E.; Takeuchi, Y.; Kawai, T.; Cua, K.; Gauthier, K. et al. Increased sensitivity to thyroid hormone in mice with complete deficiency of thyroid hormone receptor alpha. *Proc Natl Acad Sci U S A* **2001**, *98*, 349-354.

(6) Plateroti, M.; Chassande, O.; Fraichard, A.; Gauthier, K.; Freund, J. N. et al. Involvement of T3Ralpha- and beta-receptor subtypes in mediation of T3 functions during postnatal murine intestinal development. *Gastroenterology* **1999**, *116*, 1367-1378.

(7) Morte, B.; Manzano, J.; Scanlan, T.; Vennstrom, B.; Bernal, J. Deletion of the thyroid hormone receptor alpha 1 prevents the structural alterations of the cerebellum induced by hypothyroidism. *Proc Natl Acad Sci U S A* **2002**, *99*, 3985-3989.

(8) Wikstrom, L.; Johansson, C.; Salto, C.; Barlow, C.; Campos Barros, A. et al. Abnormal heart rate and body temperature in mice lacking thyroid hormone receptor alpha 1. *Embo J* **1998**, *17*, 455-461.

(9) Salto, C.; Kindblom, J. M.; Johansson, C.; Wang, Z.; Gullberg, H. et al. Ablation of TRalpha2 and a concomitant overexpression of alpha1 yields a mixed hypo- and hyperthyroid phenotype in mice. *Mol Endocrinol* **2001**, *15*, 2115-2128.

(10) Johansson, C.; Gothe, S.; Forrest, D.; Vennstrom, B.; Thoren, P. Cardiovascular phenotype and temperature control in mice lacking thyroid hormone receptor-beta or both alpha1 and beta. *Am J Physiol* **1999**, *276*, H2006-2012.

(11) Gullberg, H.; Rudling, M.; Forrest, D.; Angelin, B.; Vennstrom, B. Thyroid hormone receptor beta-deficient mice show complete loss of the normal cholesterol 7alpha-hydroxylase (CYP7A) response to thyroid hormone but display enhanced resistance to dietary cholesterol. *Mol Endocrinol* **2000**, *14*, 1739-1749.

(12) Abel, E. D.; Boers, M. E.; Pazos-Moura, C.; Moura, E.; Kaulbach, H. et al. Divergent roles for thyroid hormone receptor beta isoforms in the endocrine axis and auditory system. *J Clin Invest* **1999**, *104*, 291-300.

(13) Abel, E. D.; Kaulbach, H. C.; Campos-Barros, A.; Ahima, R. S.; Boers, M. E. et al. Novel insight from transgenic mice into thyroid hormone resistance and the regulation of thyrotropin. *J Clin Invest* **1999**, *103*, 271-279.

(14) Forrest, D.; Hanebuth, E.; Smeyne, R. J.; Everds, N.; Stewart, C. L. et al. Recessive resistance to thyroid hormone in mice lacking thyroid hormone receptor beta: evidence for tissue-specific modulation of receptor function. *Embo J* **1996**, *15*, 3006-3015.

(15) Gauthier, K.; Chassande, O.; Plateroti, M.; Roux, J. P.; Legrand, C. et al. Different functions for the thyroid hormone receptors TRalpha and TRbeta in the control of thyroid hormone production and post-natal development. *Embo J* **1999**, *18*, 623-631.

(16) Gothe, S.; Wang, Z.; Ng, L.; Kindblom, J. M.; Barros, A. C. et al. Mice devoid of all known thyroid hormone receptors are viable but exhibit disorders of the pituitary-thyroid axis, growth, and bone maturation. *Genes Dev* **1999**, *13*, 1329-1341.

(17) Nagaya, T.; Madison, L. D.; Jameson, J. L. Thyroid hormone receptor mutants that cause resistance to thyroid hormone. Evidence for receptor competition for DNA sequences in target genes. *J Biol Chem* **1992**, *267*, 13014-13019.

(18) Jameson, J. L. Mechanisms by which thyroid hormone receptor mutations cause clinical syndromes of resistance to thyroid hormone. *Thyroid* **1994**, *4*, 485-492.

(19) Hashimoto, K.; Curty, F. H.; Borges, P. P.; Lee, C. E.; Abel, E. D. et al. An unliganded thyroid hormone receptor causes severe neurological dysfunction. *Proc Natl Acad Sci U S A* **2001**, *98*, 3998-4003.

(20) Chassande, O. Do unliganded thyroid hormone receptors have physiological functions? *J Mol Endocrinol* **2003**, *31*, 9-20.

(21) Baxter, J. D.; Dillmann, W. H.; West, B. L.; Huber, R.; Furlow, J. D. et al. Selective modulation of thyroid hormone receptor action. *J Steroid Biochem Mol Biol* **2001**, *76*, 31-42.

(22) Jorgenson, E. C. Thyroid hormones. *Hormonal Proteins and Peptides*; Academic Press: New York, 1978.

(23) Dietrich, S. W.; Bolger, M. B.; Kollman, P. A.; Jorgenson, E. C. Thyroxine analogues. 23. Quantitative structure-activity correlation studies of in vivo and in vitro thyromimetic activities. *J Med Chem* **1977**, *20*, 863-880.

(24) Wagner, R. L.; Apriletti, J. W.; McGrath, M. E.; West, B. L.; Baxter, J. D. et al. A structural role for hormone in the thyroid hormone receptor. *Nature* **1995**, *378*, 690-697.

(25) Borngraeber, S.; Budny, M. J.; Chiellini, G.; Cunha-Lima, S. T.; Togashi, M. et al. Ligand selectivity by seeking hydrophobicity in thyroid hormone receptor. *Proc Natl Acad Sci U S A* **2003**, *100*, 15358-15363.

(26) Scanlan, T. S.; Yoshihara, H. A.; Nguyen, N. H.; Chiellini, G. Selective thyromimetics: tissue-selective thyroid hormone analogs. *Curr Opin Drug Discov Devel* **2001**, *4*, 614-622.

(27) Stanton, J. L.; Cahill, E.; Dotson, R.; Tan, J.; Tomaselli, H. C. et al. Synthesis and biological activity of phenoxyphenyl oxamic acid derivatives related to L-thyronine. *Bioorg Med Chem Lett* **2000**, *10*, 1661-1663.

(28) Ye, L.; Li, Y. L.; Mellstrom, K.; Mellin, C.; Bladh, L. G. et al. Thyroid receptor ligands. 1. Agonist ligands selective for the thyroid receptor beta1. *J Med Chem* **2003**, *46*, 1580-1588.

(29) Dow, R. L.; Schneider, S. R.; Paight, E. S.; Hank, R. F.; Chiang, P. et al. Discovery of a novel series of 6-azauracil-based thyroid hormone receptor ligands: potent, TR beta subtype-selective thyromimetics. *Bioorg Med Chem Lett* **2003**, *13*, 379-382.

(30) Chiellini, G.; Apriletti, J. W.; Yoshihara, H. A.; Baxter, J. D.; Ribeiro, R. C. et al. A high-affinity subtype-selective agonist ligand for the thyroid hormone receptor. *Chem Biol* **1998**, *5*, 299-306.

(31) Chiellini, G.; Nguyen, N. H.; Yoshihara, H. A.; Scanlan, T. S. Improved synthesis of the iodine-free thyromimetic GC-1. *Bioorg Med Chem Lett* **2000**, *10*, 2607-2611.

(32) Chiellini, G.; Nguyen, N. H.; Apriletti, J. W.; Baxter, J. D.; Scanlan, T. S. Synthesis and biological activity of novel thyroid hormone analogues: 5'-aryl substituted GC-1 derivatives. *Bioorg Med Chem* **2002**, *10*, 333-346.

(33) Yoshihara, H. A.; Chiellini, G.; Mitchison, T. J.; Scanlan, T. S. An efficient substitution reaction for the preparation of thyroid hormone analogues. *Bioorg Med Chem* **1998**, *6*, 1179-1183.

(34) Furlow, J. D.; Yang, H. Y.; Hsu, M.; Lim, W.; Ermio, D. J. et al. Induction of larval tissue resorption in Xenopus laevis tadpoles by the thyroid hormone receptor agonist GC-1. *J Biol Chem* **2004**, *279*, 26555-26562.

(35) Grover, G. J.; Egan, D. M.; Sleph, P. G.; Beehler, B. C.; Chiellini, G. et al. Effects of the thyroid hormone receptor agonist GC-1 on metabolic rate and cholesterol in rats and primates: selective actions relative to 3,5,3'-triiodo-L-thyronine. *Endocrinology* **2004**, *145*, 1656-1661.

(36) Trost, S. U.; Swanson, E.; Gloss, B.; Wang-Iverson, D. B.; Zhang, H. et al. The thyroid hormone receptor-beta-selective agonist GC-1 differentially affects plasma lipids and cardiac activity. *Endocrinology* **2000**, *141*, 3057-3064.

(37) Ribeiro, M. O.; Carvalho, S. D.; Schultz, J. J.; Chiellini, G.; Scanlan, T. S. et al. Thyroid hormone--sympathetic interaction and adaptive thermogenesis are thyroid hormone receptor isoform--specific. *J Clin Invest* **2001**, *108*, 97-105.

(38) Wagner, R. L.; Huber, B. R.; Shiau, A. K.; Kelly, A.; Cunha Lima, S. T. et al. Hormone selectivity in thyroid hormone receptors. *Mol Endocrinol* **2001**, *15*, 398-410.

(39) Yoshihara, H. A.; Apriletti, J. W.; Baxter, J. D.; Scanlan, T. S. Structural determinants of selective thyromimetics. *J Med Chem* **2003**, *46*, 3152-3161.

(40) Webb, P.; Nguyen, N. H.; Chiellini, G.; Yoshihara, H. A.; Cunha Lima, S. T. et al. Design of thyroid hormone receptor antagonists from first principles. *J Steroid Biochem Mol Biol* **2002**, *83*, 59-73.

(41) Hudig, F.; Bakker, O.; Wiersinga, W. M. Amiodarone-induced hypercholesterolemia is associated with a decrease in liver LDL receptor mRNA. *FEBS Lett* **1994**, *341*, 86-90.

(42) Bakker, O.; van Beeren, H. C.; Wiersinga, W. M. Desethylamiodarone is a noncompetitive inhibitor of the binding of thyroid hormone to the thyroid hormone beta 1-receptor protein. *Endocrinology* **1994**, *134*, 1665-1670.

(43) van Beeren, H. C.; Bakker, O.; Wiersinga, W. M. Desethylamiodarone is a competitive inhibitor of the binding of thyroid hormone to the thyroid hormone alpha 1-receptor protein. *Mol Cell Endocrinol* **1995**, *112*, 15-19.

(44) van Beeren, H. C.; Bakker, O.; Wiersinga, W. M. Desethylamiodarone interferes with the binding of co-activator GRIP-1 to the beta 1-thyroid hormone receptor. *FEBS Lett* **2000**, *481*, 213-216.

(45) Martino, E.; Bartalena, L.; Bogazzi, F.; Braverman, L. E. The effects of amiodarone on the thyroid. *Endocr Rev* **2001**, *22*, 240-254.

(46) Morse, R. M.; Valenzuela, G. A.; Greenwald, T. P.; Eulie, P. J.; Wesley, R. C. et al. Amiodarone-induced liver toxicity. *Ann Intern Med* **1988**, *109*, 838-840.

(47) Van Beeren, H. C.; Jong, W. M.; Kaptein, E.; Visser, T. J.; Bakker, O. et al. Dronerarone acts as a selective inhibitor of 3,5,3'-triiodothyronine binding to thyroid hormone receptor-alpha1: in vitro and in vivo evidence. *Endocrinology* **2003**, *144*, 552-558.

(48) Ribeiro, R. C.; Apriletti, J. W.; Wagner, R. L.; West, B. L.; Feng, W. et al. Mechanisms of thyroid hormone action: insights from X-ray crystallographic and functional studies. *Recent Prog. Horm. Res.* **1998**, *53*, 351-392.

(49) Schapira, M.; Raaka, B. M.; Samuels, H. H.; Abagyan, R. Rational discovery of novel nuclear hormone receptor antagonists. *Proc Natl Acad Sci U S A* **2000**, *97*, 1008-1013.

(50) Schapira, M.; Raaka, B. M.; Das, S.; Fan, L.; Totrov, M. et al. Discovery of diverse thyroid hormone receptor antagonists by high-throughput docking. *Proc Natl Acad Sci U S A* **2003**, *100*, 7354-7359.

(51) Brzozowski, A. M.; Pike, A. C.; Dauter, Z.; Hubbard, R. E.; Bonn, T. et al. Molecular basis of agonism and antagonism in the oestrogen receptor. *Nature* **1997**, *389*, 753-758.

(52) Darimont, B. D.; Wagner, R. L.; Apriletti, J. W.; Stallcup, M. R.; Kushner, P. J. et al. Structure and specificity of nuclear receptor-coactivator interactions. *Genes Dev* **1998**, *12*, 3343-3356.

(53) Yoshihara, H. A.; Apriletti, J. W.; Baxter, J. D.; Scanlan, T. S. A designed antagonist of the thyroid hormone receptor. *Bioorg Med Chem Lett* **2001**, *11*, 2821-2825.

(54) Yoshihara, H. A.; Nguyen, N. H.; Scanlan, T. S. Design and synthesis of receptor ligands. *Methods Enzymol* **2003**, *364*, 71-91.

(55) Pike, A. C.; Brzozowski, A. M.; Walton, J.; Hubbard, R. E.; Thorsell, A. G. et al. Structural insights into the mode of action of a pure antiestrogen. *Structure (Camb)* **2001**, *9*, 145-153.

(56) Baxter, J. D.; Goede, P.; Apriletti, J. W.; West, B. L.; Feng, W. et al. Structure-based design and synthesis of a thyroid hormone receptor (TR) antagonist. *Endocrinology* **2002**, *143*, 517-524.

Chapter 3

Development of a Potent Novel Thyroid Hormone Antagonist: *in vitro* and *in vivo* Characterization of NH-3

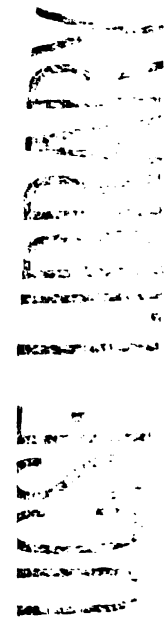

Compared to steroid ligands for nuclear receptors, T_3 analogue chemistry is relatively unexplored. Previous studies have primarily focused on structure-activity relationships (SAR) of T_3.[1,2] These results have aided the development of numerous selective TR modulators (STRMs) that have tissue- and/or receptor subtype-specific thyromimetic activity to obtain the beneficial effects of T_3, such as reduction of weight or cholesterol levels, without inducing the undesired cardiac side effects.[3] In contrast, development of thyroid hormone antagonists has been limited. To date, only a handful of T_3 antagonists have been reported,[4-6] including **GC-14** (Figure 3-1). These compounds have relatively weak binding affinity and low potency, limiting their use as potential therapeutic agents and chemical probes to understand thyroid hormone signaling pathways. The goal of the current study is to develop more potent selective T_3 antagonists that could be used as pharmacological tools for inducing TR inactivation in *in vitro* and *in vivo* systems.

We report a novel thyroid hormone antagonist **NH-3** (Figure 3-1), based on the halogen-free thyromimetic **GC-1**, that has improved efficacy and potency compared to **GC-14**. **NH-3** is a second-generation **GC-1** derivative containing a 5'-*p*-nitrophenylethynyl extension. One mechanism for antagonism appears to be the ability of **NH-3** to block TR-coactivator interactions. Furthermore, **NH-3** is the first T_3 antagonist to exhibit potent antagonism *in vivo*.

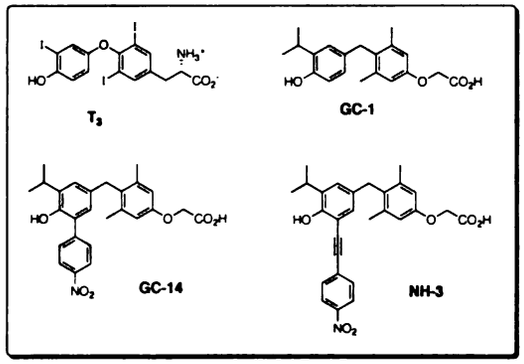

Figure 3-1. Chemical structures of thyroid hormone (T_3), thyromimetic GC-1, and antagonists GC-14 and NH-3.

3.1 Design and Synthesis of NH-3

3.1.1 Applying the Extension Hypothesis and SAR Data

The design of **NH-3** paralleled that of other thyroid hormone antagonists in applying the "extension hypothesis"[7,8] (Figure 2-4) combined with crystallographic data of human (h) TRβ LBD bound to an agonist ligand.[9-11] As mentioned previously, the C-terminal portion of the LBD corresponding to helix 12 (H12) appears to act as a molecular switch that packs against the body of the receptor upon agonist binding to close the ligand binding pocket and complete formation of a putative coactivator binding surface.[12] The X-ray structure reveals the 5'-position of the ligand oriented in the direction of the loop between helices H11 and H12. Thus, extensions of the thyronine scaffold at the 5'-position should perturb the packing of H12 and result in a disrupted coactivator binding surface.

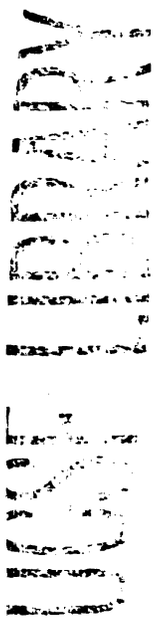

Numerous analogues containing 5'-alkyl and aryl substituents have been synthesized but only a handful of compounds, including **GC-14**, exhibited some antagonistic activity.[4,5] The majority of the 5'-analogues were agonists, suggesting that either the 5'-extensions employed were not large enough to perturb H12, or that the potential interactions between ligand and receptor that stabilize an inactive conformation had not been realized. **GC-14** also exhibited partial agonist activity, which we postulate might be due to flexibility of the 5'-aryl substitution that would still allow formation of the coactivator-binding surface. Previous studies have shown that the antagonist activity of **GC-14** requires the 5'-aryl nitro ($-NO_2$) group specifically in the *para*-position.[5] Positional isomers of **GC-14** in the *ortho*- and *meta*-positions, and isosteres of **GC-14** with carboxylic acid and amino substitutions exhibited agonistic properties, suggesting the nitro group may be involved in key stereo-electronic interactions with the receptor to stabilize an inactive conformation.

nitro group may be involved in key stereo-electronic interactions with the receptor to stabilize an inactive conformation.

Taking these factors into consideration, **NH-3** employed an ethynyl group to rigidly link the 5'-*p*-nitroaryl extension to the **GC-1** agonist scaffold. We hypothesize that increasing the length and rigidity of the 5'-extension would allow more effective perturbation of H12 and eliminate the observed partial agonist activity of **GC-14**.

3.1.2 Improved Synthesis of the Iodine-Free Thyromimetic GC-1[13]

The original synthesis of **GC-1**[14] to form the diarylmethane structure encountered synthetic challenges that limited production of **GC-1** in multi-gram quantities and adaptation for the synthesis of **GC-1** derivatives. Thus, it was necessary to optimize the synthesis of **GC-1** before pursuing analogue chemistry.

The improved synthesis of **GC-1** is outlined in Scheme 3-1.[13] The two aryl halves of **GC-1** are constructed first and the phenols are differentiated at this stage with different protecting groups. For the B-aryl ring half, 4-bromo-2-isopropylphenol is converted to the corresponding methoxymethyl ether **1** by treatment of the phenoxide with chloromethyl methyl ether (MOM-Cl). For the A-ring half the 4-bromo-3,5-dimethylphenol is treated with triisopropylsilylchloride (TiPS-Cl) to provide the triisopropylsilyl ether **2**, which is subsequently formylated via lithium-halogen exchange followed by treatment with dimethylformamide to provide aldehyde **3**. Bromide **1** and aldehyde **3** are then coupled via addition of *n*-butyllithium to give the biaryl alcohol **4**. Hydrogenolysis of alcohol **4** provides the biarylmethane compound **5**. Subsequent treatment with tetrabutylammonium fluoride (TBAF) allows selective removal of the phenolic silyl ether protecting group to yield the free phenol, which is then mono-alkylated using α-chloro-*t*-butyl acetate to give mono-ester **6**. **GC-1** is then obtained from **6** by removal of the methoxymethyl phenolic protecting group under acidic

conditions, followed by basic saponification of the *t*-butyl ester. Although *t*-butyl esters are usually hydrolyzed under acidic conditions, we found that hydrolysis with base resulted in less decomposition and higher chemical yields for this step.

The improved route provides **GC-1** in 22% overall yield from 4-bromo-3,5-dimethylphenol, compared to a 7% yield of **GC-1** in the original synthesis. In addition to improving synthetic efficiency, the differentiated phenol protecting groups offer a chemical handle for selective modification of the thyronine skeleton to produce new derivatives. The methoxymethyl protecting group can be used to direct *ortho*-metalation chemistry leading to derivatization of the 5'-position.

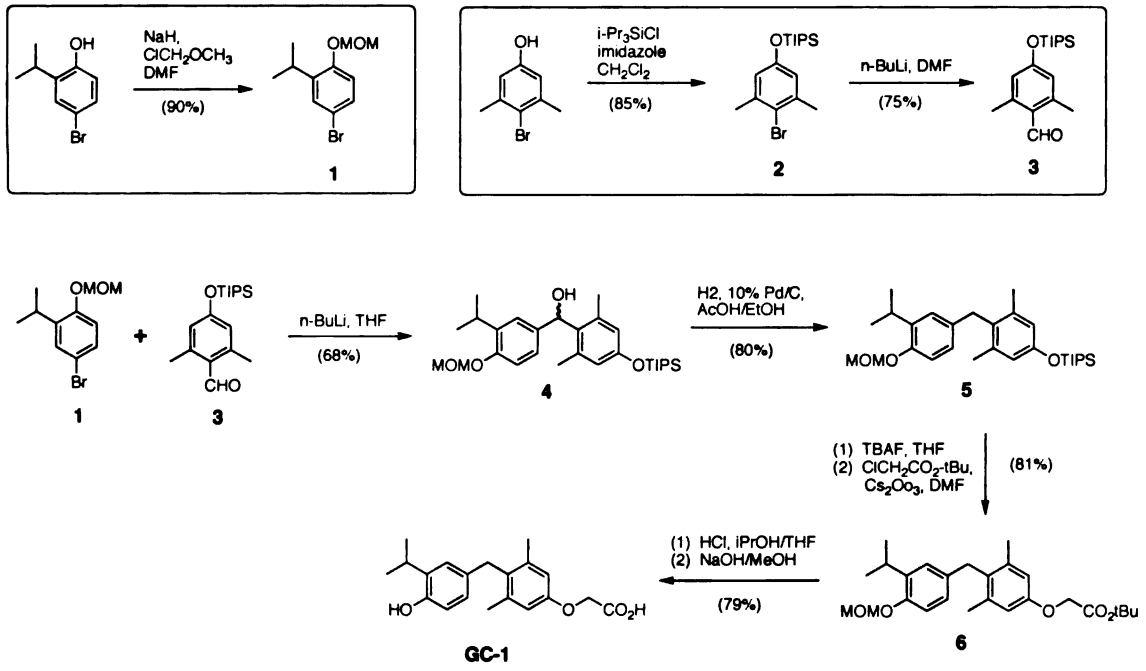

Scheme 3-1. Improved synthetic route for the preparation of GC-1. See Appendix A.

3.1.3 5'-Derivatization via Palladium Catalyzed Chemistry

Palladium (Pd)-catalyzed coupling of an organo-halide and an organo-metal is a useful tool in organic chemistry to form carbon-carbon (C-C) bonds through exchange of the coupling partners.[15,16] Various Pd-catalyzed Suzuki[17,18] and Sonogashira[19-23] conditions were tried to couple ethynylbenzene to the 5'-position of the **GC-1** scaffold, as

summarized in Table 3-1. Combinations of halide and boronate coupling partners were used. Formation of the 5'-halogenated **GC-1** intermediate **7** was achieved by *ortho*-metalation of biarylmethane intermediate **5** with *n*-BuLi followed by *in situ* halogenation with N-iodosuccinimide (NIS) or N-bromosuccinimide (NBS) in a 2:1 THF/hexanes solvent mixture (Scheme 3-2, see Appendix A). Trapping the lithiated intermediate with NIS or NBS generally resulted in a 50-60% conversion to the halogenated species, which could not be isolated from the intermediate **5** by standard silica gel chromatography. Use of other iodinating agents such as iodine, iodine monochloride, and activated iodonium sources resulted in lower yields with decomposition of starting material. Therefore, the mixture of compounds was carried through to the coupling reaction, where separation of the coupled product and intermediate **5** was achieved. Synthesis of the 5'-boronic acid **GC-1** intermediate **8** also requires *ortho*-metalation with *n*-BuLi followed by trapping with triisopropylborate and acid hydrolysis (Scheme 3-2).[5] Complete conversion to the boronic acid was achieved in 75%-85% crude yield without further purification.

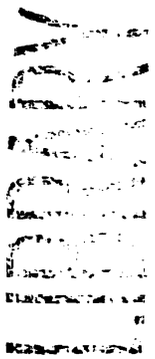

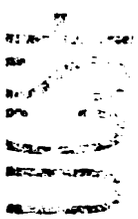

The greatest coupling yield was obtained with 5'-iodinated **GC-1** intermediate **7** and phenylethynyl boronate following the Suzuki-Miyaura procedure described by Soderquist et al. (Table 3-1, Entry 7).[18] Coupling reactions with bromides were unsuccessful due to the lower reactivity of bromides relative to iodides in palladium chemistry (Table 3-1, Entries 1-4). Switching the iodide and boronate coupling partners where a 5'-boronic acid **GC-1** intermediate is coupled with 4-ethynyl-1-iodobenzene using various palladium catalysts gave no reaction (Table 3-1, Entry 9). Suzuki coupling conditions were more suitable for this system compared to Sonogashira conditions, which generally resulted in low yields and/or decomposition of starting material (Table 3-1, Entries 5, 6, and 8).

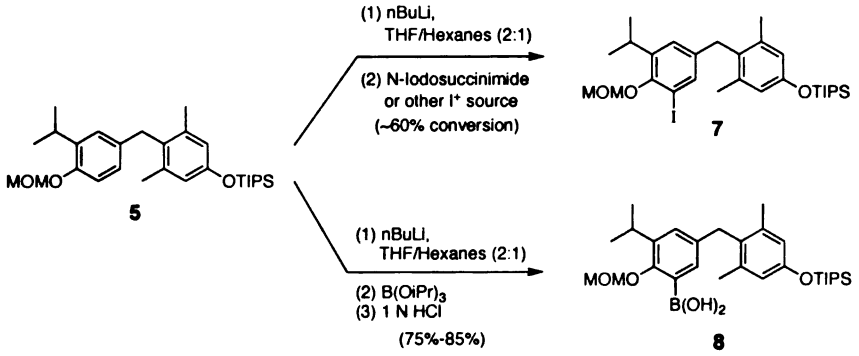

Scheme 3-2. Preparation of 5'-halogenated or 5'-boronic acid GC-1 derivatives. See Appendix A.

Table 3-1. Optimization of Suzuki and Sonogashira coupling for the synthesis of 5'-phenylethynyl GC-1 derivatives.

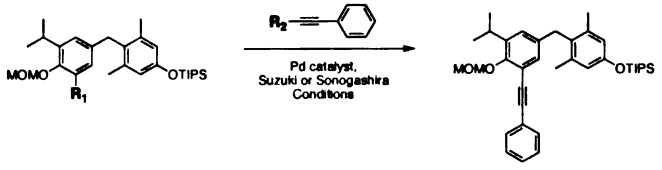

Entry	R_1	R_2	Conditions	Yield	Ref
1	-Br	-H	$PdCl_2(PPh_3)_2$ (0.01 eq), CuI (0.02 eq), iPr_2NH, DMF; 100°C 2h, rt. overnight	Decomp.	[19]
2	-Br	-H	$Pd(dba)_3CHCl_3$ (0.05 eq), CuI (0.10 eq), Et_2NH, DMF; 100°C 3 h, rt, overnight	Decomp.	[19]
3	-Br	-H	$Pd(dba)_3CHCl_3$ (0.05 eq), CuI (0.10 eq), PPh_3 (0.40 eq), piperidine; rt, overnight	Decomp.	[17]
4	-Br	-H	$Pd(dba)_3CHCl_3$ (0.05 eq), CuI (0.012 eq), PPh_3 (0.025 eq), piperidine/THF; 100°C 2h, rt. overnight	Decomp.	[22]
5	-I	-H	CuI (0.05 eq), PPh_3 (0.10 eq), K_2CO_3 (1.5 eq), DMF; 100°C overnight	No Reaction	[20, 21]
6	-I	-H	CuI (0.05 eq), PPh_3 (0.10 eq), Cs_2CO_3 (1.5 eq), DMSO; 120°C overnight	No Reaction	[20, 21]
7	-I	-H	KHMDS or n-BuLi, MeO-9-BBN, $PdCl_2(PPh_3)_2$ (0.03 eq), THF; -78°C then reflux overnight	75%*	[18]
8	-I	-H	$PdCl_2(PPh_3)_2$ (0.01 eq), CuI (0.02 eq), Et_2NH; rt. then 45°C overnight	50%*	[23]
9	$-B(OH)_2$	-I	$Pd(dba)_3CHCl_3$ (eq), Cs_2CO_3 (1.5 eq), toluene; 80°C overnight	No Reaction	[5]

* Yield obtained with recovery of starting compound **5**, which was an inseparable mixture with halogenated compound **7**.

The complete synthesis of 5'-phenylethynyl **GC-1** derivative **NH-1** as a model system using the optimized Suzuki-Miyaura coupling procedure is shown in Scheme 3-3.[24] The 5'-iodinated **GC-1** intermediate **7** was coupled with phenylethynyl boronate,

generated *in situ* under basic conditions with MeO-9-BBN, to give the 5'-phenylethynyl compound in good yield. De-silylation of **9** with TBAF generated phenol **10**, which was then mono-alkylated using *t*-butylchloroacetate to give ester **11**. Removal of the methoxymethyl phenolic protecting groups under acidic conditions, followed by basic saponification of the *t*-butyl ester gave the desired **NH-1** compound. Despite the complication with the iodination step, the current synthetic route gives fairly good overall yields and 5'-phenylethynyl **GC-1** derivatives can be prepared in gram quantities.

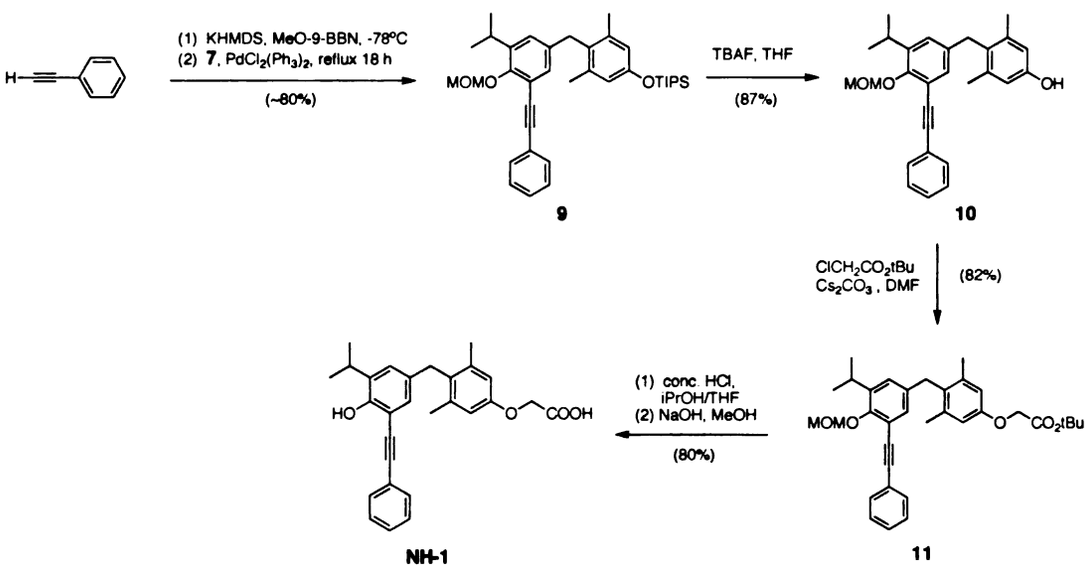

Scheme 3-3. Synthesis of NH-1 via the Suzuki-Miyaura coupling. See Appendix A.

3.1.4 NH-3 via Suzuki-Miyaura Coupling[24]

The Suzuki-Miyaura procedure outlined in Scheme 3-3 was also used to couple intermediate **7** with 1-ethynyl-4-nitro-benzene for the synthesis of **NH-3**. However, complications arose in scaling up this coupling reaction. Since palladium-catalyzed coupling is typically facilitated by electron-donating groups in close proximity to the alkyl/aryl group of the boronate species,[15,16] we suspected that the electron-withdrawing nature of the nitro substituent was hindering the transmetalation and/or the reductive

elimination steps of the catalytic cycle. Consequently, the synthesis was modified to couple intermediate **7** with 4-ethynylaniline as a precursor to the nitro compound (Scheme 3-4, see Appendix A). Following iodination, the silyl-protecting group was removed and mono-alkylated with methylbromoacetate to give **12**. Suzuki-Miyaura coupling of **12** with 4-ethynylaniline gave **13**, which was then oxidized with *m*-chloroperbenzoic acid (m-CPBA) to give the nitro compound **14**. Removal of the methoxymethyl phenolic protecting groups and saponification of methyl ester **14** gave final compound **NH-3**.

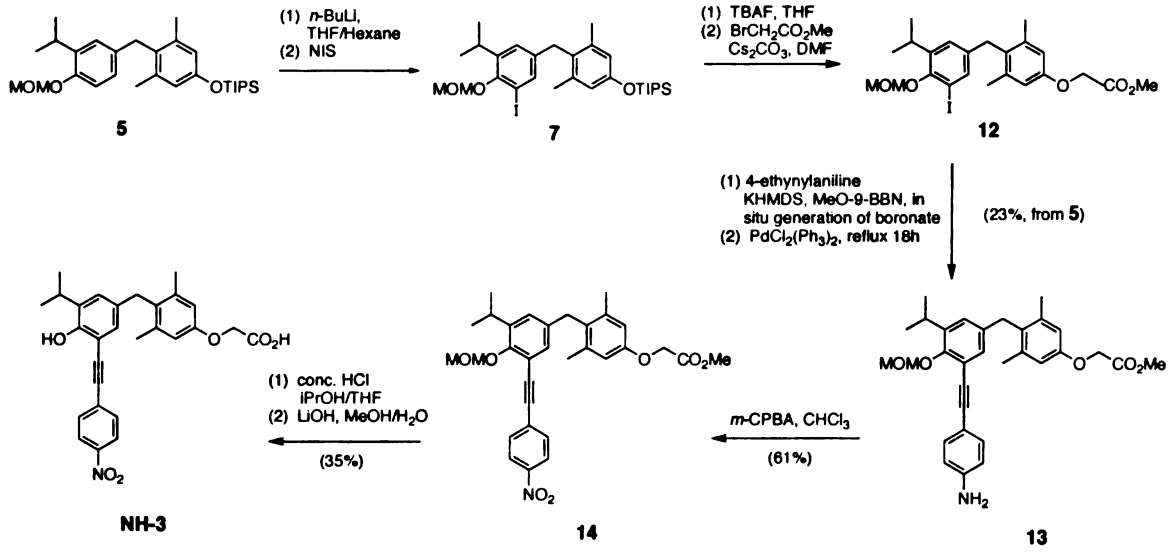

Scheme 3-4. Synthesis of NH-3 via the Suzuki-Miyaura coupling. See Appendix A.

3.2 *In Vitro* Characterization of NH-3

3.2.1 Human TR Binding and Transactivation Properties[24]

Binding assays for **NH-3** to human (h) TRα1 and TRβ1 were performed by Jim Apriletti from the Baxter lab (UCSF) as described previously (see Appendix A).[24] The binding data are summarized in Table 3-2, which also includes comparative data for T_3, **GC-1** and **GC-14**.[5] Briefly, binding affinity was measured by an *in vitro* radioligand

displacement assay using recombinant hTRα1 and hTRβ1, a fixed concentration of radiolabeled T_3, and a range of concentrations to **NH-3**. As previously observed with other **GC-1** analogues, **NH-3** has reduced binding affinity by at least one order of magnitude for both TRα and TRβ compared to **GC-1**. Although binding is impaired, the TRβ-selectivity of **NH-3** is retained. This result is consistent with structural and chemical data that suggest the molecular determinant of selectivity is located at the 1-oxyacetic acid side chain of the **GC-1** core structure.[11,25,26]

The transcriptional transactivation property of **NH-3** was characterized in human metastasized cervical cancer cell line (HeLa cells) by a reporter gene assay (see Appendix A). Briefly, HeLa cells were transiently transfected with expression plasmids for hTRα1 or hTRβ1 and a luciferase reporter containing a TRE with two tandemly linked copies of direct repeats of the consensus TR DNA binding site spaced by four base pairs (DR4 element) upstream of the thymidine kinase promoter. In this assay, **NH-3** induced minimal transactivation of reporter expression above the level of vehicle control with either TRα or TRβ (Figure 3-2A). Furthermore, **NH-3** competitively blocked 1 nM T_3-induced transactivation in a dose-dependent manner down to the maximal level of activation observed with **NH-3** alone (Figure 3-2B). Under these conditions, the IC_{50} value of antagonism by **NH-3** was 370 nM for TRβ and 950 nM for TRα, making it more potent than **GC-14**. Thus, **NH-3** is TRβ-selective in both binding and inhibition of T_3-induced transactivation

Table 3-2. Binding and transactivational activity of NH-1 and NH-3 at hTRβ1 and hTRα1.

5'-substitution	$K_D \pm SE$ (nM)[a]		% $TR\beta_1$	$TR\beta_1$ EC_{50}	% $TR\alpha_1$	$TR\alpha_1$ EC_{50}
	$hTR\beta_1$	$hTR\alpha_1$	activation[b]	(IC_{50})[c] (nM)	activation[b]	(IC_{50})[c] (nM)
T_3	0.10 ± 0.03	0.10 ± 0.03	100	2	100	2
GC-1[d] H	0.10 ± 0.02	1.8 ± 0.2	100	7	100	45
GC-14[d] 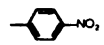	35 ± 12	200 ± 60	18	(680)[e]	35	(5000)[e]
NH-1[f] 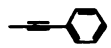	37 ± 9	490 ± 100	70	500	n.d.	n.d.
NH-3 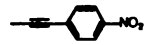	20 ± 7	93 ± 29	3	(370)[e]	10	(950)[e]

[a] The K_D and standard error (SE) values were calculated by fitting the competition data to the equations of Swillens[27] and using the Graph-Pad Prism computer program (Graph-Pad Software, Inc.).
[b] HeLa cells were co-transfected with either hTRβ or hTRα expression vector and a TRE-luciferase reporter plasmid. Luciferase activity of 10^{-5} M analogue is expressed as a percent of the $TR\beta_1$ or $TR\alpha_1$ response with 10^{-7} M T_3. Values are the mean ± SD for three separate experiments. See Appendix A for more details.
[c] The EC_{50} value is the concentration of ligand required for half-maximum activation, whereas the IC_{50} value is the concentration of ligand required for half-maximum inhibition in competition experiments with 10^{-9} M T_3. EC_{50} and IC_{50} values were calculated by nonlinear regression with the Graph-Pad Prism computer program (Graph-Pad Software, Inc.) using a sigmoidal dose response or single-site competition models, respectively. Values are the mean for three separate experiments.
[d] Refer to Chiellini, et al. 2002 (Reference 5).
[e] These are IC_{50} values for hTRβ1 and hTRα1, respectively.
[f] Compounds exhibiting thyromimetic transcriptional activation through $hTR\beta_1$ were not further characterized with $hTR\alpha_1$.

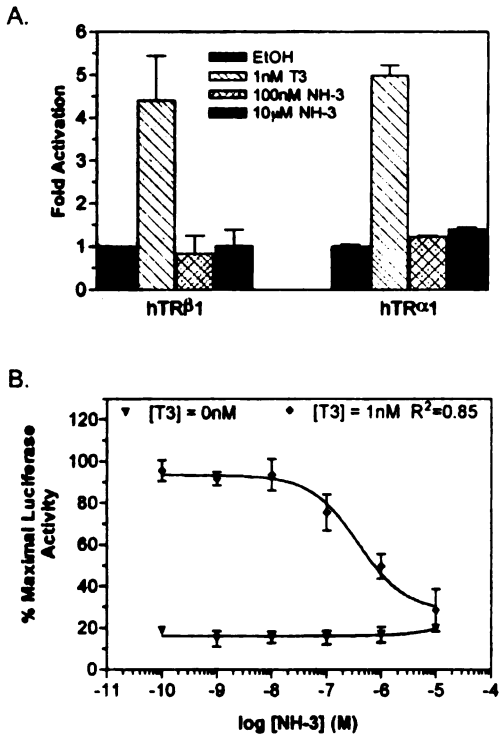

Figure 3-2. (A) Transcriptional activity of NH-3 compared to that of T_3. (B) Dose response curve with $hTR\beta_1$ for NH-3 alone and in competition with 1 nM T_3. Values are the mean ± SD for three separate experiments expressed as (A) fold activation relative to ethanol (EtOH) vehicle and (B) percent of the TRβ response with 1 nM T_3, which is set at 100%. Data were fitted by nonlinear regression using the Graph-Pad Prism computer software for a single-site competition model to generate IC_{50} values.

3.2.2 *Effect of NH-3 on TR Interaction with Coregulators*[24,28]

3.2.2.1 Mammalian Two-Hybrid and GST-Pulldown Assays

Since **NH-3** displayed antagonist activity and its 5'-extension was designed to prevent folding of TR to form the coactivator binding surface, the compound was tested for its effect on TR interaction with coactivator GRIP-1 using a mammalian two-hybrid assay system (see Appendix A).[24] Since the coactivator surface partly overlaps the corepressor binding surface, we also looked at effects of **NH-3** on TR interaction with corepressor NCoR. HeLa cells were transiently transfected with expression plasmids for the yeast GAL4 DBD linked to either NCoR (aa1925-2308) or GRIP-1 (aa618-1121), hTRβ-LBD fused to the VP16 activation domain, and a GAL4-driven luciferase reporter (Figure 3-3A). Both T_3 and **NH-3** promoted release of NCoR; the EC_{50} values of TR-NCoR interaction with bound T_3 versus bound **NH-3** are approximately 1.5 versus 45 nM, respectively (Figure 3-3 B,C). This difference is likely to reflect the difference in their binding affinities for TR. In collaboration with Suzana Cunha-Lima and Paul Webb from the Baxter lab (UCSF), we showed that **NH-3** also promoted TR release from corepressor SMRT under similar conditions indicating that the effect of **NH-3** on corepressor release is not specific to NCoR (data not shown). Moreover, **NH-3** did not promote RAR release from the corepressors suggesting that its effect is TR selective (data not shown). Thus, **NH-3** resembles T_3 in its ability to promote TR dissociation from corepressors.

We then examined the effect of **NH-3** on coactivator binding. As expected, T_3 stimulated binding of GRIP-1 to TR whereas **NH-3** did not (Figure 3-3B). In a competition assay, 1.5 μM **NH-3** blocked 50% of 10 nM T_3-induced TR-GRIP-1 interactions in a dose-dependent manner (Figure 3-3D). Thus, **NH-3** antagonizes TR-coactivator interactions in a cellular environment.

Our collaborators in the Baxter lab also confirmed that **NH-3** showed similar effects on TR interactions with corepressors and coactivators in *in vitro* GST-pulldown assays by standard procedures (Figure 3-3E).[24] In accordance with the results obtained in transfected cells, **NH-3** behaved like T_3 in promoting release of liganded TR from bacterially expressed NCoR. However, **NH-3** again failed to promote TR interactions with bacterially expressed GRIP-1 and also blocked the T_3-induced interactions between TR and this coactivator. Similar results were also obtained with bacterially expressed fragments of the alternate TR coactivator TRAP220 (data not shown).

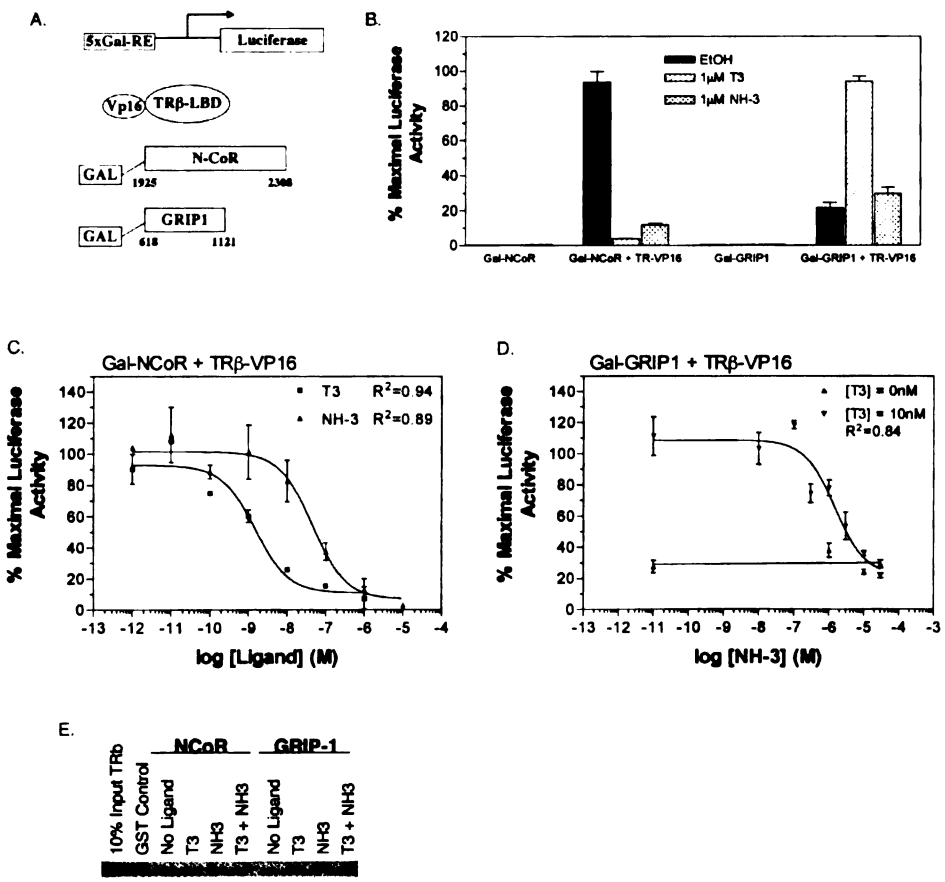

Figure 3-3. Effect of NH-3 on TR interactions with coregulators. (A) Schematic of the transfection components in mammalian two-hybrid assays. (B) T_3 and NH-3 promote TR dissociation from NCoR, but only T_3 is able to induce GRIP-1 association. (C) In a dose-response curve, T_3 and NH-3 inhibit TR-NCoR interaction. TR-NCoR interaction in the presence of ethanol (EtOH) vehicle is defined as 100% maximal luciferase activity. (D) In a competition assay, 1.5 μM NH-3 inhibits 50% of TR-GRIP1 association induced by 10 nM T_3. TR-GRIP1 interaction in the presence of 10 nM T_3 is defined as 100% maximal luciferase activity. Values are the mean ± SD for three separate experiments and analyzed by nonlinear regression using a sigmoidal dose-response model with GraphPad Prism computer software. (E) Autoradiogram of 10% SDS-polyacrylamide gel showing products of *in vitro* binding regions of NCoR and GRIP-1. A 10% input labeled TR is shown as a control. T_3 concentration was 100 nM; NH-3 concentration was 10 μM.

3.2.2.2 *High-throughput In Vitro Binding Assay to Coregulator Peptide Library*

Previous work by other investigators has shown that ligands can allosterically modulate the NR coregulator binding pocket and therefore differentially alter specific coregulator recruitment.[29-31] To understand the TR-coactivator selectivity in the presence of antagonist **NH-3** compared to natural hormone T_3 and agonist **GC-1**, we collaborated with Jamie Moore and others in the Guy lab (UCSF) to perform an expanded analysis of TR-coregulator interactions using a high throughput fluorescence polarization binding assay with TR against a library of potential coregulator peptides. The library consisted of 32 unique NR box peptides (LXXLL sequences) found in 12 different coactivators covalently attached to a fluorescent probe (Figure 3-4A), as described in a recent publication.[28] To our knowledge, this study is the first comprehensive report of the interactions of TR and natural coactivator NR boxes.

Of the 32 NR box peptides, 20 appear to interact with TRβ in the presence of T_3 with varying degrees of affinity (Figure 3-4B). Strong interactions were observed with TRBP-1, RIP140-5, TRAP220-1, DAX1-3, p300 and all of the SRC2 peptides. The coactivator peptides that did not interact with TRβ•T_3 included ARA55, all of the TRAP100 peptides, and some of the RIP140 and DAX1 peptides. In the presence of **GC-1**, the coactivator binding pattern was overall similar to that of T_3. However, the degree to which they bound TR with **GC-1** varied. In most cases, the coactivator peptides bound with similar or slightly lower affinity to TRβ•**GC-1** than TRβ•T_3. Other notable differences for TRβ•**GC-1** include saturated binding of only SRC2-2 and reduced binding of TRAP220 and TRBP. Testing of **NH-3** against the entire peptide library reveals no coactivator recruitment to the TRβ in the presence of saturating concentrations of **NH-3**. Thus, it appears **NH-3** is nonselective in disallowing

interactions between TR and its target coactivators. This is likely one of the underlying mechanisms for observed full antagonistic activity of **NH-3**.

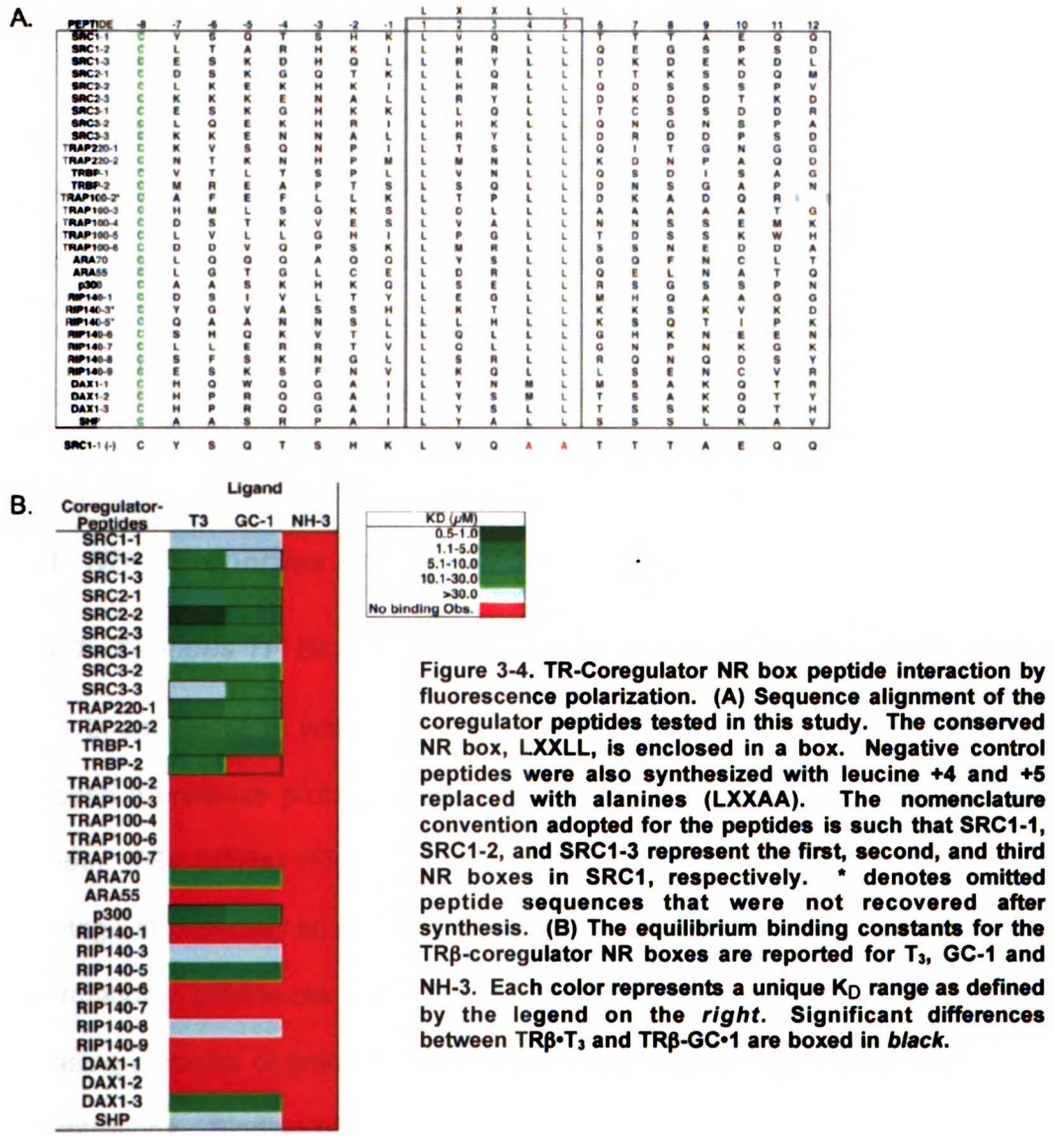

Figure 3-4. TR-Coregulator NR box peptide interaction by fluorescence polarization. (A) Sequence alignment of the coregulator peptides tested in this study. The conserved NR box, LXXLL, is enclosed in a box. Negative control peptides were also synthesized with leucine +4 and +5 replaced with alanines (LXXAA). The nomenclature convention adopted for the peptides is such that SRC1-1, SRC1-2, and SRC1-3 represent the first, second, and third NR boxes in SRC1, respectively. * denotes omitted peptide sequences that were not recovered after synthesis. (B) The equilibrium binding constants for the TRβ-coregulator NR boxes are reported for T_3, GC-1 and NH-3. Each color represents a unique K_D range as defined by the legend on the *right*. Significant differences between TRβ•T_3 and TRβ-GC•1 are boxed in *black*.

3.3 Effects of NH-3 on *Xenopus Laevis* Metamorphosis[32]

We are using *Xenopus laevis* metamorphosis as a simple and highly reproducible screen for biologically active thyroid hormone agonists and antagonists. The *Xenopus* system is a valuable model for thyroid hormone action for a number of reasons.[33,34] The *Xenopus* thyroid hormones are identical in structure to the mammalian

thyroid hormones.[35] The initiation and completion of metamorphosis is completely dependent on thyroid hormones secreted from the developing thyroid gland. The TRα and TRβ subtypes, their heterodimeric partner RXR, and the receptor-associated corepressors and coactivators are structurally and functionally well conserved with the mammalian counterparts. The TRs recognize TREs in native target genes that contain canonical direct repeats similar to mammalian DR4 elements. Tadpoles readily take up T_3 from the aqueous rearing solution and respond in a dose-dependent and highly stereotypic manner. Thus, amphibian metamorphosis presents a unique opportunity to address important questions regarding thyroid hormone actions that are common to all vertebrates.

3.3.1 NH-3 Properties Are Similar between Human and Xenopus TR

3.3.1.1 Xenopus TR Binding and Transactivation

In collaboration with Wayland Lim and others from the Furlow lab at UCD, we employed a protease protection assay to determine whether **NH-3** can bind directly to *Xenopus* TRs (xTRs) (Figure 3-5) as previously described.[32] This assay has the advantage of providing an estimate of the relative binding affinity and a means to detect conformational differences when TRs are bound to various ligands. Using elastase IV, increasing amounts of protected bands at ~35 kDa were observed with increasing **NH-3** concentrations. Binding of **NH-3** by both xTRs lead to at least one order of magnitude reduced binding affinity, with also reduced subtype selectivity, compared to agonist **GC-1**. These findings are consistent with results using human TRs. The protease protection assay also revealed a distinct protected band pattern in both xTRα and xTRβ incubated with saturating **NH-3** relative to T_3 and **GC-1**, suggesting **NH-3** induces an xTR conformation that is distinct from the agonist bound xTRs.

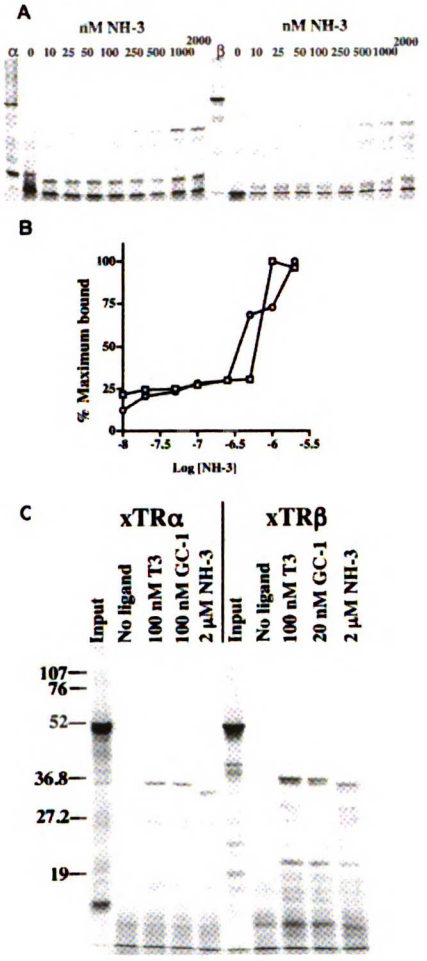

Figure 3-5. NH-3 binds to both *X. laevis* TR subtypes. (A) *In vitro* translated, ^{35}S-labeled xTRα (α) or xTRβ (β) were incubated with the indicated nM concentrations of NH-3 and then treated with 4 μg of elastase IV. The resulting bands were resolved by 12% SDS-PAGE. (B) Binding curves for xTRα (*squares*) and xTRβ (*circles*) were generated by quantization of the protected bands shown in (A) and expressed as a percentage of the maximally protected bands. (C) Elastase protection patterns of xTRα and xTRβ incubated with the indicated saturating concentrations of T_3, GC-1, or NH-3 performed as in (A). Positions of molecular mass markers in kDa are indicated to the *left*.

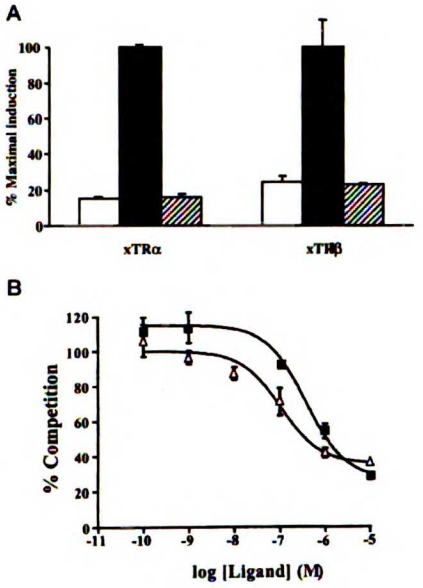

Figure 3-6. NH-3 inhibits T_3-induced transcription in a reporter gene assays. (A). HeLa cells were transiently transfected with expression plasmids for xTRα or xTRβ along with a TRE-containing reporter gene. Cells were treated for 24 h with ethanol vehicle alone (*open bars*), 1 nM T_3 (*filled bars*), or 10 μM NH-3 (*striped bars*), and luciferase activity was assayed. (B) Competition assays of NH-3 with 1 nM T_3 for xTRα (*squares*) and xTRβ (*triangles*); IC_{50} values were 100 nM (R^2 = 0.94) and 380 nM (R^2 = 0.88), respectively.

To determine the effects of NH-3 on T_3-induced transcription, xTRα or xTRβ expression plasmids were co-transfected with a TH/bZIP TRE-luciferase reporter gene into HeLa cells (see Appendix A). **NH-3** alone does not activate xTRα or xTRβ relative to untreated controls (Figure 3-6A). In competition assays, **NH-3** blocks activation by 1

nM T_3 in a dose-dependent manner (Figure 3-6B). **NH-3** is approximately 3-4 fold more potent at antagonizing 1 nM T_3 activated xTRβ relative to xTRα, which IC_{50} values of 100 nM and 380 nM, respectively. This correlates well with the competitive binding and transactivation assay data for the human TRs, which shows ~3-fold selective binding and antagonistic potency for hTRβ over hTRα.

3.3.1.2 Effect of NH-3 on Xenopus TR Interaction with Coactivators

The molecular basis for the antagonism of **NH-3** with xTR was investigated using the mammalian two-hybrid assay in HeLa cells (see Appendix A). xTRβ LBD fused to the GAL4 DBD was co-transfected with human GRIP-1 fused to VP16 activation domain or with human SRC-1 fused to the GAL4 activation domain (Figure 3-7A). As shown in Figure 3-7B, 10 μM **NH-3** completely abolishes T_3-induced interaction with GRIP-1 and SRC-1 fusion proteins. The half-maximal IC_{50} for competition against 20 nM T_3 was 920 nM **NH-3** for GRIP-1 and 870 nM **NH-3** for SRC-1. xTRα showed essentially the same result, except that the inhibition curves were shifted slightly to the right (higher concentration) as expected based on the TRβ-selectivity of **NH-3**.

Collectively, our results clearly demonstrate the degree of structural and functional relatedness between the mammalian and amphibian TRs and further underscore the usefulness of the amphibian model for identifying biologically active nuclear receptor ligands.

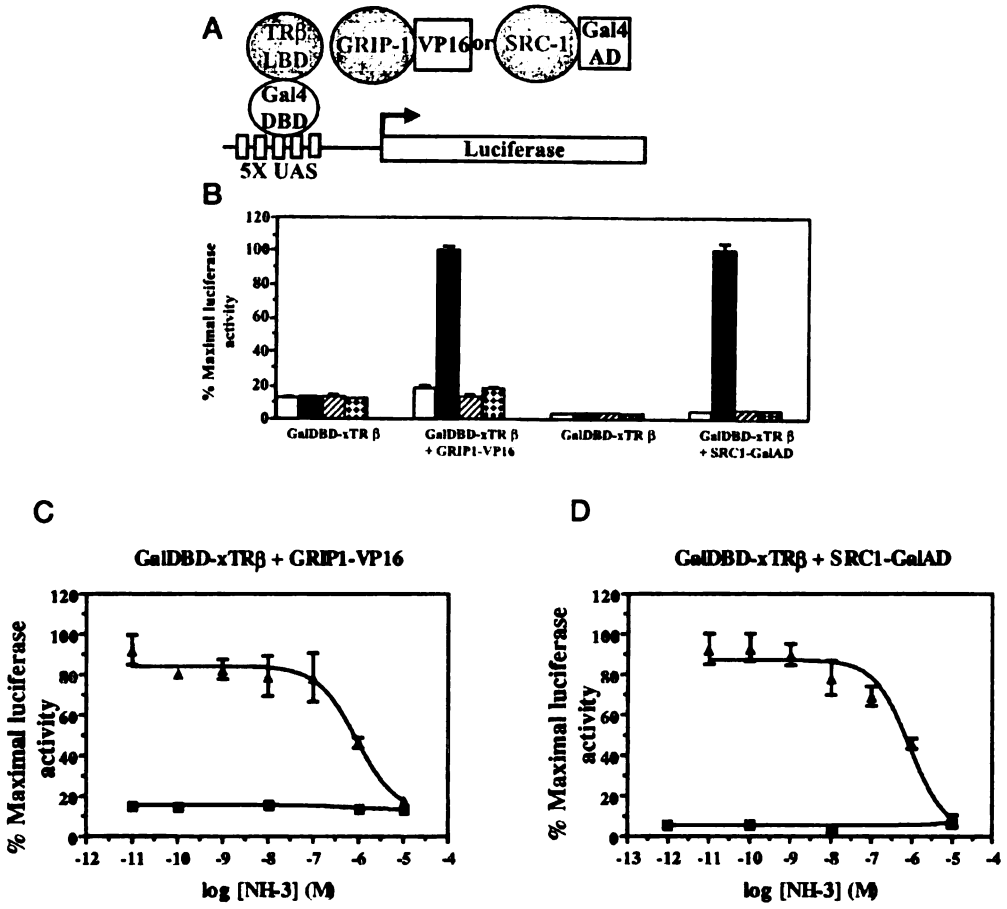

Figure 3-7. p160 family coactivator recruitment by xTRβ is inhibited by NH-3. (A) Schematic of transfection components in mammalian two-hybrid assays. (B) NH-3 completely inhibits T_3-induced TR interaction with GRIP-1 or SRC-1 fusion proteins. *Open bars*, vehicle only; *filled bars*, 20 nM T_3; *striped bars*, 10 μM NH-3; *hatched bars*, 20 nM T_3 + 10 μM NH-3. (C and D) Dose-response curve of NH-3 inhibition of T_3-induced GRIP-1 and SRC-1 interactions with TR. Values are the mean ± SD for three separate experiments and analyzed by nonlinear regression using a sigmoidal dose-response model with GraphPad Prism computer software. *Triangles*, 20 nM T_3 + NH-3; *squares*, NH-3 only.

3.3.2 NH-3 Inhibits Xenopus Metamorphosis

After we confirmed the antagonistic activity of **NH-3** observed *in vitro* with human TR is also observed with *Xenopus* TR, the Furlow lab further tested the ability of **NH-3** to inhibit T_3 action in an *in vivo* animal model. **NH-3** is remarkably effective in the inhibition of spontaneous metamorphosis in *Xenopus laevis* tadpoles as well as metamorphic changes induced by exogenously added T_3. Consistent with its lower TR subtype selectivity compared with **GC-1**, **NH-3** inhibits most observed metamorphic responses,

including tissue growth as seen in the brain and Meckel's cartilage and the death of larval tissues such as the internal gills and tail. Hind limb growth is less effectively inhibited by **NH-3**, possibly because of its slight TRβ selectivity. In addition to blocking morphological changes, **NH-3** also inhibits T_3-induced target gene up-regulation including collagenase-3 that is involved in resorbing and remodeling tissues.[32]

At concentrations above 2 μM *in vivo*, **NH-3** shows weak partial agonist activity in both gene expression and morphological assays. One plausible reason might be due to the relief of transrepression since TR•**NH-3** complexes are unable to bind corepressors, as observed *in vitro* using human TRs. The absence of partial agonist activity in transient transfection may result from the lack of proper chromatin assembly on transfected plasmids. Weak partial agonism may also result from metabolism of **NH-3** to a compound with weak agonist activity in the intact animal.

NH-3 does not simply inhibit T_3 uptake from the rearing medium as its mode of action because it potently blocks induction of spontaneous metamorphosis by circulating endogenous T_3 levels.[36] In this case, **NH-3** is a more potent inhibitor than methimazole, a compound that is clinically used to prevent thyroid hormone biosynthesis. In addition, the effects of **NH-3** are completely reversible, meaning that the antagonist is non-toxic and can be added to and removed from the animal at will. In contrast to **NH-3**, the previously described T_3 antagonists **HY-4** and **GC-14** do not inhibit induced metamorphosis or T_3-induced gene expression at concentrations below 10 μM; higher concentrations of these compounds were found to be very toxic to the animals (data not shown). Thus, the improved design of **NH-3** over previous compounds results in higher TR affinity and greater potency such that **NH-3** can be used at effective but sub-lethal concentrations *in vivo*.

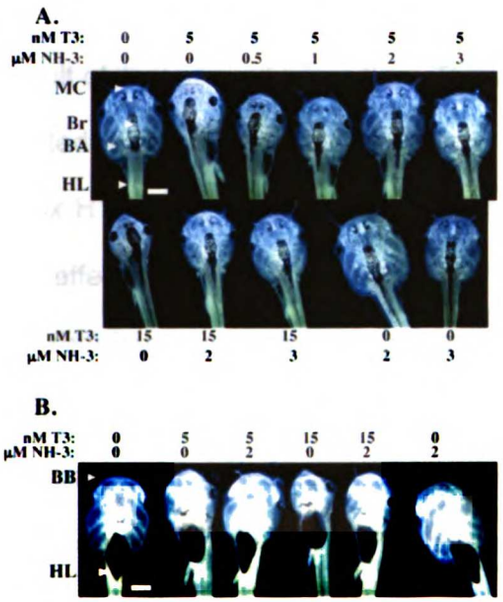

Figure 3-8. T_3-induced metamorphosis of *X. laevis* is inhibited by NH-3. Premetamorphic stage-52/53 tadpoles were treated with the indicated concentrations of T_3 and/or NH-3 for 5 days. (A) Dorsal views of the head and anterior end of the tail are shown. *Bar*, 2 mm; *MC*, Meckel's cartilage; *Br*, brain; *BA*, branchial arches; *HL*, hind limbs. (B) Ventral views of indicated animals shown in A. *B B*, barbels; *bar*, 2mm.

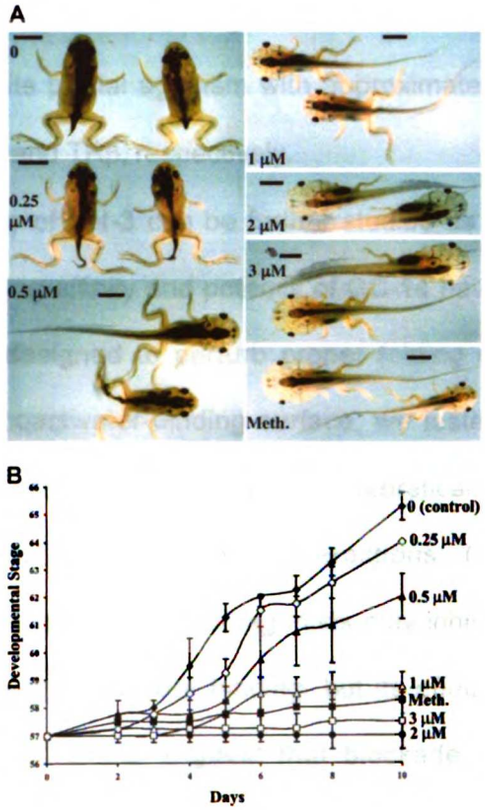

Figure 3-9. Spontaneous metamorphosis of *X. laevis* is inhibited by NH-3. (A) Four late stage-57 tadpoles were maintained in the indicated concentrations of NH-3, 1 mM methimazole, or vehicle alone for 10 days. Two animals from each treatment group are shown showing the range of development at the end of the treatments. Black bars, 5 mm. The experiment was repeated at least two additional times. (B) Animals shown in (A) were observed daily and assigned a developmental stage based on the tables of Nieuwkoop and Faber (36). Four animals were used per group; error bars indicate SD. Stage 66 is the end of metamorphosis.

3.4 Discussion

The **GC-1** derivative **NH-3** is a second generation TRβ-selective T_3 antagonist with improved properties compared to the previously reported mixed agonist/antagonist **GC-14**. **NH-3** has a modest two-fold greater binding affinity and potency for TRα and TRβ relative to **GC-14** (Table 3-1). However, its main improvement over **GC-14** is loss

of partial agonist activity observed with **GC-14**. **NH-3** is a full antagonist on the basis of the transactivation assays, whereas **GC-14** exhibits partial agonism with approximately 35% and 20% transactivation relative to T_3 for TRα and TRβ, respectively.

The mechanism for the antagonistic activity of **NH-3** can be further studied as a result of its improved properties. The weaker binding affinity and potency of **GC-14** have limited such characterization. Since **NH-3** was designed to perturb proper folding of helix H12 to complete formation of the putative coactivator-binding surface, we tested the effect of **NH-3** on TR interactions with corepressors and coactivators. Theoretically, antagonists may function in two ways to affect TR-coregulator interactions: (1) antagonists may enhance TR-corepressor interactions and/or (2) antagonists may inhibit TR-coactivator interactions. **DIBRT** weakly blocked coactivator binding, but its effects on corepressor binding were not examined. Our results suggest that blockade of coactivator binding is also responsible for the antagonism of **NH-3**. However, **NH-3** resembles T_3 in promoting corepressor release from TR. Thus, applying the "extension hypothesis" of attaching an appropriate appendage at the appropriate position of an agonist core structure may be a general strategy to design antagonists that block coactivator recruitment and impair nuclear receptor regulation of gene expression.

GC-14 and **NH-3** share a common chemical functionality with a *p*-nitroaryl group attached to the 5'-extension. In addition, **NH-3** has a unique ethynyl linkage. Previous SAR data suggest the nitro group attached to the 5'-extension dictates the antagonistic property; the size, position, and electronic properties of this nitro group are essential for the observed activity. The presence of the rigid ethynyl linkage in **NH-3** results in increased binding affinity and potency compared to **GC-14**. Thus, the improved properties of **NH-3** can be attributed directly to the internal ethynyl moiety. It has been proposed that liganded NRs exist in an equilibrium of active and inactive conformations, and that the nature of the ligand can shift the equilibrium to favor one state over the

other. The 5'-*p*-nitrophenyl extension of **GC-14** is apparently insufficient for complete perturbation of H12, thus allowing a significant concentration of a sub-optimal active conformation and the observed partial agonism. With **NH-3**, H12 may be more effectively perturbed and stabilized in the inactive conformation as indicated by the inability of TR to interact with coactivators when bound with **NH-3**. Rigidly extending the nitrophenyl group by two carbon atoms out of the ligand binding pocket potentially allows additional and/or amplified stabilizing ligand-receptor interactions that shifts the equilibrium towards an inactive conformation. Without additional structural data, these putative interactions are ill-defined. Efforts are underway to solve the crystal structure of an antagonist-bound TR LBD.

NH-3 is the first T_3 antagonist to exhibit potent antagonism *in vivo* and will be a useful tool for studying the effects of reversibly blocking TR activity in a number of different animal systems. Prior to the availability of pharmacological probes like **NH-3**, such studies have relied on TR-knockout mice that have irreversibly deprived the animal of expression of one of both TR isotypes throughout development. Certainly, the utility of **NH-3** in mammals will depend on various pharmacokinetic parameters that may differ in an amphibian model. Beyond anuran metamorphosis, T_3 has been implicated in a wide range of important biological processes in organisms that lack an available genetic approach, which can now be explored in more mechanistic detail using **NH-3**. Ultimately, potent T_3 antagonists such as **NH-3** will be useful therapeutic agents in the treatment of hyperthyroidism and other metabolic disorders.

3.5 Acknowledgements

First and foremost, we thank Dr. Grazia Chiellini for her guidance and help in developing the synthetic route for the 5'-phenylethynl **GC-1** derivatives. We are grateful to our collaborators and their contributions to this project. From the Baxter Lab at UCSF, we thank Dr. Jim Apriletti who performed *in vitro* binding assays, Dr. Suzanna Cunha-Lima and Dr. Paul Webb for their guidance and resources in the mammalian two-hybrid and GST-pulldown assays, and Phuong Nguyen for her technical assistance. We thank the Guy Lab at UCSF, in particular Dr. Jamie Moore, for conducting the TR-coactivator peptide binding assays. We are indebted to Wayland Lim and others in the Furlow Lab at UC Davis for their work on the *Xenopus* TR protease protection assays and *in vivo* tadpole studies with **NH-3**. We also thank Dr. M. Privalsky, Dr. R. Evans, and Dr. D. Moore for the gifts of plasmids used in the transfection assays.

This work was supported by grants from the National Institutes of Health (Grant DK 52798 to T.S.S.) and the UCSF Department of Pharmaceutical Chemistry (Training Grant T3207175-25 to N.H.N.).

3.6 References

(1) Jorgensen, E. C. Thyroid hormones and analogs. I. synthesis, physical properties and theoretical calculations. *Hormonal Proteins and Peptides*; Academic Press: New York, 1978; pp 57-105.

(2) Jorgensen, E. C. Thyroid hormones and analogs. II. structure-activity relationships. *Hormonal Proteins and Peptides*; Academic Press: New York, 1978; pp 107-204.

(3) Scanlan, T. S.; Yoshihara, H. A.; Nguyen, N. H.; Chiellini, G. Selective thryomimetics: Tissue-selective thyroid hormone analogs. *Curr. Op. in Drug Discovery & Development* **2001**, *4*, 614-622.

(4) Baxter, J. D.; Goede, P.; Apriletti, J. W.; West, B. L.; Feng, W. et al. Structure-based design and synthesis of a thyroid hormone receptor (TR) antagonist. *Endocrinology* **2002**, *143*, 517-524.

(5) Chiellini, G.; Nguyen, N. H.; Apriletti, J. W.; Baxter, J. D.; Scanlan, T. S. Synthesis and biological activity of novel thyroid hormone analogues: 5'-aryl substituted GC-1 derivatives. *Bioorg. and Med. Chem.* **2002**, *10*, 333-346.

(6) Yoshihara, H. A.; Apriletti, J. W.; Baxter, J. D.; Scanlan, T. S. A designed antagonist of the thyroid hormone receptor. *Bioorg. and Med. Chem. Lett.* **2001**, *11*, 2821-2825.

(7) Ribeiro, R. C.; Apriletti, J. W.; Wagner, R. L.; West, B. L.; Feng, W. et al. Mechanisms of thyroid hormone action: insights from X-ray crystallographic and functional studies. *Recent Prog. Horm. Res.* **1998**, *53*, 351-392; discussion 392-354.

(8) Weatherman, R. V.; Fletterick, R. J.; Scanlan, T. S. Nuclear-receptor ligands and ligand-binding domains. *Ann. Rev. of Biochemistry* **1999**, *68*, 559-581.

(9) Wagner, R. L.; Apriletti, J. W.; McGrath, M. E.; West, B. L.; Baxter, J. D. et al. A structural role for hormone in the thyroid hormone receptor. *Nature* **1995**, *378*, 690-697.

(10) Darimont, B. D.; Wagner, R. L.; Apriletti, J. W.; Stallcup, M. R.; Kushner, P. J. et al. Structure and specificity of nuclear receptor-coactivator interactions. *Genes Dev* **1998**, *12*, 3343-3356.

(11) Wagner, R. L.; Huber, B. R.; Shiau, A. K.; Kelly, A.; Cunha Lima, S. T. et al. Hormone selectivity in thyroid hormone receptors. *Mol. Endocrinol.* **2001**, *15*, 398-410.

(12) Feng, W.; Ribeiro, R. C.; Wagner, R. L.; Nguyen, H.; Apriletti, J. W. et al. Hormone-dependent coactivator binding to a hydrophobic cleft on nuclear receptors. *Science* **1998**, *280*, 1747-1749.

(13) Chiellini, G.; Nguyen, N. H.; Yoshihara, H. A.; Scanlan, T. S. Improved synthesis of the iodine-free thyromimetic GC-1. *Bioorg. and Med. Chem. Lett.* **2000**, *10*, 2607-2611.

(14) Chiellini, G.; Apriletti, J. W.; al Yoshihara, H.; Baxter, J. D.; Ribeiro, R. C. et al. A high-affinity subtype-selective agonist ligand for the thyroid hormone receptor. *Chemistry and Biology* **1998**, *5*, 299-306.

(15) Rossi, R.; Carpita, A.; Bellina, F. Palladium- and/or copper-mediated cross-coupling reactions between 1-alkynes and vinyl, aryl, 1-alkynyl, 1,2-propadienyl, propargyl, and allylic halides or related compounds. REVIEW. *Org. Prep. and Proc. Intl.* **1995**, *27*, 127-160.

(16) Miyaura, N.; Suzuki, A. Palladium-Catalyzed Cross-Coupling Reactions of Organoboron Compounds. *Chem. Rev.* **1995**, *95*, 2457-2483.

(17) Alami, M.; Ferri, F.; Linstrumelle, G. An efficient palladium-catalyzed reaction of vinyl and aryl halides or triflates with terminal alkynes. *Tet. Lett.* **1993**, *34*, 6403-6406.

(18) Soderquist, J. A.; Matos, K.; Rane, A.; Ramos, J. Alkynylboranes in the Suzuki-Miyaura Coupling. *Tetrahedron Letters* **1995**, *36*, 2401-2402.

(19) Sonogashira, K.; Tohda, Y.; Hagihara, N. A convenient synthesis of acetylenes: catalytic substitutions of acetylenic hydrogen with bromoalkenes, iodoarenes, and bromopyridines. *Tet. Lett.* **1975**, *50*, 4467-4470.

(20) Okuro, K.; Furuune, M.; Miura, M.; Nomura, M. Copper-catalyzed coupling reaction of aryl and vinyl halides with terminal alkynes. *Tet. Lett.* **1992**, *33*, 5363-5364.

(21) Okuro, K.; Furuune, M.; Enna, M.; Miura, M.; Nomura, M. Synthesis of aryl- and vinylacetylene derivatives by copper-catalyzed reaction of aryl and vinyl iodides with terminal alkynes. *J. Org. Chem.* **1993**, *58*, 4716-4721.

(22) Thorand, S.; Krause, N. Improved procedures for the palladium-catalyzed coupling of terminal alkynes with aryl bromides (Sonogashira coupling). *J. Org. Chem.* **1998**, *63*, 8551-8553.

(23) Takahashi, S.; Kuroyama, Y.; Sonogashira, K.; Hagihara, N. Convenient synthesis of ethynylarenes and diethynylarenes. *Synthesis Comm.* **1980**, 627-629.

(24) Nguyen, N. H.; Apriletti, J. W.; Cunha Lima, S. T.; Webb, P.; Baxter, J. D. et al. Rational design and synthesis of a novel thyroid hormone antagonist that blocks coactivator recruitment. *J Med Chem* **2002**, *45*, 3310-3320.

(25) Baxter, J. D.; Dillmann, W. H.; West, B. L.; Huber, R.; Furlow, J. D. et al. Selective modulation of thyroid hormone receptor action. *J. of Steroid Biochem. and Mol. Biol.* **2001**, *76*, 31-42.

(26) Yoshihara, H. A.; Apriletti, J. W.; Baxter, J. D.; Scanlan, T. S. Structural determinants of selective thyromimetics. *J Med Chem* **2003**, *46*, 3152-3161.

(27) Swillens, S. Interpretation of binding curves obtained with high receptor concentrations: practical aid for computer analysis. *Mol. Pharmacol.* **1995**, *47*, 1197-1203.

(28) Moore, J. M.; Galicia, S. J.; McReynolds, A. C.; Nguyen, N. H.; Scanlan, T. S. et al. Quantitative proteomics of the thyroid hormone receptor-coregulator interactions. *J Biol Chem* **2004**, *279*, 27584-27590.

(29) Geistlinger, T. R.; McReynolds, A. C.; Guy, R. K. Ligand-selective inhibition of the interaction of steroid receptor coactivators and estrogen receptor isoforms. *Chem Biol* **2004**, *11*, 273-281.

(30) Bramlett, K. S.; Wu, Y.; Burris, T. P. Ligands specify coactivator nuclear receptor (NR) box affinity for estrogen receptor subtypes. *Mol Endocrinol* **2001**, *15*, 909-922.

(31) McInerney, E. M.; Rose, D. W.; Flynn, S. E.; Westin, S.; Mullen, T. M. et al. Determinants of coactivator LXXLL motif specificity in nuclear receptor transcriptional activation. *Genes Dev* **1998**, *12*, 3357-3368.

(32) Lim, W.; Nguyen, N. H.; Yang, H. Y.; Scanlan, T. S.; Furlow, J. D. A thyroid hormone antagonist that inhibits thyroid hormone action in vivo. *J Biol Chem* **2002**, *277*, 35664-35670.

(33) Sachs, L. M.; Damjanovski, S.; Jones, P. L.; Li, Q.; Amano, T. et al. Dual functions of thyroid hormone receptors during Xenopus development. *Comp Biochem Physiol B Biochem Mol Biol* **2000**, *126*.

(34) Tata, J. R. Amphibian metamorphosis as a model for studying the developmental actions of thyroid hormone. *Biochimie (Paris)* **1999**, *81*, 359-366.

(35) Dodd, M. H. I.; Dodd, J. M. *Physiology of the Amphibia*; Academic Press: New York, 1976; pp 467-599.

(36) Nieuwkoop, P. D.; Faber, J. *Normal Table of Xenopus laevis (Daudin)*; 2nd Ed. ed.; Garland Publishing, Inc.: New York & London, 1994.

Chapter 4

Structural and Electronic Requirements for Thyroid Hormone Receptor Antagonists

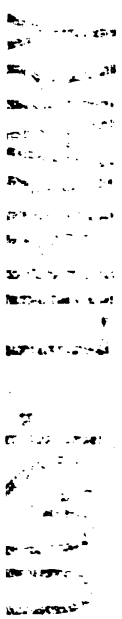

Selective thyroid hormone modulators (STRMs) that function as isoform-selective agonists or antagonists of the thyroid hormone receptors (TRs) might be therapeutically useful in diseases associated with aberrant hormone signaling. The most potent thyroid hormone antagonist reported to date is **NH-3**.[1] We have previously shown that the rigid ethynyl moiety of **NH-3** gave improved antagonist efficacy and potency compared to the parent compound **GC-14**.[1,2] However, the contribution of the 5'-*p*-nitroaryl group to antagonist activity is unknown. To better understand the molecular basis of the antagonistic activity of **NH-3** and the significance of the 5'-*p*-nitroaryl pharmacophore, we sought to expand the structure-activity relationship (SAR) data for the 5'-phenylethynyl series of **GC-1** derivatives. Herein we describe the synthesis of eighteen 5'-phenylethynyl **GC-1** derivatives having variable electronic properties. Based on modeling studies, we hypothesize that the nitro group is not required for antagonism and that the electronic nature of the 5'-aryl extension will dictate a spectrum of agonist versus antagonist activity. We show that these analogues bind TR with moderate nanomolar affinity and TRβ selectivity, exhibit selective TR modulation that indeed correlates with electronic character, and function similar to **NH-3** with respect to ligand-induced TR interaction with coactivators and corepressors to neutralize TR transcriptional activity.

4.1 Modeling Approach[3]

Using SYBL, molecular modeling was used to study the possible structural basis for antagonism of **NH-3** (Figure 4-1). Building the 5'-extension into the crystal structure of **GC-1** bound to TRβ LBD shows that the 4-nitrophenylethynyl group runs into significant steric clutter from residues of helices H5-6, H11, and H12, which presumably would alter the receptor conformation relative to the agonist fold. Modeling suggests that the 5'-extension sterically perturbs His435, which is involved in hydrogen-bonding interactions

with and recognition of the 4'-phenolic oxygen. This may account for the reduced binding affinity observed for **NH-3** relative to **GC-1**. However, in accommodating the ligand extension, the receptor might adopt a conformation such that the nitro group is involved in stabilizing interactions that would favor a transcriptionally inactive conformation. Knowing what residues are involved in ligand contacts in the agonist-bound TR crystal structure and surveying the secondary structure for nearby contacts (within 5 Å distance) allows prediction of potential ligand-receptor interactions. The nitro group may be involved in aromatic π-interactions (center-to-edge, edge-to-face, and/or face-to-face)[4] with proximal phenylalanine residues (ex. Phe455 and Phe459) from H12 that lay along the rim of the ligand binding pocket. Additionally the strong dipole of the nitro group may participate in electrostatic interactions with Lys306 of H5-6. The modeled structure of **GC-14** in the TRβ LBD shows that there are larger gaps between the nitrophenyl extension and the Phe/Lys receptor residues compared to the **NH-3**•TRβ complex. Thus, the 5'-nitrophenyl extension of **GC-14** may have sub-optimal interactions with the receptor compared to that of **NH-3** to shift the equilibrium towards an inactive conformation.

Based on the predicted electronic and electrostatic interactions of **NH-3** and TRβ receptor residues, we hypothesize that the nitro group is not needed for antagonism and that the electronic nature of the 5'-aryl extension will dictate ligand activity. That is, ligands with extensions containing electron-donating groups (EDG) would have agonist activity by productively interacting with receptor residues to stabilize an active receptor conformation. In contrast, ligands with extensions containing electron-withdrawing groups (EWG) would stabilized an inactive receptor conformation and therefore have antagonist activity.

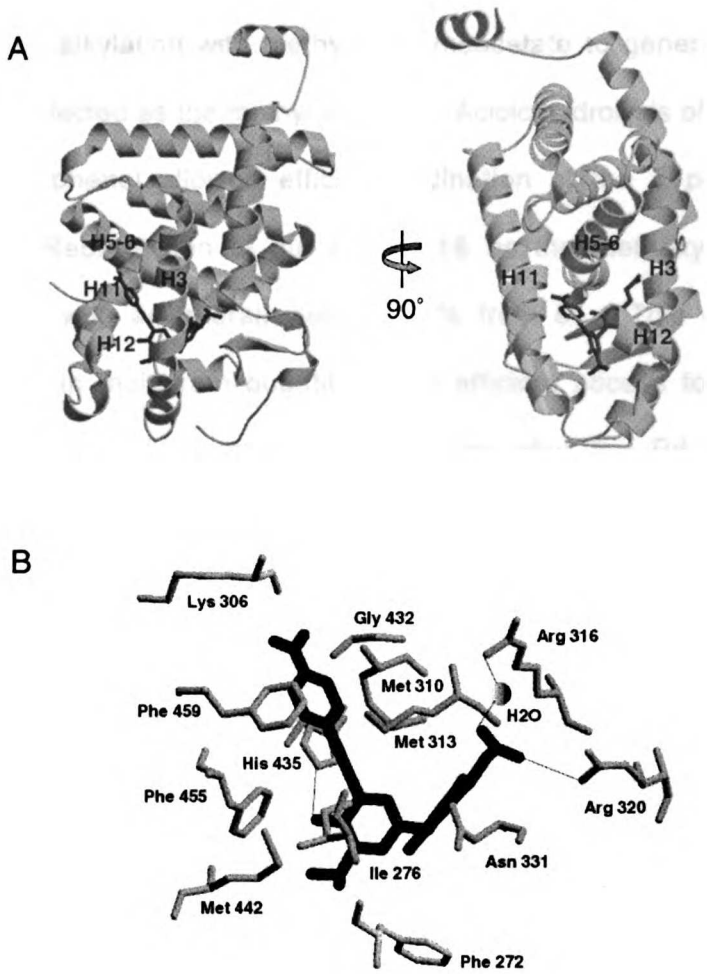

Figure 4-1. Molecular modeling of NH-3 bound to hTRβ-LBD. (A) The 5'-*p*-nitrophenylethynyl extension protrudes from the ligand binding pocket, resulting in steric clash with residues from helices H5-6, H11, and H12. (B) Receptor residues involved in ligand contact within 5 Å of NH-3 are shown. Modeling reveal residues 435, 459, 306, 432, and 310 lie within 3 Å proximity to the 5'-extension, suggesting these residues must undergo some rearrangement in order to accommodate the ligand extension. Figures were prepared with MolScript (P. J. Kraulis, *J. Appl. Cryst.* 24, 946 (1991).) and Raster3D (E. A. Merritt and D. J. Bacon, *Methods Enzymol.* 277, 505 (1997).)

4.2 Expanding SAR Data for 5'-phenylethynyl GC-1 Derivatives[5]

4.2.1 Chemical Synthesis

For more efficient access to a series of 5'-phenylethynyl **GC-1** derivatives, the synthesis previously described using the palladium-catalyzed Suzuki-Miyaura coupling[1] was modified to improve the 5'-iodination reaction to generate the key intermediate **12**

(Scheme 4-1A). The starting **GC-1** biarylmethane intermediate **5** was treated with TBAF followed by alkylation with methyl 2-bromoacetate to generate the 1-oxyacetic acid side chain protected as the methyl ester **15**. Acidic hydrolysis of the methoxymethyl (MOM)-protected phenol allowed efficient iodination at the 5'-position with iodine monochloride. Reprotection of the phenol **16** as the methoxymethyl ether gave intermediate **12**, with an overall yield of 51% from **5**. This new route allowed preparation of **12** in multigram quantities and efficient access to the 5'-substituted compounds with minimal chemical manipulations after the Pd-catalyzed coupling reaction.

With the exception of **NH-2** (Scheme 4-2), which was synthesized following the original synthetic route outlined in Scheme 3-3, all 5'-phenylethynyl derivatives were generated by palladium-catalyzed Suzuki-Miyaura coupling[6] of **12** with phenylethynyl boronate derivatives, generated *in situ* under basic conditions with MeO-9-BBN. The 5'-phenylethynyl analogues were synthesized in good yields (Scheme 4-1B). Many of the starting phenylacetylenic compounds are commercially available; others were generated via Sonogashira[7] or Sandmeyer[8,9] conditions (see Appendix A). The resulting coupled products **17a-l** were then subjected to acidic hydrolysis of the methoxymethyl phenolic protecting group followed by basic saponification of the methyl ester to afford the desired 5'-phenylethynyl **GC-1** analogues **18a-l** as outlined in Scheme 4-1B.

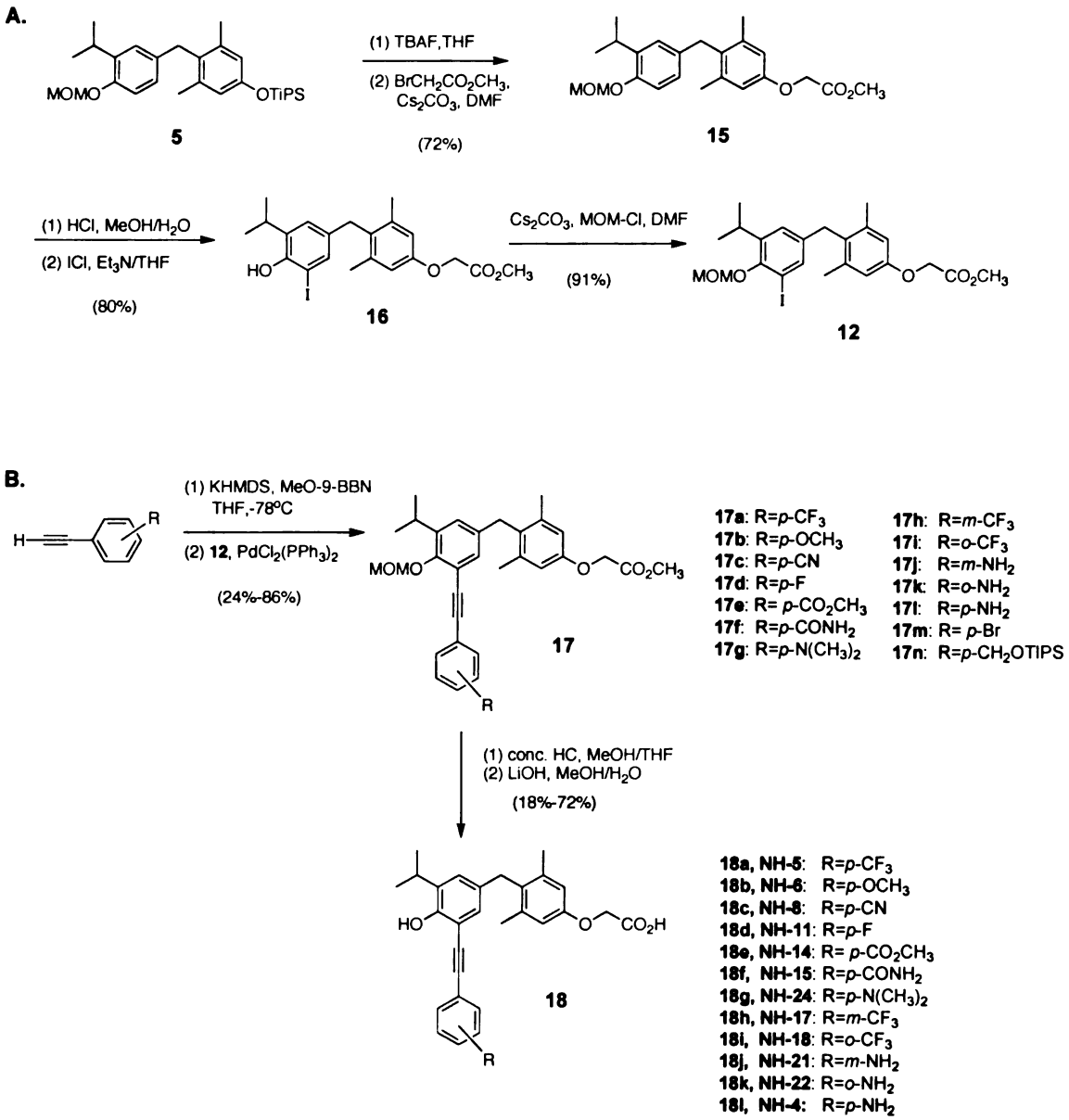

Scheme 4-1. General synthetic route to 5'-phenylethynyl GC-1 derivatives via the Suzuki-Miyaura coupling. (A) Improved synthesis of the 5'-iodinated key intermediate 4. (B) Suzuki-Miyaura coupling of 12 with phenylacetylenic derivatives followed by deprotection afforded the desired compounds 18a-l. Most phenylacetylenic derivatives were commercially available; others were readily synthesized via standard procedures as described in the Appendix A.

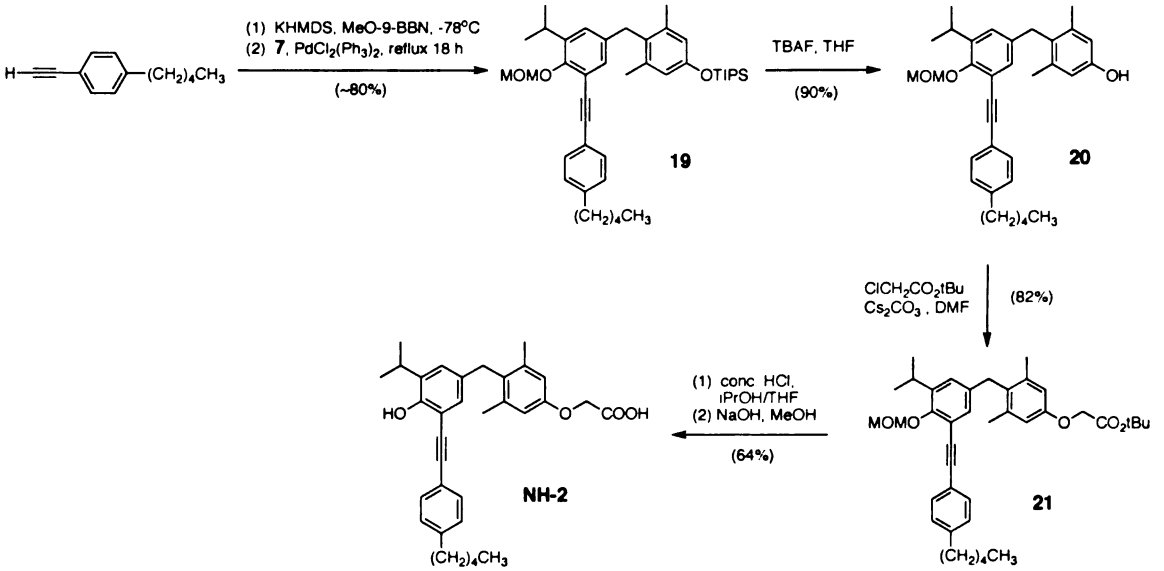

Scheme 4-2. Synthesis of NH-2. See Appendix A.

Some analogues required additional chemical manipulations after palladium coupling and/or after deprotection steps. The 5'-*p*-azidophenylethynyl analogue **NH-7** was prepared from the aniline precursor **17l** (Scheme 4-1B) using Sandmeyer[10] conditions of aqueous sodium nitrate in acid and sodium azide (Scheme 4-3A). Subsequent deprotection of the MOM group and the methyl ester gave the final compound **NH-7** in high yield.

Analogue **NH-16** was obtained by methylation of the 5'-*p*-dimethylamino-phenylethynyl intermediate **17g** with methyl trifluoromethanesulfonate (MeTf) in refluxing dichloromethane[11] (Scheme 4-3B). **NH-16** was not hydrolyzed to the carboxylic acid due to solubility issues in the workup and isolation of the final compound. Analogue **NH-19** was prepared from MOM-deprotected intermediate **22** by oxidation with *m*-chloroperbenzoic acid (*m*-CPBA) in chloroform[12] followed by basic hydrolysis of the methyl ester providing the desired compound in good yield (Scheme 4-3C). Attempts to oxidize intermediate **17k** (Scheme 4-2B) to form the 5'-*o*-nitrophenylethynyl analogue unexpectedly resulted in degradation.

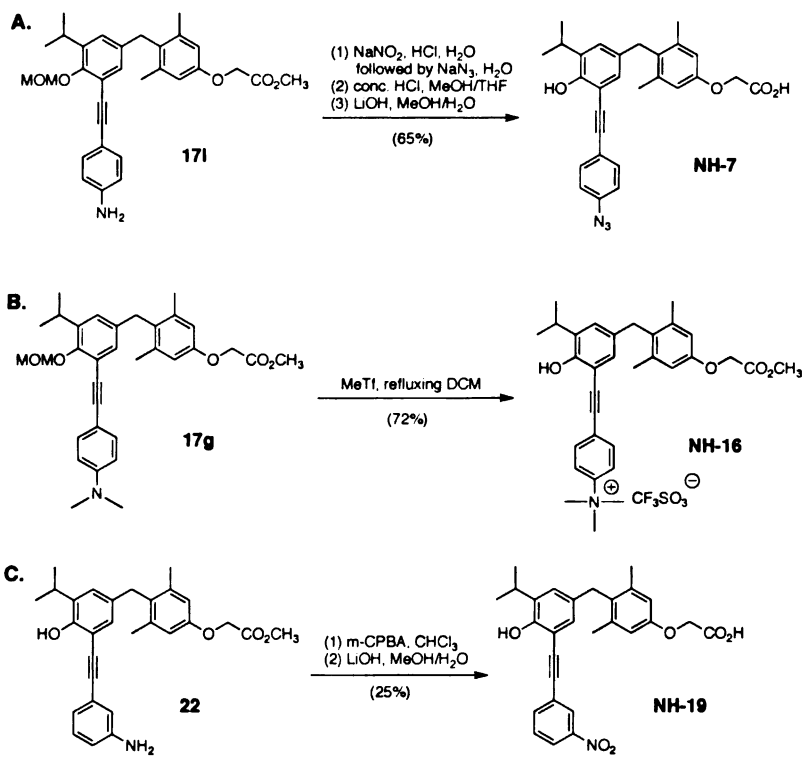

Scheme 4-3. Synthesis of NH-7, NH-16 and NH-19. See Appendix A.

The synthesis of analogue **NH-9** started with the coupling of **12** with 1-bromo-4-ethynylbenzene to give intermediate **17m** (Scheme 4-1B). However, the Suzuki-Miyaura coupling did not go to completion and the coupled product was an inseparable mixture with the aryl iodide **12**. This mixture was carried through another palladium-catalyzed coupling for the synthesis of nitroalkane **23**, adopting the procedure described by Vogl and Buchwald[13] (Scheme 4-4A). The reaction yield for this coupling was low with multiple by-products, which likely was due to use of impure bromide **17m**. The MOM protecting group was removed under acidic conditions. Upon treatment with aqueous lithium hydroxide in methanol for deprotection of the methyl ester, the *p*-nitroethane group underwent hydrolysis in a Nef reaction[14] after acidic workup to give the ketone product **NH-9** (Scheme 4-4A).

Analogue **NH-23** was synthesized from the triisopropylsilyl (TiPs) protected benzyl alcohol **17n** (Scheme 4-1B) as outlined in Scheme 4-4B. De-silylation with TBAF generated the free benzyl alcohol, which was readily converted to the benzyl azide **24** via formation of the benzyl chloride in a one-pot synthesis with chlorotrimethylsilane in DMSO[15] and sodium azide.[16] Subsequent cleavage of the MOM group and the methyl ester afforded **NH-23**.

Under the basic conditions of the final saponification step, a number of 5'-phenylethynyl derivatives underwent cyclization of the *o*-alkynylphenolic moiety to form the benzofuran product. The key diagnostic signals in the ^{1}H NMR indicating benzofuran formation were additional peaks near 1.4 ppm (-CH_3, *i*Pr, doublet), near 3.4 ppm (-CH, *i*Pr, heptet), and a peak ranging from 7.2 to 7.8 ppm (vinyl -H, singlet). Cyclization generally occurred at a much slower rate than ester hydrolysis and was limited by controlling the reaction time. Benzofuran formation was also observed for some analogues under slight acidic conditions needed for NMR characterization and consequently limited acquisition of ^{13}C NMR spectra.

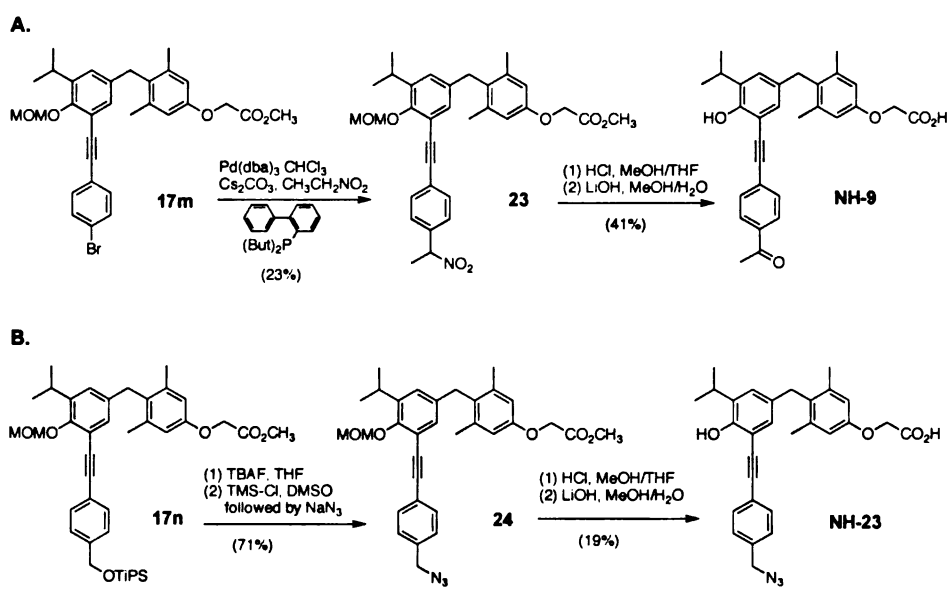

Scheme 4-4. Synthesis of NH-9 and NH-23. See Appendix A.

4.2.2 TR Binding and Transactivation Properties

All compounds were tested for binding to hTRα_1 and hTRβ_1 by *in vitro* radioligand displacement assays as described previously (see Appendix A) and the results are summarized in Table 4-1.[1] K_D values reported are expressed relative to the K_D of T_3 and were calculated by fitting the data to the equations of Swillens.[17] Data of T_3, **GC-1**[2], and previously reported **NH** compounds are included for comparison. As observed with other 5'-substituted analogues having the core **GC-1** scaffold, analogues **NH-2** through **NH-24** retained TRβ-selectivity with impaired affinity compared to **GC-1**. The TRβ-selectivity was consistent with structural and chemical data that suggest the key molecular determinant of selectivity is located on the 1-oxyacetic acid side chain of the **GC-1** core structure.[18,19] The analogues bound hTRβ with low nanomolar affinity with K_D values ranging from 0.5 to 450 nM. Analogue **NH-16** with the masked 1-oxyacetic acid moiety also bound TRβ with reasonable affinity, suggesting the compound might be partially hydrolyzed to the acid form under the conditions of the binding assays. Varying the position of the aryl substituent from *para*- to *ortho*- or *meta*-positions generally led to a decrease in binding affinity. For example, **NH-19** exhibited almost 2-fold decreased binding affinity compared to **NH-3**. Likewise, **NH-17** and **NH-18** had 25-fold lower affinity relative to **NH-5**, respectively.

The analogues were then tested in human HeLa cells for transcriptional transactivation properties using a luciferase reporter assay. HeLa cells were transiently transfected with expression plasmids for hTRα_1 or hTRβ_1 and a TRE-driven (DR4 element) luciferase reporter as described previously (see Appendix A).[1] Similar to **NH-1**, analogues **NH-2**, **NH-6**, **NH-16**, and **NH-24** exhibited partial agonism at TRβ by at least 60% activity relative to saturating T_3-induced transactivation (Figure 4-2A). The EC_{50} values are reported in Table 4-1. **NH-16** exhibited similar maximal transactivation

activity with reduced potency compared to **NH-24**. We surmise that the apparent agonist activity of **NH-16** resulted from partial demethylation of the trimethyl ammonium salt and partial hydrolysis of methyl ester to give **NH-24**. Analogues **NH-8** and **NH-14** exhibited mixed agonist and antagonist activity at TRβ. These compounds alone were able to induce luciferase expression by approximately 40% relative to saturating T_3-induced transactivation, while in competition assays they were able to partially block 2 nM T_3-induced activity down to the level of compound alone with micromolar potency (Figure 4-2B). EC_{50} values were not calculated for **NH-6**, **NH-8**, **NH-14**, and **NH-16** at TRα because their relatively poor affinity and potency for TRα made it difficult to obtain complete dose response curves. Analogues **NH-4**, **NH-15**, **NH-21** and **NH-22** displayed weak activity at TRα and TRβ. These compounds did not induce TR-mediated transactivation above the level of vehicle control and failed to compete with 2 nM T_3-induced transactivation in a dose-dependent manner (Table 4-1). At 10 μM concentration, **NH-4**, **NH-15**, **NH-21** and **NH-22** exhibited mild antagonism to block T_3 activity by approximately 10% (data not shown). All 5'-phenylethynyl analogues generally became toxic to the cells at doses above 10 μM.

Analogues **NH-5**, **NH-7**, **NH-9**, **NH-11**, and **NH-23** induced minimal reporter expression above the level of vehicle control with either TRα or TRβ (Figure 4-2A). In competition assays these compounds exhibited full antagonism in completely blocking 2 nM T_3-induced transactivation in a dose-dependent manner down to the level of activation observed with vehicle alone (Figure 4-2C). The IC_{50} values for antagonism under these conditions are shown in Table 4-1. For TRβ, **NH-5** and **NH-7** (IC_{50} = 590 nM and 630 nM, respectively) had 2- to 3-fold reduced potency compared to **NH-3** (IC_{50} = 270nM). The other antagonists in this group had IC_{50} values in the micromolar range. For TRα, the antagonists exhibited approximately 4-fold to 5-fold reduced potency

compared to TRβ. Thus, these compounds are TRβ-selective in binding affinity as well as transcriptional activity.

Transactivation data for **NH-17**, **NH-18**, and **NH-19** revealed the significance of substitution at the *para*-position on the 5'-aryl extension for antagonism. The *meta*- and *ortho*-substituted analogues induced minimal transactivation above that of vehicle control (Figure 2A). However, these compounds inefficiently blocked 2 nM T_3-induced transactivation and complete dose-response curves could not be obtained. **NH-19** at 10 μM blocked approximately 60% of T_3-induced response at TRβ(data not shown Similarly, 10 μM of **NH-17** and **NH-18** partially blocked the T_3 response by 50% and 30%, respectively, at TRβ (data not shown The relative lower affinity of these compounds can partially account for their impaired transactivation activity compared to the *para*-substituted counterparts **NH-3** and **NH-5**. Combined, these results suggest that substitution at the *para*-position on the 5'-aryl extension is optimal for ligand binding and antagonist activity.

Table 4-1. Binding and transcriptional activation data of 5'-substituted derivatives at hTRα_1 and hTRβ_1.

5'-substitution		$K_D \pm SE$ (nM)[a]		% TRβ_1 activation[b]	TRβ_1 EC_{50} (IC_{50}) (nM)[c]	% TRα_1 activation[b]	TRα_1 EC_{50} (IC_{50}) (nM)[c]	Activity
		hTRβ_1	hTRα_1					
T_3		0.10 ± 0.03	0.10 ± 0.03	100	2	100	2	Full Agonist
GC-1[d]	H	0.10 ± 0.02	1.8 ± 0.2	100	7	100	45	Full Agonist
NH-1		37 ± 9	490 ± 100	70	500	n.d.[e]	n.d.[e]	Partial Agonist
NH-2[f]	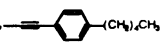	0.52 ± 0.05	5.2 ± 0.7	85	380	n.d.[e]	n.d.[e]	Partial Agonist
NH-3[g]	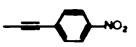	2.8 ± 0.4	14 ± 3	3	(230)	5	(1200)	Full Antagonist
NH-4	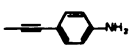	90 ± 6	330 ± 60	2	n.d.[h]	n.d.	n.d.	-
NH-5	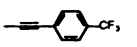	0.97 ± 0.05	8.4 ± 0.1	6	(590)	1	(1600)	Full Antagonist
NH-6[f]	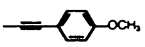	1.7 ± 0.2	13.6 ± 0.3	75	99	n.d.[e]	n.d.[e]	Partial Agonist
NH-7	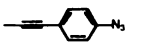	2.5 ± 0.4	23.7 ± 0.5	5	(630)	1	(2600)	Full Antagonist
NH-8[f]	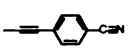	3.1 ± 0.5	17.0 ± 0.4	40	750 (>2000)	n.d.	n.d.	Mixed Agonist/ Antagonist
NH-9	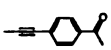	3.1 ± 0.5	23.0 ± 0.5	2	(1700)	1	(>5000)	Full Antagonist
NH-11	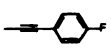	12 ± 2	46 ± 13	1	(4200)	2	(>5000)	Full Antagonist
NH-14[f]	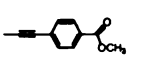	3 ± 1	38 ± 5	37	350 (>3000)	n.d.	n.d.	Mixed Agonist/ Antagonist
NH-15	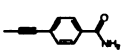	10 ± 1	41 ± 6	1	n.d.[h]	n.d.	n.d.	-
NH-16	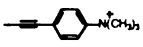	453 ± 30	629 ± 32	58	2700	n.d.[e]	n.d.[e]	Partial Agonist
NH-24	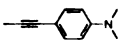	0.23 ± 0.02	3.9 ± 0.6	57	180	63	280	Partial Agonist
NH-23	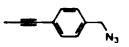	0.68 ± 0.04	8.1 ± 0.8	2	(1100)	1	(>5000)	Full Antagonist
NH-17	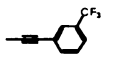	57 ± 22	332 ± 16	1	(>2500)	n.d.	n.d.	Weak Antagonist
NH-18	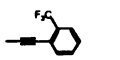	62 ± 14	80 ± 24	1	(>2500)	n.d.	n.d.	Weak Antagonist
NH-19	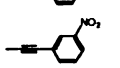	5 ± 1	31 ± 9	1	(>2500)	n.d.	n.d.	Weak Antagonist
NH-21	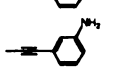	11 ± 2	50 ± 14	1	n.d.[h]	n.d.	n.d.	-
NH-22	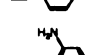	11 ± 3	67 ± 3	1	n.d.[h]	n.d.	n.d.	-

[a] The K_D and standard error (SE) values are expressed relative to the K_D of T_3 and were calculated by fitting the competition data to the equations of Swillens[17] and using the Graph-Pad Prism computer program (Graph-Pad Software, Inc.).

[b] Luciferase activity of 10^{-5} M analogue is expressed as a percent of the TRβ1 or TRα1 response with 10^{-6} M T_3. Values are the mean ± SD for three separate experiments. See Supporting Information for more details.

[c] The EC_{50} value is the concentration of ligand required for half-maximum activation, whereas IC_{50} value is the concentration of ligand required for half-maximum inhibition in competition experiments with 2×10^{-9} M T_3. EC_{50} and IC_{50} values were calculated by nonlinear regression with the Graph-Pad Prism computer program (Graph-Pad Software, Inc.) using a sigmoidal dose-response and single-site competition models, respectively. Values reported are the mean for three separate experiments with R^2 fit of at least 0.85 unless value is expressed as greater than (">"), indicating a poor R^2 fit.

[d] Refer to Chiellini et al. (2002) (see Reference 2).

[e] Compounds exhibiting thyromimetic transcriptional activation through hTRβ1 were not further characterized with hTRα_1.

[f] For transactivation assays, HeLa cells were cultured in 10% hormone-depleted, heat-treated (80°C, 20 min) newborn calf serum during incubation with ligand. Incubation with serum not heat-treated resulted in little or no ligand activity (data not shown), suggesting serum components are significantly sequestering ligand.

[g] NH-3 was retested in binding and transactivation assays. Results were comparable to previously reported values of 20 ± 7 nM for hTRβ_1 and 93 ± 29 nM for hTRα_1 in binding, and IC_{50} = 370 nM for hTRβ_1 in antagonist potency.

[h] Compound did not induce TR-mediated transactivation at 10^{-5} M nor antagonize 2×10^{-9} M T_3-induced transactivation in a dose-dependent manner. Therefore EC_{50} and IC_{50} could not be obtained for TRα1 and TRβ1.

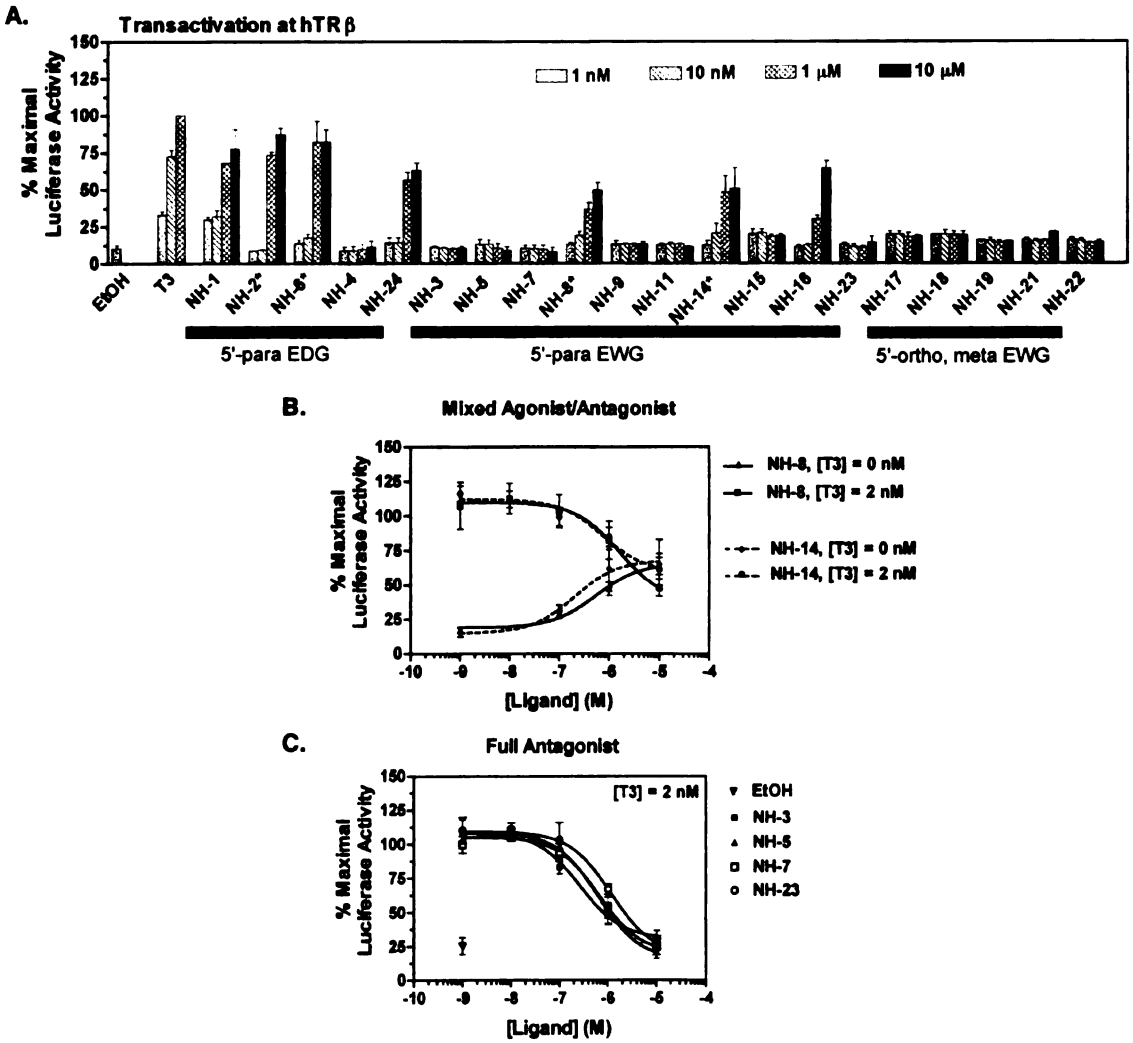

Figure 4-2. (A) Transcriptional activation of T_3 and 5'-phenylethynyl analogues in luciferase reporter gene assays at hTRβ_1 (see Appendix A). Analogues with electron donating character generally have agonist activity, while those with electron withdrawing character are non-agonists. [*] indicates data obtained using media supplemented with 10% heat-treated (80°C, 20 min.) newborn calf serum. (B) Dose-response curves of mixed agonist/antagonist NH-8 and NH-14 at hTRβ_1 with and without 2 nM T_3. NH-8 and NH-14 induced approximately 40% transactivation relative to 2 nM T_3. In competition assays, the compounds blocked T_3-induced transactivation to the level of activation observed for compound alone. (C) Dose-response curves of NH-3, NH-5, NH-7 and NH-23 at hTRβ_1 in competition with 2 nM T_3. NH-9 and NH-11 show similar competition dose-response curves (data not shown). These compounds failed to induce transactivation and completely inhibited the T_3-induced response to the level of ethanol vehicle control. IC_{50} values under these conditions are shown in Table 1. Transactivation induced by 2 nM T_3 is defined as 100% maximal luciferase activity. Values are the mean $\pm$ SD for three separate experiments. Dose-response data were fitted by nonlinear regression using the Graph Pad Prism computer program (Graph Pad Software Inc.) for a single site competition model to generate IC_{50} values.

4.2.3 Effect of Antagonists on TR interaction with NCoR and GRIP-1

The full antagonists **NH-5**, **NH-7**, **NH-9**, **NH-11**, and **NH-23** were tested for their affect on TR interaction with coactivator GRIP-1 and corepressor NCoR in mammalian two hybrid assays. HeLa cells were transiently transfected with expression plasmids for the yeast GAL4 DBD linked to either NCoR (*aa*1925-2308) or GRIP-1 (*aa*618-1121), hTRβ-LBD fused to the VP16 activation domain, and a GAL4-driven luciferase reporter (see Appendix A).[1] As shown in Figure 4-3A, the 5'-phenylethynyl antagonists failed to stimulate binding of GRIP-1 to TR. The analogues also blocked 10 nM T_3-induced TR-GRIP-1 interactions albeit with weak potency. Increasing antagonist concentration led to decreased T_3-induced TR-coactivator interaction. Dose-response curves could not be obtained due to concentration and toxicity limitations. As with **NH-3**, the inability of these compounds to promote interaction between TR and its target coactivators is one of the underlying mechanisms for their observed antagonist activities.

We then examined the ability of the analogues to promote release of NCoR upon binding to TR. Like T_3 and **GC-1**, the antagonists induced TR-NCoR dissociation in a dose-dependent manner (Figure 4-3B,C). The IC_{50} values of TR-NCoR interaction with bound **GC-1** versus bound 5'-phenylethynyl analogues vary by at least one order of magnitude, consistent with the difference in their relative binding affinities for TR. These results suggest that in the presence of **NH-5**, **NH-7**, **NH-9**, **NH-11**, and **NH-23**, TR adopts an inactive conformation where neither corepressors nor coactivators are recruited and TR transcriptional activity is nullified. This mechanism of action is not unique to **NH-3** and can be generalized to the class of 5'-*para*-substituted phenylethynyl derivatives bearing 5'-electron-withdrawing substituents.

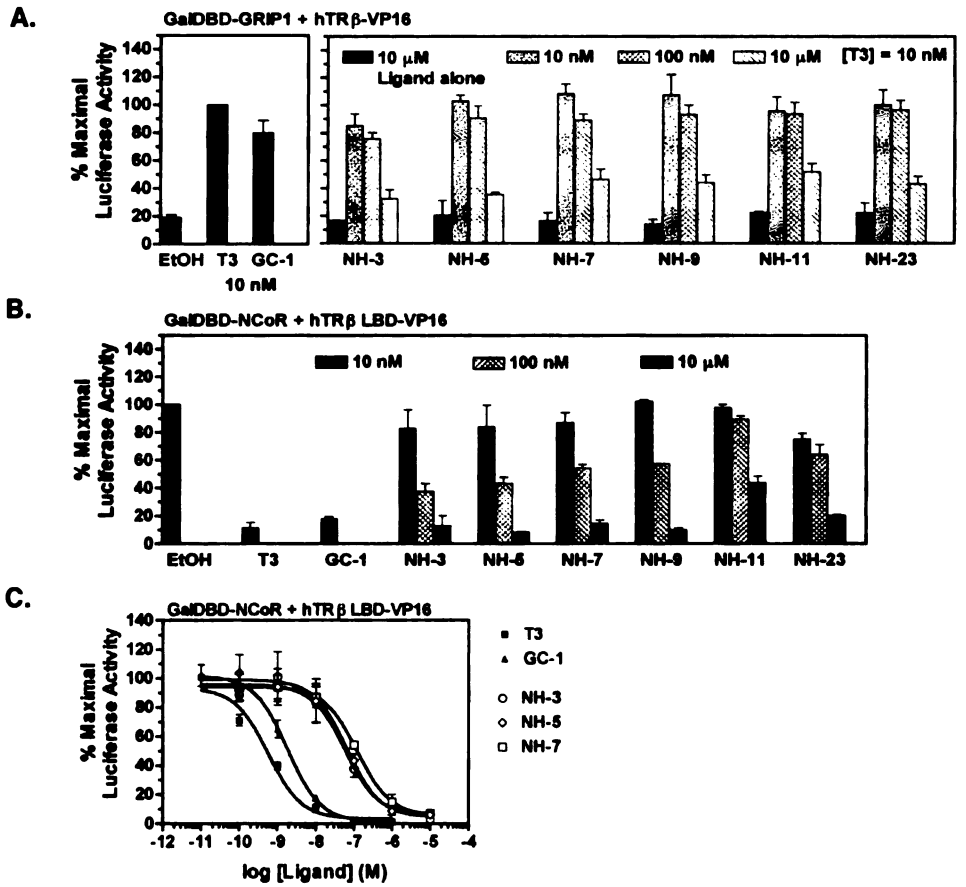

Figure 4-3. Affect of antagonists NH-3, NH-5, NH-7, NH-9, NH-11 and NH-23 on TR interactions with corepressor and coactivator in mammalian two-hybrid assays (see Appendix A). (A) At 10 μM concentration, the antagonists fail to recruit GRIP-1 to TR. However, increasing antagonist concentration inhibited with micromolar potency the TR-GRIP-1 interactions induced by 10 nM T_3. Competition dose-response curves could not be obtained due to concentration and toxicity limits. TR-GRIP-1 interaction in the presence of 10 nM T_3 is defined as 100% maximal luciferase activity. (B) Like T_3 and GC-1, the antagonists were able to promote NCoR dissociation from TR in a dose-dependent manner. (C) NH-3, NH-5, and NH-7 inhibited TR-NCoR interaction by 50% (IC_{50}) at 58 nM, 64 nM and 120 nM, respectively. TR-NCoR interaction in the presence of ethanol vehicle control is defined as 100% maximal luciferase activity. All values are expressed as the mean ± SD for three separate experiments. IC_{50} values were calculated using the Graph-Pad computer program (Graph-Pad Software Inc.) by nonlinear regression of a sigmoid dose-response model.

4.2.4 Hammett Analysis

Based on the transactivation data of the 5'-*para*-substituted phenylethynyl derivatives, we generated a Hammett semi-log plot of relative ligand potency [log (IC_{50H} / IC_{50X})] versus the Hammett σ substituent value[20,21] (Figure 4-4A). A general trend was observed between the +σ value of substituted aromatics and ligand antagonist activity where greater electron withdrawing character translated to improved antagonist potency.

For example, **NH-5** (σ = +0.54) possessed greater electronic character relative to **NH-11** (σ = +0.06) and exhibited stronger antagonist potency. **NH-3** had the greatest +σ value (σ = +0.78) for the 5'-phenylethynyl derivatives and remained the most potent TR antagonist reported. Qualitative Hammett analysis of –σ value and relative ligand potency revealed no significant correlation (data not shown); however, compounds bearing an EDG such as **NH-1**, **NH-2**, **NH-6**, and **NH-24** had partial or full agonist activity.

While trends were observed between electronic character and TR modulation, Hammett analysis suggests additional factors are important for antagonist activity. In particular, analogue **NH-7** (σ = +0.08) had comparable electronic character yet exhibited nearly 7-fold improved potency relative to **NH-11** (σ = +0.06). Extending the azido group of **NH-7** by one carbon from the 5'-aryl ring, as with **NH-23**, significantly reduced the electronic contribution of the azido group to the aryl extension but resulted in a slight 2-fold decrease in antagonist potency. These results imply the azido group may be involved in specific interactions with receptor residues to stabilize an inactive receptor conformation.

Similar Hammett analysis of the relative ligand binding affinity [log (K_{dH}/K_{dX})] versus the σ parameter revealed no significant correlation between binding affinity and electronic character of the 5'-aryl extension (Figure 4-4B). The presence of a strong EDG or EWG did not improve nor impair binding. For example **NH-6** (σ = -0.27) has electron donating character while **NH-3** (σ = +0.78) and **NH-5** (σ = +0.54) have electron withdrawing character, yet these compounds had comparable binding affinity and selectivity to TRβ (Table 4-1). Lack of correlation between binding affinity and electronic properties of the 5'-aryl extension suggests that altering the electronic properties

primarily affects TR functional activity through downstream transactivation signaling events.

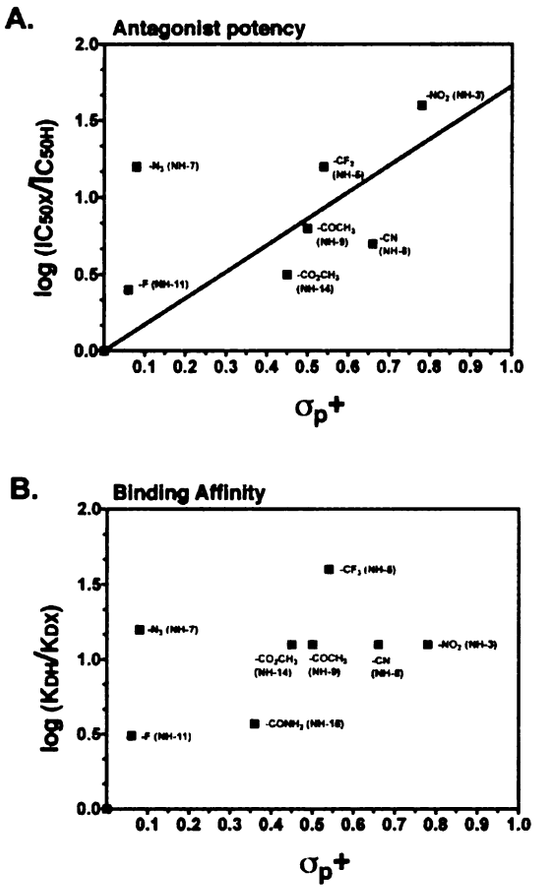

Figure 4-4. (A) Hammett analysis of electronic character ($+\sigma_p$) and relative transcriptional activity (log IC_{50H}/IC_{50X}) showed improved antagonist potency with increased electron withdrawing character of the 5'-*para*-substituted aryl extension. (B) Hammett analysis of electronic character ($+\sigma_p$) and relative binding affinity (log K_{DH}/K_{DX}) revealed no correlation between the two parameters. Hammett σ substituent values were based on values reported by Hansch, et al. and Jaffe.[20,21] IC_{50H} was assigned a value of 10 μM.

4.3 Discussion

In the present study we evaluated the significance and role of the 5'-*p*-nitroaryl moiety of **NH-3** for T_3 antagonist activity. We synthesized a series of 5'-phenylethynyl **GC-1** derivatives varying in size and electronic property. All analogues bound TRα and TRβ with moderate nanomolar affinity and 4-fold to 20-fold TRβ selectivity (Table 4-1).

In transactivation assays with TRβ (Figure 4-2), **NH-1**, **NH-2**, **NH-6**, **NH-16**, and **NH-24** had partial agonist activity while **NH-8** and **NH-14** exhibited mixed agonist/antagonist activity. **NH-5**, **NH-7**, **NH-9**, **NH-11**, and **NH-23** were full antagonists with reduced potency relative to **NH-3**.

We further tested the affect of the antagonists **NH-5, NH-7, NH-9, NH-11** and **NH-23** on TR interactions with NCoR and GRIP-1 (Figure 4-3). Similar to **NH-3**, these compounds functioned like agonists to promote corepressor release from TR but failed to induce recruitment of coactivators to TR. Thus, the 5'-phenylethynyl derivatives containing *para*-substituted EWG are a unique class of STRMs that effectively induce a chemical TR knockout by preventing TR-mediated hormone transactivation and relieving transrepression of positively regulated target gene expression.

These results indicate that simple steric blockade of H12 packing with large hydrophobic extensions alone, as with **NH-2**, are not sufficient to confer antagonism. Closer analysis of the chemical features important for TR modulation by Hammett correlation between TR-mediated ligand activity and electronic character revealed 5'-aryl extensions with EDG (-σ value) had agonist activity while those carrying charge neutral EWG (+σ value) had antagonist activity (Figure 4-4A). Moreover, greater antagonist potency was observed with greater electron withdrawing character (greater +σ value) as with **NH-3**, **NH-5**, and **NH-7**. **NH-3** had the greatest +σ value in this class of compounds and remained the most potent T_3 antagonist. The combined SAR data reveal the 5'-*p*-nitroaryl moiety was not required for antagonism. However, substitution with a strong EWG on the 5'-aryl extension was essential for antagonist activity.

Hammett analysis of the ligand binding affinity relative to the σ substituent values confirmed that varying the electronic character of the ligand predominantly affects the downstream signaling interactions of TR and not binding. As shown in Figure 4B,

there was variability in the binding affinities of the 5'-phenylethynyl derivatives but no correlation was observed between electronic property and binding. Compounds having EDG aryl extensions bound TR with similar affinities as those bearing EWG. Moreover, stronger electronic character does not enhance binding affinity.

Our data further lends support to the observation that the nature and position of the 5'-aryl substituent is critical for T_3 antagonist activity and potency. Analogues with EWG in the *ortho*- or *meta*-positions exhibited significantly reduced antagonist potency as seen with analogues **NH-17**, **NH-18** and **NH-19** compared to the *para*-substituted counterparts **NH-3** and **NH-5**. This result can partially be accounted for by the reduction in electronic contribution to the aryl extension in the *meta*- and *ortho*-positions relative to the *para*-position.[20] However, compounds with weaker *para*-electron withdrawing substituents, such as **NH-7** and **NH-23**, also displayed full antagonist activity indicating electronic properties alone do not dictate antagonism. The azido groups of **NH-7** and **NH-23** may be involved in stabilizing an inactive TR conformation.

To rationalize the molecular basis of antagonism for this class of STRMs, the 5'-phenylethynyl extension was modeled into the TR ligand binding pocket based on the X-ray crystal structure of **GC-1** bound to hTRβ-LBD.[3,18] Modeling revealed that the 5'-extension clashed with numerous receptor residues in the active conformation, including Phe455 and Phe459 of helix H12. Our results suggest that, in addition to sterically perturbing proper folding and rearrangement of H12, the EWG on the 5'-aryl extension promotes favorable aromatic π-interactions (center-to-edge, edge-to-face, and/or face-to-face)[4] with the phenylalanine residues to stabilize an inactive receptor conformation. Given that the 5'-phenylethynyl **GC-1** antagonists induce a conformation that occluded binding of both coactivators and corepressors, the ligand extension may induce a conformation of H12 that packs against the hydrophobic groove where the coactivator and corepressor binding sites overlap.[22-24] This mode of "active antagonism"[25] is similar

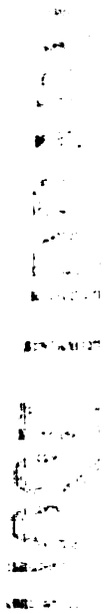

to that observed for the estrogen receptor (ER) bound to selective ER modulators (SERMs) raloxifene[26] and 4-hydroxytamoxifen[27] where H12 adopts an auto-inhibitory conformation to compete with coactivator recruitment by mimicking the interactions of the coactivator with the ER-LBD.

In summary, the results of this study confirmed our hypothesis that the 5'-*p*-nitroaryl extension is not required for antagonism and that the size, position, and electronic nature of the 5'-aryl extension will dictate a spectrum of agonist and antagonist activity. A better understanding of the pharmacophore important for T_3 antagonism will be useful for the development of therapeutics for the treatment of diseases associated with excessive thyroid hormone production and action such as hyperthyroidism (thyrotoxicosis).[28] Furthermore, TR subtype-selective STRMs will be useful pharmacological probes for studying thyroid hormone signaling pathways.

4.4 Acknowledgments

We gratefully thank our collaborators in the Baxter Lab at UCSF for their contributions to this project. Dr. Jim Apriletti performed the *in vitro* binding assays. Dr. Suzana Cunha-Lima and Dr. Paul Webb provided expertise and resources in the mammalian two-hybrid. We also thank Dr. R. Evans and Dr. D. Moore for the gifts of plasmids used in the transfection assays. This work was supported by grants from the National Institutes of Health (Grant DK52798 to T.S.S; Grant DK41842 to J.D.B).

4.5 References

(1) Nguyen, N. H.; Apriletti, J. W.; Cunha Lima, S. T.; Webb, P.; Baxter, J. D. et al. Rational design and synthesis of a novel thyroid hormone antagonist that blocks coactivator recruitment. *J. Med. Chem.* **2002**, *45*, 3310-3320.

(2) Chiellini, G.; Nguyen, N. H.; Apriletti, J. W.; Baxter, J. D.; Scanlan, T. S. Synthesis and biological activity of novel thyroid hormone analogues: 5'-aryl substituted GC-1 derivatives. *Bioorg. Med. Chem.* **2002**, *10*, 333-346.

(3) Yoshihara, H. A.; Nguyen, N. H.; Scanlan, T. S. Design and synthesis of receptor ligands. *Methods Enzymol.* **2003**, *364*, 71-91.

(4) Cozzi, F.; Annunziata, R.; Benaglia, M.; Cinquini, M.; Raimondi, L. et al. Through-space interactions between face-to-face, center-to-edge oriented arenes: importance of polar-pi effects. *Org Biomol Chem* **2003**, *1*, 157-162.

(5) Nguyen, N. H.; Apriletti, J. W.; Scanlan, T. S. Hammett analysis of selective thyroid hormone modulators reveal structural and electronic requirements for hormone antagonists. *J Am Chem Soc* **2004**, *Submitted for publication.*

(6) Soderquist, J. A.; Matos, K.; Rane, A.; Ramos, J. Alkynylboranes in the Suzuki-Miyaura Coupling. *Tetrahedron Lett.* **1995**, *36*, 2401-2402.

(7) Takahashi, S.; Kuroyama, Y.; Sonogashira, K.; Hagihara, N. Convenient synthesis of ethynylarenes and diethynylarenes. *Synthesis Comm.* **1980**, 627-629.

(8) Suzuki, N.; Kaneko, Y.; Nomoto, T.; Izawa, Y. Synthetic reactions in polyethylene glycol. Diazotization and Sandmeyer Reactions of anilines in polyethylene glycol-methylene dichloride. *J. Chem. Soc. Chem. Commun.* **1984**, 1523-1524.

(9) Suzuki, N.; Azuma, T.; Kaneko, Y.; Izawa, Y.; Tomioka, H. Diazotization and Sandmeyer Reactions of arylamines in poly(ethylene glycol)-methylene

dichloride: usefulness of PEG in synthetic reactions. *J. Chem. Soc. Perkin Trans. I* **1987**, 645-647.

(10) Tanno, M.; Sueyoshi, S.; Kamiya, S. Synthesis of arylcyanotriazenes and related compounds. *Chem. Pharm. Bull.* **1982**, *30*, 3125-3132.

(11) Oya, S.; Choi, S. R.; Coenen, H.; Kung, H. F. New PET imaging agent for the serotonin transporter: [(18)F]ACF (2-[(2-amino-4-chloro-5-fluorophenyl)thio]-N,N-dimethyl-benzenmethanamine). *J. Med. Chem.* **2002**, *45*, 4716-4723.

(12) Craig, J. C.; Purushothaman, K. K. An improved preparation of tertiary amine N-oxides. *J. Org. Chem.* **1970**, *35*, 1721-1722.

(13) Vogl, E. M.; Buchwald, S. L. Palladium-catalyzed monoarylation of nitroalkanes. *J. Org. Chem.* **2002**, *67*, 106-111.

(14) Smith, M. B.; March, J. Hydrolysis of Aliphatic Nitro Compounds. *March's Advanced Organic Chemistry*; 5th ed.; Wiley-Interscience: New York, 2001; pp 1178-1179.

(15) Snyder, D. C. Conversion of alcohols to chlorides by TMSCl and DMSO. *J. Org. Chem.* **1994**, *60*, 2638-2639.

(16) Alvarez, S. G.; Alvarez, M. T. A practical procedure for the synthesis of alkyl azides at ambient temperature in dimethyl sulfoxide in high purity and yield. *Synthesis* **1997**, 413-414.

(17) Swillens, S. Interpretation of binding curves obtained with high receptor concentrations: practical aid for computer analysis. *Mol. Pharmacol.* **1995**, *47*, 1197-1203.

(18) Wagner, R. L.; Huber, B. R.; Shiau, A. K.; Kelly, A.; Cunha Lima, S. T. et al. Hormone selectivity in thyroid hormone receptors. *Mol. Endocrinol.* **2001**, *15*, 398-410.

(19) Yoshihara, H. A.; Apriletti, J. W.; Baxter, J. D.; Scanlan, T. S. Structural determinants of selective thyromimetics. *J. Med. Chem.* **2003**, *46*, 3152-3161.

(20) Hansch, C.; Leo, A.; Taft, R. W. A survey of Hammett substituent constants and resonance and field parameters. *Chem. Rev.* **1991**, *91*, 165-195.

(21) Jaffe, H. H. A reexamination of the Hammett equation. *Chem. Rev.* **1953**, *53*, 191-261.

(22) Marimuthu, A.; Feng, W.; Tagami, T.; Nguyen, H.; Jameson, J. L. et al. TR surfaces and conformations required to bind nuclear receptor corepressor. *Mol. Endocrinol.* **2002**, *16*, 271-286.

(23) Darimont, B. D.; Wagner, R. L.; Apriletti, J. W.; Stallcup, M. R.; Kushner, P. J. et al. Structure and specificity of nuclear receptor-coactivator interactions. *Genes and Development* **1998**, *12*, 3343-3356.

(24) Perissi, V.; Staszewski, L. M.; McInerney, E. M.; Kurokawa, R.; Krones, A. et al. Molecular determinants of nuclear receptor-corepressor interaction. *Genes and Development* **1999**, *13*, 3198-3208.

(25) Shiau, A. K.; Barstad, D.; Radek, J. T.; Meyers, M. J.; Nettles, K. W. et al. Structural characterization of a subtype-selective ligand reveals a novel mode of estrogen receptor antagonism. *Nat. Struct. Biol.* **2002**, *9*, 359-364.

(26) Brzozowski, A. M.; Pike, A. C.; Dauter, Z.; Hubbard, R. E.; Bonn, T. et al. Molecular basis of agonism and antagonism in the oestrogen receptor. *Nature* **1997**, *389*, 753-758.

(27) Shiau, A. K.; Barstad, D.; Loria, P. M.; Cheng, L.; Kushner, P. J. et al. The structural basis of estrogen receptor/coactivator recognition and the antagonism of this interaction by tamoxifen. *Cell* **1998**, *95*, 927-937.

(28) Utiger, R. D. The thyroid: physiology, thyrotoxicosis, hypothyroidism, and the painful thyroid. *Endocrinology and Metabolism*; McGraw-Hill: New York, 1995; pp 435-519.

Conclusions and Future Directions

Currently, there is no clear-cut recipe for designing antagonist ligands for nuclear receptors. Given the available SAR and structural information, important general considerations can be made to help direct rational ligand design. For antagonist ligands, as well as agonist ligands, filling ligand binding pocket volume and satisfying key polar interactions for molecular recognition are critical for receptor-selectivity, ligand-binding, and activity. Unlike agonist ligands, antagonist ligands have an addition hydrophobic extension stemming from an agonist scaffold, as described by the "extension hypothesis". We have had success using guiding principles from crystal structures combined with standard medicinal chemistry to develop selective thyroid hormone (T_3) receptor modulating (STRM) antagonists. **NH-3** is the most potent *in vitro* and *in vivo* antagonist reported to date. While the "extension hypothesis" appears broadly applicable for antagonist design, the nature of the chemical groups on the ligand extension are important in establishing specific interactions with receptor residues to help stabilize an inactive receptor conformation. However, without additional structural data, these putative interactions are ill-defined. It is difficult at present to predict what ligand extensions moieties will induce antagonism. We have found that simple steric blockade with large hydrophobic extensions is not sufficient to confer T_3 antagonist activity. Instead, correctly positioned groups of the correct chemistry, specifically 5'-aryl extensions containing electron withdrawing groups (EWG), are required to block T_3 action. Thus, the results presented herein may serve as starting points in the design of new TR modulators.

Based on our current understanding of NR function, antagonist ligands can potentially function through several mechanisms: (1) enhance NR corepressor binding,

(2) prevent NR coactivator recruitment, (3) disrupt NR dimerization, (4) disrupt NR interaction with DNA, (5) reducing NR half-life, or (6) a combination of these mechanisms. We have shown one possible mode of antagonism by the class of 5'-phenylethynyl derivatives is by preventing coactivator recruitment to TR. Additionally, these compounds are unique in that they can induce corepressor release from TR and thereby alleviate the transcriptional transrepression effect associated with unliganded TR. Thus, these compounds are useful pharmacological tools to effectively induce a chemical TR knockout to neutralize TR-mediated gene expression. Whether these compounds also elicit antagonistic activity by other mechanisms remains to be studied.

Developing a panel of antagonist ligands that function through various mechanisms will be instrumental in furthering our understanding of thyroid hormone signaling pathways. More SAR and structural data are needed to better define the recipe for developing antagonists. A useful feature of the rigid ethynyl linker between the 5'-aryl extension and the **GC-1** scaffold is that it can be reduced to the ethylene or saturated ethyl moiety. This allows access to a series of derivatives that can sample a conical space and explore alternative interactions with the receptor residues, which may enhance the potency and efficacy of the existing antagonists for improved therapeutic utility.

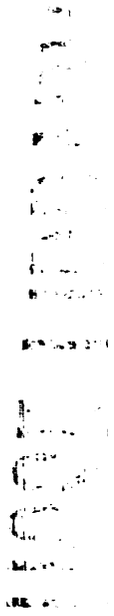

Appendix A

Experimental Procedures

A.1 Chemistry

A.1.1 General Methods, Chapter 3

^{1}H and ^{13}C NMR were recorded on the Varian Utility 400MHz spectrometer, in $CDCl_3$ or CD_3OD solvent. Chemical shifts were reported as parts per million downfield from an internal tetramethylsilane standard (δ = 0.0 for ^{1}H NMR) or from solvent references. HRMS was performed by the Biomedical Mass Spectrometry Resource at UCSF, or the Mass Spectrometry Facility at UC Berkeley. Anhydrous solvents and starting reagents were commercially available and used without further purification. Glassware was oven- or flame-dried prior to use. Reactions were performed under argon inert atmosphere. Crude products were purified by either flash chromatography using 230-400 mesh silica gel or preparative TLC (Aldrich Chemical Co.). Target compounds were analyzed for purity by analytical HPLC, which was performed using Rainin HP controller and Varian UV detector with an Alltech Hypersil 100 Silica column (250mm x 4.6mm). Condition A: isocratic 60% (v/v) hexanes (spiked with 0.5% TFA) in ethyl acetate; Condition B: isocratic 1% (v/v) MeOH (spiked with 0.5% TFA) in CH_2Cl_2.

A.1.2 General Methods, Chapter 4

^{1}H and ^{13}C NMR were recorded on the Varian Utility 400MHz spectrometer, in $CDCl_3$, CD_3OD, or *d*-DMSO solvent. Chemical shifts were reported as parts per million (ppm) downfield from an internal tetramethylsilane standard (δ = 0.0 for ^{1}H NMR) or from solvent references. High-resolution mass spectrometry (HRMS) using electrospray ionization (EI) was performed by the National Bio-Organic, Biomedical Mass Spectrometry Resource at UCSF, or the Mass Spectrometry Facility at UC Berkeley. Glassware was oven- or flame-dried prior to use. Reactions were performed under

argon inert atmosphere that was passed through a Drierite drying tube. Dichloromethane, dimethylformamide, methanol, tetrahydrofuran, and toluene were dried using the procedure recommended by Grubbs using the solvent purification system manufactured by Glass Contour, Inc. (Laguna Beach, CA). Prior to installation of the purification system and all other anhydrous solvents were purchased from Aldrich Chemical Company. Commercially available starting reagents were used without further purification. Crude products were purified by either flash chromatography using 230-400 mesh silica gel (Aldrich Chemical Co.) or 40-63 μm EMD (Geduran Silica Gel 60, VWR International) or preparative TLC (Aldrich Chemical Co.). For final compounds, purity was assessed as 95% pure or greater by NMR analysis.

A.1.3 Synthesis

4-Bromo-2-isopropyl phenyl methoxymethyl ether (1). 4-Bromo-2-isopropylphenol (22.0 g, 0.120 mol) was added dropwise to a slurry of sodium hydride pellets (3.70 g, 0.128 mol) in dimethylformamide (100 ml) at room temperature. Stirring at this temperature was continued until the evolution of hydrogen ceased (20 min). Monochloromethylether (9.47 g, 0.117 mol) was then added during 30 min and stirring was continued for an additional 30 min after which excess sodium hydride was destroyed by cautious addition of methanol (30 ml). The reaction mixture was diluted with 200 ml of ether and washed with of water (3×100 ml) and of brine (5×100 ml). The organic portion was dried over $MgSO_4$, filtered, and evaporated to give an oil, which was purified by flash column chromatography (5% ethyl acetate in hexanes) to give 24.0 g of pure product (90% yield). ^{1}H NMR ($CDCl_3$, 300 MHz, δ): 1.2 (d, 6H, J = 6.9 Hz), 3.29 (heptet, 1H, J = 6.9 Hz), 3.47 (s, 3H), 5.17 (s, 2H), 6.94 (d, 1H, J = 8.7 Hz), 7.22 (dd, 1H, J = 8.7, 2.7 Hz), 7.30 (d, 1H, J = 2.7 Hz). ^{13}C NMR ($CDCl_3$, 300 MHz, δ): 22.6, 26.9,

56.03, 94.5, 114.4, 115.7, 129.2, 139.9, 153.4. HR-MS calcd for $C_{11}H_{15}O_2Br$: 258.0255, found: 258.0253.

O-Triisopropylsilyl-4-bromo-3,5-dimethylphenol (2). A solution of 4-bromo-3, 5-dimethyl-phenol (30 g, 0.149 mol), imidazole (25.3 g, 0.327 mol), and triisopropylsilyl chloride (27.3 g, 0.142 mol) in CH_2Cl_2 (300 ml) was stirred for 1 h. The reaction mixture was diluted with 600 ml of CH_2Cl_2, washed with water (500 ml), brine (500 ml), dried ($MgSO_4$), filtered and evaporated to give an oil, which was purified by flash column chromatography (10% ethyl acetate in hexanes) to give 43.4 g of product as an oil (81% yield). ^1H NMR ($CDCl_3$, 300 MHz, δ): 1.09 (d, 18H, *J* = 6.9 Hz), 1.26 (m, 3H), 2.34 (s, 6H), 6.61 (s, 2H). ^{13}C NMR ($CDCl_3$, 300 MHz, δ): 12.7, 17.7, 23.9, 117.5, 119.6, 138.9, 155.9. HR-MS calcd for $C_{17}H_{29}OBrSi$: 358.1150, found: 358.1144.

2,6-Dimethyl-4-O-triisopropylsilylbenzaldehyde (3). To **2** (30 g, 0.084 mol) in 200 ml of tetrahydrofuran at -78°C was added n-butyllithium (2.0 M, 92 ml). The reaction mixture was stirred for 30 min at -78°C and then for 1.5 h at rt., diluted with 200 ml of ether, and washed with 100 ml of water, acidified with 1N HCl, and washed with 5x50 ml of brine. The organic portion was dried ($MgSO_4$), filtered, and evaporated to give the crude product, which was purified by flash column chromatography (10% ethyl acetate in hexanes) to yield the desired product as a clear oil (18 g, 70% yield). ^1H NMR ($CDCl_3$, 300 MHz, δ): 1.1 (d, 18H, *J* = 6.9 Hz), 1.26 (m, 3H), 2.57 (s, 6H), 6.56 (s, 2H), 10.47 (s, 1H). ^{13}C NMR ($CDCl_3$, 300 MHz, δ): 12.6, 17.8, 20.9, 119.5, 120.8, 144.4, 159.8, 191.8. HR-MS calcd for $C_{18}H_{30}O_2Si$: 306.2015, found: 306.2014.

3,5-Dimethyl-4-(3'-isopropyl-4'-O-methoxymethylbenzylhydroxy)-O-triisopropyl-silyl-phenol (4). To **1** (10 g, 0.038 mol) in 100 ml of THF at -78°C was added *n*-butyllithium (2.0 M, 29 ml) and the reaction mixture was stirred for 30 min at -78°C under argon. The aldehyde **3** (11.8 g, 0.039 mol) in THF anhydrous (100 ml) was added and the mixture was stirred for 1 h at -78°C and for 6 h at rt. Then, the reaction mixture was diluted with 150 ml of ether, washed with 200 ml of water and 5×50 ml of brine. The combined extracts were dried over $MgSO_4$, filtered, and evaporated to give the crude product, which was purified by flash chromatography (10% ethyl acetate in hexanes) to yield **4** (12 g, 68% yield) as an oil. ^{1}H NMR ($CDCl_3$, 300 MHz, δ): 1.1 (d, 18H, *J* = 6.9 Hz), 1.2 (dd, 6H, *J* = 6.6, 6.9 Hz), 1.26 (m, 3H), 2.20 (s, 6H), 3.3 (heptet, 1H, *J* = 6.9 Hz), 3.48 (s, 3H), 5.17 (s, 2H), 6.22 (s, 1H), 6.55 (s, 2H), 6.93 (m, 2H), 7.15 (s, 1H). ^{13}C NMR ($CDCl_3$, 300 MHz, δ): 12.7, 17.7, 20.8, 22.7, 27.0, 31.6, 56.03, 70.9, 94.63, 113.6, 120.4, 123.7, 132.2, 136.4, 137.2, 138.4, 153.1, 154.9. HR-MS calcd for $C_{29}H_{46}O_4Si$: 486.3165, found: 486.3159.

3,5-Dimethyl-4-(3'-isopropyl-4'-O-methoxymethylbenzyl)-O-triisopropylsilylphenol (5). A solution of **4** (7.3 g, 0.015 mol) in 50 ml of 9% (v/v) AcOH in EtOH containing 10% Pd/C (500 mg) was hydrogenated at 1 atm at rt. When hydrogen uptake was complete (12 h), the catalyst was filtered off and the filtrate was diluted with 250 ml of ether, washed with sat. $NaHCO_3$ solution (3×50 ml), dried over $MgSO_4$ and concentrated *in vacuo*. The solvent was evaporated to yield 5.65 g (0.012 mol, 80%) of **5** as an oil. This material was used in the next step without further purification. ^{1}H NMR ($CDCl_3$, 300 MHz, δ): 1.1 (d, 18H, *J* = 6.9 Hz), 1.16 (d, 6H, *J* = 6.9 Hz), 1.23 (m, 3H), 2.16 (s, 6H), 3.27 (heptet, 1H, *J* = 6.9 Hz), 3.48 (s, 3H), 3.91 (s, 2H), 5.15 (s, 2H), 6.59 (s, 2H), 6.67 (dd, 1H, *J* = 2.4, 8.4 Hz), 6.9 (m, 2H). ^{13}C NMR ($CDCl_3$, 300 MHz, δ): 12.7, 17.0, 20.32,

22.78, 26.9, 33.73, 55.97, 94.71, 113.9, 119.4, 125.5, 129.8, 133.4, 137.3, 138.1, 152.4, 153.8. HR-MS calcd for $C_{29}H_{46}O_3Si$: 470.3216, found 470.3194.

[3,5-Dimethyl-4-(3'-isopropyl-4'-O-methoxymethylbenzyl)-phenoxy]-tert-butyl-acetate (6). Compound **5** (4 g, 8.5 mmol) and tetrabutylammonium fluoride (1.0 M, 10.6 ml) were combined in a round-bottom flask. Deprotection was determined to be nearly instantaneous by TLC. The reaction mixture was diluted with ethyl acetate (100 ml) and washed with water (2×75 ml) and brine (100 ml), dried and concentrated. The crude product was purified by flash column chromatography (20% ethyl acetate in hexanes) to yield the desired phenol (2.40 g, 90% yield). ^{1}H NMR ($CDCl_3$, 300 MHz, δ): 1.17 (d, 6H, J = 6.9 Hz), 2.18 (s, 6H), 3.28 (heptet, 1H, *J* = 6.9 Hz), 3.47 (s, 3H), 3.89 (s, 2H), 5.15 (s, 2H), 6.55 (s, 2H), 6.65 (dd, 1H, *J* = 2.4, 8.4 Hz), 6.88 (d, 1H, *J* = 8.4 Hz), 6.94 (d, 1H, *J* = 2.4 Hz). ^{13}C NMR ($CDCl_3$, 300 MHz, δ): 20.52, 23.01, 27.18, 33.9, 56.2, 94.88, 114.2, 114.9, 125.5, 126.1, 129.8, 133.5, 137.6, 138.8, 153.6. HR-MS calcd for $C_{20}H_{26}O_3$: 314.1882, found 314.1869.

To cesium carbonate (10.4 g, 32 mmol) and the phenol (2 g, 6.4 mmol) in 50 ml of DMF was added tert-butylchloroacetate (1.2 g, 8 mmol). The reaction mixture was stirred for 30 min at room temperature, poured into 100 ml of cold 1N HCl, and extracted with ethyl acetate (3×100 ml). The combined organic portions were dried ($MgSO_4$) and evaporated to yield 3.0 g of crude, which was purified using flash column chromatography (10% ethyl acetate in hexanes) to yield **6** (2.50 g, 90% yield). ^{1}H NMR ($CDCl_3$, 300 MHz, δ): 1.16 (d, 6H, *J* = 6.9 Hz), 1.50 (s, 9H), 2.2 (s, 6H), 3.27 (heptet, 1H, *J* = 6.9 Hz), 3.47 (s, 3H), 3.90 (s, 2H), 4.49 (s, 2H), 5.14 (s, 2H), 6.61 (s, 2H), 6.67 (s, 1H), 6.9 (m, 2H). ^{13}C NMR ($CDCl_3$, 300 MHz, δ): 20.73, 23.01, 27.18, 28.28, 29.92, 34.01, 56.2, 82.35, 94.89,

114.2, 125.6, 126.1, 120.64, 133.37, 137.6, 138.61, 152.7, 156.09, 168.57. HR-MS calcd for $C_{26}H_{36}O_5$: 428.2563, found 428.2567.

[3,5-Dimethyl-4-(4'-hydroxy-3'-isopropylbenzyl)-phenoxy]-acetic acid (GC-1). To the ester **6** (2.0 g, 4.7 mmol) in 40 ml of a 50% (v/v) mixture of *i*-PrOH and THF was added 2.0 ml of 1N HCl. The reaction mixture was stirred for 2 h at rt., diluted with 50 ml of water and extracted with ethyl acetate (2×75 ml). The combined organic portions were dried ($MgSO_4$) and evaporated to yield 1.70 g of the corresponding *O*-methoxymethyl deprotected phenol, which was used directly in the following step. To the above phenol (1.50 g, 3.9 mmol) in 40 ml of methanol was added 26 ml of 1N NaOH. The reaction mixture was stirred for 1 h at rt., acidified with 30 ml of 2N HCl, and extracted with ethyl acetate (2×100 ml). The combined organic portions were dried ($MgSO_4$) and evaporated to give **GC-1** (1.20 g, 79% yield). ^{1}H NMR (CD_3OD, 300 MHz, δ): 1.15 (d, 6H, *J* = 6.6 Hz), 2.18 (s, 6H), 3.21 (heptet, 1H, *J* = 6.6 Hz), 3.86 (s, 2H), 4.40 (s, 2H), 6.49-6.62 (m, 2H), 6.65 (s, 2H), 6.84 (s, 1H). ^{13}C NMR (CD_3OD, 300 MHz, δ): 20.8, 23.0, 27.6, 34.4, 68.3, 115.2, 115.6, 126.0, 126.4, 126.5, 131.6, 135.6, 139.1, 152.8, 157.0, 177.9. HR-MS calcd for $C_{20}H_{24}O_4$: 328.1675, found: 328.1679.

[4-(3-Iodo-5-isopropyl-4-methoxymethoxy-benzyl)-3,5-dimethyl-phenoxy]-triisopropyl-silane (7). To a solution of 1 (1.2 g, 2.55 mmol) in 30mL of a 2:1 mixture of anhydrous THF/hexanes cooled to –78°C was added *n*-BuLi (2.5 M in hexanes, 5.61 mmol). The resulting mixture was warmed to rt. and after 2 h, it was cooled back to –78°C before N-iodosuccinimide (0.70 g, 3.06 mmol) was added as a solution in THF. The reaction was stirred at rt. for an additional 5 h, then quenched with water and extracted with ethyl acetate (2×20 ml). The organic phase was washed with brine, dried

over $MgSO_4$, filtered and concentrated in vacuo. ^1H NMR of the crude material showed > 60% conversion to the desired product, which has identical Rf to the starting compound **5**. Thus, the desired product was not isolated. Other impurities were removed by flash chromatography (100% hexanes) to give 1.35 g of a 2:1 mixture of product:starting material.

{5'-[2,6-Dimethyl-4-(triisopropyl-silanyloxy)-benzyl]-3-iospropyl-2-methoxy-methoxy-phenyl}-boronic acid (8). A solution of **5** (0.5 g, 1.06 mmol) in 5 ml of a 2:1 mixture of dry THF/hexanes was treated with *n*-BuLi (2.5 M, 2.12 mmol) and the mixture was stirred 2 h at rt. to give a cloudy white suspension. Triisopropyl borate (0.3 ml, 1.2 mmol) was added and the mixture was stirred 1 h at rt. The reaction was quenched by pouring into 1 N HCl aq., extracted with ethyl acetate, dried and filtered. The crude boronic acid **8** was used in subsequent Suzuki coupling reactions without further purification.

General procedure for Suzuki-Miyaura Coupling of Aryl Iodides. To a well-stirred solution of aryl acetylene (1.2 equiv.) in THF at –78°C was added KHMDS (0.5M in toluene, 1.2 equiv.). After 30 min, methoxy-9-BBN (1.0M in hexanes, 1.2 equiv.) was added, and after 2 h, this solution was transferred via cannula to a second solution consisting of $PdCl_2(PPh_3)_2$ (0.3 equiv.) and aryl iodine (1.0 equiv.) in THF. The reaction mixture was heated at reflux for ca. 18 h (overnight), allowed to cool to room temperature and diluted with ethyl acetate (20 ml). The organic phase was washed with water (3×50 ml) and brine (3×50 ml), dried over $MgSO_4$, filtered through Celite, and concentrated *in vacuo*. The crude material was purified by flash chromatography on silica gel.

Triisopropyl-[4-(3-isopropyl-4-methoxymethoxy-5-phenylethynyl-benzyl)-3,5-dimethyl-phenoxy]-silane (9). The coupling of **7** with phenylacetylene (0.06 ml, 0.56 mmol) was effected using the general procedure to afford 202mg (50%, 2 steps from **5**) of the title compound as a colorless oil. ^{1}H NMR ($CDCl_3$, 400MHz, δ): 1.11 (d, 18H, *J* = 7.2Hz), 1.15 (d, 6H, *J* = 6.8Hz), 1.25 (m, 3H), 2.17 (s 6H), 3.40 (heptet, 1H, *J* = 6.8Hz), 3.61 (s, 3H), 3.91 (s, 2H), 5.25 (s, 2H), 6.62 (s, 2H), 6.90 (s, 2H), 7.33 (m, 3H), 7.48 (m, 2H). ^{13}C NMR ($CDCl_3$, 400MHz, δ): 12.7,18.0, 20.4, 23.4, 26.4, 33.7, 57.6, 86.9, 92.7, 99.8, 116.4, 119.6, 123.5, 126.6, 128.3, 129.1, 129.8, 131.4, 136.0, 138.2, 141.9, 153.8, 154.1. HR-MS calcd for $C_{37}H_{50}O_3Si$: 570.3529, found: 570.3528.

4-(3-Isopropyl-4-methoxymethoxy-5-phenylethynyl-benzyl)-3,5-dimethyl-phenol (10). Compound **9** (30mg, 0.05 mmol) and Bu_4NF (1.0 M, 0.8 ml) were combined in 2 ml THF. Deprotection was nearly instantaneous, as determined by TLC. The reaction mixture was diluted with ethyl acetate (10 ml), washed with water (2×15 ml) and brine (2×15 ml), dried over $MgSO_4$, and concentrated. The crude product was purified by flash column chromatography (5% ethyl acetate in hexanes) to yield **10** (19 mg, 87%). ^{1}H NMR ($CDCl_3$, 400 MHz, δ): 1.18 (d, 6H, *J* = 6.8Hz), 2.19 (s, 6H), 3.41 (heptet, 1H, *J* = 6.8Hz), 3.61 (s, 3H), 3.91 (s, 2H), 5.26 (s, 2H), 6.57 (s, 2H), 6.87 (s, 1H), 6.96 (s, 1H), 7.3 (m, 3H), 7.5 (m, 2H). ^{13}C NMR ($CDCl_3$, 400 MHz, δ): 20.3, 23.4, 26.4, 33.7, 57.6, 86.9, 92.8, 99.8, 114.8, 116.5, 123.3, 126.8, 128.2, 128.3, 128.9, 129.6, 131.4, 135.9, 138.7, 141.9, 153.6, 153.8. HR-MS calcd for $C_{28}H_{30}O_3$: 414.2195, found: 414.2181.

[4-(3-Isopropyl-4-methoxymethoxy-5-phenylethynyl-benzyl)-3,5-dimethyl-phenoxy]-acetic acid tert-butyl ester (11). To a dry solution of **10** (15 mg, 0.036 mmol) and Cs_2CO_3 (59 mg, 0.18 mmol) in 2 ml DMF was added *t*-butylchloroacetate (7 μl, 0.045

mmol). The reaction mixture was stirred for 30 min at rt., neutralized with cold 1N aq. HCl to pH 7, and extracted with ethyl acetate (3×10 ml). The combined organic portions were washed with brine (3×15 ml), dried over $MgSO_4$, and concentrated. Crude product was purified by preparative TLC (5% ethyl acetate in hexanes) to yield the MOM-deprotected phenol (16mg, 82%). ^1H NMR ($CDCl_3$, 400 MHz, δ): 1.17 (d, 6H, *J* = 6.8 Hz), 1.49 (s, 9H), 2.21 (s, 6H), 3.41 (heptet, 1H, *J* = 6.8Hz), 3.61 (s, 3H), 3.91 (s, 2H), 4.51 (s, 2H), 5.25 (s, 2H), 6.63 (s, 2H), 6.85 (s, 1H), 6.95 (s, 1H), 7.32 (m, 3H), 7.48 (m, 2H). ^{13}C NMR ($CDCl_3$, 400 MHz, δ): 20.6, 23.4, 26.4, 28.0, 33.8, 57.6, 65.7, 82.2, 86.8, 92.8, 99.8, 114.2, 116.4, 123.3, 126.7, 128.2, 128.3, 129.6, 131.4, 135.8, 138.4, 141,9, 153.9, 156.0, 168.3. HR-MS calcd for $C_{34}H_{40}O_5$: 528.2876, found: 528.2876.

[4-(4-Hydroxy-3-isopropyl-5-phenylethynyl-benzyl)-3,5-dimethyl-phenoxy]-acetic acid (NH-1). To the ester **11** (15 mg, 0.03 mmol) in 1ml of 50% (v/v) mixture of *i*-PrOH and THF was added 1N aq. HCl (60 μl). The reaction mixture was stirred for 6 h at rt., diluted with water, neutralized with 1N aq. NaOH to pH 6, and then extracted with ethyl acetate (2×15 ml). The combined organic portions were dried with $MgSO_4$ and concentrated to yield 14mg of the corresponding *O*-methoxymethyl deprotected phenol, which was used directly in the following step. To the resulting phenol in 1 ml methanol was added 150 μl of 1N aq. NaOH. The reaction mixture was stirred at rt. for 4 h, acidified with 1N aq. HCl to pH 6, and diluted with ethyl acetate (15 ml). The organic portion was extracted with water (2×15 ml) and brine (2×15 ml), dried over $MgSO_4$ and concentrated *in vacuo* to yield 10mg desired product (80% yield, 2 steps) as a yellow solid. ^1H NMR ($CDCl_3$, 400 MHz, δ): 1.22 (d, 6H, *J* = 6.8 Hz), 2.23 (s, 6H), 3.26 (heptet, 1H, *J* = 6.8 Hz), 3.89 (s, 2H), 4.67 (s, 2H), 6.66 (s, 2H), 6.72 (s, 1H), 6.95 (s, 1H), 7.34 (m, 3H), 7.48 (m, 2H). ^{13}C NMR ($CDCl_3$, 400 MHz, δ): 20.6, 22.3, 27.6, 29.7, 33.7, 83.9,

95.9, 108.9, 114.2, 122.5, 127.1, 127.5, 128.5, 128.7, 130.8, 131.4, 131.6, 134.2, 138.9, 152.2, 155.3. HR-MS calcd for $C_{28}H_{28}O_4$: 428.1988, found: 428.1980. HPLC: Condition A, ret. time 4.6 min; Condition B ret. time 4.5 min; 95.2% pure.

[4-(3-Iodo-5-isopropyl-4-methoxymethoxy-benzyl)-3,5-dimethyl-phenoxy]-acetic acid methyl ester (12). Compound **7** (2:1 mixture with **5**, 1.35 g, 2.3 mmol) and Bu_4NF (1.0 M, 3.4 ml) were combined in 30 ml THF. Deprotection was nearly instantaneous, as determined by TLC. The reaction mixture was diluted with ethyl acetate (20 ml), washed with water (2×50 ml) and brine (2×50 ml), dried over $MgSO_4$, and concentrated. Filtration through a silica gel plug (5% ethyl acetate in hexanes) yields the silyl-deprotected phenol (2:1 mixture, 0.72 g). The crude mixture was then dissolved in 20 ml DMF and Cs_2CO_3 (2.7 g, 8.2 mmol) was added, followed by methylbromoacetate (0.2 ml, 2 mmol). The reaction mixture was stirred for 30 min at rt. and then neutralized with cold 1N aq. HCl to pH 7, and extracted with ethyl acetate (3×25 ml). The combined organic portions were washed with brine (3×75 ml), dried over $MgSO_4$, and concentrated. The resulting product was filtered through a silica gel plug (5% ethyl acetate in hexanes) to yield the methyl ester **12** (2:1 mixture, 0.73 g).

{4-[3-(4-Amino-phenylethynyl)-5-isopropyl-4-methoxymethoxy-benzyl]-3,5-dimethyl-phenoxy}-acetic acid methyl ester (13). The ester **12** was used in the Suzuki-Miyaura coupling with 4-ethynylaniline (200mg, 1.7mmol) following the general procedure described above to afford 0.29g (23%, 4 steps from **5**) of the title compound as a yellow oil. ^1H NMR ($CDCl_3$, 400 MHz, δ): 1.17 (d, 6H, J = 7.2 Hz), 2.21 (s, 6H), 3.41 (heptet, 1H, J = 7.2 Hz), 3.60 (s, 3H), 3.82 (s, 3H), 3.90 (s, 2H), 4.63 (s, 3H), 5.24 (s, 2H), 6.60 (d, 2H, J = 8.0 Hz), 6.81 (s, 1H), 6.91 (s, 1H), 7.28 (d, 2H, J = 8.0 Hz). ^{13}C

NMR ($CDCl_3$, 400 MHz, δ): 20.5, 23.3, 26.4, 33.8, 52.2, 57.5, 65.3, 84.6, 93.6, 99.6, 112.7, 114.2, 114.7, 117.0, 126.1, 129.3, 130.1, 132.7, 135.5, 138.6, 141.7, 146.6, 153.6, 155.9, 169.7. HR-MS calcd for $C_{31}H_{35}NO_5$: 501.2515, found: 501.2519.

{4-[3-Isopropyl-4-methoxymethoxy-5-(4-nitro-phenylethynyl)-benzyl]-3,5-dimethyl-phenoxy}-acetic acid methyl ester (14). A solution of *m*-CPBA (60% in mineral oil, 260 mg, 0.90 mmol) in 10 ml $CHCl_3$ was added gradually at 0°C to an ice cooled, stirred solution of **13** (150 mg, 0.30 mmol) in 10ml $CHCl_3$. Stirring was continued for 3 h, during which time the mixture was allowed to come to rt. The reaction was quenched with water (20 ml) and extracted with ethyl acetate (3×25 ml). The combined organic phase was washed with saturated $NaHCO_3$ (3×50 ml), brine (3×50 ml), dried over $MgSO_4$, and concentrated. The crude product was purified by flash column chromatography (10% ethyl acetate in hexanes) to give the nitro compound **14** (97mg, 61% yield) as a bright yellow oil. ^1H NMR ($CDCl_3$, 400 MHz, δ): 1.20 (d, 6H, *J* = 6.8 Hz), 2.22 (s, 6H), 3.41 (heptet, 1H, *J* = 6.8 Hz), 3.61 (s, 3H), 3.93 (s, 2H), 4.64 (s, 2H), 5.23 (s, 2H), 6.65 (s, 2H), 6.85 (s, 1H), 7.05 (s, 1H), 7.62 (d, 2H, *J* = 8.4 Hz), 8.19 (d, 2H, *J* = 8.4 Hz). ^{13}C NMR ($CDCl_3$, 400 MHz, δ): 20.5, 22.2, 23.3, 26.5, 33.7, 52.2, 57.6, 65.2, 90.9, 92.4, 99.9, 114.2, 115.5, 123.6, 128.0, 129.6, 130.3, 132.0, 136.0, 138.6, 142.2, 146.9, 154.3, 156.0, 169.6. HR-MS calcd for $C_{31}H_{35}NO_7$: 531.2257, found: 531.2252.

{4-[4-Hydroxy-3-isopropyl-5-(4-nitro-phenylethynyl)-benzyl]-3,5-dimethyl-phenoxy}-acetic acid (NH-3). To ester **14** (95 mg, 0.18 mmol) in 5 ml of 50% (v/v) mixture of *i*-PrOH and THF was added 1N aq. HCl (0.35 ml). The reaction mixture was stirred for 6 h at rt., diluted with 10 ml of water, neutralized with 1N aq. NaOH to pH 6, and extracted with ethyl acetate (2×15 ml). The combined organic portions were dried

with $MgSO_4$ and concentrated to yield the corresponding *O*-methoxymethyl deprotected phenol. Purification by flash column chromatography (10% ethyl acetate in hexanes) gave the MOM-deprotected phenol (55mg, 63% yield). ^1H NMR ($CDCl_3$, 400 MHz, δ): 1.23 (d, 6H, *J* = 6.8 Hz), 2.22 (s, 6H), 3.26 (heptet, 1H, *J* = 6.8 Hz), 3.82 (s, 3H), 3.90 (s, 2H), 4.64 (s, 2H), 5.68 (s, 1H), 6.65 (s, 2H), 6.71 (s, 1H), 7.02 (s, 1H), 7.64 (d, 2H, *J* = 8.8 Hz), 8.21 (d, 2H, *J* = 8.8 Hz). ^{13}C NMR ($CDCl_3$, 400 MHz, δ): 20.5, 22.2, 27.5, 33.5, 52.2, 65.2, 89.5, 93.9, 107.9, 114.1, 123.7, 127.3, 128.6, 129.4, 130.0, 131.9, 132.1, 134.6, 138.6, 147.1, 152.4, 155.9, 169.7. HR-MS calcd for $C_{29}H_{29}NO_6$: 487.1995, found: 487.1989.

To the above phenol (40 mg, 0.10 mmol) in 3 ml methanol was added $LiOH•H_2O$ (10 mg, 0.22 mmol) and H_2O (10 ml, 0.10 mmol). The reaction mixture was stirred at rt. for 4 h, acidified with 1N aq. HCl to pH 6, and diluted with ethyl acetate (15 ml). The organic portion was extracted with water (2×15 ml) and brine (2×15 ml), dried over $MgSO_4$ and concentrated *in vacuo*. The product was purified by flash column chromatography (2% MeOH in $CHCl_3$) to yield 30 mg desired product (78% yield) as a bright yellow solid. ^1H NMR ($CDCl_3$, 400 MHz, δ): 1.22 (d, 6H, *J* = 6.8 Hz), 2.23 (s, 6H), 3.26 (heptet, 1H, *J* = 6.8Hz), 3.90 (s, 2H), 4.69 (s, 2H), 5.7 (broad, 1H), 6.67 (s, 2H), 6.71 (s, 1H), 7.02 (s, 1H), 7.63 (d, 2H, *J* = 8.8 Hz), 8.20 (d, 2H, *J* = 8.8 Hz). ^{13}C NMR ($CDCl_3$, 400 MHz, δ): 20.5, 22.3, 27.5, 33.6, 64.8, 89.4, 93.9, 107.9, 114.2, 123.7, 127.3, 128.6, 129.4, 130.5, 131.8, 132.1, 134.7, 138.8, 147.1, 152.4, 155.5, 173.3. HR-MS calcd for $C_{28}H_{27}NO_6$: 473.1838, found: 473.1839. HPLC: Condition A ret. time 4.5 min; Condition B ret. time 5.4 min; 98.0% pure.

[4-(3-Isopropyl-4-methoxymethoxy-benzyl)-3,5-dimethyl-phenoxy]-acetic acid methyl ester (15). To a dry solution of **5** (41.9 g, 89 mmol) in THF (500 ml) was added

tetrabutyl ammonium fluoride (TBAF, 1.0 M in THF, 110 ml). The reaction was stirred at rt. for 30 min. and quenched with H_2O (200 ml). The aqueous layer was extracted with ethyl acetate (3×100 ml). The combined organic phased was washed with water (2×100 ml) and brine (2×100 ml), dried over Mg_2SO_4 and concentrated *in vacuo*. The crude oil was purified through a silica plug using 5% ethyl acetate in hexanes to give 26.0 g (93% yield) of TIPS-deprotected phenol, which was redissolved in DMF (200 ml). To the phenol was added Cs_2CO_3 (81 g, 248 mmol) and 2-bromoacetate (8.6 ml, 91 mmol). The reaction was stirred at rt. for 30 min. The organic phase was washed with water (3×100 ml) and brine (3×100 ml), dried over Mg_2SO_4 and concentrated *in vacuo*. Purification through a silica plug using 5% ethyl acetate in hexanes afforded the desired compound (25.0 g, 78% yield). ^{1}H NMR (400 MHz, $CDCl_3$, δ): 1.17 (d, *J* = 6.8 Hz, 6H), 2.21 (s, 6H), 3.28 (heptet, *J* = 6.8 Hz, 1H), 3.46 (s, 3H), 3.81 (s, 3H), 3.90 (s, 2H), 4.62 (s, 2H), 5.14 (s, 2H), 6.62 (s 2H), 6.64 (s, 1H), 6.88 (d, *J* = 8.0 Hz, 1H), 6.93 (s, 1H). ^{13}C NMR (400 MHz, $CDCl_3$, δ): 20.5, 22.7, 26.9, 33.7, 52.2, 55.9, 65.3, 94.6, 113.9, 114.0, 125.3, 125.9, 130.8, 133.0, 137.3, 138.5, 152.5, 155.7, 169.7. HRMS calcd for $C_{23}H_{30}O_5$, 386.2093; found, 386.2133.

[4-(4-Hydroxy-3-iodo-5-isopropyl-benzyl)-3,5-dimethyl-phenoxy]-acetic acid methyl ester (16). To a solution of **15** (25.0 g, 64.7 mmol) in 440 ml of 40% (v/v) MeOH in THF was added conc. HCl (12 N, 34 ml). The reaction mixture was stirred for 6 h at rt., diluted with water, neutralized with saturated $NaHCO_3$ to pH 7, and then extracted with ethyl acetate (2×100 ml). The combined organic portions were washed with water (3×100 ml) and brine (3×100 ml), dried with $MgSO_4$ and concentrated in vacuo. Purification through a silica plug using 10% ethyl acetate in hexanes gave the desired *O*-methoxymethyl deprotected phenol (22.0 g, 99% yield). ^{1}H NMR (400 MHz, $CDCl_3$, δ):

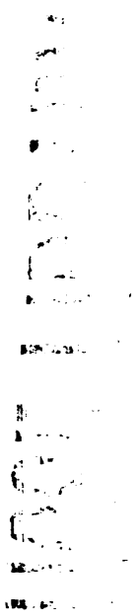

1.20 (d, J = 6.8 Hz, 6H), 2.20 (s, 6H), 3.15 (heptet, J = 6.8 Hz, 1H), 3.81 (s, 3H), 3.89 (s, 2H), 4.62 (s, 2H), 4.71 (s, 1H), 6.56 (q, J = 6.0 Hz, 2H), 6.62 (s, 2H), 6.91 (s, 1H). ^{13}C NMR (400 MHz, $CDCl_3$, δ): 20.5, 22.5, 27.1, 33.7, 52.2, 65.3, 114.0, 115.1, 125.3, 126.1, 130.9, 132.0, 134.1, 138.6, 150.8, 155.7, 169.8. HRMS calcd for $C_{21}H_{26}O_4$, 342.1831; found, 342.1837.

A dry solution of the phenol (22.0 g, 64.2 mmol) in THF (300 ml) and triethylamine (100 ml), cooled to –40°C, was added iodine monochloride (1.0 M in dichloromethane, 71 ml). After stirring at –40°C for 1 h, the reaction was slowly warmed to rt. and then neutralized with 1N HCl to pH 7. The aqueous phase was extracted with H_2O (3×100 ml). The combined organic phase was washed with brine (2×100 ml), dried over $MgSO_4$ and concentrated *in vacuo*. Purification by flash column chromatography (10% ethyl acetate in hexanes) gave 18.6 g (61% yield) of desired product as a green-colored oil. ^1H NMR (400 MHz, $CDCl_3$, δ): 1.17 (d, J = 7.2 Hz, 6H), 2.20 (s, 6H), 3.23 (heptet, J = 7.2 Hz, 1H), 3.81 (s, 3H), 3.86 (s, 2H), 4.63 (s, 2H), 5.16 (s, 1H), 6.63 (s 2H), 6.85 (s, 1H), 6.97 (s, 1H). ^{13}C NMR (400 MHz, $CDCl_3$, δ): 20.5, 22.3, 28.5, 33.3, 52.2, 65.3, 87.1, 114.2, 126.8, 129.9, 133.7, 133.9, 135.1, 138.5, 149.9, 155.9, 169.6. HRMS calcd for $C_{21}H_{25}IO_4$, 468.0798; found, 468.0792.

[4-(3-Iodo-5-isopropyl-4-methoxymethoxy-benzyl)-3,5-dimethyl-phenoxy]-acetic acid methyl ester (12). To a dry solution of **16** (18.6 g, 39.7 mmol) and Cs_2CO_3 (39 g, 119 mmol) in 200 ml of DMF, cooled to 0°C, was added chloromethoxy methane (3.3 ml, 43.7 mmol). The reaction mixture was stirred at 0°C for 1 h and slowly warmed to rt. It was then diluted with H_2O (3×50 ml)and extracted with ethyl acetate (3×50 ml). The combined organic portion was washed with brine (3×50 ml), dried over $MgSO_4$, and concentrated *in vacuo*. The crude oil was purified by flash column chromatography (5%

ethyl acetate in hexanes) to yield 4 (17.8 g, 88% yield) as a pale yellow solid. ^{1}H NMR (400 MHz, $CDCl_3$, δ): 1.13 (d, *J* = 6.8 Hz, 6H), 2.19 (s, 6H), 3.36 (heptet, *J* = 6.8 Hz, 1H), 3.64 (s, 3H), 3.82 (s, 3H), 3.88 (s, 2H), 4.64 (s, 2H), 5.00 (s, 2H), 6.63 (s 2H), 6.89 (s, 1H), 7.15 (s, 1H). ^{13}C NMR (400 MHz, $CDCl_3$, δ): 20.5, 23.6, 27.3, 33.5, 52.2, 57.8, 65.3, 92.9, 100.3, 114.2, 126.5, 129.7, 135.8, 138.4, 138.5, 143.2, 152.4, 156.0, 169.6. HRMS calcd for $C_{23}H_{29}IO_5$, 512.1060; found, 512.1057.

{4-[3-Isopropyl-4-methoxymethoxy-5-(4-trifluoromethyl-phenylethynyl)-benzyl]-3,5-dimethyl-phenoxy}-acetic acid methyl ester (17a). The coupling of **12** with 1-ethynyl-4-trifluoromethyl-benzene (0.175 ml, 1.07 mmol) was effected using the general procedure with refluxing for 6 h to afford 443 mg (82% yield) of the title compound after purification by flash column chromatography (2% ethyl acetate in hexanes). ^{1}H NMR (400 MHz, $CDCl_3$, δ): 1.18 (d, *J* = 6.8 Hz, 6H), 2.22 (s, 6H), 3.40 (heptet, *J* = 6.8 Hz, 1H), 3.61 (s, 3H), 3.82 (s, 3H), 3.92 (s, 2H), 4.64 (s, 2H), 5.23 (s, 2H), 6.65 (s, 2H), 6.85 (s, 1H), 7.00 (s, 1H), 7.58 (s, 4H). ^{13}C NMR (400 MHz, $CDCl_3$, δ): 20.6, 23.4, 26.5, 33.8, 52.2, 57.6, 65.3, 89.4, 91.3, 99.9, 114.2, 115.9, 125.3, 127.2, 127.4, 129.6, 129.9, 131.6, 135.9, 138.6, 142.1, 154.1, 155.9, 169.7. HRMS calcd for $C_{32}H_{33}F_3O_5$, 554.2280; found, 554.2272.

{4-[4-Hydroxy-3-isopropyl-5-(4-trifluoromethyl-phenylethynyl)-benzyl]-3,5-dimethyl-phenoxy}-acetic acid (18a, NH-5). To a solution of **17a** (425 mg, 0.77 mmol) in 19.5 ml of 40% (v/v) MeOH in THF was added conc. HCl (12 N, 1.5 ml). The reaction mixture was stirred for 6 h at rt., diluted with water, neutralized with 1N aq. NaOH to pH 6, and then extracted with ethyl acetate (2×15 ml). The combined organic portions were dried with $MgSO_4$ and concentrated *in vacuo*. The crude product was purified by flash

column chromatography (2% ethyl acetate in hexanes) to give the corresponding *O*-methoxymethyl deprotected phenol (263 mg, 67% yield). ^{1}H NMR (400 MHz, $CDCl_3$, δ): 1.22 (d, *J* = 6.8 Hz, 6H), 2.22 (s, 6H), 3.26 (heptet, *J* = 6.8 Hz, 1H,), 3.82 (s, 3H), 3.89 (s, 2H), 4.63 (s,2H), 5.74 (s, 1H), 6.64 (s, 2H), 6.72 (s, 1H), 6.99 (s, 1H), 7.60 (s, 4H). ^{13}C NMR (400 MHz, $CDCl_3$, δ): 20.5, 22.3, 27.5, 33.6, 52.2, 65.3, 86.4, 94.4, 108.2, 114.2, 125.3, 125.4, 126.3, 127.2, 128.1, 130.2, 131.7, 134.4, 138.6, 152.3, 155.9, 169.7.

To the phenol (260 mg, 0.51 mmol) in 4 ml methanol was added $LiOH{\cdot}H_2O$ (47 mg, 1.12 mmol, dissolved in 1 ml H_2O). The reaction mixture was stirred at rt. for 4 h, acidified with 1N aq. HCl to pH 6, and diluted with ethyl acetate (15 ml). The organic portion was extracted with water (2×15 ml) and brine (2×15 ml), dried over $MgSO_4$ and concentrated *in vacuo*. The product was purified by preparative TLC (3: 2: 0.2 ratio of hexanes: ethyl acetate: MeOH) and isolated with 10% MeOH in ethyl acetate to afford the desired product (65 mg, 26 yield). ^{1}H NMR (400 MHz, $CDCl_3$ spiked w/ 0.1% TFA, δ): 1.22 (d, *J* = 6.8 Hz, 6H), 2.24 (s, 6H), 3.26 (heptet, *J* = 6.8 Hz, 1H), 3.91 (s, 2H), 4.73 (s, 2H), 6.37 (broad s, 1H), 6.66 (s, 2H), 6.71 (s, 1H), 6.98 (s, 1H), 7.60 (s, 4H). ^{13}C NMR (400 MHz, $CDCl_3$, δ): 20.4, 22.2, 27.5, 33.5, 86.4, 94.4, 108.2, 114.4, 122.4, 125.3, 126.3, 127.2, 128.1, 130.0, 130.3, 130.4, 131.6, 134.4, 138.6, 152.3, 155.9. HRMS calcd for $C_{29}H_{27}F_3O_4$, 496.1861; found, 496.1857.

{4-[3-Isopropyl-4-methoxymethoxy-5-(4-methoxy-phenylethynyl)-benzyl]-3,5-dimethyl-phenoxy}-acetic acid methyl ester (17b). The coupling of **12** with 1-ethynyl-4methoxy-benzene (142 mg, 1.07 mmol) was effected using the general procedure with refluxing for 3 h to afford 434 mg (86% yield) of the title compound after purification by flash column chromatography (2% ethyl acetate in hexanes). ^{1}H NMR ($CDCl_3$, 400 MHz, δ): 1.18 (d, 6H, *J* = 6.8 Hz), 2.21 (s, 6H), 3.41 (heptet, 1H, *J* = 6.8 Hz), 3.60 (s, 3H), 3.80

(s, 3H), 3.81 (s, 3H), 3.91 (s, 2H), 4.63 (s, 2H), 5.25 (s, 2H), 6.64 (s, 2H), 6.84 (s, 1H), 6.85 (d, 2H, J = 8.4 Hz), 6.94 (s, 1H), 7.42 (d, 2H, J = 8.2 Hz). ^{13}C NMR ($CDCl_3$, 400 MHz): δ 20.5, 23.3, 26.4, 33.8, 52.2, 55.2, 57.5, 65.2, 85.4, 92.8, 99.6, 113.9, 114.1, 115.4, 116.7, 126.4, 129.4, 130.0, 132.8, 135.6, 138.6, 141.8, 153.7, 155.9, 159.6, 169.6. HRMS calcd for $C_{32}H_{36}O_6$: 516.2517. Found: 516.2512.

{4-[4-Hydroxy-3-isopropyl-5-(4-methoxy-phenylethynyl)-benzyl]-3,5-dimethyl-phenoxy}-acetic acid (18b, NH-6). To a solution of **17b** (400 mg, 0.77 mmol) in 19.5 ml of 40% (v/v) MeOH in THF was added conc. HCl (12 N, 1.5 ml). The reaction mixture was stirred for 6 h at rt., diluted with water, neutralized with 1N aq. NaOH to pH 6, and then extracted with ethyl acetate (2×15 ml). The combined organic portions were dried with $MgSO_4$ and concentrated *in vacuo*. The resulting *O*-methoxymethyl deprotected phenol (339 mg crude, 93% yield) was used directly in the following step. The phenol (260 mg, 0.51 mmol) was redissolved in 4 ml methanol. $LiOH•H_2O$ (66 mg, 1.12 mmol, dissolved in 1 ml H_2O) was added and the reaction mixture was stirred at rt. for 10 h, acidified with 1N aq. HCl to pH 6, and diluted with ethyl acetate (15 ml). The organic portion was extracted with water (2×15 ml) and brine (2×15 ml), dried over $MgSO_4$ and concentrated *in vacuo*. The product was purified by flash column chromatography (40% ethyl acetate in hexanes to 5% MeOH in ethyl acetate gradient) and isolated with 10% MeOH in ethyl acetate to afford the desired product (235 mg, 66% yield from **17b**). ^1H NMR (400 MHz, $CDCl_3$, δ): 1.19 (d, J = 6.8 Hz, 6H), 2.16 (s, 6H), 3.23 (heptet, J = 6.8 Hz, 1H), 3.78 (s, 3H), 3.82 (s, 2H), 4.57 (s, 2H), 5.80 (broad, 1H), 6.63 (s, 2H), 6.68 (s, 1H), 6.83 (d, J = 8.4 Hz, 2H), 6.89 (s, 1H), 7.38 (d, J = 8.4 Hz, 2H). ^{13}C NMR (400 MHz, $CDCl_3$, δ): 20.5, 22.3, 27.6, 33.6, 55.3, 82.4, 95.9, 109.2, 114.1, 114.5, 126.9, 127.1,

131.3, 133.0, 134.0, 138.7, 152.0, 155.4, 159.9. HRMS calcd for $C_{29}H_{30}O_5$, 458.2093; found, 458.2090.

{4-[3-(4-Cyano-phenylethynyl)-5-isopropyl-4-methoxymethoxy-benzyl]-3,5-dimethyl-phenoxy}-acetic acid methyl ester (17c). The coupling of **12** with 4-ethynyl benzonitrile (136 mg, 1.07 mmol), prepared as previously described by Takahashi,[1] was effected using the general procedure with refluxing for 7 h to afford 278 mg (56% yield) of the title compound after purification by flash column chromatography (5% to 10% gradient ethyl acetate in hexanes). ^{1}H NMR (400 MHz, $CDCl_3$, δ): 1.19 (d, *J* = 6.8 Hz, 6H), 2.21 (s, 6H), 3.41 (heptet, *J* = 6.8 Hz, 1H), 3.60 (s, 3H), 3.82 (s, 3H), 3.92 (s, 2H), 4.64 (s, 2H), 5.21 (s, 2H), 6.65 (s, 2H), 6.83 (s, 1H), 7.03 (s, 1H), 7.55 (d, *J* = 8.4 Hz, 2H,), 7.61 (d, *J* = 8.2 Hz, 2H). ^{13}C NMR (400 MHz, $CDCl_3$, δ): 20.5, 23.3, 26.4, 33.8, 52.2, 57.6, 65.2, 91.1, 91.4, 99.9, 111.4, 114.2, 115.6, 118.5, 127.8, 128.3, 129.6, 129.8, 131.8, 132.0, 136.0, 138.6, 142.2, 154.2, 156.0, 169.7. HRMS calcd for $C_{32}H_{33}NO_5$, 511.2359; found, 511.2354.

{4-[3-(4-Cyano-phenylethynyl)-4-hydroxy-5-isopropyl-benzyl]-3,5-dimethyl-phenoxy}-acetic acid (18c, NH-8). To a solution of **17c** (425 mg, 0.77 mmol) in 8 ml of 40% (v/v) MeOH in THF was added conc. HCl (12 N, 1.5 ml). The reaction mixture was stirred for 9 h at rt., diluted with water, neutralized with saturated $NaHCO_3$ to pH 7, and then extracted with ethyl acetate (2 × 15 ml). The combined organic portions were dried with $MgSO_4$ and concentrated *in vacuo*. The crude product was purified by flash column chromatography (15% ethyl acetate in hexanes) to give the corresponding *O*-methoxymethyl deprotected phenol (104 mg, 79% yield). ^{1}H NMR (400 MHz, $CDCl_3$, δ): 1.22 (d, *J* = 7.2 Hz, 6H), 2.21 (s, 6H), 3.26 (heptet, *J* = 7.2 Hz, 1H), 3.82 (s, 3H), 3.89 (s, 2H), 4.64 (s, 2H), 5.69 (s, 1H), 6.64 (s, 2H), 6.70 (s, 1H), 7.01 (s, 1H), 7.57 (d, *J* = 8.4

Hz, 2H), 7.63 (d, J = 8.4 Hz, 2H). ^{13}C NMR (400 MHz, $CDCl_3$, δ): 20.5, 23.3, 33.6, 52.2, 65.2, 88.5, 94.1, 108.0, 111.8, 114.2, 118.3, 127.2, 127.4, 128.5, 130.1, 131.8, 131.9, 132.1, 134.5, 138.6, 152.3, 155.9, 169.7. HRMS calcd for $C_{30}H_{29}NO_4$, 467.2097; found, 467.2085.

To the phenol (60 mg, 0.13 mmol) in 2 ml methanol was added $LiOH•H_2O$ (12 mg, 0.29 mmol, dissolved in 0.5 ml H_2O). The reaction mixture was stirred at rt. for 4 h, acidified with 1N aq. HCl to pH 5, and diluted with ethyl acetate (15 ml). The organic portion was extracted with water (2×15 ml) and brine (2×15 ml), and concentrated *in vacuo*. The crude residue was redissolved in chloroform, giving a white insoluble precipitate. The precipitate was rinsed with chloroform (3×5 ml), collected by filtration through a Buchner funnel, and redissolved in MeOH. NMR reveals product was obtained with reasonable purity (53 mg, 91% yield). ^1H NMR (400 MHz, $CDCl_3$, δ): 1.20 (d, J = 7.2 Hz, 6H), 2.20 (s, 6H), 3.26 (heptet, J = 7.2 Hz, 1H), 3.87 (s, 2H), 4.39 (s, 2H), 6.68 (s, 2H), 6.71 (s, 1H), 6.98 (s, 1H), 7.59 (d, J = 8.4 Hz, 2H), 7.62 (d, J = 8.2 Hz, 2H). HRMS calcd for $C_{29}H_{27}NO_4$, 453.1940; found, 454.0626 (M+H).

{4-[3-(4-Fluoro-phenylethynyl)-5-isopropyl-4-methoxymethoxy-benzyl]-3,5-dimethyl-phenoxy}-acetic acid methyl ester (17d). The coupling of **12** with 1-ethynyl-4-fluoro-benzene (100 mg, 0.83 mmol) was effected using the general procedure with refluxing for 6 h to afford 294 mg (77% yield) of the title compound after purification by flash column chromatography (5% ethyl acetate in hexanes). ^1H (400 MHz, $CDCl_3$, δ): 1.18 (d, J = 7.2 Hz, 6H), 2.21 (s, 6H), 3.41 (heptet, J = 7.2 Hz, 1H), 3.60 (s, 3H), 3.82 (s, 3H), 3.91 (s, 2H), 4.64 (s, 2H), 5.23 (s, 2H), 6.64 (s, 2H), 6.82 (s, 1H), 6.97 (s, 1H), 7.02 (dd J = 8.8, 8.8 Hz, 2H), 7.46 (dd, J = 8.8, 5.2 Hz, 2H). HRMS calcd for $C_{31}H_{33}FO_5$, 504.2312; found, 504.2310.

{4-[3-(4-Fluoro-phenylethynyl)-4-hydroxy-5-isopropyl-benzyl]-3,5-dimethyl-phenoxy}-acetic acid (18d, NH-11). To a solution of **17d** (290 mg, 0.57 mmol) in 15 ml of 40% (v/v) MeOH in THF was added conc. HCl (12 N, 1.14 ml). The reaction mixture was stirred for 6 h at rt., diluted with water, neutralized with saturated $NaHCO_3$ to pH 7, and then extracted with ethyl acetate (2×15 ml). The combined organic portions were dried with $MgSO_4$ and concentrated *in vacuo*. Purification by flash column chromatography (5% ethyl acetate in hexanes) gave the desired *O*-methoxymethyl deprotected phenol (135 mg, 51% yield). ^1H NMR (400 MHz, $CDCl_3$, δ): 1.22 (d, *J* = 6.8 Hz, 6H), 2.22 (s, 6H), 3.25 (heptet, *J* = 6.8 Hz, 1H), 3.82 (s, 3H), 3.88 (s, 2H), 4.63 (s, 2H), 5.74 (s, 1H), 6.64 (s, 2H), 6.70 (s, 1H), 6.95 (s, 1H), 7.04 (dd 2H, *J* = 8.8, 8.8 Hz), 7.48 (dd *J* = 8.8, 5.6 Hz, 2H). ^{13}C NMR (400 MHz, $CDCl_3$, δ): 20.5, 22.3, 27.5, 33.6, 52.2, 65.3, 83.6, 94.7, 108.7, 114.2, 115.7, 155.9, 118.6, 127.1, 127.6, 130.3, 131.5, 133.4, 134.2, 138.6, 138.6, 152.1, 155.9, 169.7. HRMS calcd for $C_{29}H_{29}FO_4$, 460.2049; found, 460.2053.

To the phenol (135 mg, 0.29 mmol) in 10 ml methanol was added $LiOH•H_2O$ (27 mg, 0.64 mmol, dissolved in 1 ml H_2O). The reaction mixture was stirred at rt. for 4 h, acidified with 1N aq. HCl to pH 6, and diluted with ethyl acetate (15 ml). The organic portion was extracted with water (2×15 ml) and brine (2×15 ml), and concentrated *in vacuo*. Purification by preparative TLC (5% MeOH in $CHCl_3$) afforded the desired product (76 mg, 58% yield). ^1H NMR (400 MHz, *d*-DMSO, δ): 1.14 (d, *J* = 6.8 Hz, 6H), 2.15 (s, 6H), 3.23 (heptet, *J* = 6.8 Hz, 1H), 3.82 (s, 2H), 4.43 (broad s, 2H), 6.61 (broad s, 3H), 6.98 (s, 1H), 6.96 (s, 1H), 7.22 (dd, *J* = 8.4, 8.4 Hz, 2H), 7.62 (broad s, 2H). HRMS calcd for $C_{28}H_{27}FO_4$: 446.1893, found: 446.1887.

4-[3-Isopropyl-5-(4-methoxycarbonylmethoxy-2,6-dimethyl-benzyl)-2-methoxy-methoxy-phenylethynyl]-benzoic acid methyl ester (17e). The coupling of **12** with 4-ethynyl-benzoic acid methyl ester (137 mg, 0.86 mmol), prepared as previously described by Takahashi,[1] was effected using the general procedure with refluxing for 18 h to afford 192 mg (45% yield) with of the title compound after purification by flash column chromatography (5% to 10% gradient ethyl acetate in hexanes). ^{1}H NMR (400 MHz, $CDCl_3$, δ): 1.18 (d, *J* = 6.8 Hz, 6H), 2.22 (s, 6H), 3.41 (heptet, *J* = 6.8 Hz, 1H), 3.61 (s, 3H), 3.82 (s, 3H), 3.92 (s, 5H), 4.64 (s, 2H), 5.24 (s, 2H), 6.65 (s, 2H), 6.85 (s, 1H), 7.00 (s, 1H), 7.54 (d, *J* = 8.4 Hz, 2H), 7.99 (d, *J* = 8.4 Hz, 2H). ^{13}C NMR (400 MHz, $CDCl_3$, δ): 20.6, 23.3, 26.5, 33.8, 52.2, 57.6, 65.3, 90.0, 92.0, 99.9, 114.2, 116.0, 127.4, 128.0, 129.4, 129.5, 129.6, 129.9, 131.3, 135.9, 138.6, 142.1, 154.1, 156.0, 166.5, 169.7. HRMS calcd for $C_{33}H_{36}O_7$, 544.2461; found, 544.2457.

4-[5-(4-Methoxycarbonylmethoxy-2,6-dimethyl-benzyl)-2-hydroxy-3-isopropyl-phenylethynyl]-benzoic acid (18e, NH-14). To a solution of **17e** (190 mg, 0.35 mmol) in 8 ml of 40% (v/v) MeOH in THF was added conc. HCl (12 N, 0.6 ml). The reaction mixture was stirred for 6 h at rt., diluted with water, neutralized with 2N NaOH to pH 7, and then extracted with ethyl acetate (2×15 ml). The combined organic portions were dried with $MgSO_4$ and concentrated *in vacuo*. Purification by flash column chromatography (20% ethyl acetate in hexanes) gave the desired *O*-methoxymethyl deprotected phenol (134 mg, 77% yield). ^{1}H NMR (400 MHz, $CDCl_3$, δ): 1.22 (d, *J* = 6.8 Hz, 6H), 2.22 (s, 6H), 3.26 (heptet, *J* = 6.8 Hz, 1H), 3.82 (s, 2H), 3.89 (s, 2H), 3.92 (s, 3H), 4.64 (s, 2H), 5.76 (s, 1H), 6.64 (s, 2H), 6.72 (s, 1H), 6.98 (s, 1H), 7.55 (d, *J* = 8.4 Hz), 2H), 8.01 (d, *J* = 8.4 Hz, 2H). ^{13}C NMR (400 MHz, $CDCl_3$, δ): 20.5, 22.8, 27.5, 33.6, 52.2, 65.3, 86.9, 95.0, 108.4, 114.2, 127.2, 128.1, 129.6, 129.8, 130.2, 131.4,

131.7, 134.4, 138.6, 152.2, 155.9, 166.4, 169.7. HRMS calcd for $C_{31}H_{32}O_6$, 500.2199; found, 500.2204.

To the phenol (130 mg, 0.26 mmol, 1.0 equiv) in 5 ml methanol was added $LiOH \cdot H_2O$ (44 mg, 1.0 mmol, dissolved in 2 ml H_2O). The reaction mixture was stirred at rt. for 4 h, acidified with 1N aq. HCl to pH 6, and diluted with ethyl acetate (15 ml). The organic portion was extracted with water (2×15ml) and brine (2×15ml), and concentrated *in vacuo*. Purification by preparative TLC (10% MeOH in CH_2Cl_2) afforded the desired product (58 mg, 45% yield). ^1H NMR (400 MHz, $CDCl_3$ spiked w/ 0.1% TFA δ): 1.22 (d, J = 6.8 Hz, 6H), 2.24 (s, 6H), 3.26 (heptet, J = 6.8 Hz, 1H), 3.91 (s, 2H), 3.96 (s, 3H), 4.74 (s, 2H), 6.64 (s, 2H), 6.72 (s, 1H), 6.99 (s, 1H), 7.56 (d, J = 8.0 Hz, 2H), 8.01 (d, J = 8.0 Hz, 2H). HRMS calcd for $C_{29}H_{28}O_6$, 486.2042; found, 486.2019.

{4-[3-(4-Carbamoyl-phenylethynyl)-5-isopropyl-4-methoxymethoxy-benzyl]-3,5-dimethyl-phenoxy}-acetic acid methyl ester (17f). 4-Ethynyl benzamide was prepared following a modified procedure of Takahashi[1] for the synthesis of ethynylarenes. To a mixture of trimethylsilylacetylene (1.06 ml, 7.5 mmol) and 4-bromobenzamide (0.50 g, 2.5 mmol) in diethylamine (20 ml) were added $PdCl_2(PPh_3)_2$ (70 mg, 0.10 mmol) and CuI (10 mg, 0.05 mmol). The reaction mixture was stirred at rt. for 48 h and then solvent is removed under reduced pressure. The residue was diluted with ethyl acetate and filtered through Celite. The organic portion was washed with water (2×15 ml) and brine (2×15 ml), dried over $MgSO_4$ and concentrated *in vacuo*. Purification by flash column chromatography (2% *i*PrOH in CH_2Cl_2) gave the *C*-silyl-protected intermediate (280 mg, 53% yield). This was then treated with tetrabutyl ammonium fluoride (1.0 M, 1.4 ml) in THF (15ml) at rt. for 30 min. The reaction was diluted with ethyl acetate (15 ml), washed with water (2×25 ml) and brine (2×25 ml),

dried over $MgSO_4$ and concentrated *in vacuo*. Filtration through a silica gel plug (2% *i*PrOH in CH_2Cl_2) gave the desired product (178mg, 95% yield). ^1H NMR (400 MHz, $CDCl_3$, δ): 3.22 (s, 1H), 5.65 (broad s, 1H), 6.05 (broad s, 1H), 7.57 (d, *J* = 8.4 Hz, 2H), 7.78 (d, *J* = 8.4 Hz, 2H)

The coupling of **12** with 4-ethynyl-benzamide (93 mg, 0.64 mmol) was effected using the general procedure with refluxing for 12 h to afford 156 mg (50% yield) of the title compound after purification by flash column chromatography (5% *i*PrOH in CH_2Cl_2). ^1H NMR (400 MHz, $CDCl_3$, δ): 1.19 (d, *J* = 6.8 Hz, 6H), 2.22 (s, 6H), 3.41 (heptet, *J* = 6.8 Hz, 1H), 3.61 (s 3H), 3.82 (s, 3H), 3.92 (s, 5H), 4.64 (s, 2H), 5.24 (s, 2H), 6.65 (s, 2H), 6.85 (s, 1H), 7.00 (s, 1H), 7.56 (d, *J* = 8.4 Hz, 2H), 7.77 (d, *J* = 8.4 Hz, 2H). ^{13}C NMR (400 MHz, $CDCl_3$, δ): 20.6, 23.3, 26.4, 33.8, 52.2, 57.6, 65.3, 89.6, 91.8, 99.9, 114.2, 116.0, 127.2, 127.4, 129.6, 129.9, 131.5, 132.5, 135.9, 138.6, 142.1, 154.1, 155.9, 168.4, 169.7. HRMS calcd for $C_{32}H_{35}NO_6$, 529.2464; found, 529.2440.

{4-[3-(4-Carbamoyl-phenylethynyl)-4-hydroxy-5-isopropyl-benzyl]-3,5-dimethyl-phenoxy}-acetic acid (18f, NH-15). To a solution of **17f** (150 mg, 0.28 mmol) in 8 ml of 40% (v/v) MeOH in THF was added conc. HCl (12 N, 0.6 ml). The reaction mixture was stirred for 18 h at rt., diluted with water, neutralized with 5N KOH to pH 6, and then extracted with ethyl acetate (2×15 ml). The combined organic portions were dried with $MgSO_4$ and concentrated *in vacuo*. Purification by flash column chromatography (15% *i*PrOH in CH_2Cl_2) gave the desired *O*-methoxymethyl deprotected phenol (109 mg, 84% yield). ^1H NMR (400 MHz, $CDCl_3$, δ): 1.22 (d, *J* = 6.8 Hz, 6H), 2.21 (s, 6H), 3.27 (heptet, *J* = 6.8 Hz, 1H), 3.81 (s, 3H), 3.88 (s, 2H), 4.63 (s, 2H), 6.00 (s, 1H), 6.40 (broad s, 2H), 6.63 (s, 2H), 6.72 (s, 1H), 6.98 (s, 1H), 7.53 (d, *J* = 8.4 Hz, 2H), 7.77 (d, *J* = 8.4 Hz, 2H). ^{13}C NMR (400 MHz, $CDCl_3$, δ): 20.4, 25.2, 27.4, 33.5, 52.2, 65.2, 86.7, 94.7, 108.4,

114.1, 126.2, 127.2, 127.4, 127.9, 129.0, 130.1, 131.5, 132.8, 134.4, 138.5, 152.2, 155.8, 168.8, 169.7. HRMS calcd for $C_{30}H_{31}NO_5$, 485.2202; found, 485.2220.

To the phenol (20 mg, 0.041 mmol) in 3 ml methanol was added LiOH (2 mg, 0.082 mmol, dissolved in 0.5 ml H_2O). The reaction mixture was stirred at rt. for 4 h, acidified with 1N aq. HCl to pH 5, and diluted with ethyl acetate (15 ml). The organic portion was extracted with water (2×15 ml) and brine (2×15 ml), and concentrated *in vacuo*. Purification by preparative TLC (10% MeOH in CH_2Cl_2) afforded the desired product (6 mg, 29% yield). ^1H NMR (400 MHz, $CDCl_3$, δ): 1.08 (d, *J* = 6.8 Hz, 6H), 2.11 (s, 6H), 3.19 (heptet, *J* = 6.8 Hz, 1H), 3.81 (s, 2H), 4.47 (s, 2H), 6.58 (s, 2H), 6.60 (s, 1H), 6.86 (s, 1H), 7.52 (d, *J* = 8.0 Hz, 2H), 7.75 (d, *J* = 8.0 Hz, 2H). ^{13}C NMR (400 MHz, $CDCl_3$, δ): 20.6, 22.9, 28.4, 34.3, 79.5, 89.1, 93.9, 111.2, 115.2, 128.3, 128.5, 128.7, 129.4, 131.1, 132.5, 132,9, 137.1, 139.4, 154.2, 157.7, 171.6. HRMS calcd for $C_{29}H_{29}NO_5$: 471.2046, found: 471.2041.

{4-[3-(4-Dimethylamino-phenylethynyl)-5-isopropyl-4-methoxymethoxy-benzyl]-3,5-dimethyl-phenoxy}-acetic acid methyl ester (17g). (4-Ethynyl-phenyl)-dimethyl-amine. Ethynylaniline (1.0 g, 8.5 mmol) was heated to 40°C with methyl iodide (1.6 ml, 25.5 mmol) and cesium carbonate (8.3 g, 25.5 mmol) in 50 ml DMF for 15 h. The reaction mixture was cooled to rt. and diluted with ether (50 ml). The organic portion was washed with water (3 × 50 ml) and brine (3 × 50 ml), dried over $MgSO_4$ and concentrated *in vacuo*. The N, N-dimethyl product was purified by flash column chromatography (2% ethyl acetate in hexanes) as a white solid (480 mg, 39% yield). ^1H NMR (400 MHz, $CDCl_3$, δ): 2.97 (s, 1H), 6.62 (d, *J* = 8.8 Hz, 2H), 7.36 (d, *J* = 8.8 Hz, 2H).

The coupling of **12** with (4-ethynyl-phenyl)-dimethyl-amine (160 mg, 1.07 mmol) was effected using the general procedure with refluxing for 24 h to afford 391 mg (76% yield) of the title compound after purification by flash column chromatography (5% to 15% gradient ethyl acetate in hexanes). ^{1}H NMR (400 MHz, $CDCl_3$, δ): 1.17 (d, *J* = 7.2 Hz, 6H), 2.22 (s, 6H), 2.98 (s, 6H), 3.41 (heptet, *J* = 7.2 Hz, 1H), 3.60 (s, 3H), 3.82 (s, 3H), 3.90 (s, 2H), 4.64 (s, 2H), 5.25 (s, 2H), 6.63 (d, *J* = 8.8 Hz, 2H), 6.64 (s, 2H), 6.83 (s, 1H), 6.90 (s, 1H), 7.36 (d, *J* = 8.8 Hz, 2H). HRMS calcd for $C_{33}H_{39}NO_5$, 529.2828; found, 529.2842.

{4-[3-(4-Dimethylamino-phenylethynyl)-4-hydroxy-5-isopropyl-benzyl]-3,5-dimethyl-phenoxy}-acetic acid (18g, NH-24). To a solution of **17g** (120 mg, 0.23 mmol) in 7 ml of 40% (v/v) MeOH in THF was added conc. HCl (12 N, 0.5 ml). The reaction mixture was stirred for 6 h at rt., diluted with water, neutralized with 2N KOH to pH 6, and then extracted with ethyl acetate (2×15 ml). The combined organic portions were dried with $MgSO_4$ and concentrated *in vacuo*. Purification by preparative TLC (33% ethyl acetate in hexanes) gave the desired *O*-methoxymethyl deprotected phenol (88 mg, 80% yield). ^{1}H NMR ($CDCl_3$, 400 MHz): δ 1.21 (d 6H, *J* = 6.8 Hz), 2.22 (s 6H), 2.98 (s 6H), 3.25 (heptet 1H, *J* = 6.8 Hz), 3.81 (s 3H), 3.87 (s 2H), 4.63 (s 2H), 5.88 (s 1H), 6.63 (d 2H, *J* = 8.4 Hz), 6.63 (s 2H), 6.70 (s 1H), 6.89 (s 1H), 7.36 (d 2H, *J* = 8.4 Hz).

To the phenol (85 mg, 0.17 mmol) in 3 ml methanol was added LiOH (9 mg, 0.37 mmol, dissolved in 3 ml H_2O). The reaction mixture was stirred at rt. for 1.5 h, acidified with 1N aq. HCl to pH 6, and diluted with ethyl acetate (15 ml). The organic portion was extracted with water (2×15 ml) and brine (2×15 ml), and concentrated *in vacuo*. Purification by preparative TLC (1: 1: 0.1 ratio of hexanes: ethyl acetate: MeOH) and

isolated using 10% MeOH in CH_2Cl_2 afforded the desired product (12 mg, 14% yield). ^1H NMR (CD_3OD, 400 MHz, δ): 1.23 (d, 6H, *J* = 6.8 Hz), 2.23 (s, 6H), 3.26 (heptet, 1H, *J* = 6.8 Hz), 3.32 (s, 6H), 3.91 (s, 2H), 4.76 (s, 2H), 6.66 (s, 2H), 6.69 (s, 1H), 7.02 (s, 1H), 7.51 (d, 2H, *J* = 8.0 Hz), 7.66 (d, 2H, *J* = 8.0 Hz). HRMS calcd for $C_{30}H_{33}NO_4$: 471.2410, found: 471.2403.

{4-[2-Hydroxy-3-isopropyl-5-(4-methoxycarbonylmethoxy-2,6-dimethyl-benzyl)-phenylethynyl]-phenyl}-trimethyl-ammonium trifluoromethane sulfonate salt (NH-16). Compound **17g** (250 mg, 0.23 mmol) and methyl trifluoromethanesulfonate (80 μl, 0.71 mmol) in 15 ml CH_2Cl_2 was heated at reflux (*ca.* 45°C) for 3 h. After cooling to rt., the reaction was diluted with ether and concentrated *in vacuo*. The resulting residue was rinsed (3×5 ml) with 10% ethyl acetate in ether with heating and sonication to afford the desired product with reasonable purity (220mg, 72%). Product cannot be purified by silica chromatography and attempts to recrystallize from CH_2Cl_2/ether were unsuccessful. ^1H NMR (400 MHz, $CDCl_3$ spiked w/ CD_3OD, δ): 1.22 (d, *J* = 7.2 Hz, 6H), 2.22 (s, 6H), 3.26 (heptet, *J* = 7.2 Hz, 1H), 3.75 (s, 9H), 3.82 (s, 3H), 3.89 (s, 2H), 4.64 (s, 2H), 6.64 (s, 2H), 6.70 (s, 1H), 7.02 (s, 1H), 7.69 (d, *J* = 8.8 Hz, 2H), 7.76 (d, *J* = 8.8 Hz, 2H). HRMS calcd for $C_{33}H_{38}F_3O_7S$, 649.2321; found, 499.2695 (M-CF_3SO_3H).

{4-[3-(4-Amino-phenylethynyl)-5-isopropyl-4-methoxymethoxy-benzyl]-3,5-dimethyl-phenoxy}-acetic acid methyl ester (17l). The coupling of **12** with 1-ethynyl aniline (274 mg, 2.34 mmol) was effected using the general procedure with refluxing for 15 h to afford 567 mg (58% yield) of the title compound after purification by flash column chromatography (25% ethyl acetate in hexanes). ^1H (400 MHz, $CDCl_3$, δ): 1.17 (d, *J* = 7.2 Hz, 6H), 2.21 (s, 6H), 3.41 (heptet, *J* = 7.2 Hz, 1H), 3.60 (s, 3H), 3.82 (s, 3H), 3.90

(s, 2H), 4.63 (s, 3H), 5.24 (s, 2H), 6.60 (d, *J* = 8.0 Hz, 2H), 6.81 (s, 1H), 6.91 (s, 1H), 7.28 (d, *J* = 8.0 Hz, 2H). ^{13}C NMR (400 MHz, $CDCl_3$, δ): 20.5, 23.3, 26.4, 33.8, 52.2, 57.5, 65.3, 84.6, 93.6, 99.6, 112.7, 114.2, 114.7, 117.0, 126.1, 129.3, 130.1, 132.7, 135.5, 138.6, 141.7, 146.6, 153.6, 155.9, 169.7. HRMS calcd for $C_{31}H_{35}NO_5$, 501.2515; found, 501.2519.

{4-[3-(4-Amino-phenylethynyl)-4-hydroxy-5-isopropyl-benzyl]-3,5-dimethyl-phenoxy}-acetic acid (18l, NH-4). To ester **17l** (83 mg, 0.16 mmol) in 5 ml of 50% (v/v) mixture of *i*-PrOH and THF was added 1N aq. HCl (0.20 ml). The reaction mixture was stirred for 6 h at rt., diluted with 10 ml of water, neutralized with 1N aq. NaOH to pH 6, and extracted with ethyl acetate (2×15 ml). The combined organic portions were dried with $MgSO_4$ and concentrated to yield the corresponding *O*-methoxymethyl deprotected phenol. Purification by flash column chromatography (50% ethyl acetate in hexanes) gave the desired product **9** (34mg, 45%). ^1H NMR (400 MHz, $CDCl_3$, δ): 1.21 (d, *J* = 6.8 Hz, 6H), 2.21 (s, 6H), 3.25 (heptet, *J* = 6.8 Hz, 1H), 3.81 (s, 3H), 3.88 (s, 2H), 4.63 (s, 2H), 6.61 (d, *J* = 8.8 Hz, 2H), 6.63 (s, 2H), 6.69 (s, 1H), 6.91 (s, 1H), 7.29 (d, *J* = 8.8 Hz, 2H). ^{13}C NMR (400 MHz, $CDCl_3$, δ): 20.5, 22.3, 27.5, 33.6, 52.2, 65.3, 81.6, 96.6, 109.5, 111.6, 113.7, 114.1, 114.7, 126.9, 130.4, 130.8, 131.2, 132.9, 133.9, 138.6, 146.98, 151.8, 155.8, 169.7. HR-MS calcd for $C_{29}H_{31}NO_4$: 457.2253, found: 457.2249.

To the above phenol **9** (34 mg, 0.07 mmol) in 4 ml methanol was added $LiOH \cdot H_2O$ (7 mg, 0.16 mmol) and H_2O (7 μL, 0.70 mmol). The reaction mixture was stirred at rt. for 4 h, acidified with 1N aq. HCl to pH 6, and diluted with ethyl acetate (15ml). The organic portion was extracted with water (2×15 ml) and brine (2×15 ml), dried over $MgSO_4$ and concentrated in vacuo. The product was purified by preparative TLC (5% MeOH in $CHCl_3$) to yield 13 mg desired product (41%) as a yellow solid. ^1H NMR (400 MHz, 1%

CD_3OD, in $CDCl_3$, δ): 1.20 (d, *J* = 6.8 Hz, 2H), 2.22 (s, 6H), 3.25 (heptet, 1H, J=6.8Hz), 3.88 (s, 2H), 4.60 (s, 2H), 6.65 (s, 2H), 6.67 (m, 3H), 6.91 (s, 1H), 7.31 (d, *J* = 8.4 Hz, 2H). ^{13}C NMR (400 MHz, 1% CD_3OD in $CDCl_3$, δ):20.3, 22.1, 27.3, 33.5, 60.5, 64.9, 81.8, 96.1, 109.4, 114.0, 115.1, 126.7, 126.9, 130.2, 131.2, 132.7, 133.9, 138.5, 151.7, 155.7, 171.5, 174.0. HR-MS calcd for $C_{28}H_{29}NO_4$: 443.2097, found: 443.2099.

{4-[3-(4-Azido-phenylethynyl)-4-hydroxy-5-isopropyl-benzyl]-3,5-dimethyl-phenoxy}-acetic acid (NH-7). A solution of **17I** (250 mg, 0.50 mmol) in acetone (1 ml) and 10% (v/v) aq. HCl (5 ml) and was cooled to 0°C. $NaNO_2$ (35 mg, 0.50 mmol, dissolved in 2.5 ml H_2O) was then added dropwise and the reaction mixture was stirred at 0°C. After 30 min, NaN_3 (36 mg, 0.55 mmol, dissolved in 2.5 ml H_2O) was added to the reaction mixture and stirring continued at 0°C for an additional 1 h and slowly warmed to rt. The reaction was quenched with saturated $NaHCO_3$ to pH 7 and diluted with ethyl acetate. The organic portion was extracted with water (2×15 ml) and brine (2×15 ml), dried over $MgSO_4$ and concentrated *in vacuo*. Purification by flash column chromatography (5% ethyl acetate in hexanes) afforded 220 mg (84% yield) of the azide compound. ^1H NMR (400 MHz, $CDCl_3$, δ): 1.18 (d, *J* = 7.2 Hz, 6H), 2.21 (s, 6H), 3.40 (heptet, *J* = 7.2 Hz, 1H), 3.60 (s, 3H), 3.81 (s, 3H), 3.91 (s, 2H), 4.64 (s, 2H), 5.23 (s, 2H), 6.64 (s, 2H), 6.83 (s, 1H), 6.97 (s, 1H), 6.98 (d, *J* = 8.4 Hz, 2H), 7.47 (d, *J* = 8.2 Hz, 2H). ^{13}C (400 MHz, $CDCl_3$, δ): 20.6, 23.3, 26.4, 33.8, 52.2, 57.5, 65.3, 87.2, 92.1, 99.8, 114.2, 116.4, 119.1, 119.9, 126.9, 129.4, 130.0, 132.9, 135.8, 138.6, 139.9, 142.0, 153.9, 155.9, 169.7. HRMS calcd for $C_{31}H_{33}N_3O_5$, 527.2420; found, 527.2421.

To a solution of the azide (200 mg, 0.38 mmol) in 10 ml of 40% (v/v) MeOH in THF was added conc. HCl (12 N, 0.8 ml). The reaction mixture was stirred for 6 h at rt., diluted with water, neutralized with 1N aq. NaOH to pH 6, and then extracted with ethyl acetate

(2 × 15 ml). The combined organic portions were dried with $MgSO_4$ and concentrated *in vacuo*. The resulting *O*-methoxymethyl deprotected phenol (170 mg crude, 93% yield) was used directly in the following step. The phenol (170 mg, 0.35 mmol) was redissolved in 4 ml methanol. $LiOH \cdot H_2O$ (33 mg, 0.77 mmol, dissolved in 1 ml H_2O) was added and the reaction mixture was stirred at rt. for 10 h, acidified with 1N aq. HCl to pH 5, and diluted with ethyl acetate (15 ml). The organic portion was extracted with water (2×15ml) and brine (2×15 ml), dried over $MgSO_4$ and concentrated *in vacuo*. The product was purified by flash column chromatography (40% ethyl acetate in hexanes to 5% MeOH in ethyl acetate gradient) and isolated with 10% MeOH in ethyl acetate to afford the desired product (128 mg, 65% yield from **17a**). ^1H NMR (400 MHz, $CDCl_3$, δ): 1.18 (d, *J* = 6.8 Hz, 6H), 2.21 (s, 6H), 3.25 (heptet, *J* = 6.8 Hz, 1H), 3.87 (s, 2H), 4.63 (s, 2H), 5.78 (broad, 1H), 6.65 (s, 2H), 6.69 (s, 1H), 6.94 (s, 1H), 6.98 (d, *J* = 8.4 Hz, 2H), 7.45 (d, *J* = 8.4 Hz, 2H). ^{13}C NMR (400 MHz, $CDCl_3$, δ): 20.5, 22.3, 27.5, 33.6, 84.2, 95.2, 108.8, 114.3, 118.9, 119.1, 127.0, 127.6, 130.7, 131.4, 133.0, 134.2, 138.8, 140.4, 152.1, 155.4. HRMS calcd for $C_{28}H_{27}N_3O_4$, 469.2002; found: 469.2007.

{4-[3-(4-Bromo-phenylethynyl)-5-isopropyl-4-methoxymethoxy-benzyl]-3,5-dimethyl-phenoxy}-acetic acid methyl ester (17m). 4-Bromo-ethynylbenzene was synthesized via the Sandmeyer reaction as described by Galli.[2] 4-ethylnylaniline (100 mg, 0.85 mmol) was dissolved in a 50% (v/v) mixture of HBF_4 and H_2O (6 ml) and cooled to 0°C. Sodium nitrate (60 mg, 0.85 mmol) was added dropwise as a solution in H_2O and the resulting mixture was kept at 0°C for 30 min. Solid $Cu(II)Br_2$ (190 mg, 0.85 mmol) was then added followed ascorbic acid (2M, 150 mg in 0.4 ml H_2O). The reaction continued to stir at rt. for 20 min, diluted with H_2O (3×10ml), and extracted with ethyl

acetate (3×10ml). The combined organic portion was washed with brine (3×10ml), dried over $MgSO_4$, and concentrated *in vacuo*.

The coupling of **12** with 1-bromo-4-ethynylbenzene (194 mg, 1.07 mmol) was effected using the general procedure with refluxing for 9 h to afford 419 mg (~76% yield) of the title compound after purification by flash column chromatography (10% ethyl acetate in hexanes). Product had ~80% purity as an inseparable mixture with **12**, and used in the next reaction for synthesis of **23**. ^{1}H NMR (400 MHz, $CDCl_3$, δ): 1.18 (d, *J* = 6.8 Hz, 6H), 2.21 (s, 6H), 3.40 (heptet, *J* = 6.8 Hz, 1H), 3.60 (s, 3H), 3.81 (s, 3H), 3.91 (s, 2H), 4.64 (s, 2H), 5.22 (s, 2H), 6.64 (s, 2H), 6.82 (s, 1H), 6.98 (s, 1H), 7.34 (d, *J* = 8.4 Hz, 2H), 7.45 (d, *J* = 8.4 Hz, 2H).

(4-{3-Isopropyl-4-methoxymethoxy-5-[4-(1-nitro-ethyl)-phenylethynyl]-benzyl}-3,5-dimethyl-phenoxy)-acetic acid methyl ester (23). Following a modified procedure for monoarylation of nitroalkanes described by Vogl and Buchwald,[3] a dry flask charged with **17m** (120 mg, 0.21 mmol) was added $Pd_2(dba)_3$•$CHCl_3$ (13 mg, 0.013 mmol), 2-di-*tert*-butylphosphinobiphenyl (7.5 mg, 0.025 mmol), and Cs_2CO_3 (140 mg, 0.42 mmol). The reaction flask was capped with a rubber septum, evacuated, and backfilled with argon three times. Dimethoxyethane (5 ml) and nitroethane (30 μl, 0.42 mmol) were added and the reaction mixture was stirred vigorously at rt. for 2 min. The flask was then equipped with a reflux condenser and heated to 60°C for 4 h. Upon cooling to rt., the reaction was quenched with saturated NH_4Cl (5 ml) and extracted with ethyl acetate (3×15 ml). The combined organic phases was washed with water (2×15 ml) and brine (2×15 ml), dried over $MgSO_4$ and concentrated *in vacuo*. Purification by preparative TLC (25% ethyl acetate in hexanes) gave desired product (27 mg, 23% yield). ^{1}H NMR (400 MHz, $CDCl_3$, δ): 1.18 (d, *J* = 6.8 Hz, 6H), 1.89 (d, *J* = 6.8 Hz, 3H), 2.22 (s, 6H), 3.40

(heptet, J = 6.8 Hz, 1H), 3.60 (s, 3H), 3.82 (s, 3H), 3.92 (s, 2H), 4.64 (s, 2H), 5.22 (s, 2H), 5.60 (quartet, J = 6.8 Hz, 1H), 6.65 (s, 2H), 6.84 (s, 1H), 6.98 (s, 1H), 7.42 (d, J = 8.4 Hz, 2H), 7.52 (d, J = 8.4 Hz, 2H). ^{13}C (400 MHz, $CDCl_3$, δ): 19.3, 20.6, 23.4, 26.4, 33.8, 52.2, 57.6, 65.3, 85.8, 88.4, 91.8, 99.8, 114.2, 116.1, 125.1, 127.2, 127.4, 129.6, 129.9, 131.9, 135.1, 135.8, 138.6, 142.0, 154.0, 155.9, 169.7. HRMS calcd for $C_{33}H_{37}NO_7$, 559.2570; found, 513.2646 (M-NO_2).

{4-[3-(4-Acetyl-phenylethynyl)-4-hydroxy-5-isopropyl-benzyl]-3,5-dimethyl-phenoxy}-acetic acid (NH-9). To a solution of **23** (20 mg, 0.04 mmol) in 3 ml of 40% (v/v) MeOH in THF was added conc. HCl (12 N, 3 drops). The reaction mixture was stirred for 6 h at rt., diluted with water, neutralized with saturated $NaHCO_3$ to pH 7, and then extracted with ethyl acetate (2×15 ml). The combined organic portions were dried with $MgSO_4$ and concentrated *in vacuo*. Purification by preparative TLC (25% ethyl acetate in hexanes) gave the desired *O*-methoxymethyl deprotected phenol (13 mg, 72% yield). ^1H NMR (400 MHz, $CDCl_3$, δ): 1.22 (d, J = 6.8 Hz, 6H), 1.90 (d, J = 6.8 Hz, 3H), 2.22 (s, 6H), 3.26 (heptet, J = 6.8 Hz, 1H), 3.82 (s, 3H), 3.89 (s, 2H), 4.63 (s, 2H), 5.61 (quartet, J = 6.8 Hz, 1H), 5.74 (s, 1H), 6.64 (s, 2H), 6.71 (s, 1H), 6.97 (s, 1H), 7.43 (d, J = 8.4 Hz, 2H), 7.52 (d, J = 8.4 Hz, 2H). ^{13}C NMR (400 MHz, $CDCl_3$, δ): 19.3, 20.5, 22.3, 27.5, 33.6, 52.2, 65.3, 85.4, 85.7, 94.8, 108.5, 114.1, 124.2, 127.1, 127.5, 127.9, 130.2, 131.6, 132.0, 134.3, 135.6, 138.6, 152.2, 155.9, 169.7. HRMS calcd for $C_{31}H_{33}NO_6$, 515.2308, found, 469.2356 (M-NO_2).

To the phenol (10 mg, 0.019 mmol) in 2 ml methanol was added $LiOH \cdot H_2O$ (2 mg, 0.043 mmol, dissolved in 0.5 ml H_2O). The reaction mixture was stirred at rt. for 4 h, acidified with 1N aq. HCl to pH 5, and diluted with ethyl acetate (15 ml). The organic portion was extracted with water (2×15 ml) and brine (2×15 ml), and concentrated *in vacuo*.

Purification by preparative TLC (10% MeOH in CH_2Cl_2) afforded the desired product (5.2 mg, 57% yield). ^1H NMR (400 MHz, $CDCl_3$, δ): 1.18 (d, *J* = 6.8 Hz, 6H), 2.21 (s, 6H), 2.59 (s, 3H), 3.91 (s, 2H), 4.60 (s, 2H), 6.68 (s, 2H), 6.71 (s, 1H), 6.96 (s, 1H), 7.64 (d, *J* = 8.4 Hz, 2H), 7.96 (d, *J* = 8.2 Hz, 2H). ^{13}C NMR (CD_3OD, 400 MHz): δ 20.6, 22.9, 26.7, 28.4, 34.3, 71.4, 90.2, 93.9, 111.1, 115.2, 128.5, 129.4, 129.5, 129.9, 131.2, 132.7, 132,9, 137.2, 137.3, 139.5, 154.3, 157.7, 199.7. HRMS calcd for $C_{30}H_{30}NO_5$, 470.2093, found, 470.2104.

(4-{3-Isopropyl-4-methoxymethoxy-5-[4-(triisopropyl-silanyloxymethyl)-phenyl-ethynyl]-benzyl}-3,5-dimethyl-phenoxy)-acetic acid methyl ester (17n). (4-Ethynyl-benzyloxy)-triisopropyl-silane was prepared following the procedure of Takahashi, *et al.* (1980) for the synthesis of ethynylarenes. 4-iodobenzyl alcohol (1.0 g, 4.3 mmol) was first protected as a triisopropyl silyl ether by addition of imidazole (0.35 g, 5.2 mmol) and chlorotriisopropyl silane (1.1 ml, 5.1 mmol) in DMF (50 ml) at rt. for 48 h. The reaction was diluted with ether (10 ml) and extracted with water (3×15 ml) and brine (3×15 ml). The organic portion was dried over $MgSO_4$ and concentrated *in vacuo* to give 1.54 g (92% yield) of crude product with reasonable purity. To the *O*-silyl protected benzyl alcohol was added diethylamine (30 ml), trimethylsilylacetylene (1.2 ml, 7.8 mmol), $PdCl_2(PPh_3)_2$ (55 mg, 0.08 mmol) and CuI (7.5 mg, 0.04 mmol). The reaction mixture was stirred at rt. for 5 h and then solvent was removed under reduced pressure. The resulting residue was diluted with ethyl acetate and filtered through Celite. The organic portion was washed with water (2×15 ml) and brine (2×15 ml), dried over $MgSO_4$ and concentrated *in vacuo*. Purification by flash column chromatography (100% hexanes) gave the silyl-protected ethynylarene intermediate (1.18 g, 83% yield). This intermediate was then treated with 5 N KOH (5 ml) in MeOH (20 ml) at rt. for 2 h. The reaction was

diluted with ether (15 ml) and washed with water (2×25 ml) and brine (2×25 ml), dried over $MgSO_4$ and concentrated *in vacuo*. Filtration through a silica gel plug (100% hexanes) gave the desired product (0.92 g, 97% yield). ^1H NMR (400 MHz, CDCl3, δ): 1.09 (d, *J* = 6.8 Hz, 18 Hz), 1.15 (m, *J* = 6.8 Hz, 3H), 3.12 (s, 1H), 4.83 (s, 2H), 7.30 (d, *J* = 8.0 Hz, 2H), 7.46 (d, *J* = 8.0 Hz, 2H).

The coupling of **12** with (4-ethynyl-benzyloxy)-triisopropyl-silane (620 mg, 2.2 mmol) was effected using the general procedure with refluxing for 18 h to afford 900 mg (69% yield) of the title compound after purification by flash column chromatography (2% ethyl acetate in hexanes). ^1H NMR ($CDCl_3$, 400 MHz, δ): 1.09 (d, *J* = 6.4 Hz, 18H), 1.18 (d, *J* = 6.4 Hz, 6H,), 2.22 (s, 6H), 3.41 (m, 1H), 3.60 (s, 3H), 3.82 (s, 3H), 3.91 (s, 2H), 4.64 (s, 2H), 4.83 (s, 2H), 5.25 (s, 2H), 6.64 (s, 2H), 6.85 (s, 1H), 6.95 (s, 1H), 7.31 (d, *J* = 8.0 Hz, 2H), 7.45 (d, *J* = 8.0 Hz, 2H). HRMS calcd for $C_{41}H_{56}O_6Si$: 672.3846. Found: 672.3828.

{4-[3-(4-Azidomethyl-phenylethynyl)-5-isopropyl-4-methoxymethoxy-benzyl]-3,5-dimethyl-phenoxy}-acetic acid methyl ester (24). To a stirred solution of **17n** in THF (20 ml) was added tetrabutyl ammonium fluoride (1.0 M, 0.38 mmol). The reaction stirred at rt. for 15 min., diluted with ethyl acetate (20 ml), extracted with water (3×20 ml) and brine (3×20 ml), dried over $MgSO_4$ and concentrated in vacuo. Purification by flash column chromatography (10% to 50% gradient ethyl acetate in hexanes) gave the desired benzyl alcohol (163 mg, 93% yield). ^1H NMR (400 MHz, $CDCl_3$, δ): 1.18 (d, *J* = 6.8 Hz, 6H), 2.22 (s, 6H), 3.41 (m, *J* = 6.8 Hz, 1H), 3.60 (s, 3H), 3.82 (s, 3H), 3.92 (s, 2H), 4.64 (s, 2H), 4.70 (s, 2H), 5.25 (s, 2H), 6.64 (s, 2H), 6.85 (s, 1H), 6.96 (s, 1H), 7.33 (d, *J* = 7.6 Hz, 2H), 7.48 (d 2H, *J* = 7.6 Hz). HRMS calcd for $C_{32}H_{36}O_6$, 516.2512; found, 516.2508.

To the benzyl alcohol (230 mg, 0.45 mmol) in DMSO (3 ml) was added chlorotrimethylsilane (0.11 ml, 0.90 mmol). The reaction was stirred at rt. for 30 min. before NaN_3 was added (0.5 M in DMSO, 1.3 ml). Stirring continued for another 35 min. and the reaction was diluted with ethyl acetate (10 ml), washed with water (3×10 ml) and brine (3×10 ml), dried over $MgSO_4$, and concentrated *in vacuo*. Purification by flash column chromatography (10% to 20% gradient ethyl acetate in hexanes) gave the desired benzyl azide product (183 mg, 76% yield). ^1H NMR (400 MHz, $CDCl_3$, δ): 1.18 (d, J = 6.8 Hz, 6H), 2.22 (s, 6H), 3.41 (heptet, J = 6.8 Hz, 1H), 3.61 (s, 3H), 3.82 (s, 3H), 3.92 (s, 2H), 4.35 (s, 2H), 4.64 (s, 2H), 5.24 (s, 2H), 6.65 (s, 2H), 6.84 (s, 1H), 6.98 (s, 1H), 7.28 (d, J = 8.0 Hz, 2H), 7.50 (d, J = 8.0 Hz, 2H). ^{13}C NMR (400 MHz, $CDCl_3$, δ): 20.5, 23.3, 26.4, 33.8, 52.2, 54.5, 57.5, 65.3, 87.5, 92.2, 99.8, 114.2, 116.3, 123.4, 126.9, 128.1, 129.5, 129.9, 131.8, 135.4, 135.7, 138.6, 142.0, 154.0, 155.9, 169.7. HRMS calcd for $C_{32}H_{35}N_3O_5$, 541.2577; found, 541.2579.

{4-[3-(4-Azidomethyl-phenylethynyl)-4-hydroxy-5-isopropyl-benzyl]-3,5-dimethyl-phenoxy}-acetic acid (NH-23). To a solution of **24** (140 mg, 0.26 mmol) in 7 ml of 40% (v/v) MeOH in THF was added conc. HCl (12 N, 0.5 ml). The reaction mixture was stirred for 5 h at rt., diluted with water, neutralized with 2N NaOH to pH 6, and then extracted with ethyl acetate (2×15 ml). The combined organic portions were washed with water (2×15 ml) and brine (2×15 ml), dried with $MgSO_4$, and concentrated *in vacuo*. Purification by flash column chromatography (5% to 10% gradient ethyl acetate in hexanes) gave the desired *O*-methoxymethyl deprotected phenol (82 mg, 64% yield). ^1H NMR (400 MHz, $CDCl_3$, δ): 1.22 (d, J = 6.8 Hz, 6H), 2.22 (s, 6H), 3.25 (heptet, J = 6.8 Hz, 1H), 3.82 (s, 3H), 3.89 (s, 2H), 4.36 (s, 2H), 4.64 (s, 2H), 5.77 (s, 1H), 6.64 (s, 2H),

6.71 (s, 1H), 6.96 (s, 1H), 7.30 (d, J = 8.0 Hz, 2H), 7.51 (d, J = 8.0 Hz, 2H). HRMS calcd for $C_{30}H_{31}N_3O_4$: 497.2315. Found: 497.2310.

To the phenol (120 mg, 0.23 mmol) in 3 ml methanol was added LiOH (2 mg, 0.51 mmol, dissolved in 0.5 ml MeOH). The reaction mixture was stirred at rt. for 24 h, acidified with 1N aq. HCl to pH 5, and diluted with ethyl acetate (15 ml). The organic portion was extracted with water (2×15 ml) and brine (2×15 ml), and concentrated *in vacuo*. Purification by preparative TLC (3: 2: 0.5 ratio of hexanes: ethyl acetate: MeOH) and isolated using 10% MeOH in CH_2Cl_2 afforded the desired product (35 mg, 30% yield). ^{1}H NMR (400 MHz, $CDCl_3$, δ): 1.21 (d, J = 6.8 Hz, 6H), 2.20 (s, 6H), 3.25 (heptet, J = 6.8 Hz, 1H), 3.87 (s, 2H), 4.33 (s, 2H), 4.63 (s, 2H), 6.65 (s, 2H), 6.71 (s, 1H), 6.95 (s, 1H), 7.27 (d, J = 8.0 Hz, 2H), 7.48 (d, J = 8.0 Hz, 2H). ^{13}C NMR (400 MHz, $CDCl_3$, δ): 20.5, 22.3, 27.5, 33.6, 54.4, 84.5, 95.3, 108.7, 114.2, 122.5, 127.0, 127.6, 128.1, 130.5, 131.4, 131.9, 134.2, 135.9, 138.7, 152.1, 155.5. HRMS calcd for $C_{29}H_{29}N_3O_4$, 483.2158; found, 483.2161.

{4-[3-Isopropyl-4-methoxymethoxy-5-(3-trifluoromethyl-phenylethynyl)-benzyl]-3,5-dimethyl-phenoxy}-acetic acid methyl ester (17h). The coupling of **12** with 1-ethynyl-3-trifluoromethyl-benzene (110 mg, 0.64 mmol) was effected using the general procedure with refluxing for 12 h to afford 243 mg (75% yield) of the title compound after purification by flash column chromatography (2% ethyl acetate in hexanes). ^{1}H NMR (400 MHz, $CDCl_3$, δ): 1.18 (d, J = 6.8 Hz, 6H), 2.21 (s, 6H), 3.40 (heptet, J = 6.8 Hz, 1H), 3.60 (s, 3H), 3.81 (s, 3H), 3.92 (s, 2H), 4.64 (s, 2H), 5.23 (s, 2H), 6.65 (s, 2H), 6.83 (s, 1H), 7.00 (s, 1H), 7.45 (t, J = 8.0 Hz, 1H), 7.55 (d, J = 8.0 Hz, 1H), 7.64 (d, J = 8.0 Hz, 1H), 7.74 (s 1H). ^{13}C NMR (400 MHz, $CDCl_3$, δ): 20.5, 23.3, 26.4, 33.8, 52.2, 57.5, 65.3, 70.9, 88.4, 91.1, 99.9, 114.2, 115.9, 124.3, 124.6, 124.7, 128.1, 128.8, 129.5, 129.9,

134.4, 135.9, 138.6, 142.1, 154.1, 155.9, 169.6. HRMS calcd for $C_{32}H_{33}F_3O_5$, 554.2280; found, 554.2294.

{4-[4-Hydroxy-3-isopropyl-5-(3-trifluoromethyl-phenylethynyl)-benzyl]-3,5-dimethyl-phenoxy}-acetic acid (18h, NH-17). To a solution of **17h** (240 mg, 0.43 mmol) in 10 ml of 40% (v/v) MeOH in THF was added conc. HCl (12 N, 0.9 ml). The reaction mixture was stirred for 9 h at rt., diluted with water, neutralized with 5N KOH to pH 6, and then extracted with ethyl acetate (2×15 ml). The combined organic portions were dried with $MgSO_4$ and concentrated *in vacuo*. Purification by flash column chromatography (5% to 10% gradient ethyl acetate in hexanes) gave the desired *O*-methoxymethyl deprotected phenol (138 mg, 63% yield). ^{1}H NMR (400 MHz, $CDCl_3$, δ): 1.22 (d, *J* = 6.8 Hz, 6H), 2.22 (s, 6H), 3.27 (heptet, *J* = 6.8 Hz, 1H), 3.81 (s, 3H), 3.89 (s, 2H), 4.63 (s, 2H), 5.79 (s, 1H), 6.64 (s, 2H), 6.72 (s, 1H), 7.00 (s, 1H), 7.46 (t, *J* = 7.6 Hz, 1H), 7.57 (d, *J* = 7.6 Hz, 1H), 7.65 (d, *J* = 7.6 Hz, 1H), 7.76 (s, 1H). ^{13}C NMR (400 MHz, $CDCl_3$, δ): 20.5, 22.2, 27.5, 33.6, 52.1, 65.2, 70.9, 85.6, 94.1, 108.2, 114.1, 123.5, 125.0, 127.2, 128.0, 128.2, 128.9, 130.1, 131.6, 134.4, 134.5, 138.6, 152.2, 155.9, 169.7. HRMS calcd for $C_{30}H_{29}F_3O_4$, 510.2018; found, 510.1992.

To the phenol (120 mg, 0.23 mmol) in 3 ml methanol was added LiOH (2 mg, 0.51 mmol, dissolved in 0.5 ml MeOH). The reaction mixture was stirred at rt. for 24 h, acidified with 1N aq. HCl to pH 5, and diluted with ethyl acetate (15 ml). The organic portion was extracted with water (2×15 ml) and brine (2×15 ml), and concentrated *in vacuo*. Purification by preparative TLC (3: 2: 0.5 ratio of hexanes: ethyl acetate: MeOH) and isolated using 10% MeOH in CH_2Cl_2 afforded the desired product (35 mg, 30% yield). ^{1}H NMR (400 MHz, CD_3OD, δ): 1.21 (d, *J* = 6.8 Hz, 6H), 2.23 (s, 6H), 3.30 (heptet, *J* = 6.8 Hz, 1H), 3.91 (s, 2H), 4.62 (s, 2H), 6.68 (s, 2H), 6.74 (s, 1H), 6.97 (s, 1H), 7.50 (t, *J* =

7.6 Hz, 1H), 7.74 (d, J = 7.6 Hz, 1H), 7.82 (s, 1H). ^{13}C NMR (400 MHz, CD_3OD, δ): 20.7, 22.7, 27.8, 34.0, 65.5, 87.4, 93.1, 109.9, 114.7, 124.9, 125.1, 128.1, 128.6, 129.5, 130.8, 132.1, 135.2, 136.1, 139.1, 153.3, 156.6, 172.3. HRMS calcd for $C_{29}H_{27}F_3O_4$, 496.1861; found, 496.1852.

{4-[3-Isopropyl-4-methoxymethoxy-5-(2-trifluoromethyl-phenylethynyl)-benzyl]-3,5-dimethyl-phenoxy}-acetic acid methyl ester (17i). 1-Ethynyl-2-trifluoromethyl-benzene was prepared following a modified procedure of Takahashi, et al. (1980) for the synthesis of ethynylarenes. To a stirred solution of 1-iodo-2-trifluoromethyl-benzene (1.0 g, 3.7 mmol) in diethylamine (15 ml) was added trimethylsilylacetylene (0.8 ml, 5.5 mmol), $PdCl_2(PPh_3)_2$ (52 mg, 0.074 mmol) and CuI (7.0 mg, 0.037 mmol). The reaction mixture was stirred at rt. overnight. Solvent was removed under reduced pressure and the resulting residue was diluted with ether (15 ml) and filtered through Celite. The organic portion was washed with water (2×15 ml) and brine (2×15 ml), dried over $MgSO_4$ and concentrated *in vacuo*. Purification by flash column chromatography (100% hexanes) gave the silyl-protected ethynylarene intermediate (0.41 g, 46% yield). This intermediate was then treated with tetrabutyl ammonium fluoride (1.0M, 1.9 ml) in THF (10 ml) at rt. for 10 min. The reaction was diluted with ether (15 ml), washed with water (2×15 ml) and brine (2×15 ml), dried over $MgSO_4$ and concentrated *in vacuo*. Filtration through a silica gel plug (100% hexanes) gave the desired product (84 mg, 29% yield). Low yield of the reaction was due to the volatile property of the ethynylarene product. ^1H NMR (400 MHz, $CDCl_3$, δ): 3.36 (s, 1H), 7.44 (t, J = 6.8 Hz, 1H), 7.50 (t, J = 7.2 Hz, 1H), 7.66 (t, J = 6.8 Hz, 2H).

The coupling of **12** with 1-ethynyl-2-trifluoromethyl-benzene (80 mg, 0.47 mmol) was effected using the general procedure with refluxing for 18 h to afford 58 mg (24% yield)

of the title compound after purification by flash column chromatography (2% ethyl acetate in hexanes). The coupling efficiency was low in this system and starting compound **12** was recovered from the reaction.

{4-[4-Hydroxy-3-isopropyl-5-(2-trifluoromethyl-phenylethynyl)-benzyl]-3,5-dimethyl-phenoxy}-acetic acid (18i, NH-18). To a solution of **17i** (50 mg, 0.09 mmol) in 2.5 ml of 40% (v/v) MeOH in THF was added conc. HCl (12 N, 200 μl). The reaction mixture was stirred for 9 h at rt., diluted with water, neutralized with 5N KOH to pH 6, and then extracted with ethyl acetate (2×5 ml). The combined organic portions were washed with water (3×5 ml) and brine (3×5 ml), dried with $MgSO_4$ and concentrated *in vacuo*. Purification by preparative TLC (5% ethyl acetate in hexanes) gave the desired *O*-methoxymethyl deprotected phenol (40 mg, 87% yield). ^1H NMR (400 MHz, $CDCl_3$, δ): 1.21 (d, *J* = 6.8 Hz, 6H), 2.22 (s, 6H), 3.28 (heptet, *J* = 6.8 Hz, 1H), 3.82 (s, 3H), 3.89 (s, 2H), 4.64 (s, 2H), 5.94 (s, 1H), 6.65 (s, 2H), 6.73 (s, 1H), 6.97 (s, 1H), 7.41 (t, *J* = 7.6 Hz, 1H), 7.51 (t, *J* = 7.6 Hz, 1H), 7.66 (t, *J* = 6.8 Hz, 2H). ^{13}C NMR (400 MHz, $CDCl_3$, δ): 20.5, 22.3, 27.3, 33.6, 52.2, 65.3, 90.0, 91.6, 108.2, 114.1, 125.9, 127.1, 128.1, 130.2, 131.5, 131.6, 133.6, 134.5, 138.6, 152.8, 155.9, 169.7. HRMS calcd for $C_{30}H_{29}F_3O_4$, 510.2018; found, 510.2026.

To the phenol (35 mg, 0.069 mmol) in 3 ml methanol was added LiOH (3.6 mg, 0.15 mmol, dissolved in 0.5 ml MeOH). The reaction mixture was stirred at rt. for 36 h, acidified with 1N aq. HCl to pH 5, and diluted with ethyl acetate (5 ml). The organic portion was extracted with water (3×5 ml) and brine (3×5 ml), and concentrated *in vacuo*. Purification by preparative TLC (3: 2: 0.5 ratio of hexanes: ethyl acetate: MeOH) and isolated using 10% MeOH in CH_2Cl_2 afforded the desired product (12 mg, 35% yield). ^1H NMR (400 MHz, $CDCl_3$, δ): 1.20 (d, *J* = 6.8 Hz, 6H), 2.20 (s, 6H), 3.27 (heptet, *J* = 6.8

Hz, 1H), 3.87 (s, 2H), 4.63 (s, 3H), 6.66 (s, 2H), 6.72 (s, 1H), 6.96 (s, 1H), 7.40 (t, *J* = 7.6 Hz, 1H), 7.49 (t, *J* = 7.6 Hz, 1H), 7.64 (m, *J* = 8.0 Hz, 2H). ^{13}C NMR (400 MHz, $CDCl_3$, δ): 20.5, 22.3, 27.4, 33.6, 65.0, 90.0, 91.7, 108.3, 114.2, 120.9, 122.4, 125.1, 125.8, 125.9, 127.0, 128.1, 130.5, 131.4, 131.6, 133.5, 134.6, 138.7, 152.9, 155.5. HRMS calcd for $C_{29}H_{27}F_3O_4$, 496.1861; found, 496.1862.

{4-[3-(3-Amino-phenylethynyl)-5-isopropyl-4-methoxymethoxy-benzyl]-3,5-dimethyl-phenoxy}-acetic acid methyl ester (17j). The coupling of **12** with 3-ethynylaniline (126 mg, 1.07 mmol) was effected using the general procedure with refluxing for 16 h to afford 260 mg (53% yield) of the title compound after purification by flash column chromatography (10% to 20% gradient ethyl acetate in hexanes). ^1H NMR (400 MHz, $CDCl_3$, δ): 1.17 (d, *J* = 6.8 Hz, 6H), 2.21 (s, 6H), 3.41 (heptet, *J* = 6.8 Hz, 1H), 3.60 (s, 3H), 3.82 (s, 3H), 3.91 (s, 2H), 4.64 (s, 2H), 5.24 (s, 2H), 6.64 (s, 2H), 6.82 (d, *J* = 4.0 Hz, 1H), 6.89 (d, *J* = 7.6 Hz, 1H), 6.95 (s, 1H), 7.10 (t, *J* = 8.0 Hz, 1H). ^{13}C NMR (400 MHz, $CDCl_3$, δ): 20.5, 23.3, 26.4, 33.8, 52.2, 57.5, 65.3, 86.2, 93.1, 99.7, 114.2, 115.3, 116.5, 117.6, 121.8, 124.0, 126.6, 129.2, 129.5, 130.0, 135.6, 138.6, 141.8, 146.2, 153.9, 155.9, 169.7. HRMS calcd for $C_{31}H_{35}NO_5$, 501.2515; found, 501.2522.

{4-[3-(3-Amino-phenylethynyl)-4-hydroxy-5-isopropyl-benzyl]-3,5-dimethyl-phenoxy}-acetic acid methyl ester (22). To a solution of **17j** (220 mg, 0.44 mmol) in 10 ml of 40% (v/v) MeOH in THF was added conc. HCl (12 N, 880 μl). The reaction mixture was stirred for 16 h at rt., diluted with water, neutralized with 5N KOH to pH 6, and then extracted with ethyl acetate (2×10 ml). The combined organic portions were washed with water (3×10 ml) and brine (3×10 ml), dried with $MgSO_4$ and concentrated *in vacuo*. Purification by preparative TLC (50% ethyl acetate in hexanes) gave the desired

O-methoxymethyl deprotected phenol (120 mg, 60% yield). ^{1}H NMR (400 MHz, $CDCl_3$, δ): 1.21 (d, *J* = 7.2 Hz, 6H), 2.21 (s, 6H), 3.26 (heptet, *J* = 7.2 Hz, 1H), 3.80 (s, 3H), 3.88 (s, 2H), 4.62 (s, 2H), 5.85 (broad s, 1H), 6.63 (s, 2H), 6.64 (m, 1H), 6.70 (s, 1H), 6.79 (s, 1H), 6.88 (d, J = 8.0 Hz, 1H), 6.94 (s, 1H), 7.10 (t, *J* = 8.0 Hz, 1H). ^{13}C (400 MHz, $CDCl_3$, δ): 20.4, 22.2, 27.5, 33.5, 52.1, 65.2, 83.2, 96.1, 108.9, 114.1, 115.6, 117.5, 121.8, 123.0, 127.0, 127.3, 129.3, 130.3, 131.3, 134.0, 138.5, 146.3, 152.0, 155.8, 169.7. HRMS calcd for $C_{29}H_{31}NO_4$, 457.2253; found, 457.2256.

{4-[3-(3-Amino-phenylethynyl)-4-hydroxy-5-isopropyl-benzyl]-3,5-dimethyl-phenoxy}-acetic acid (18j, NH-21). To phenol **22** (15 mg, 0.033 mmol) in 1 ml methanol was added LiOH (1.6 mg, 0.066 mmol) and water (1 drop). The reaction mixture was stirred at rt. for 5 h, acidified with 1N aq. HCl to pH 5, and diluted with ethyl acetate (5 ml). The organic portion was extracted with water (3×5 ml) and brine (3×5 ml), and concentrated *in vacuo*. Purification by preparative TLC (5% MeOH in CH_2Cl_2) and isolated using 10% MeOH in CH_2Cl_2 afforded the desired product (13 mg, 95% yield). ^{1}H NMR (400 MHz, CD_3OD, δ): 1.21 (d, *J* = 6.8 Hz, 6H), 2.22 (s, 6H), 3.26 (heptet, *J* = 6.8 Hz, 1H), 3.89 (s, 2H), 4.60 (s, 2H), 6.66 (s, 2H), 6.69 (broad s, 2H), 6.85 (s, 1H), 6.87 (d, *J* = 7.2 Hz, 1H), 6.94 (s, 1H), 7.10 (t, *J* = 7.6 Hz, 1H). ^{13}C NMR (400 MHz, CD_3OD, δ): 20.2, 22.1, 27.2, 33.4, 64.9, 83.3, 95.5, 108.9, 114.0, 115.7, 117.7, 121.8, 123.1, 127.1, 129.1, 130.1, 131.3, 134.1, 138.4, 146.2, 151.9, 155.7, 171.5. HRMS calcd for $C_{28}H_{29}NO_4$, 443.2097; found: 443.2088.

{4-[4-Hydroxy-3-isopropyl-5-(3-nitro-phenylethynyl)-benzyl]-3,5-dimethyl-phenoxy}-acetic acid (NH-19). A solution of *m*-CPBA (60% pure, 150 mg, 0.51 mmol) in 5 ml $CHCl_3$ was added gradually at 0°C to an ice cooled, stirred solution of **22** (80 mg,

0.17 mmol) in 5 ml $CHCl_3$. Stirring continued at 0°C for 1.5 h and warmed to rt. The reaction mixture was quenched with saturated $NaHCO_3$ (5 ml) and water (5 ml), and extracted with ethyl acetate (3×10 ml). The combined organic phase was washed with washed with brine (3×10 ml), dried over $MgSO_4$, and concentrated *in vacuo*. Purification by preparative TLC (25% ethyl acetate in hexanes) afforded the desired product (26 mg, 31% yield). ^1H NMR (400 MHz, $CDCl_3$, δ): 1.23 (d, *J* = 6.8 Hz, 6H), 2.22 (s, 6H), 3.27 (heptet, *J* = 6.8 Hz, 1H), 3.82 (s, 3H), 3.90 (s, 2H), 4.64 (s, 2H), 5.70 (s, 1H), 6.65 (s, 2H), 6.72 (s, 1H), 7.01 (s, 1H), 7.53 (t, *J* = 8.0 Hz, 1H), 7.79 (d, *J* = 8.0 Hz, 1H), 8.18 (d, *J* = 8.0 Hz, 1H), 8.34 (s, 1H). ^{13}C NMR (400 MHz, $CDCl_3$, δ): 20.5, 22.3, 27.5, 33.6, 52.2, 65.2, 86.8, 93.2, 107.9, 114.2, 123.1, 124.4, 126.2, 127.3, 128.4, 129.5, 130.1, 131.8, 134.5, 137.0, 138.6, 148.1, 152.3, 155.9, 169.7. HRMS calcd for $C_{29}H_{29}NO_6$, 487.1995; found, 487.1965.

To the phenol (20 mg, 0.041 mmol) in 3 ml methanol was added LiOH (2.0 mg, 0.082 mmol) and water (0.5 ml). The reaction mixture was stirred at rt. for 8 h, acidified with 1N aq. HCl to pH 5, and diluted with ethyl acetate (5 ml). The organic portion was extracted with water (3×5 ml) and brine (3×5 ml), and concentrated *in vacuo*. Purification by preparative TLC (5% MeOH in CH_2Cl_2) and isolated using 10% MeOH in CH_2Cl_2 afforded the desired product (16 mg, 83% yield). ^1H NMR (400 MHz, $CDCl_3$, δ): 1.22 (d, *J* = 6.8 Hz, 6H), 2.19 (s, 6H), 3.25 (heptet, *J* = 6.8 Hz, 1H), 3.87 (s, 2H), 4.62 (s, 2H), 6.64 (s, 2H), 6.70 (s, 1H), 6.99 (s, 1H), 7.50 (t, *J* = 8.0 Hz, 1H), 7.76 (d, *J* = 8.0 Hz, 1H), 8.15 (d, *J* = 8.0 Hz, 1H), 8.31 (s, 1H). ^{13}C NMR (400 MHz, $CDCl_3$, δ): 20.5, 22.3, 27.5, 33.6, 65.1, 86.7, 93.2, 107.9, 114.2, 123.2, 124.4, 126.2, 127.3, 128.4, 129.5, 130.4, 131.7, 134.6, 137.0, 138.7, 148.1, 152.4, 155.5. HRMS calcd for $C_{28}H_{27}NO_6$, 473.1838; found, 473.1859.

{4-[3-(2-Amino-phenylethynyl)-5-isopropyl-4-methoxymethoxy-benzyl]-3,5-dimethyl-phenoxy}-acetic acid methyl ester (17k). 2-Ethynylaniline was prepared following a modified procedure of Takahashi, et al. (1980) for the synthesis of ethynylarenes. To a stirred solution of 2-iodoaniline (1.0 g, 4.6 mmol) in diethylamine (15 ml) was added trimethylsilylacetylene (1.0 ml, 6.8 mmol), $PdCl_2(PPh_3)_2$ (65 mg, 0.092 mmol) and CuI (9.0 mg, 0.046 mmol). The reaction mixture was stirred at rt. overnight. Solvent was removed under reduced pressure and the resulting residue was diluted with ethyl acetate (15 ml) and filtered through Celite. The organic portion was washed with water (2×15 ml) and brine (2×15 ml), dried over $MgSO_4$ and concentrated *in vacuo*. Purification by flash column chromatography (10% ethyl acetate in hexanes) gave the silyl-protected ethynylarene intermediate (0.82 g, 95% yield). This intermediate was then treated with tetrabutyl ammonium fluoride (1.0 M, 4.8 ml) in THF (20 ml) at rt. for 10 min. The reaction was diluted with ether (15 ml), washed with water (2×15 ml) and brine (2×15 ml), dried over $MgSO_4$ and concentrated *in vacuo*. Filtration through a silica gel plug (5% ethyl acetate in hexanes) gave the desired product (0.45 g, 89% yield). ^{1}H NMR (400 MHz, $CDCl_3$, δ): 3.38 (s, 1H), 4.24 (broad s, 2H), 6.68 (m, 2H), 7.14 (t, *J* = 7.6 Hz, 1H), 7.32 (d, *J* = 7.6 Hz, 1H).

The coupling of **12** with 2-ethynylaniline (126 mg, 1.07 mmol) was effected using the general procedure with refluxing for 18 h to afford 136 mg (28% yield) of the title compound after purification by flash column chromatography (2% ethyl acetate in hexanes). The coupling efficiency was low in this system and starting compound **12** was recovered from the reaction. ^{1}H NMR (400 MHz, $CDCl_3$, δ): 1.17 (d, *J* = 6.8 Hz, 6H), 2.21 (s, 6H), 3.43 (heptet, *J* = 6.8 Hz, 1H), 3.58 (s, 3H), 3.81 (s, 3H), 3.91 (s, 2H), 4.34 (broad s, 2H), 4.63 (s, 2H), 5.21 (s, 2H), 6.64 (s, 2H), 6.67 (t, *J* = 8.0 Hz, 2H), 6.85 (s, 1H), 6.94 (s, 1H), 7.10 (t, J = 7.8 Hz, 1H), 7.30 (d, *J* = 7.6 Hz, 1H). ^{13}C NMR (400 MHz,

$CDCl_3$, δ): 20.6, 23.4, 26.4, 33.8, 52.2, 57.6, 65.3, 89.5, 92.0, 99.9, 107.9, 114.2, 116.9, 117.3, 126.6, 129.3, 129.7, 130.0, 131.9, 135.8, 138.6, 142.0, 147.9, 153.5, 155.9, 169.7. HRMS calcd for $C_{31}H_{35}NO_5$, 501.2515; found, 501.2509.

{4-[3-(2-Amino-phenylethynyl)-4-hydroxy-5-isopropyl-benzyl]-3,5-dimethyl-phenoxy}-acetic acid (18k, NH-22). To a solution of **17k** (130 mg, 0.26 mmol) in 8 ml of 40% (v/v) MeOH in THF was added conc. HCl (12 N, 520 μl). The reaction mixture was stirred for 9 h at rt., diluted with water, neutralized with 5N KOH to pH 6, and then extracted with ethyl acetate (2×10 ml). The combined organic portions were washed with water (3×10 ml) and brine (3×10 ml), dried with $MgSO_4$ and concentrated *in vacuo*. Purification by preparative TLC (50% ethyl acetate in hexanes) gave the desired *O*-methoxymethyl deprotected phenol (66 mg, 55% yield). ^1H NMR (400 MHz, $CDCl_3$, δ): 1.21 (d, *J* = 6.8 Hz, 6H), 2.21 (s, 6H), 3.26 (heptet, *J* = 6.8 Hz, 1H), 3.80 (s, 3H), 3.88 (s, 2H), 4.22 (broad s, 2H), 4.62 (s, 2H), 5.88 (broad s, 1H), 6.63 (s, 2H), 6.68-6.73 (m, 2H), 6.94 (s, 1H), 7.13 (t, *J* = 8.0 Hz, 1H), 7.31 (d, *J* = 8.0 Hz, 1H). ^{13}C NMR (400 MHz, $CDCl_3$, δ): 20.5, 22.3, 27.5, 33.6, 52.2, 65.2, 89.0, 92.2, 107.2, 109.0, 114.1, 114.5, 118.0, 127.1, 127.4, 130.2, 131.5, 132.2, 134.2, 138.5, 147.8, 151.9, 155.8, 169.7. HRMS calcd for $C_{29}H_{31}NO_4$, 457.2253; found, 457.2239.

To the phenol (10 mg, 0.022 mmol) in 1 ml methanol was added LiOH (1.0 mg, 0.044 mmol) and water (1 drop). The reaction mixture was stirred at rt. for 4 h, acidified with 1N aq. HCl to pH 5, and diluted with ethyl acetate (5 ml). The organic portion was extracted with water (3×5 ml) and brine (3×5 ml), and concentrated *in vacuo*. Purification by preparative TLC (5% MeOH in CH_2Cl_2) and isolated using 10% MeOH in CH_2Cl_2 afforded the desired product (5 mg, 57% yield). ^1H NMR (400 MHz, $CDCl_3$, δ): 1.21 (d, *J* = 6.8 Hz, 6H), 2.22 (s, 6H), 3.26 (heptet, *J* = 6.8 Hz, 1H), 3.89 (s, 2H), 4.65 (s,

2H), 6.65 (s, 2H), 6.68 (s, 1H), 6.72 (d, J = 7.6 Hz, 2H), 6.95 (s, 1H), 7.15 (t, J = 7.6 Hz, 1H), 7.31 (d, J = 6.8 Hz, 1H). ^{13}C NMR (400 MHz, $CDCl_3$, δ): 20.5, 22.3, 27.5, 33.6, 64.9, 89.0, 92.3, 107.4, 109.0, 114.2, 114.7, 118.2, 127.0 127.5, 130.2, 130.7, 131.4, 132.2, 134.3, 138.8, 147.7, 152.0, 155.3. HRMS calcd for $C_{28}H_{29}NO_4$, 443.2097; found, 433.2108.

Triisopropyl-{4-[3-isopropyl-4-methoxymethoxy-5-(4-pentyl-phenylethynyl)-benzyl]-3,5-dimethyl-phenoxy}-silane (19) The coupling of **2** with 1-ethynyl-4-pentylbenzene (0.15 ml, 0.80 mmol) was effected using the general procedure to afford 312 mg (49%, 2 steps from **1**) of the title compound as a colorless oil. ^1H NMR ($CDCl_3$, 400 MHz, δ): 0.89 (t, 3H, J = 6.8 Hz), 1.1 (d, 18H, J = 7.2 Hz), 1.4 (d, 6H, J = 6.8 Hz), 1.3 (m, 9H), 1.6 (m, 2H), 2.60 (t, 2H, J = 7.6 Hz), 3.39 (heptet, 1H, J = 6.8 Hz), 3.60 (s, 3H), 3.90 (s, 2H), 5.25 (s, 2H), 6.61 (s, 2H), 6.87 (s, 2H), 7.13 (d, 2H, J = 8.0 Hz), 7.39 (d, 2H, J = 8.0 Hz). HR-MS calcd for $C_{42}H_{60}O_3Si$: 640.4312, found: 640.4300.

4-[3-Isopropyl-4-methoxymethoxy-5-(4-pentyl-phenylethynyl)-benzyl]-3,5-dimethyl-phenol (20) Compound **19** (310 mg, 0.5 mmol) and Bu_4NF (0.8 ml, 1.0 M in THF) were combined in 10 ml THF. Deprotection was nearly instantaneous, as determined by TLC. The reaction mixture was diluted with ethyl acetate (20 ml), washed with water (2×25 ml) and brine (2×25 ml), dried over $MgSO_4$, and concentrated. The crude product was purified by flash column chromatography (5% ethyl acetate in hexanes) to yield **20** (215 mg, 90%). ^1H NMR ($CDCl_3$, 400 MHz, δ): 0.89 (t, 3H, J = 6.8 Hz), 1.3 (m, 4H), 1.6 (m, 2H), 2.19 (s, 6H), 2.60 (t, 2H, J = 7.6 Hz), 3.41 (heptet, 1H, J = 7.0 Hz), 3.60 (s, 3H), 3.90 (s, 2H), 4.62 (s, broad, 1H), 5.25 (s, 2H), 6.56 (s, 2H), 6.86 (s, 1H), 6.94 (s, 1H), 7.13 (d, 2H, J = 8.0 Hz), 7.39 (d, 2H, J = 8.0 Hz). ^{13}C NMR ($CDCl_3$, 400 MHz, δ): 14.0,

20.3, 20.8, 22.5, 23.4, 26.4, 30.9, 31.4, 33.7, 35.8, 57.5, 86.2, 93.0, 99.7, 114.8, 116.7, 120.4, 126.5, 128.4, 129.5, 131.3, 135.9, 138.7, 141.8, 143.4, 153.6, 153.8. HR-MS calcd for $C_{33}H_{40}O_3$: 484.2977, found: 484.2976.

{4-[3-Isopropyl-4-methoxymethoxy-5-(4-pentyl-phenylethynyl)-benzyl]-3,5-dimethyl-phenoxy}-acetic acid *tert*-butyl ester (21) To a dry rbf containing a solution of **20** (100 mg, 0.21 mmol) and Cs_2CO_3 (336 mg, 1.05 mmol) in 10 ml DMF was added t-butylbromoacetate (35 μL, 0.23 mmol). The reaction mixture was stirred for 30 min at rt., neutralized with cold 1N aq. HCl to pH 7, and extracted with ethyl acetate (3×10 ml). The combined organic portions were washed with brine (3×15 ml), dried over $MgSO_4$, and concentrated. Crude product was purified by flash column chromatography (5% ethyl acetate in hexanes) to yield **21** (102mg, 82%). ^{1}H NMR ($CDCl_3$, 400 MHz, δ): 0.88 (t, 3H, *J* = 6.8 Hz), 1.17 (d, 6H, *J* = 6.8 Hz), 1.3 (m, 6H), 1.48 (s, 9H), 1.60 (m, 2H), 2.21 (s, 6H), 2.59 (t, 2H, *J* = 7.6 Hz), 3.41 (heptet, 1H, *J* = 6.8 Hz), 3.60 (s, 3H), 3.91 (s, 2H), 4.51 (s, 2H), 5.25 (s, 2H), 6.63 (s, 2H), 6.85 (s, 1H), 6.94 (s, 1H), 7.13 (d, 2H, *J* = 8.0 Hz), 7.39 (d, 2H, J = 8.0 Hz). ^{13}C NMR ($CDCl_3$, 400 MHz, δ): 14.0, 20.5, 22.4, 23.3, 26.3, 28.0, 30.8, 31.4, 33.7, 35.8, 57.5, 65.6, 82.1, 86.1, 93.0, 99.7, 114.1, 116.6, 120.4, 126.5, 128.4, 129.5, 129.6, 131.2, 135.7, 138.4, 141.8, 143.3, 153.8, 155.9, 168.3. HR-MS calcd for $C_{39}H_{50}O_5$: 598.3658, found: 598.3658.

{4-[4-Hydroxy-3-isopropyl-5-(4-pentyl-phenylethynyl)-benzyl]-3,5-dimethyl-phenoxy}-acetic acid (NH-2) To ester **21** (50 mg, 0.08 mmol) in 2ml of 50% (v/v) mixture of *i*-PrOH and THF was added 1N aq. HCl (0.2 ml). The reaction mixture was stirred for 6 h at rt., diluted with water, neutralized with 1N aq. NaOH to pH 6, and then extracted with ethyl acetate (2×15 ml). The combined organic portions were dried with

$MgSO_4$ and concentrated to yield 40mg of the corresponding *O*-methoxymethyl deprotected phenol, which was used directly in the following step. To the resulting phenol in 1mL methanol was added 300 μL of 1N aq. NaOH. The reaction mixture was stirred at rt. for 4 h, acidified with 1N aq. HCl to pH 6, and diluted with ethyl acetate (15 ml). The organic portion was extracted with water (2×15 ml) and brine (2×15 ml), dried over $MgSO_4$ and concentrated *in vacuo* to yield 27 mg desired product (64%, 2 steps) as a yellow solid. ^{1}H NMR ($CDCl_3$, 400 MHz, δ): 0.88 (t, 3H, *J* = 6.8 Hz), 1.21 (d, 6H, *J* = 6.8 Hz), 1.3 (m, 4H), 1.6 (m, 2H), 2.23 (s, 6H), 2.60 (t, 2H, *J* = 7.6Hz), 3.25 (heptet, 1H, *J* = 6.8Hz), 3.88 (s, 2H), 4.67 (s, 2H), 6.65 (s, 2H), 6.71 (s, 1H), 6.93 (s, 1H), 7.14 (d, 2H, *J* = 8.0 Hz), 7.41 (d, 2H, *J* = 8.0 Hz). ^{13}C NMR ($CDCl_3$, 400 MHz, δ): 14.0, 20.5, 22.3, 22.5, 27.5, 30.9, 31.4, 33.6, 35.9, 64.8, 83.1, 96.2, 109.1, 114.2, 119.5, 127.0, 127.3, 128.6, 130.8, 131.3, 131.4, 134.1, 138.8, 143.9, 152.0, 155.4. HR-MS calcd for $C_{33}H_{38}O_4$: 498.2770, found: 498.2766. HPLC: Condition A, ret. time 4.2 min; Condition B ret. time 5.5 min; 95.2% pure.

A.2 TR Ligand Binding Assays

Hormone binding and analogue competition assays were carried out as described previously.[4] The K_d and standard error (SE) values are were calculated by fitting the competition data to the equations of Swillens[5] (1995) using the Graph-Pad Prism computer program (Graph-Pad Software Inc., San Diego, CA).

A.3 TR Transcriptional Activation Assays

The reporter vector for the luciferase reporter containing a two copies of a synthetic DR-4 TRE upstream of a minimal thymidine kinase (tk) promoter and pSG5 expression vectors for the human hTRα$_1$ and hTRβ$_1$ were gifts from Dr. M. Privalsky (UCD, Davis CA). The TH/bZIP TRE-ΔMTV luciferase reporter plasmid and expression

vectors for the *xenopus miw* xTRα_1 and xTRβ_1 were gifts from Dr. J. D. Furlow (UCD, Davis CA).

Human uterine cervix cancer (HeLa) cells (Cell Culture Facility, UCSF) were grown to ~80% confluency in Dulbecco's modified Eagle's (DME)/H-21 containing 10% newborn calf serum. Cells (~1.5 x 10^6) were collected and resuspended in 0.5 ml of electroporation buffer (Dulbecco's phosphate-buffered saline (PBS) containing 0.1% dextrose, 10 mg/ml bioprene) with 5 μg of luciferase reporter plasmid, 0.5 μg per transfection of pRL-TK constitutive renilla luciferase reporter (Promega), and 1 μg of either TRα or TRβ expression vector per transfection. Cells were transfected by electroporation (Bio-Rad Gene Pulser; 0.32 kV, 960 mF, 0.4 cm cuvettes) and plated in 12-well plates in growth medium (DME H-21 with 10% charcoal-treated, hormone striped newborn calf serum or 10% charcoal-treated, hormone striped, heat-treated 80°C/20min, as indicated). After 6 h incubation, ligand or vehicle (EtOH) were added in triplicate. After additional 24 h incubation, cells were harvested and assayed for luciferase activity using the Promega Dual Luciferase kit (Promega) and Analytical Luminescence Laboratory Monolight® 3010 luminometer. Data were normalized to the renilla luciferase and analyzed with the Graph-Pad computer program (GraphPad Software Inc., San Diego, CA) using the sigmoidal dose-response or single-site competition models to generate EC_{50} and IC_{50} values, respectively.

A.4 Mammalian Two-Hybrid Assays

The following expression plasmids were derived as previously described: GAL-NCoR and luciferase reporter containing GAL promoter. GAL-SMRT (*aa*987-1491) and GAL-GRIP (*aa*618-1121) were synthesized by standard PCR methods and cloned into the mammalian GAL4-DBD expression vector pM (Clontech, Palo Alto, CA) between the

EcoRI and SalI sites. The expression vector for VP16-hTRβ LBD was a gift from Dr. R. Evans (UCSD, San Diego CA) and for VP16-RAR LBD was a gift from Dr. D. Moore (Baylor College of Medicine, Houston TX). The pSG5 expression vector for xTRα- and xTRβ-LBD/GAL4 DBD fusion was a gift from Dr. J. D. Furlow (UCD, Davis CA). The GRIP-1/VP16 fusion protein was a gift from Dr. J. Baxter (UCSF) and SRC-1/GAL4-AD fusion protein was a gift from Dr. M. Privalsky.

HeLa cells (Cell Culture Facility, UCSF) were maintained in culture and transfected as described above. Cells (5×10^6) were collected and resuspended in Dulbecco's PBS (0.5ml/transfection) containing 0.1% dextrose, 10 μg/ml bioprene, and mixed with 2.5 μg luciferase reporter, 2.5 μg of a constitutive β-galactosidase expression vector, 1 μg of the appropriate TR fusion vector, and 1 μg of the appropriate corepressor or coactivator fusion vector per transfection. After electroporation (see above), cells were resuspended in medium containing 10% charcoal-treated, hormone-depleted newborn calf serum and incubated with ligand for 24h. Luciferase activity was measured using the Promega Luciferase Kit (Promega) and data were analyzed with the Graph-Pad computer program (GraphPad Software Inc., San Diego, CA) using the sigmoidal dose-response model to generate EC_{50} values.

A.5 References

(1) Takahashi, S.; Kuroyama, Y.; Sonogashira, K.; Hagihara, N. Convenient synthesis of ethynylarenes and diethynylarenes. *Synthesis Comm.* **1980**, 627-629.

(2) Galli, C. Investigation of the two-step nature of the Sandmeyer Reaction. *J. Chem. Soc. Perkin Trans. II* **1981**, 1459-1461.

(3) Vogl, E. M.; Buchwald, S. L. Palladium-catalyzed monoarylation of nitroalkanes. *J. Org. Chem.* **2002**, *67*, 106-111.

(4) Apriletti, J. W.; Baxter, J. D.; Lau, K. H.; West, B. L. Expression of the rat alpha 1 thyroid hormone receptor ligand binding domain in Escherichia coli and the use of a ligand-induced conformation change as a method for its purification to homogeneity. *Protein Expr Purif* **1995**, *6*, 363-370.

(5) Swillens, S. Interpretation of binding curves obtained with high receptor concentrations: practical aid for computer analysis. *Mol. Pharmacol.* **1995**, *47*, 1197-1203.

Appendix B

^{1}H and ^{13}C NMR Spectra

4-Bromo-2-isopropyl phenyl methoxymethyl ether (1)

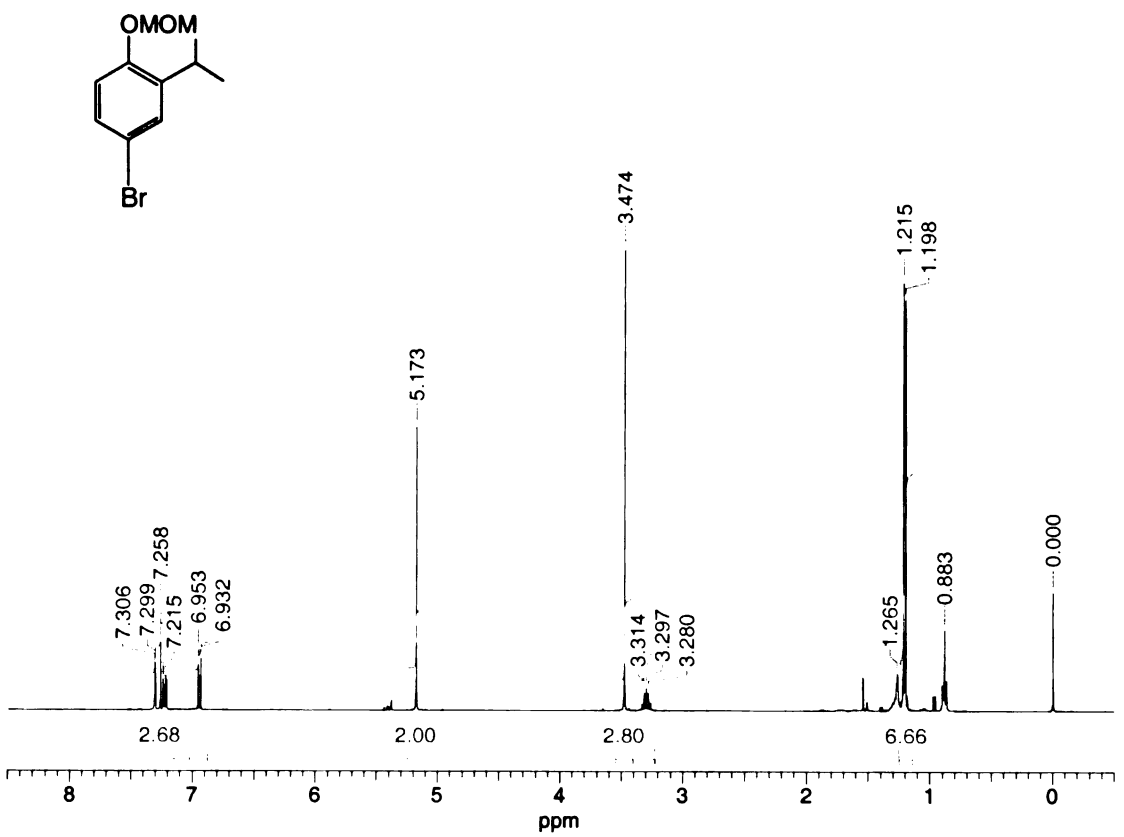

O-Triisopropylsilyl-4-bromo-3,5-dimethylphenol (2)

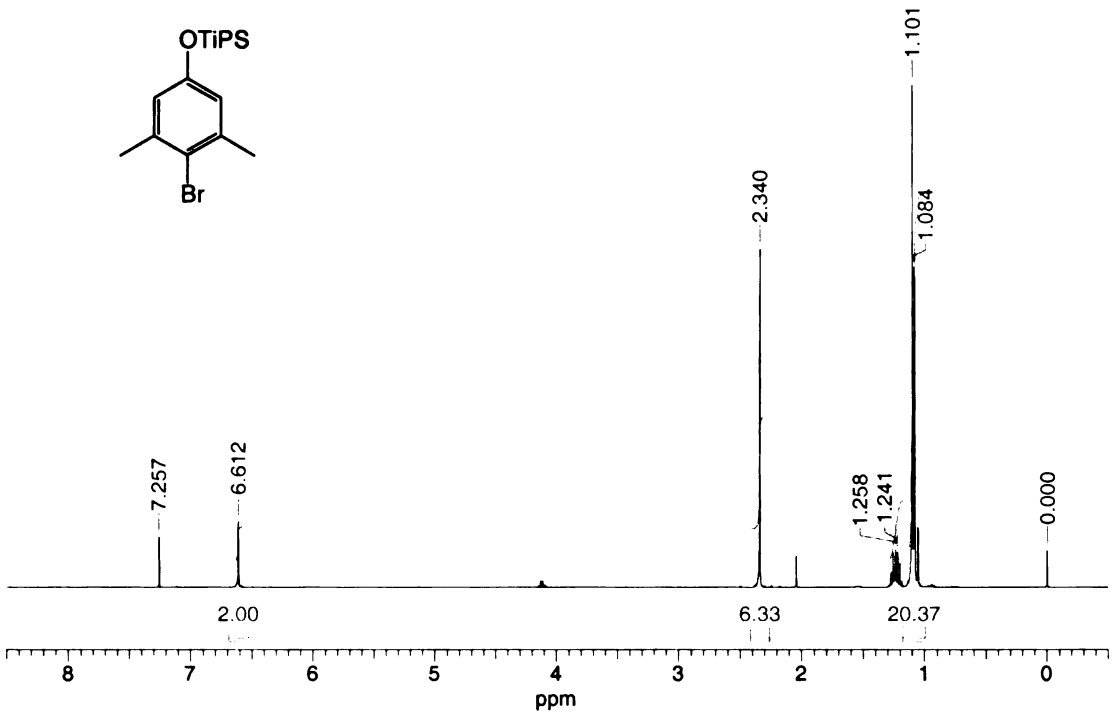

2,4-Dimethyl-4-*O*-triisopropylsilylbenzaldehyde (3)

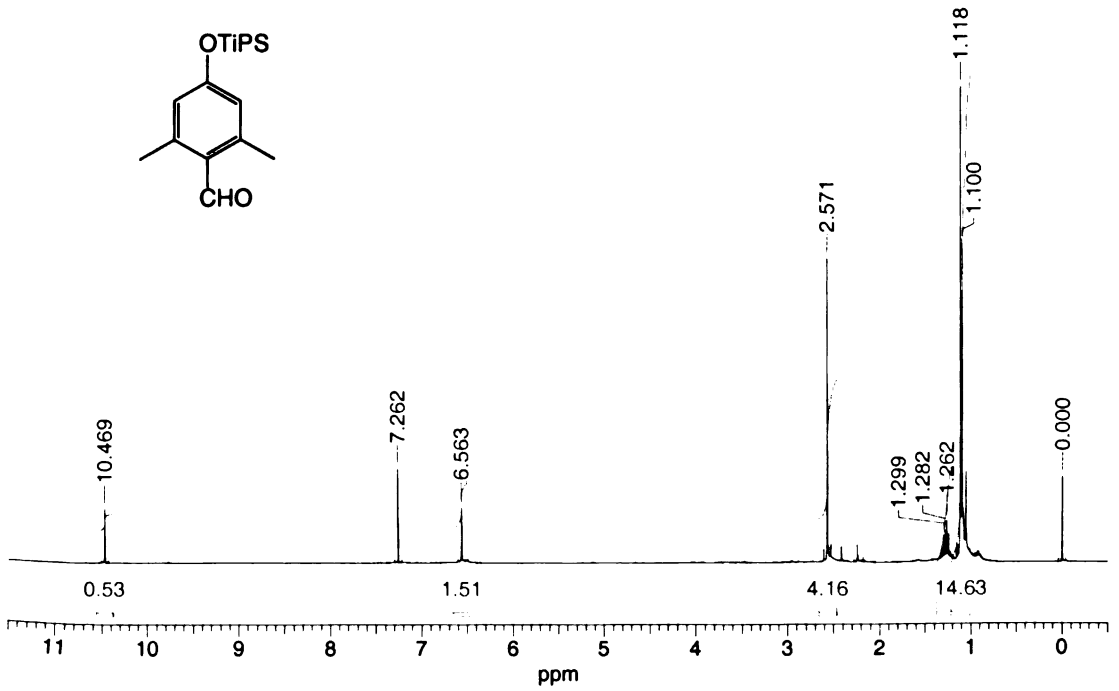

3,5-Dimethyl-4-(3-isopropyl-4-methoxymethylbenzylhydroxy)-*O*-tri-isopropylsilyl phenol (4)

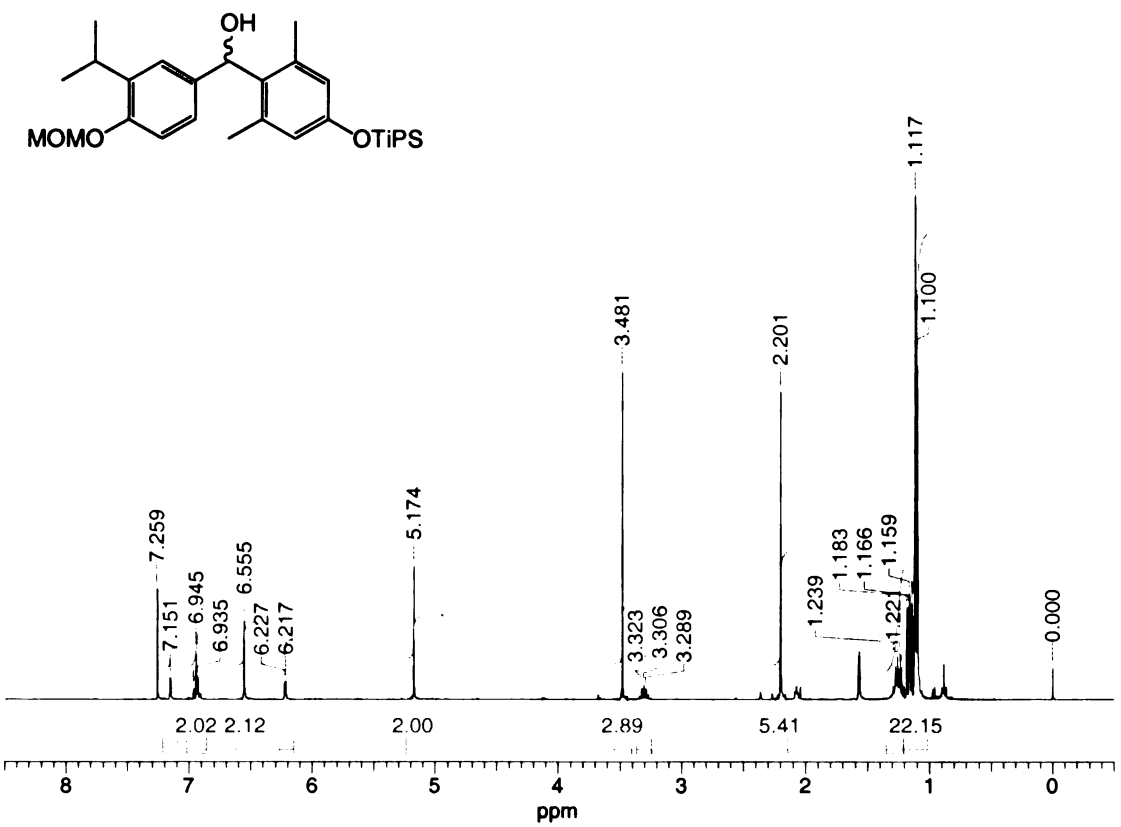

[3,5-Dimethyl-4-(4-hydroxy-3-isopropylbenzyl)-phenoxy]-acetic acid (GC-1)

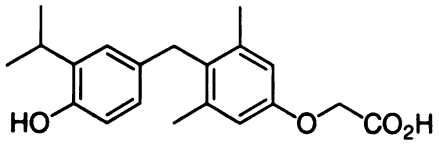

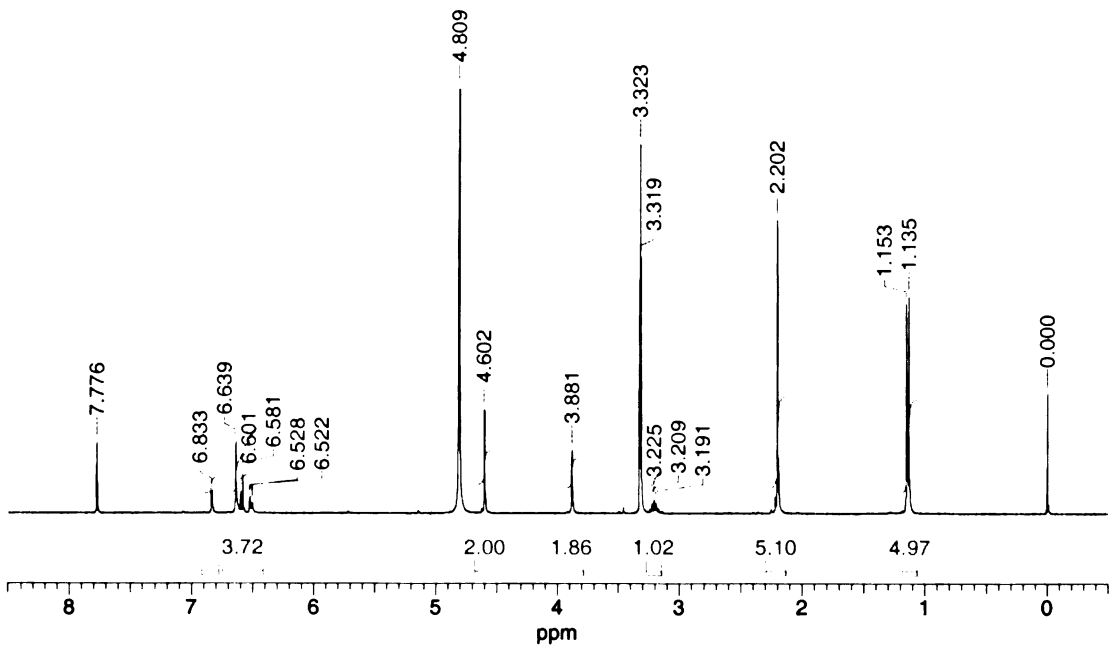

3,5-Dimethyl-4-(3-isopropyl-4-methoxymethylbenzyl)-*O*-triisopropylsilyl phenol (5)

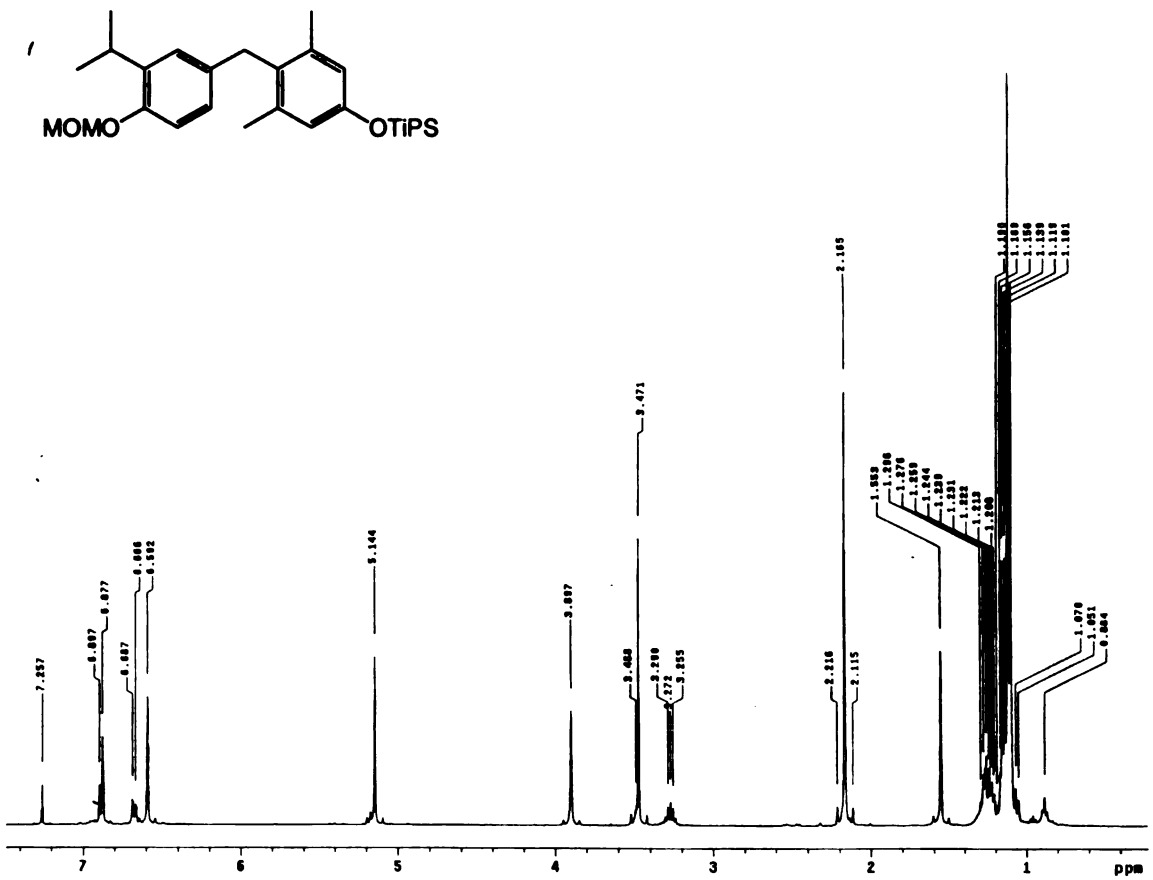

[3,5-Dimethyl-4-(3-isopropyl-4-methoxymethylbenzyl)-phenoxy]-*tert*-butylacetate (6)

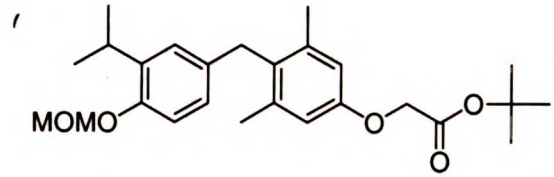

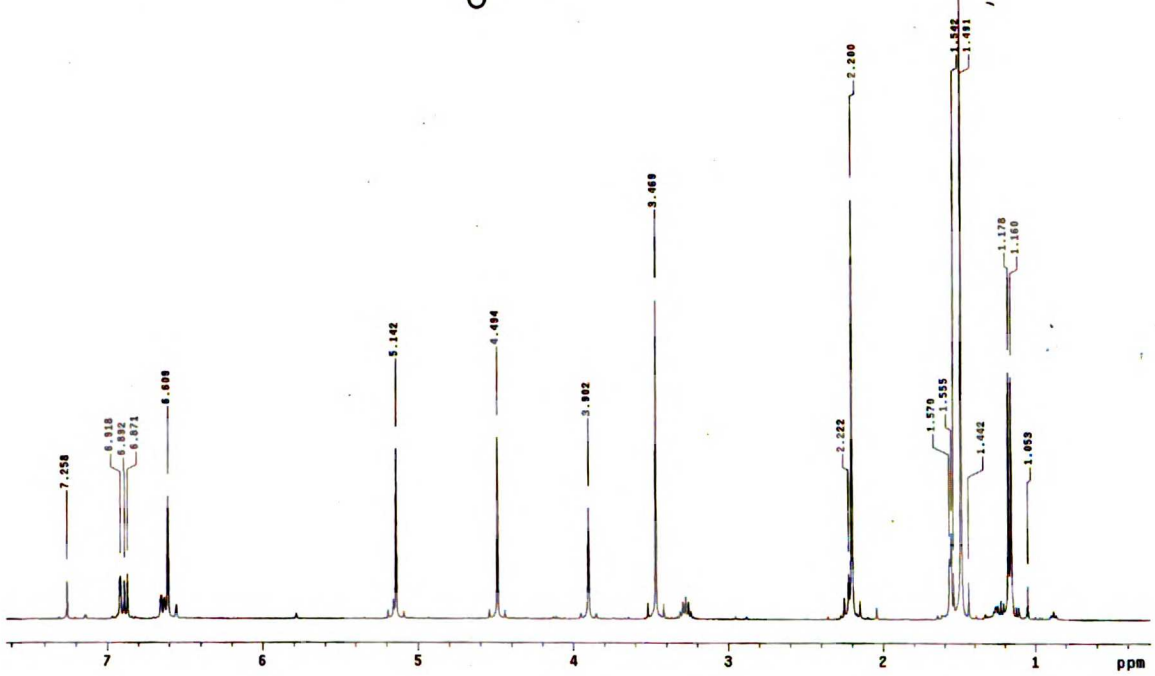

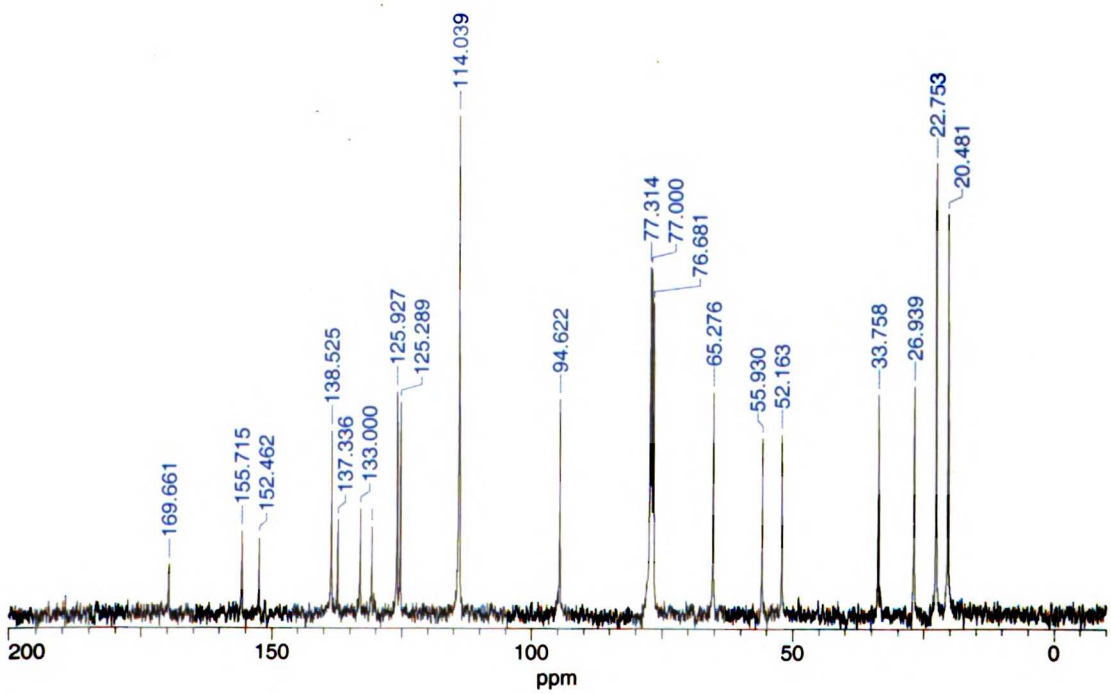

Triisopropyl-[4-(3-isopropyl-4-methoxymethoxy-5-phenylethynyl-benzyl)-3,5-dimethyl-phenoxy]-silane (9)

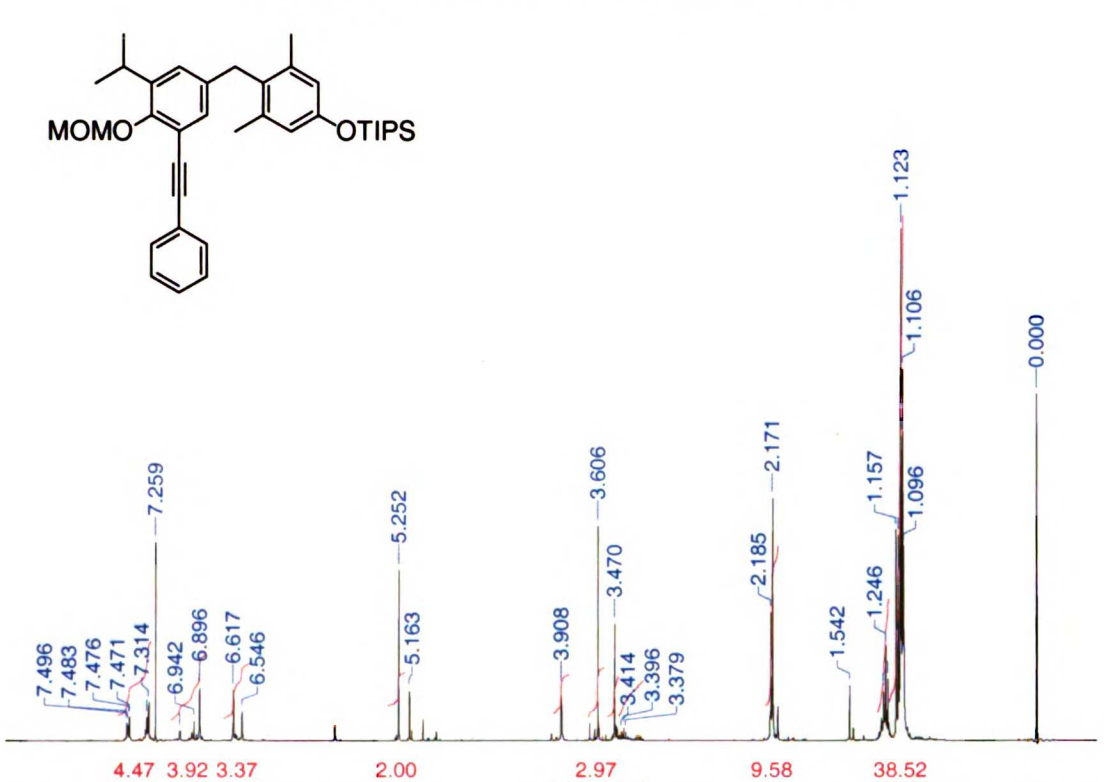

4-(3-Isopropyl-4-methoxymethoxy-5-phenylethynyl-benzyl)-3,5-dimethyl-phenol (10)

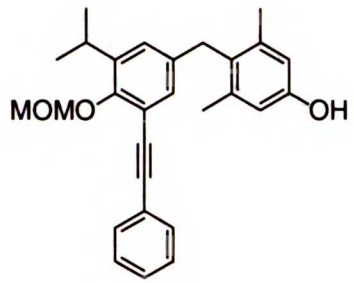

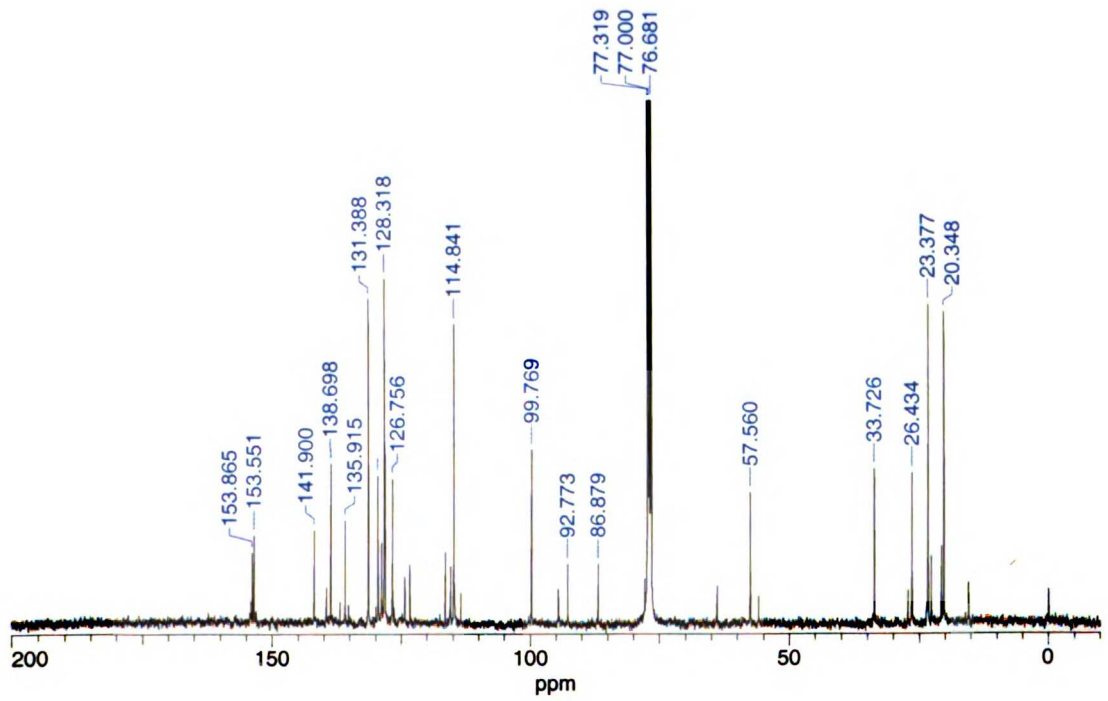

[4-(3-Isopropyl-4-methoxymethoxy-5-phenylethynyl-benzyl)-3,5-dimethyl-phenoxy]-acetic acid *tert*-butyl ester (11)

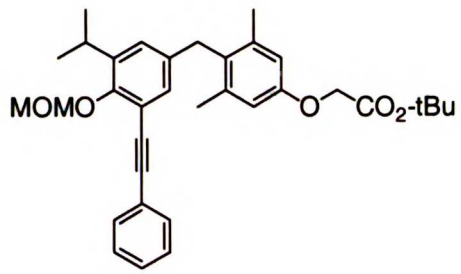

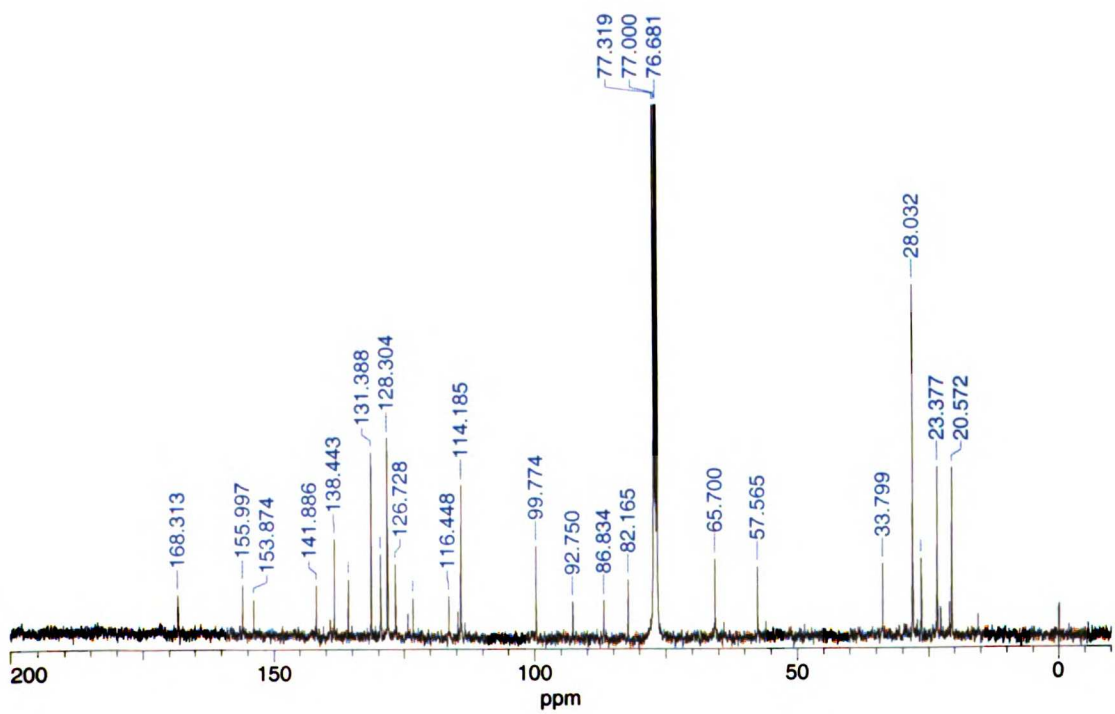

[4-(4-Hydroxy-3-isopropyl-5-phenylethynyl-benzyl)3,5-dimethyl-phenoxy]-acetic acid (NH-1)

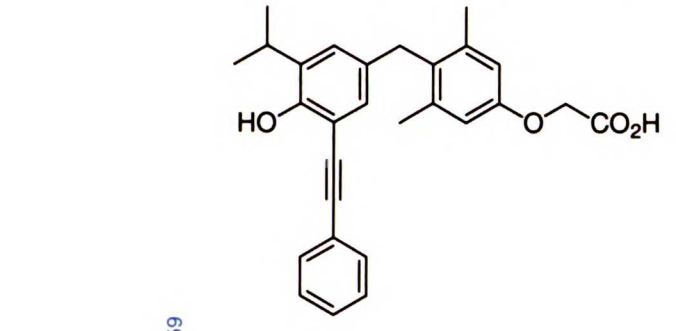

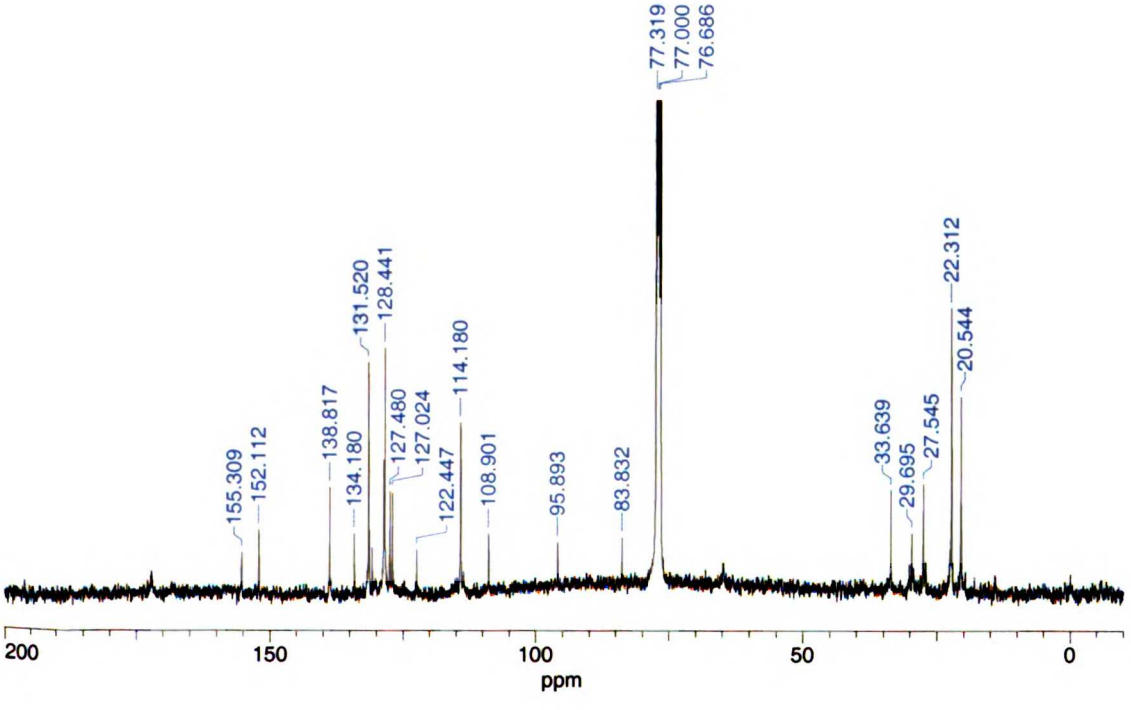

[4-(3-Iodo-5-isopropyl-4-methoxymethoxy-benzyl)-3,5-dimethyl-phenoxy]-acetic acid methyl ester (12)

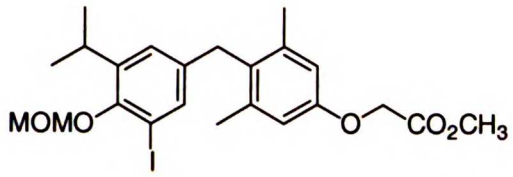

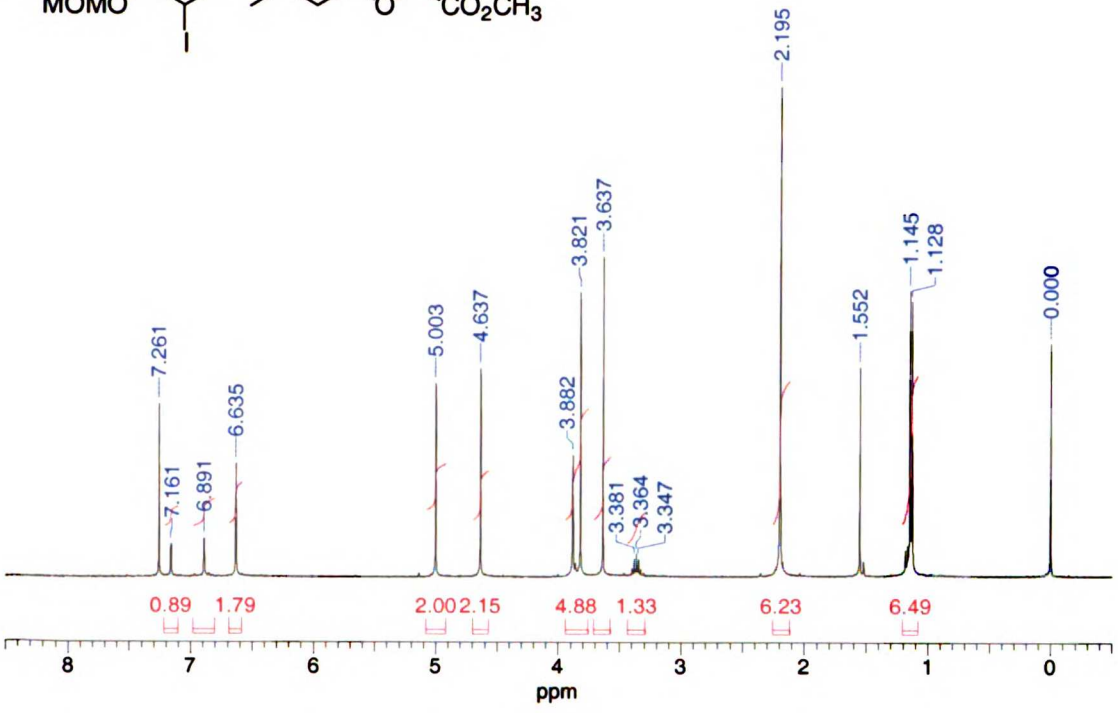

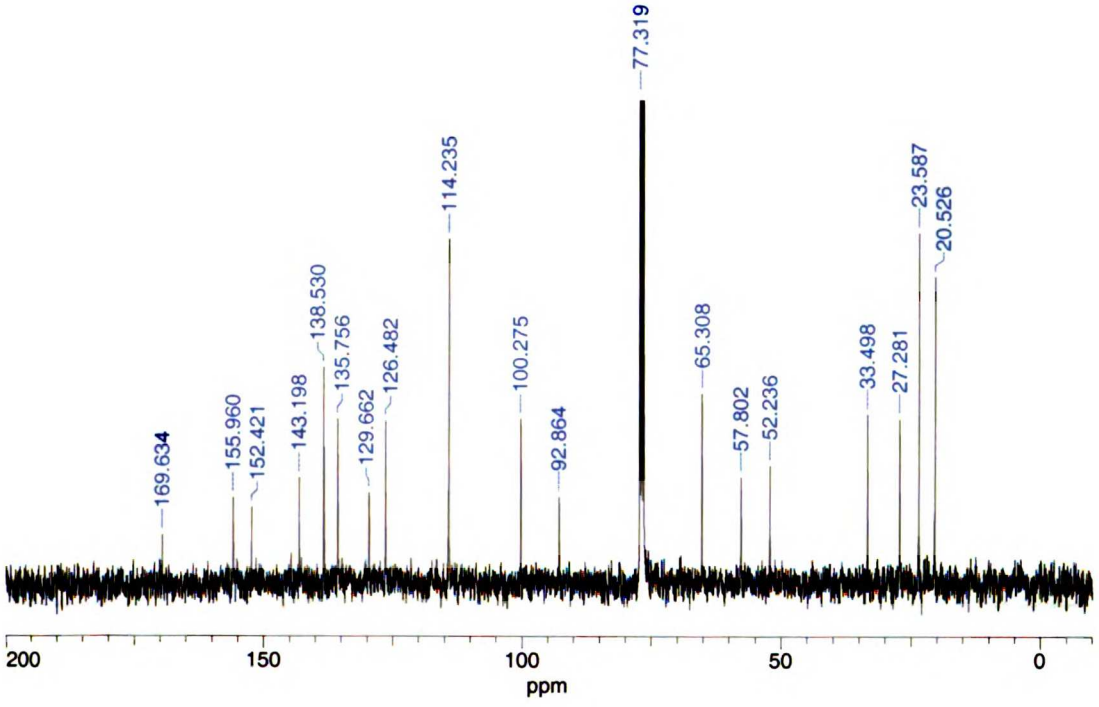

{4-[3-(4-Amino-phenylethynyl)-5-isopropyl-4-methoxymethoxy-benzyl]-3,5-dimethyl-phenoxy}-acetic acid methyl ester (13)

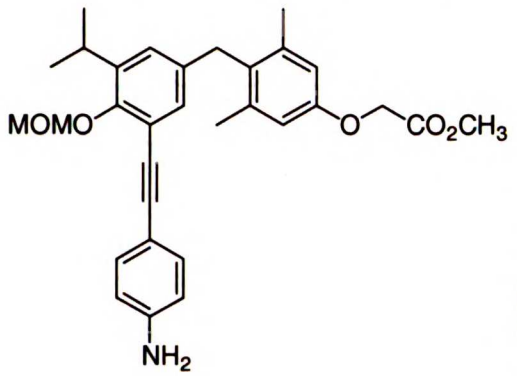

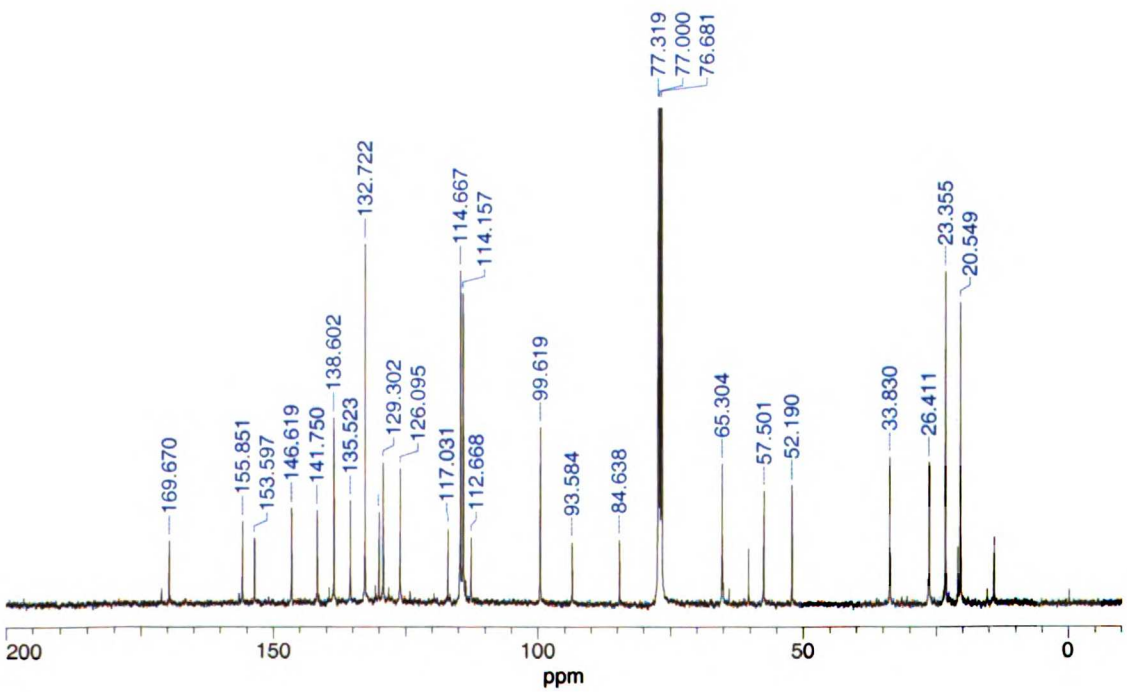

{4-[3-Isopropyl-4-methoxymethoxy-5-(4-nitro-phenylethynyl)-benzyl]-3,5-dimethyl-phenoxy}-acetic acid methyl ester (14)

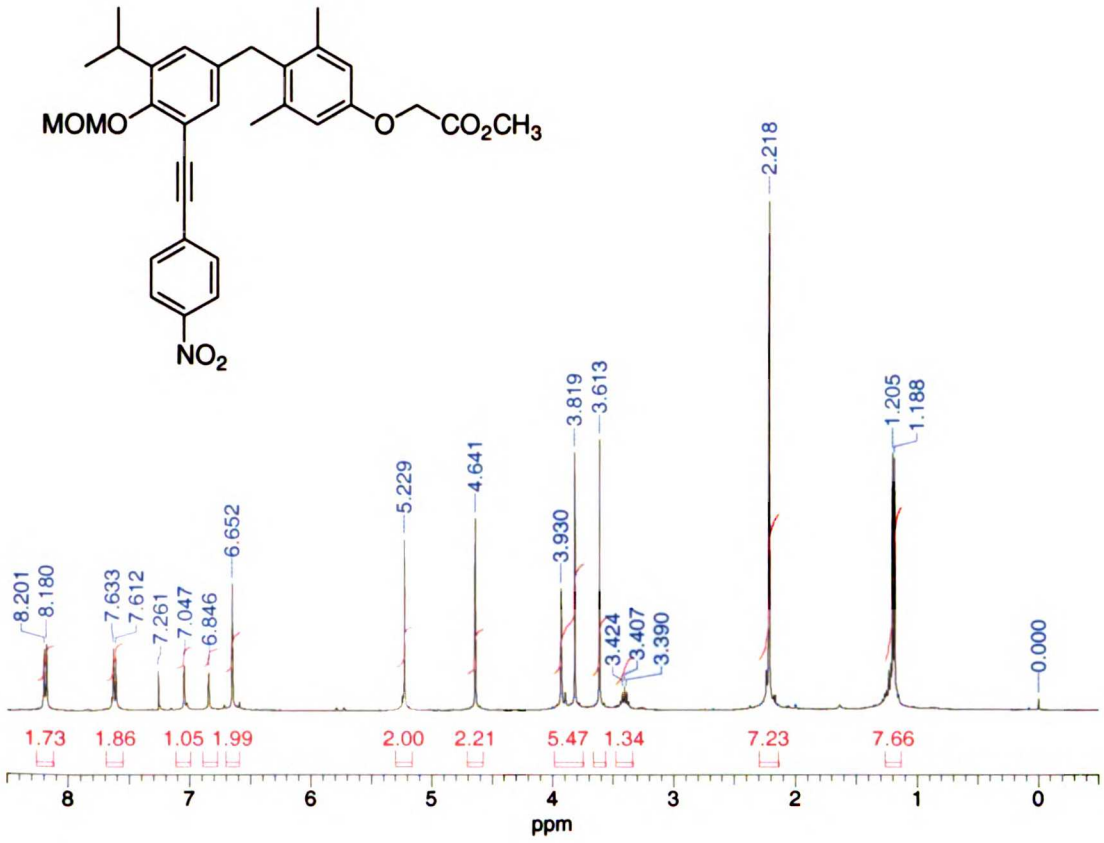

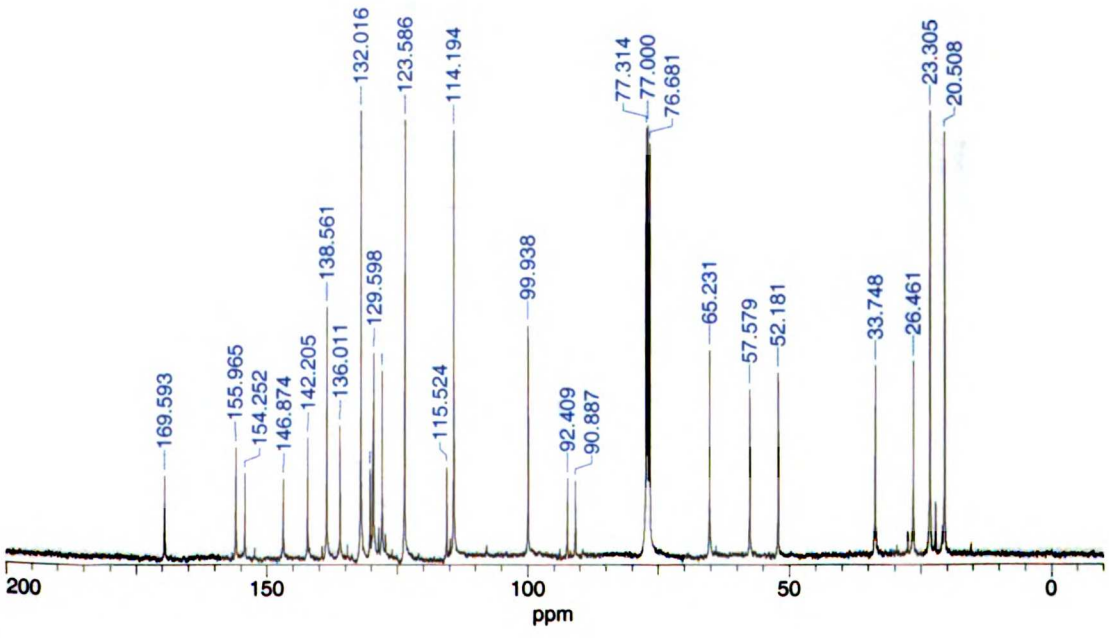

{4-[4-Hydroxy-3-isopropyl-5-(4-nitro-phenylethynyl)-benzyl]-3,5-dimethyl-phenoxy}-acetic acid methyl ester

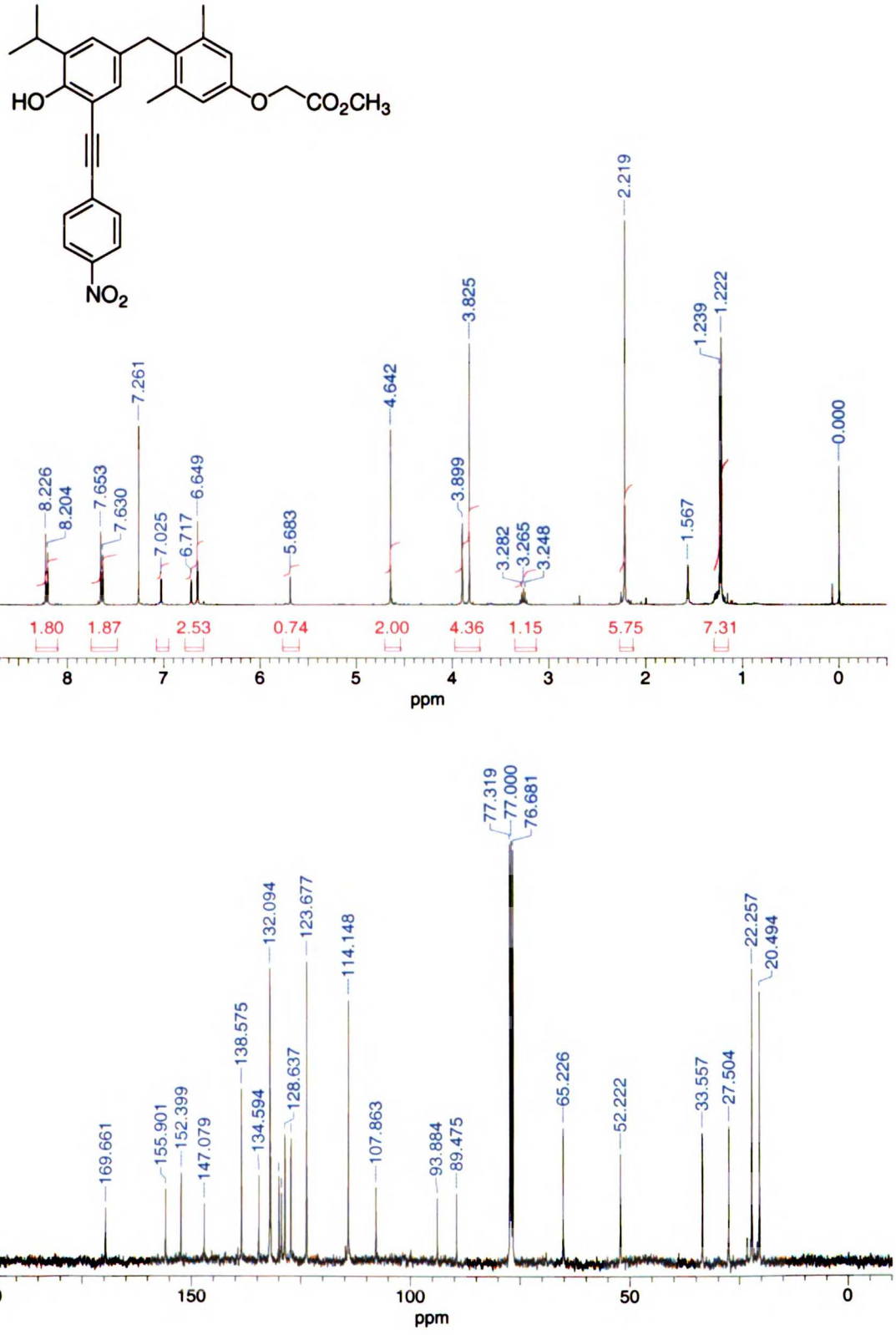

{4-[4-Hydroxy-3-isopropyl-5-(4-nitro-phenylethynyl)-benzyl]-3,5-dimethyl-phenoxy}-acetic acid (NH-3)

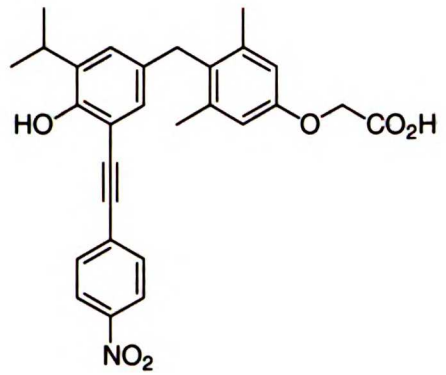

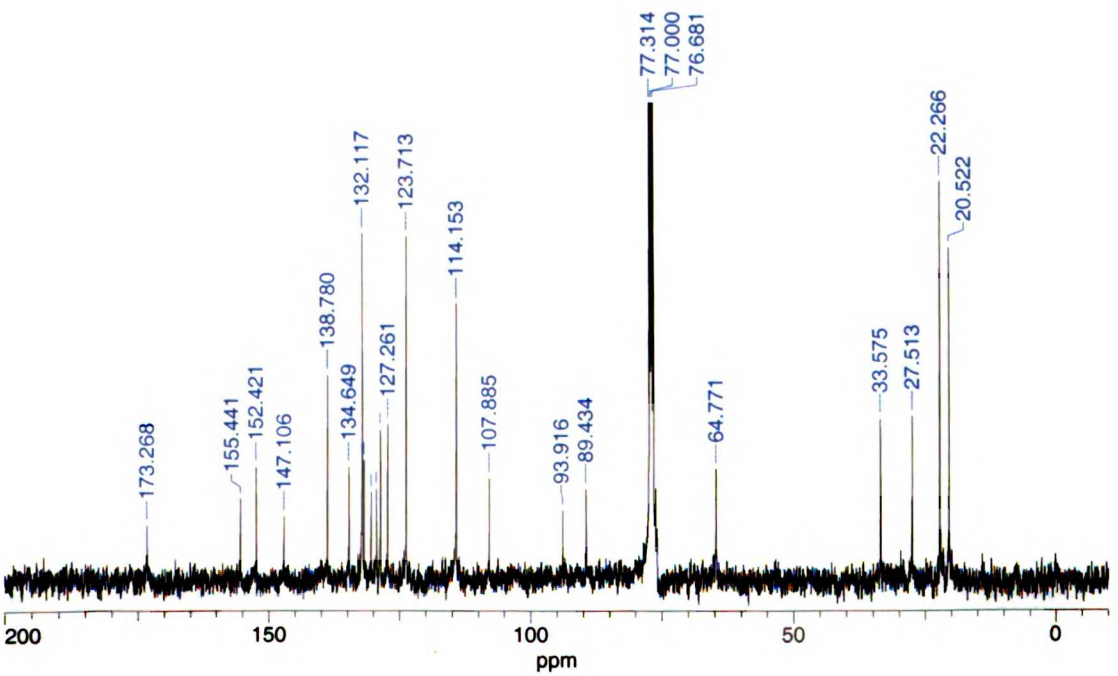

[4-(3-Isopropyl-4-methoxymethoxy-benzyl)-3,5-dimethyl-phenoxy]-acetic acid methyl ester (15)

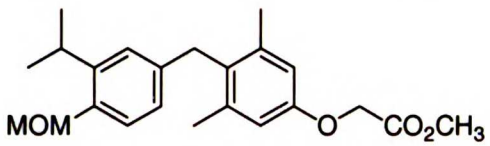

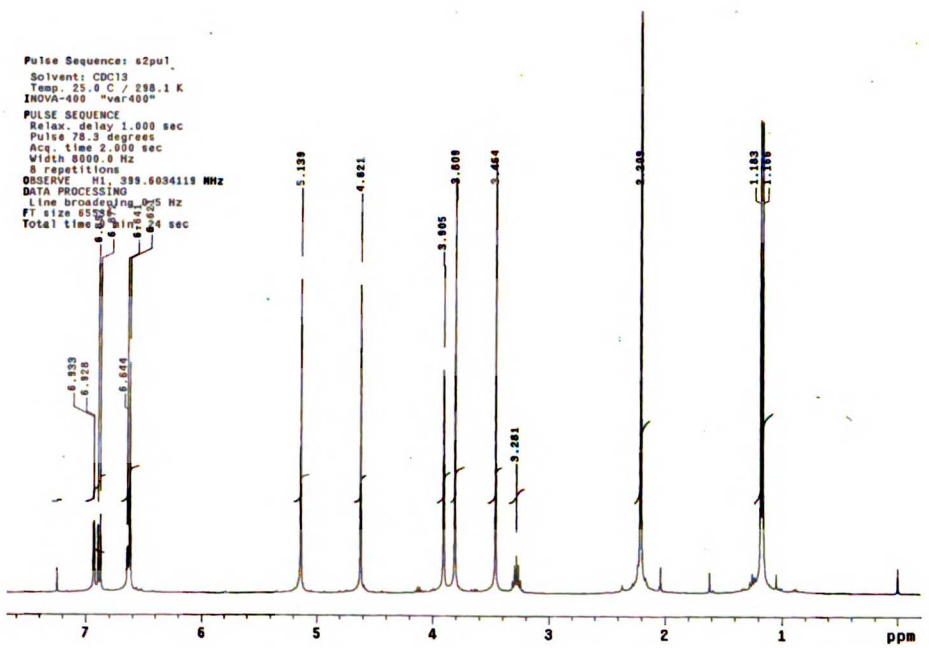

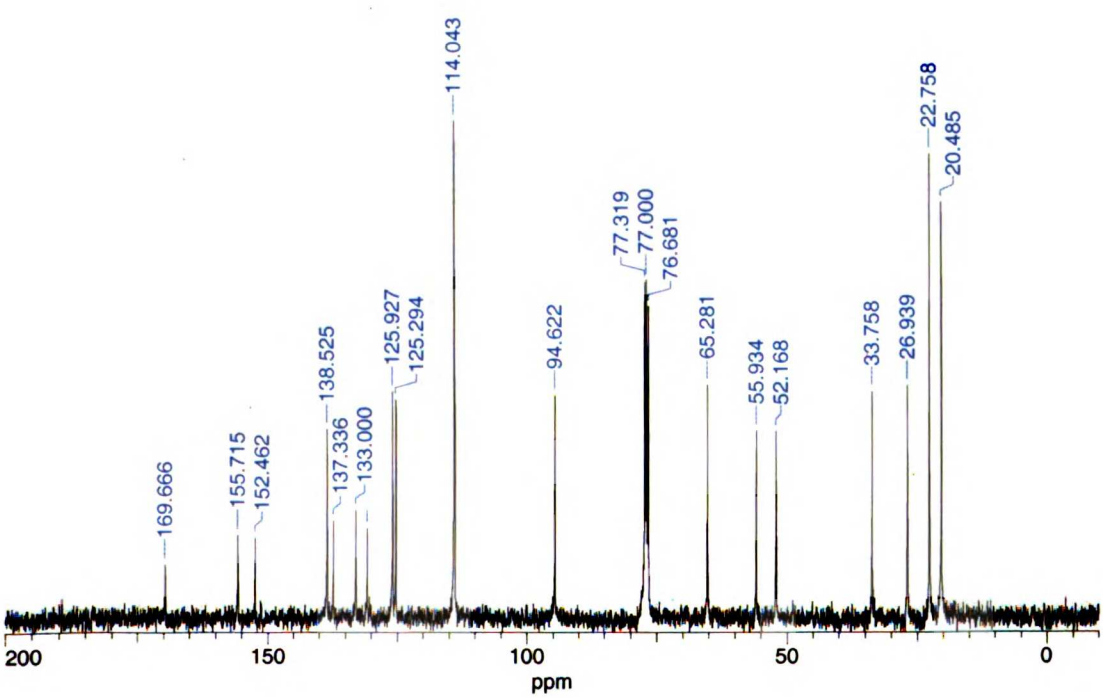

[4-(4-Hydroxy-5-isopropyl-benzyl)-3,5-dimethyl-phenoxy]-acetic acid methyl ester

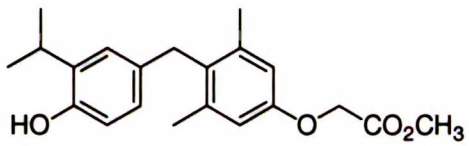

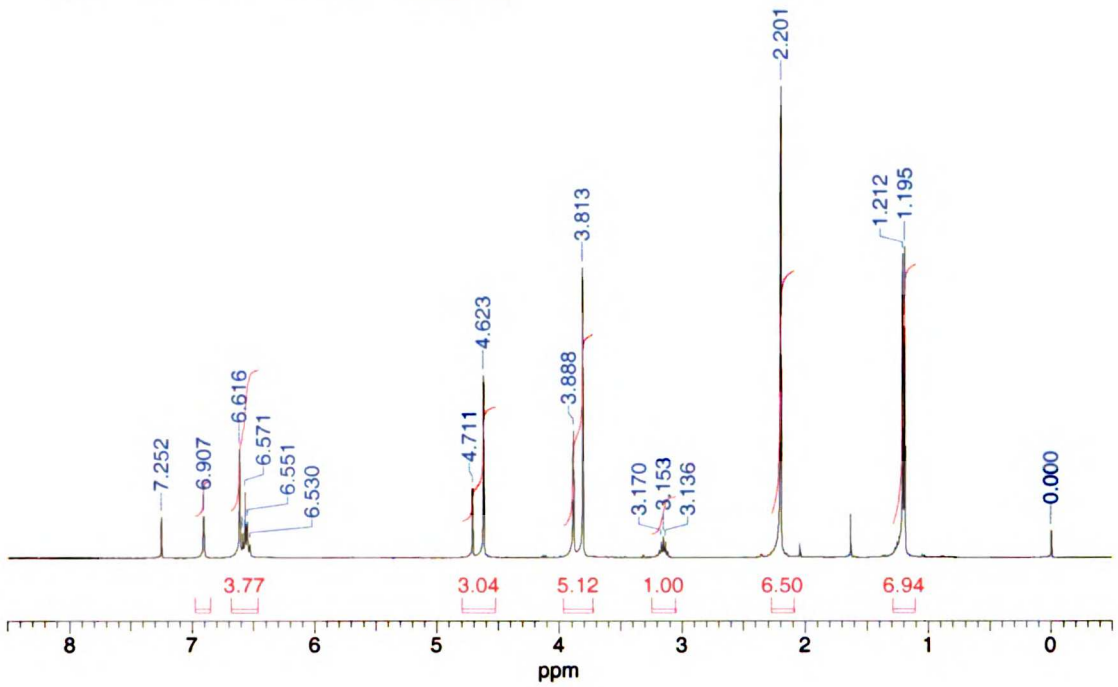

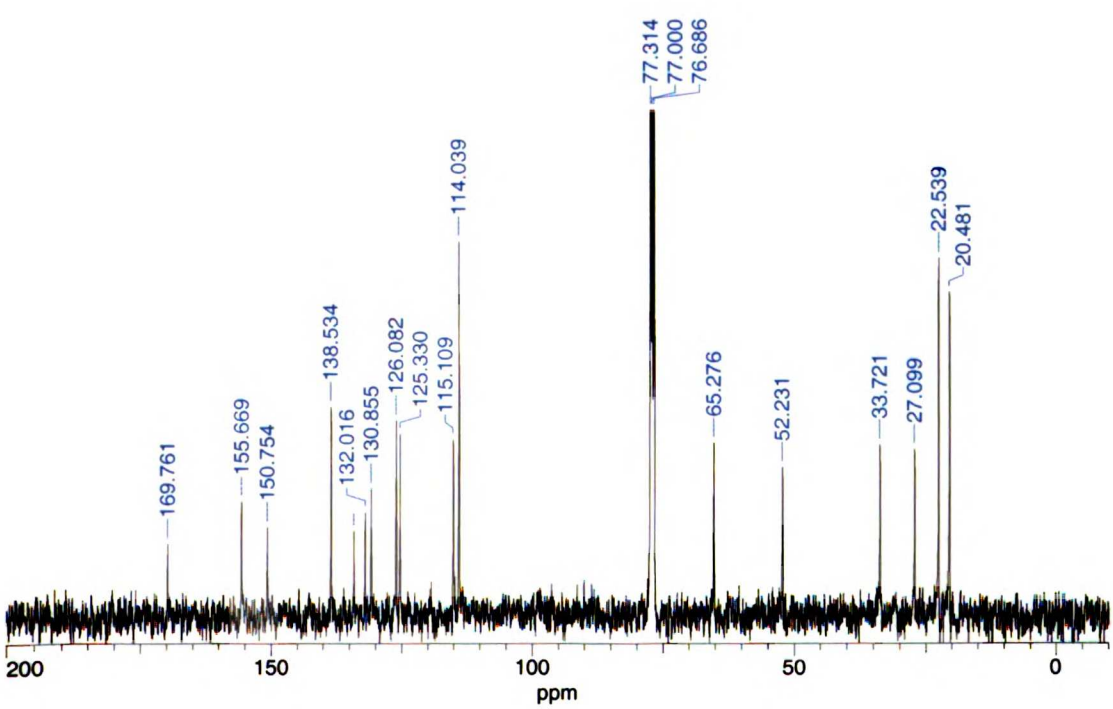

[4-(4-Hydroxy-3-iodo-5-isopropyl-benzyl)-3,5-dimethyl-phenoxy]-acetic acid methyl ester (16)

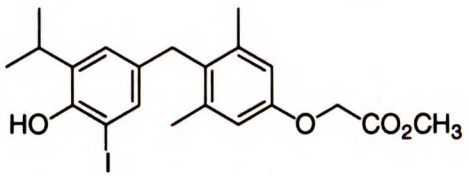

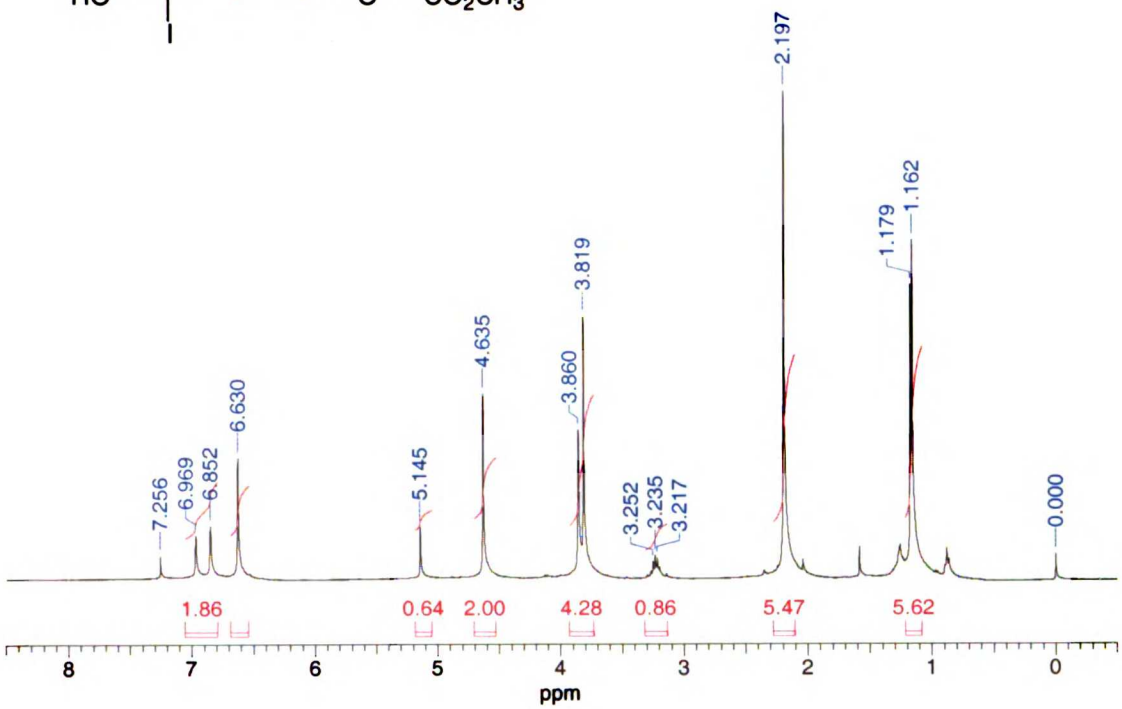

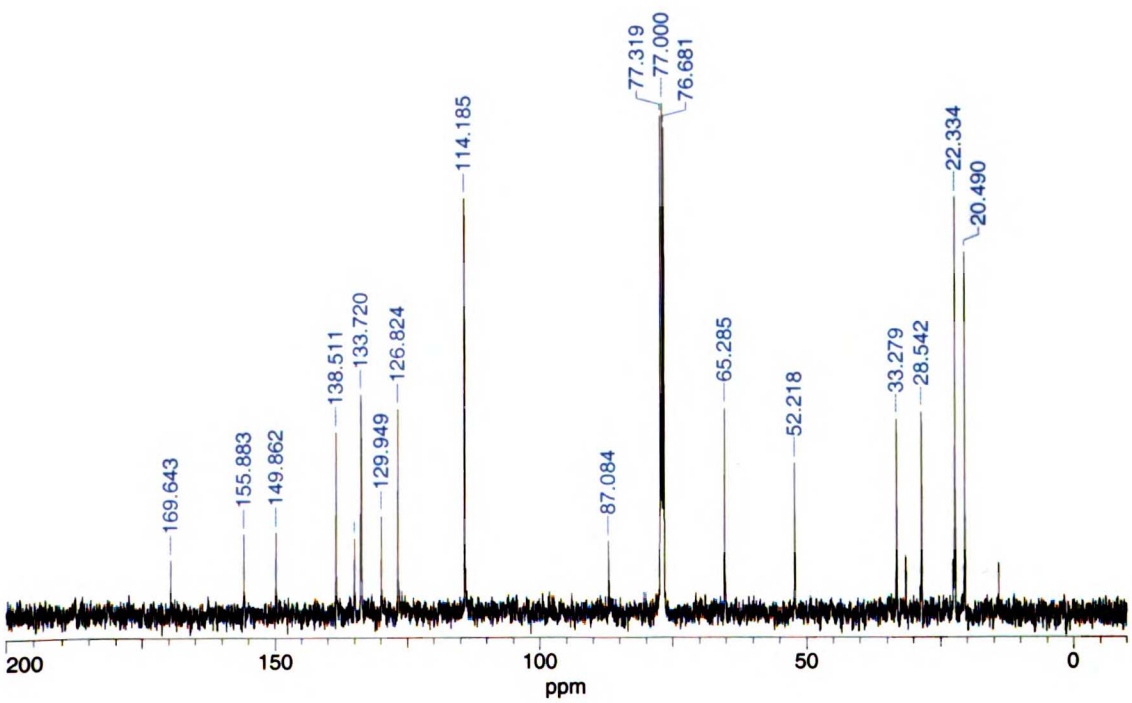

{4-[3-Isopropyl-4-methoxymethoxy-5-(4-trifluoromethyl-phenylethynyl)-benzyl]-3,5-dimethyl-phenoxy}-acetic acid methyl ester (17a)

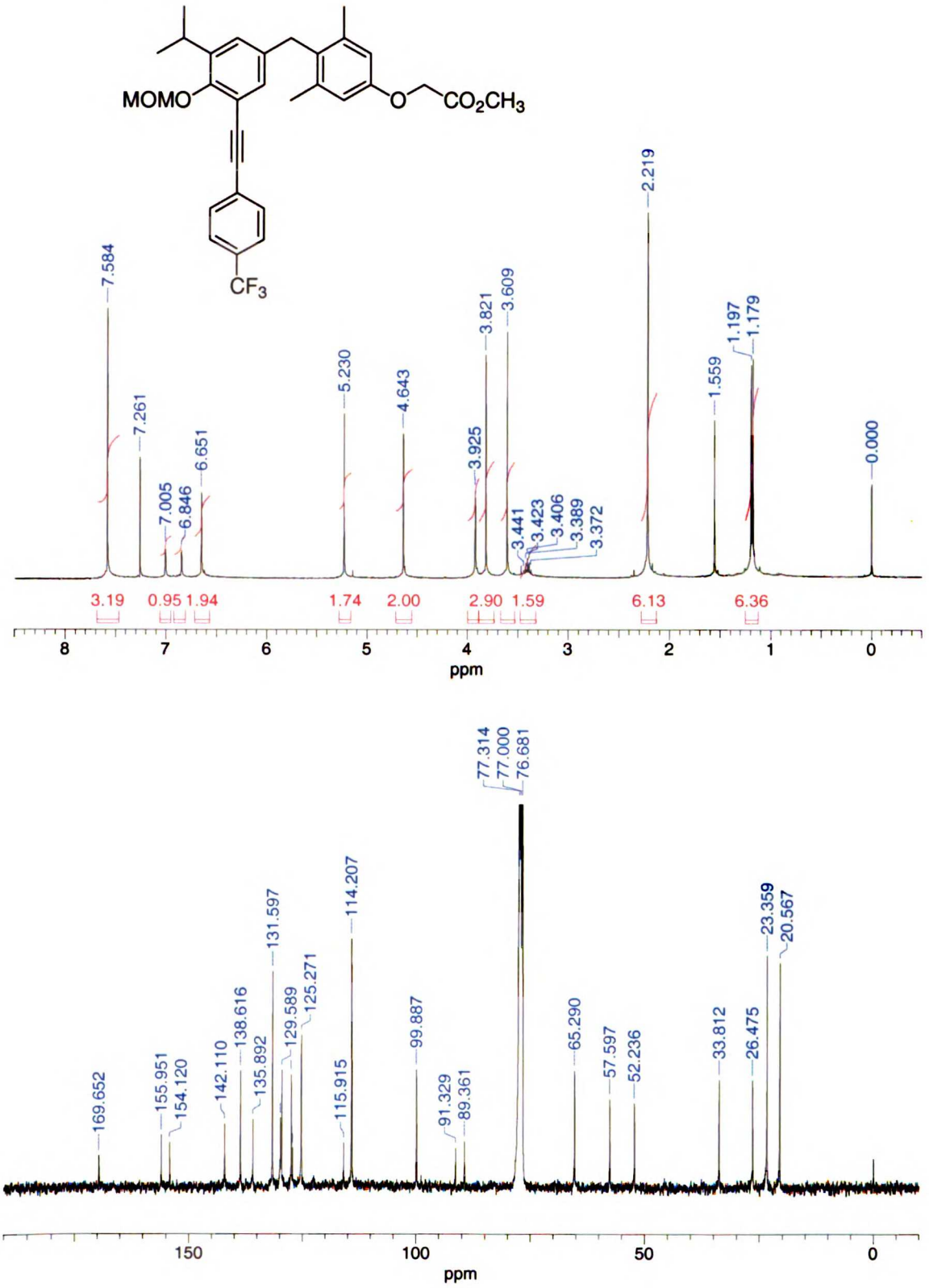

{4-[4-Hydroxy-3-isopropyl-5-(4-trifluoromethyl-phenylethynyl)-benzyl]-3,5-dimethyl-phenoxy}-acetic acid methyl ester

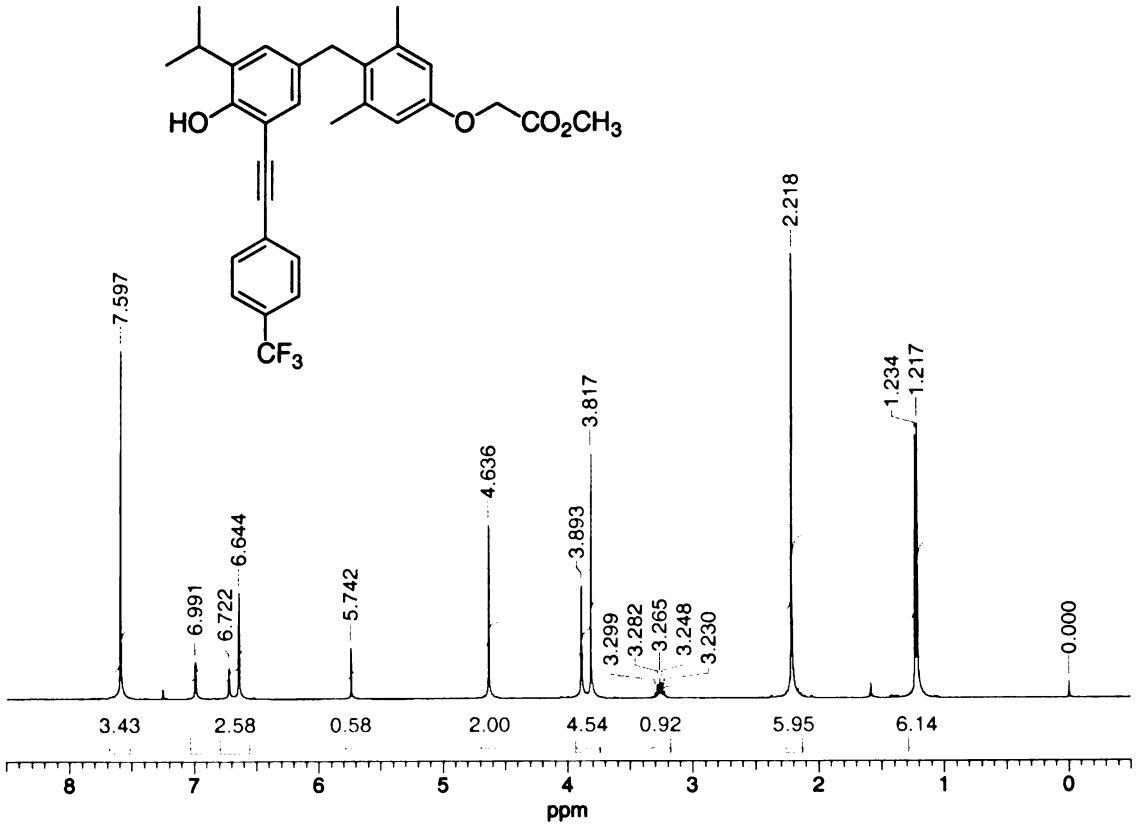

{4-[4-Hydroxy-3-isopropyl-5-(4-trifluoromethyl-phenylethynyl)-benzyl]-3,5-dimethyl-phenoxy}-acetic acid (18a, NH-5)

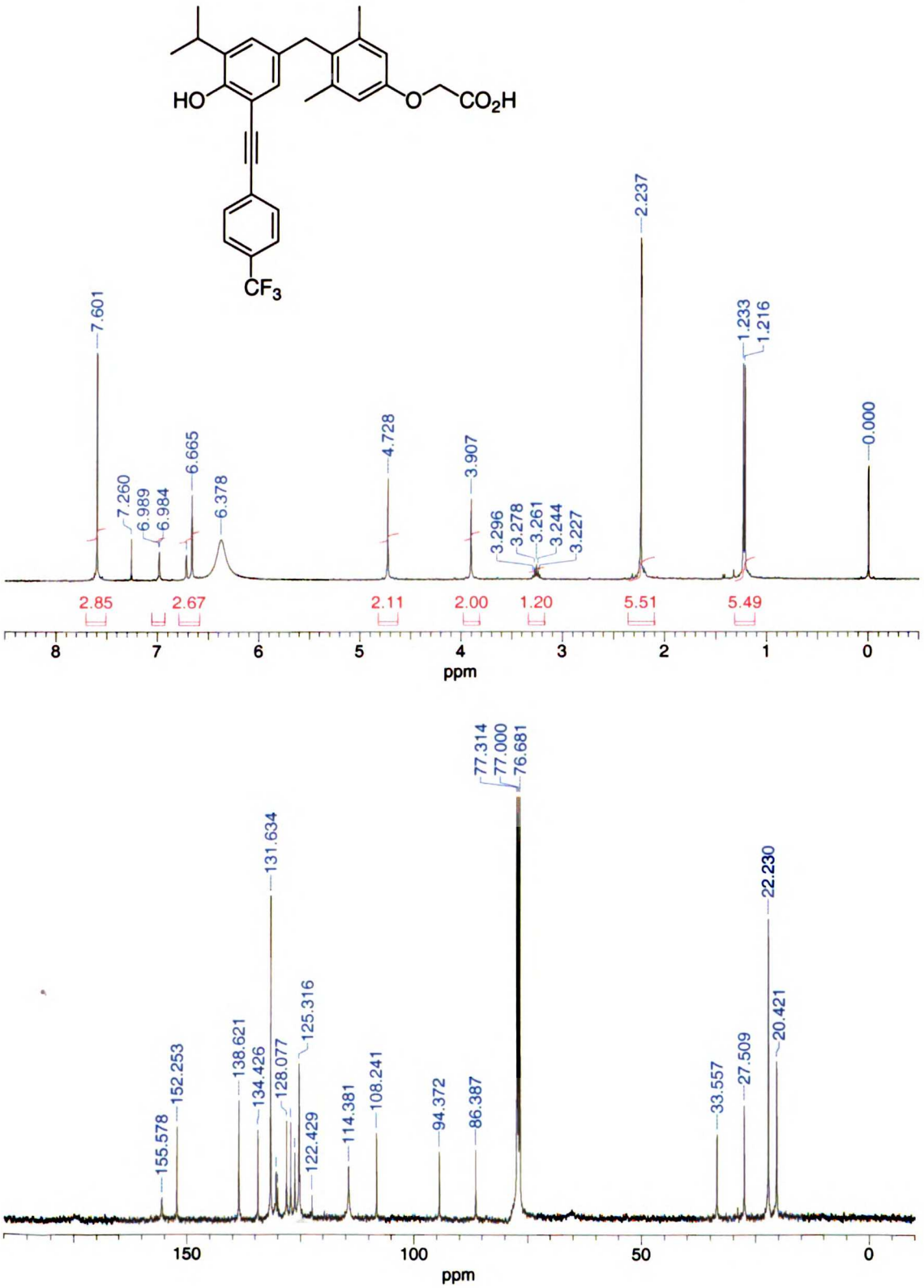

{4-[3-Isopropyl-4-methoxymethoxy-5-(4-methoxy-phenylethynyl)-benzyl]-3,5-dimethyl-phenoxy}-acetic acid methyl ester (17b)

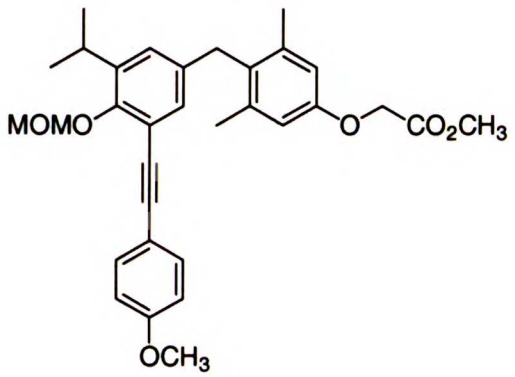

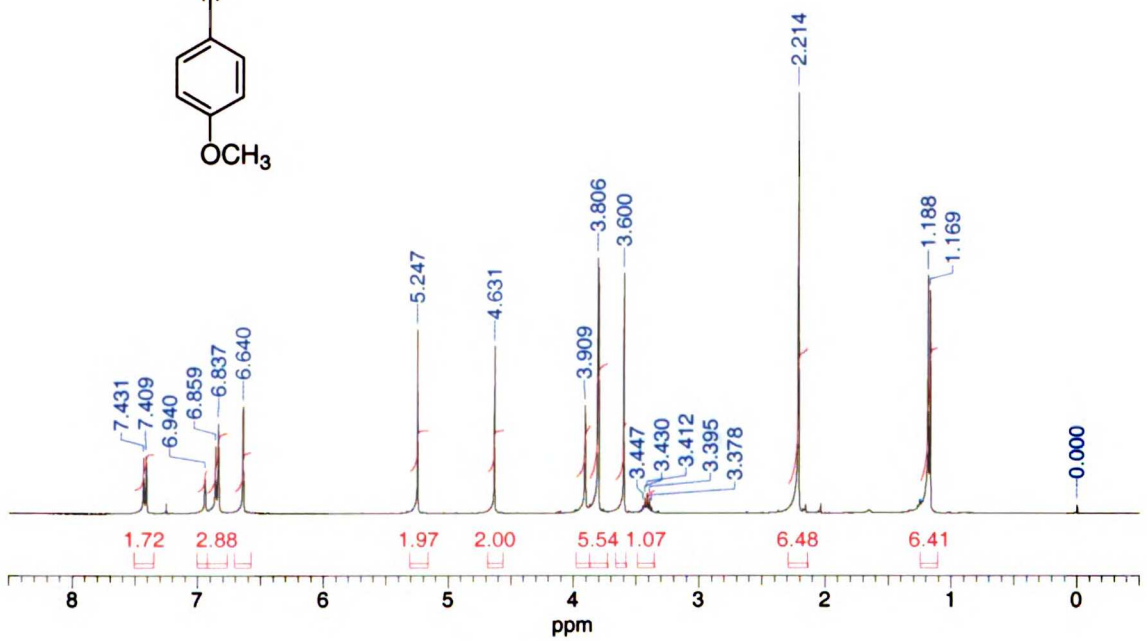

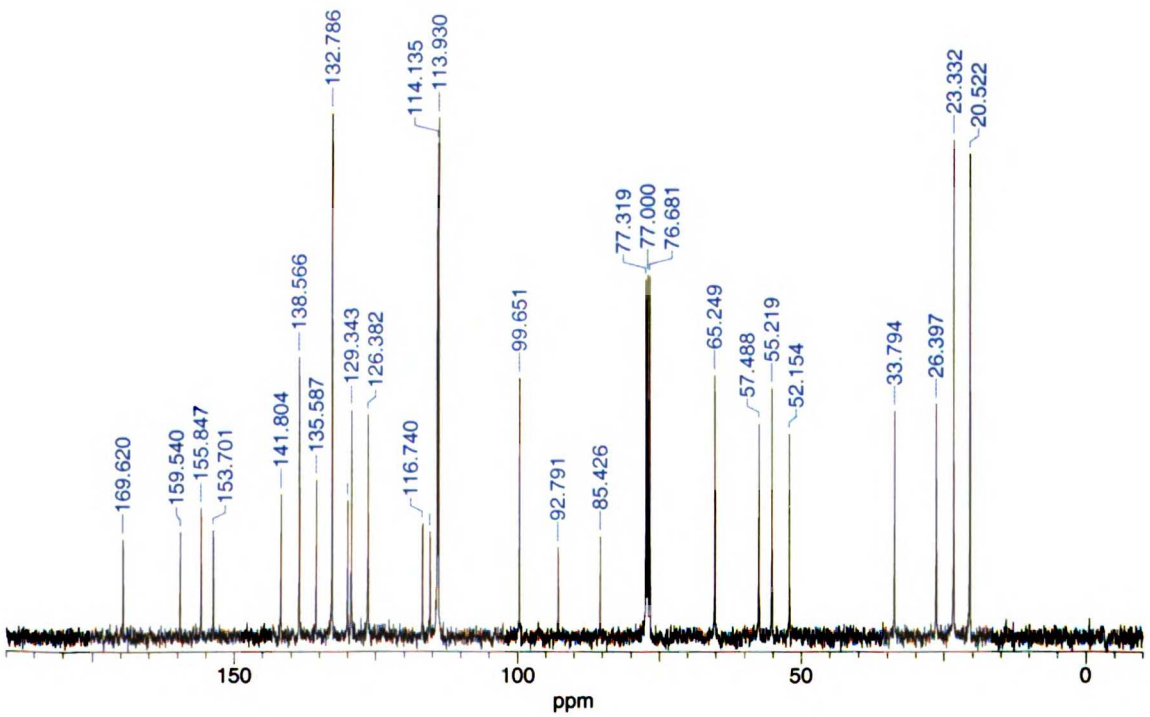

{4-[4-Hydroxy-3-isopropyl-5-(4-methoxy-phenylethynyl)-benzyl]-3,5-dimethyl-phenoxy}-acetic acid (18b, NH-6)

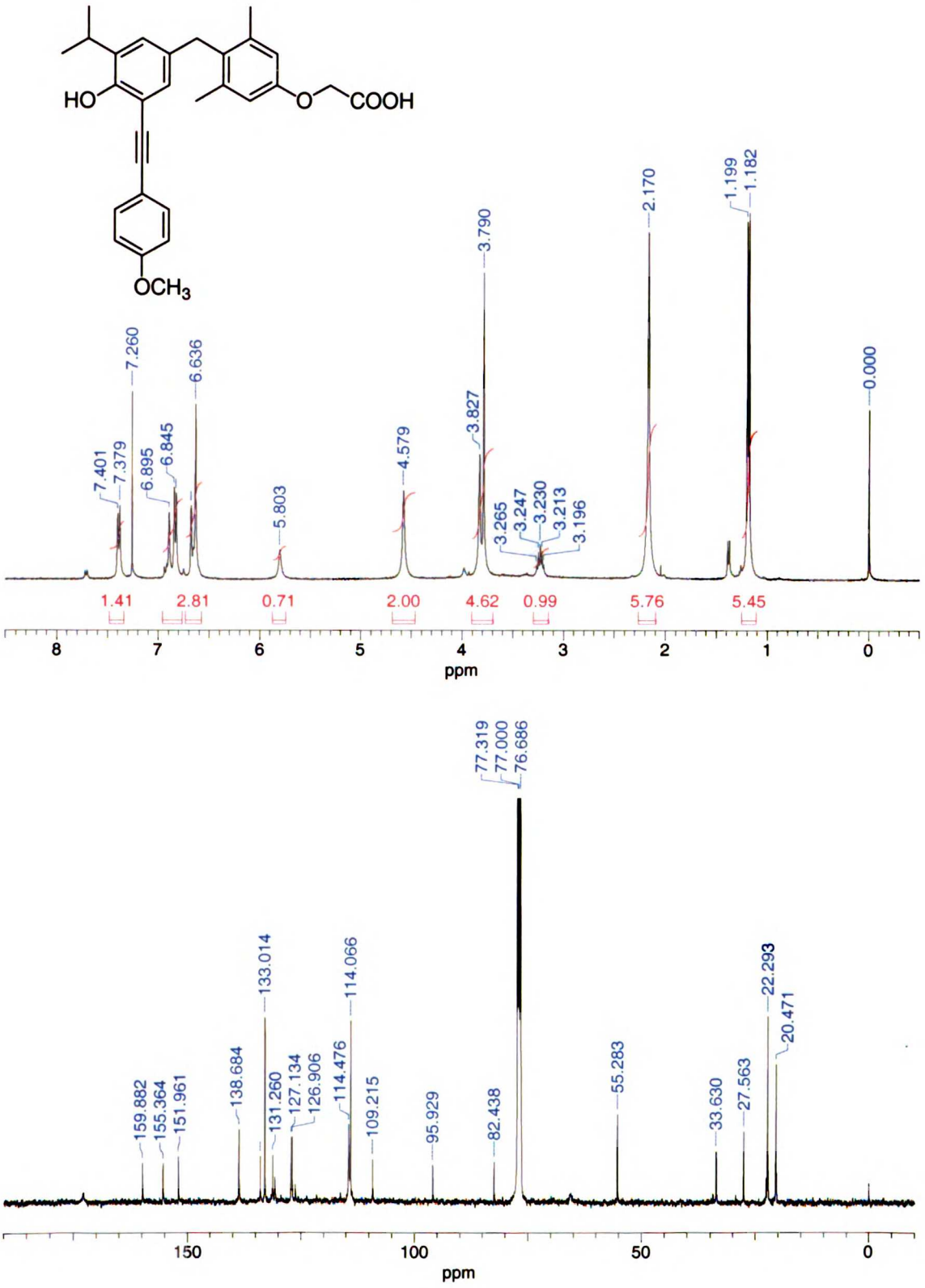

{4-[3-(4-Cyano-phenylethynyl)-5-isopropyl-4-methoxymethoxy-benzyl]-3,5-dimethyl-phenoxy}-acetic acid methyl ester (17c)

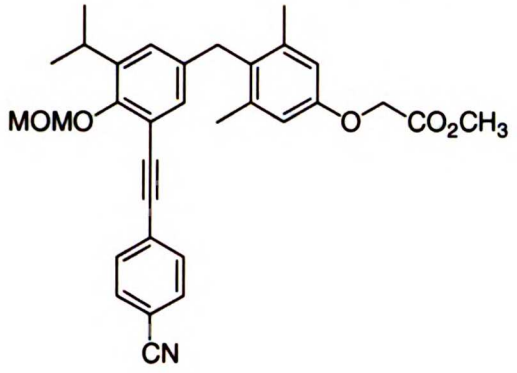

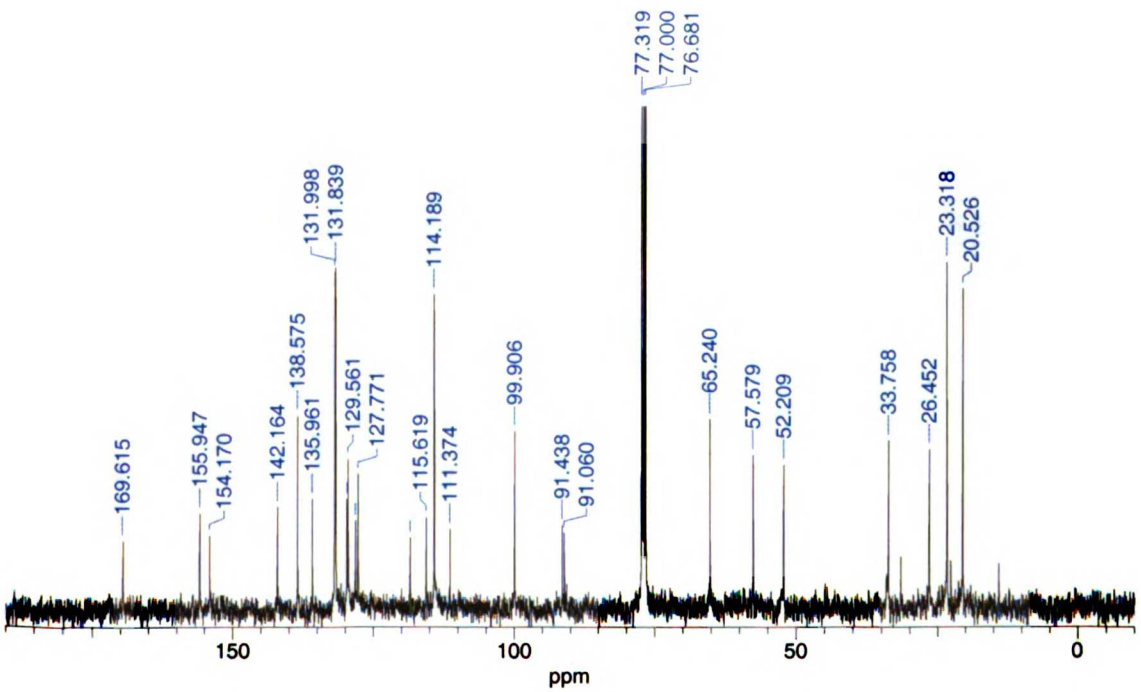

{4-[3-(4-Cyano-phenylethynyl)-4-hydroxy-5-isopropyl-benzyl]-3,5-dimethyl-phenoxy}-acetic acid methyl ester

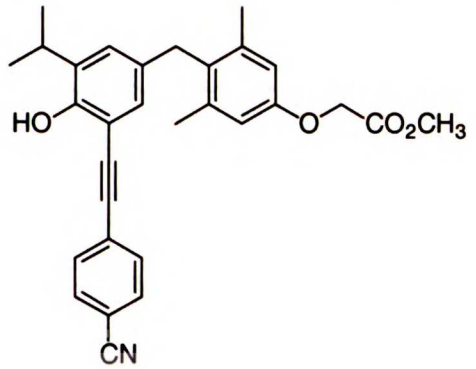

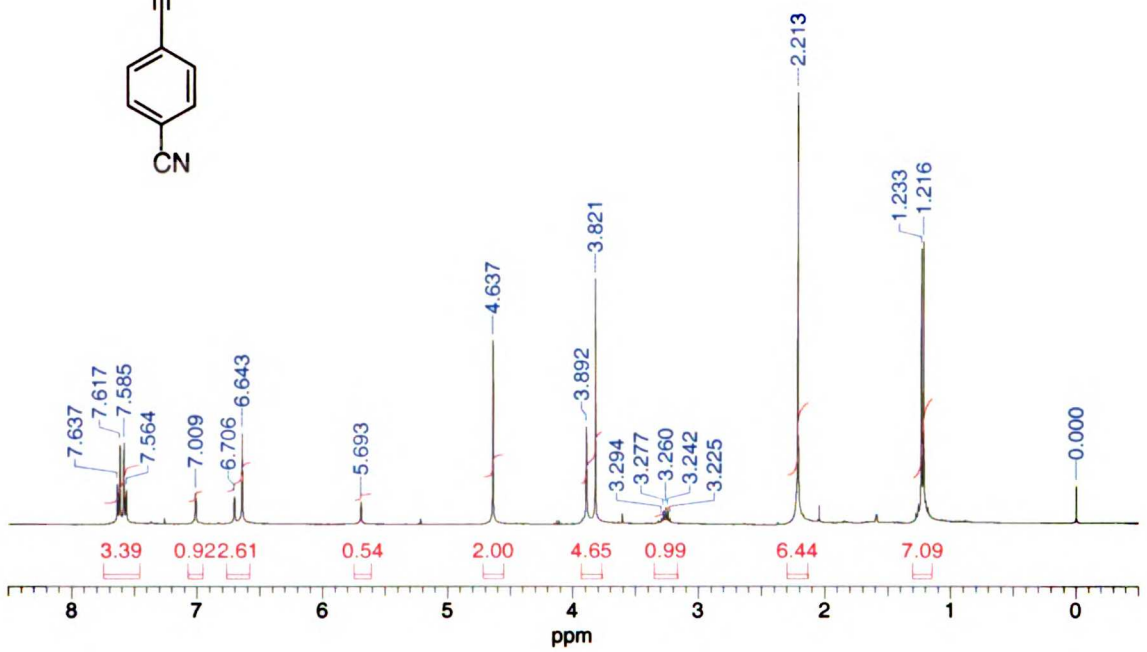

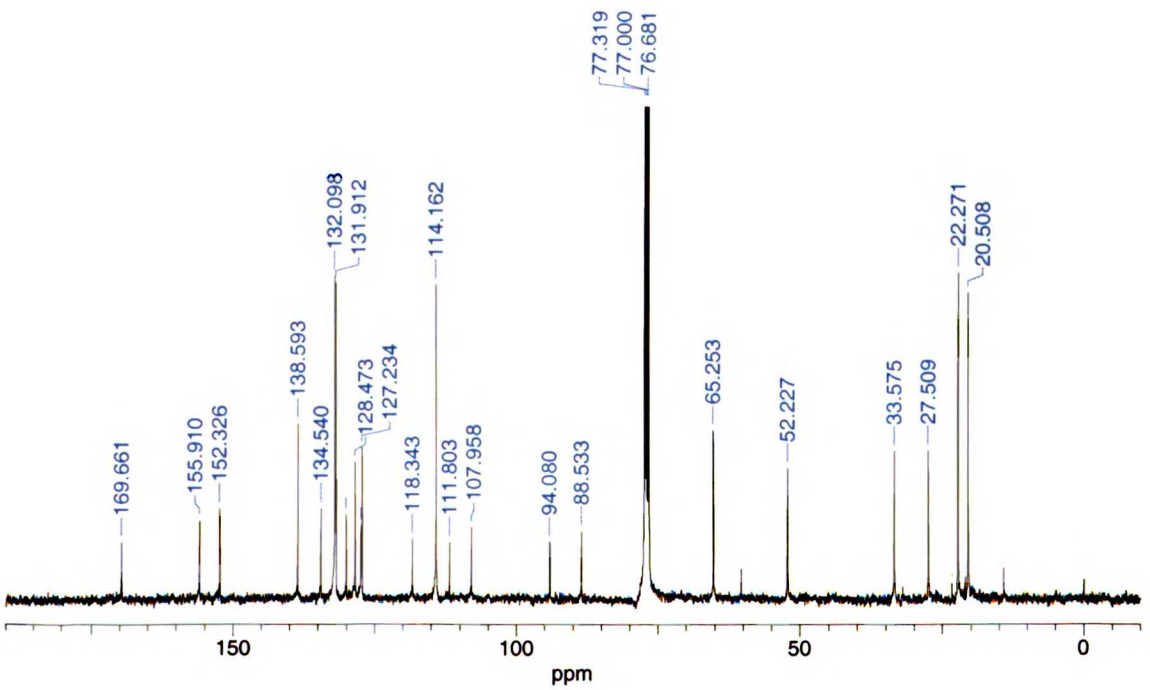

{4-[3-(4-Cyano-phenylethynyl)-4-hydroxy-5-isopropyl-benzyl]-3,5-dimethyl-phenoxy}-acetic acid (18c, NH-8)

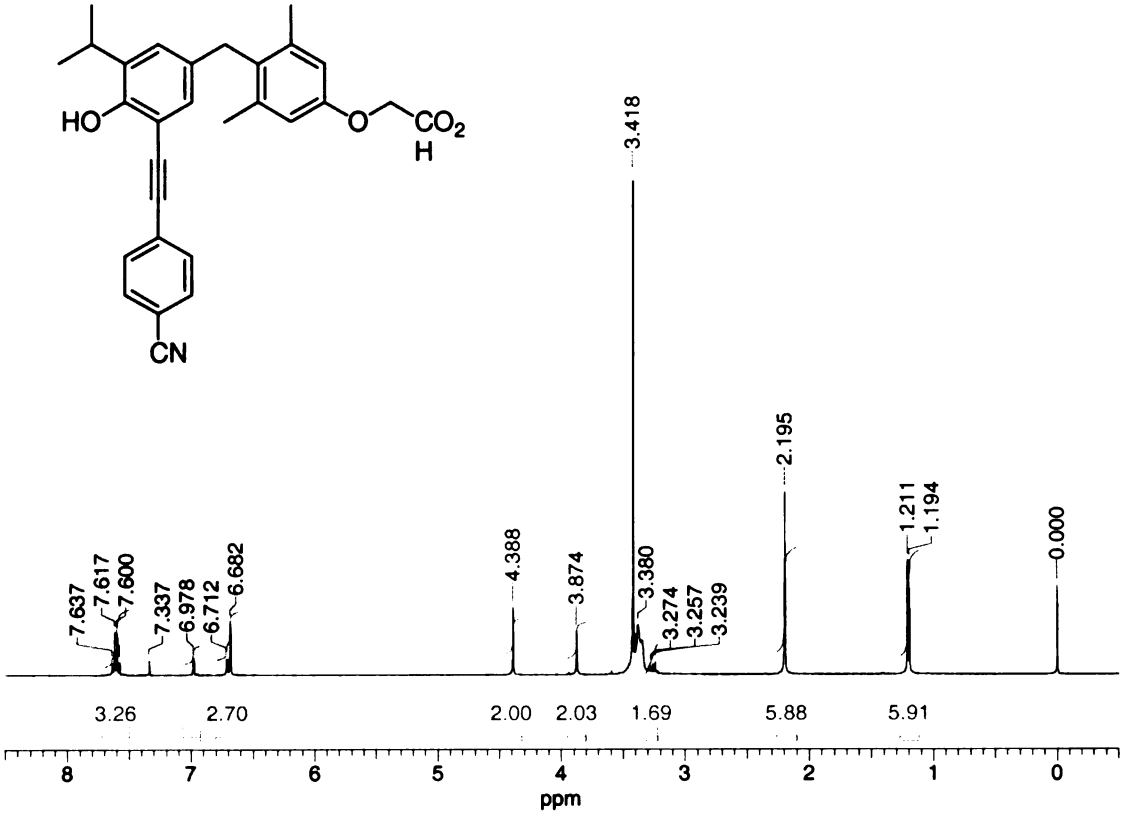

{4-[3-(4-Fluoro-phenylethynyl)-5-isopropyl-4-methoxymethoxy-benzyl] 3,5-dimethyl-phenoxy}-acetic acid methyl ester (17d)

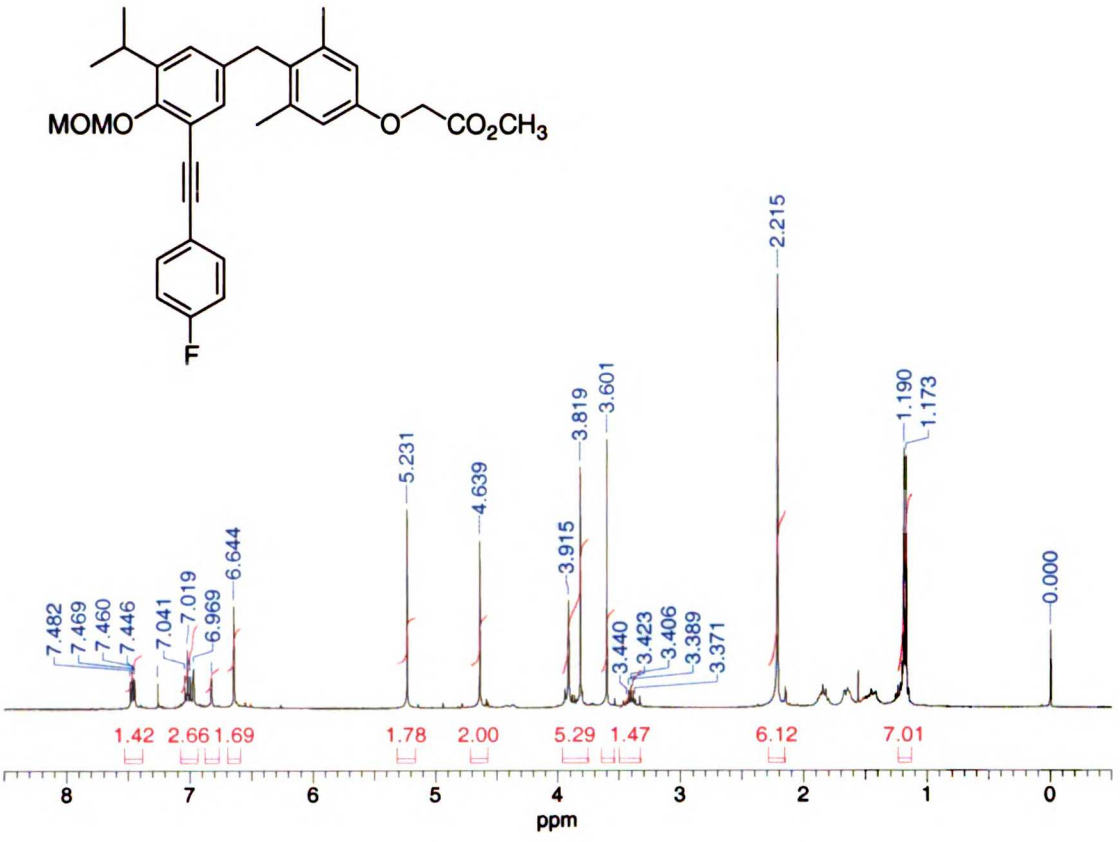

{4-[3-(4-Fluoro-phenylethynyl)-4-hydroxy-5-isopropyl-benzyl]3,5-dimethyl-phenoxy}-acetic acid methyl ester

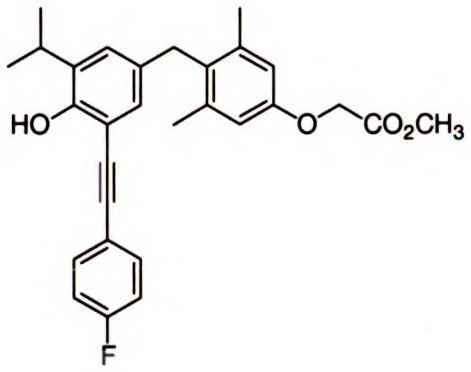

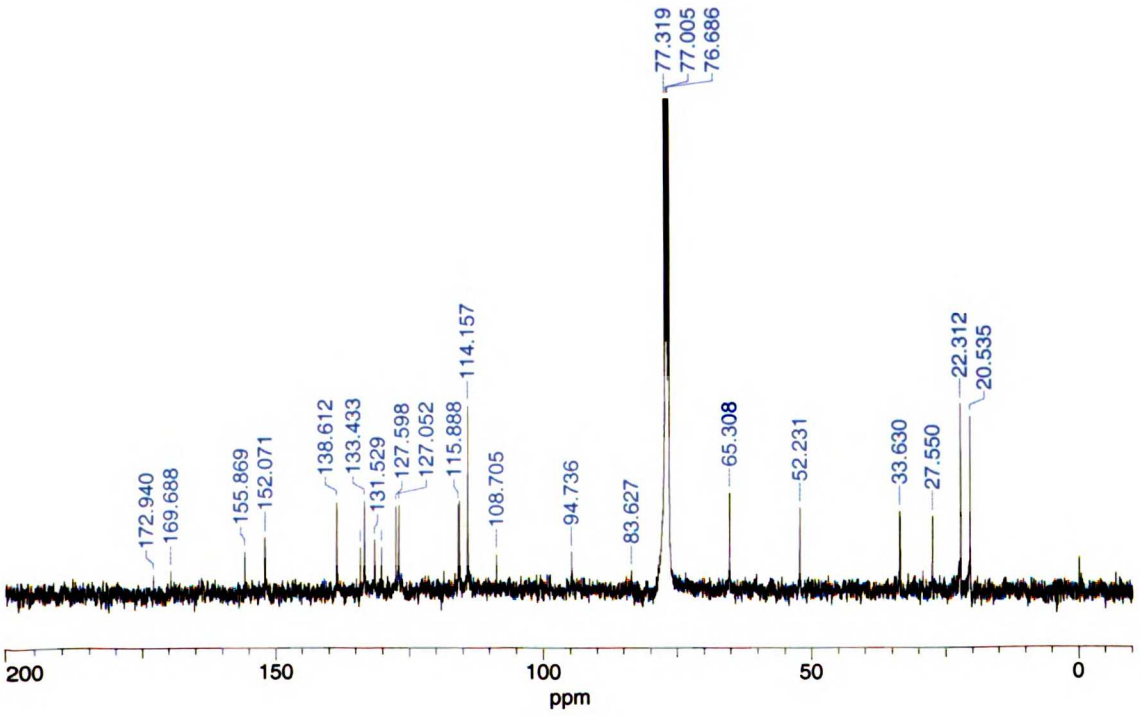

{4-[3-(4-Fluoro-phenylethynyl)-4-hydroxy-5-isopropyl-benzyl]3,5-dimethyl-phenoxy}-acetic acid (18d, NH-11)

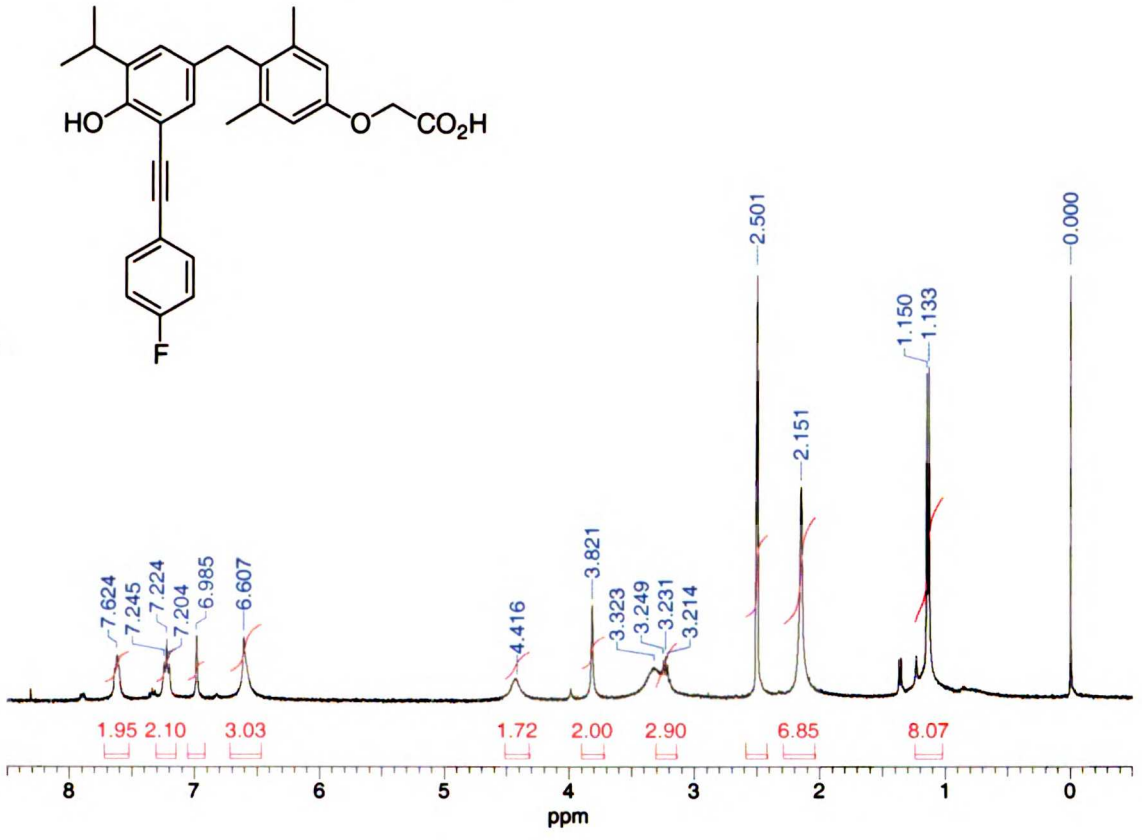

4-[3-Isopropyl-5-(methoxycarbonylmethoxy-2,6-dimethyl-benzyl)-2-methoxymethoxy-phenylethynyl] benzoic acid methyl ester (17e)

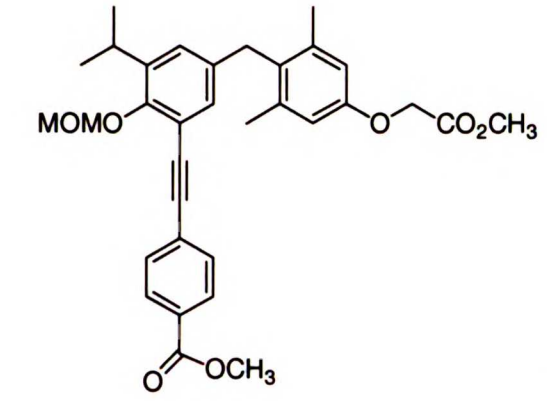

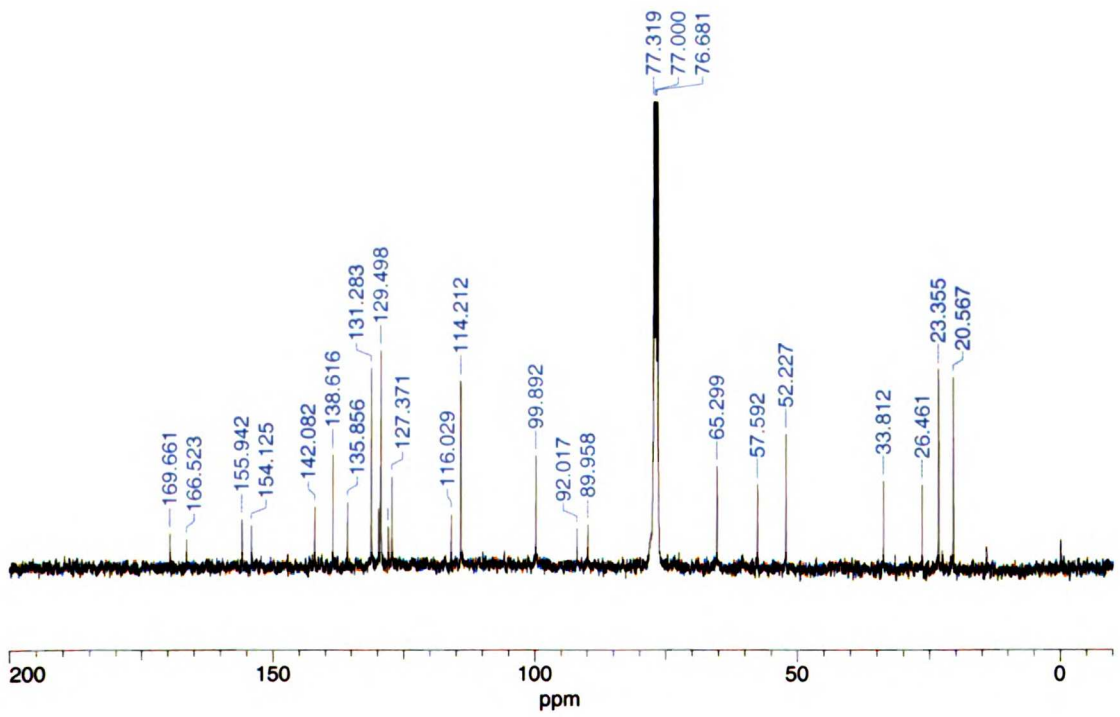

4-[5-(4-Methoxycarbonylmethoxy-2,6-dimethyl-benzyl)-2-hydroxy-3-isopropyl-phenylethynyl]-benzoic acid methyl ester

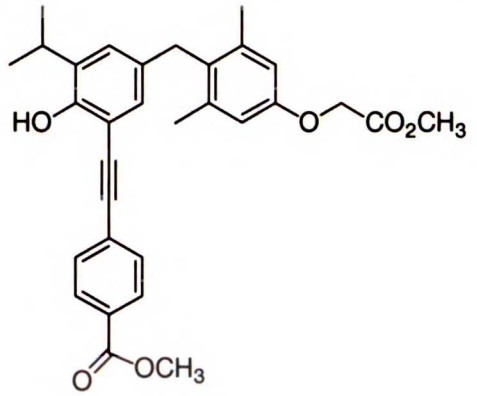

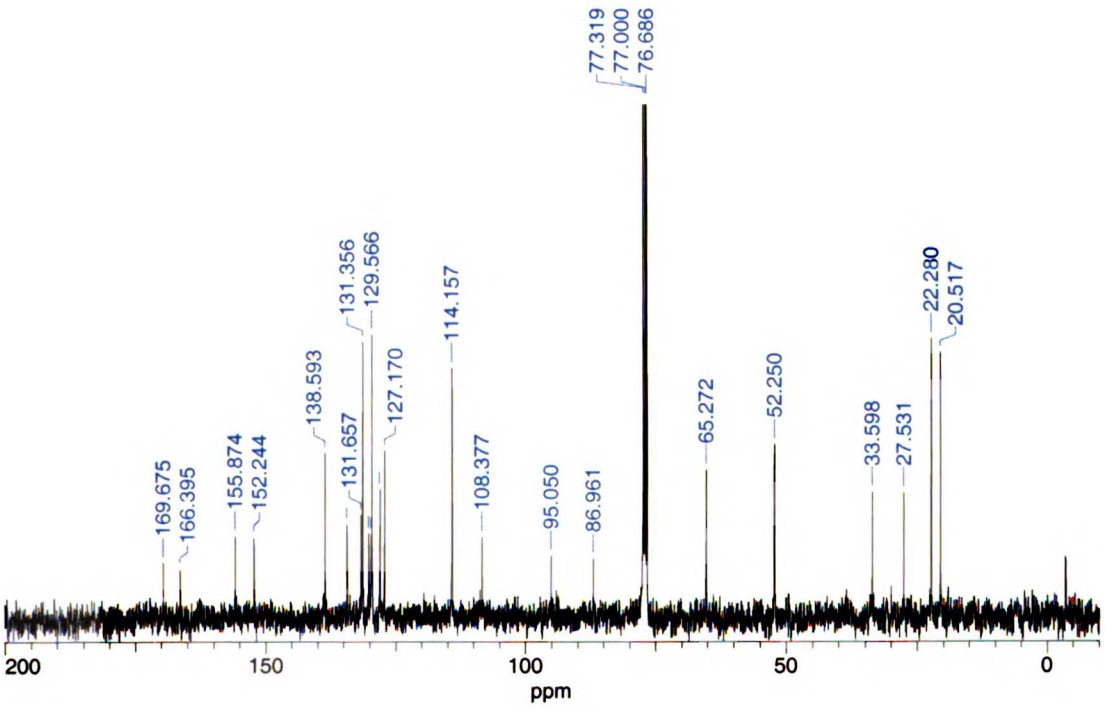

4-[5-(4-Methoxycarbonylmethoxy-2,6-dimethyl-benzyl)-2-hydroxy-3-isopropyl-phenylethynyl]-benzoic acid (18e, NH-14)

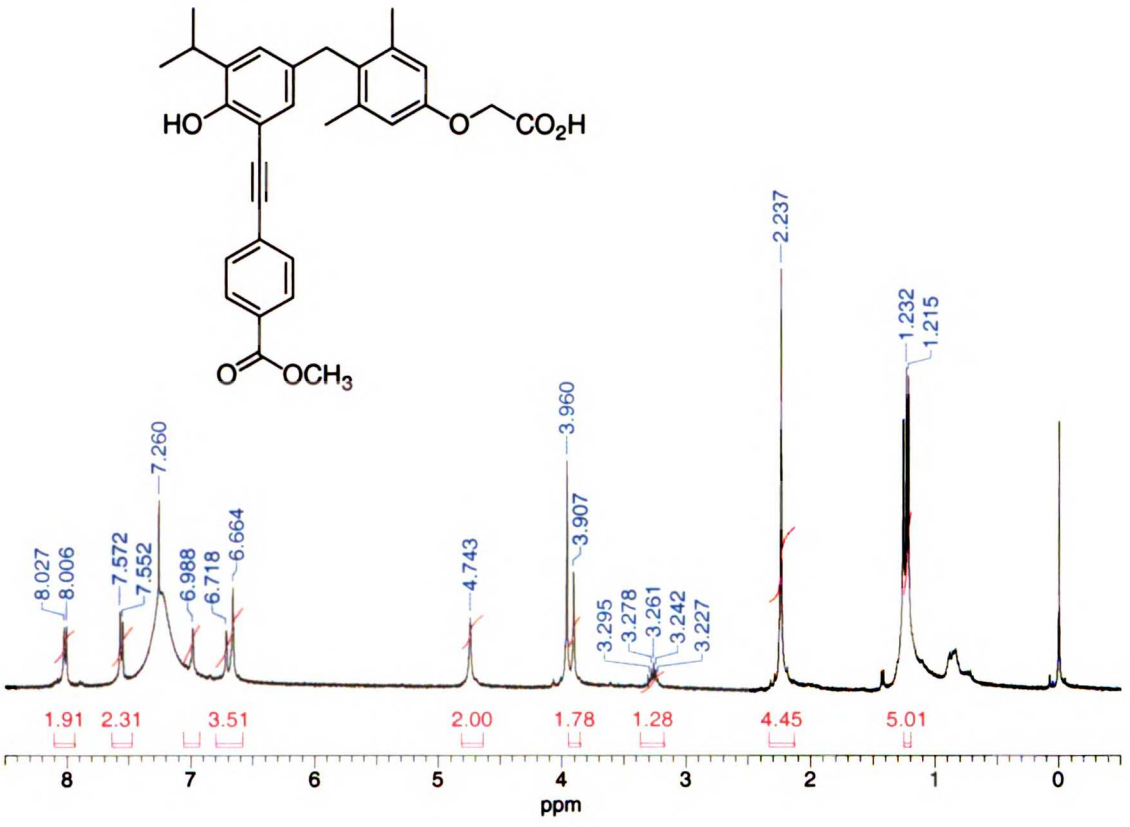

{4-[3-(4-Carbamoyl-phenylethynyl)-5-isopropyl-4-methoxymethoxy-benzyl]-3,5-dimethylphenoxy}-acetic acid methyl ester (17f)

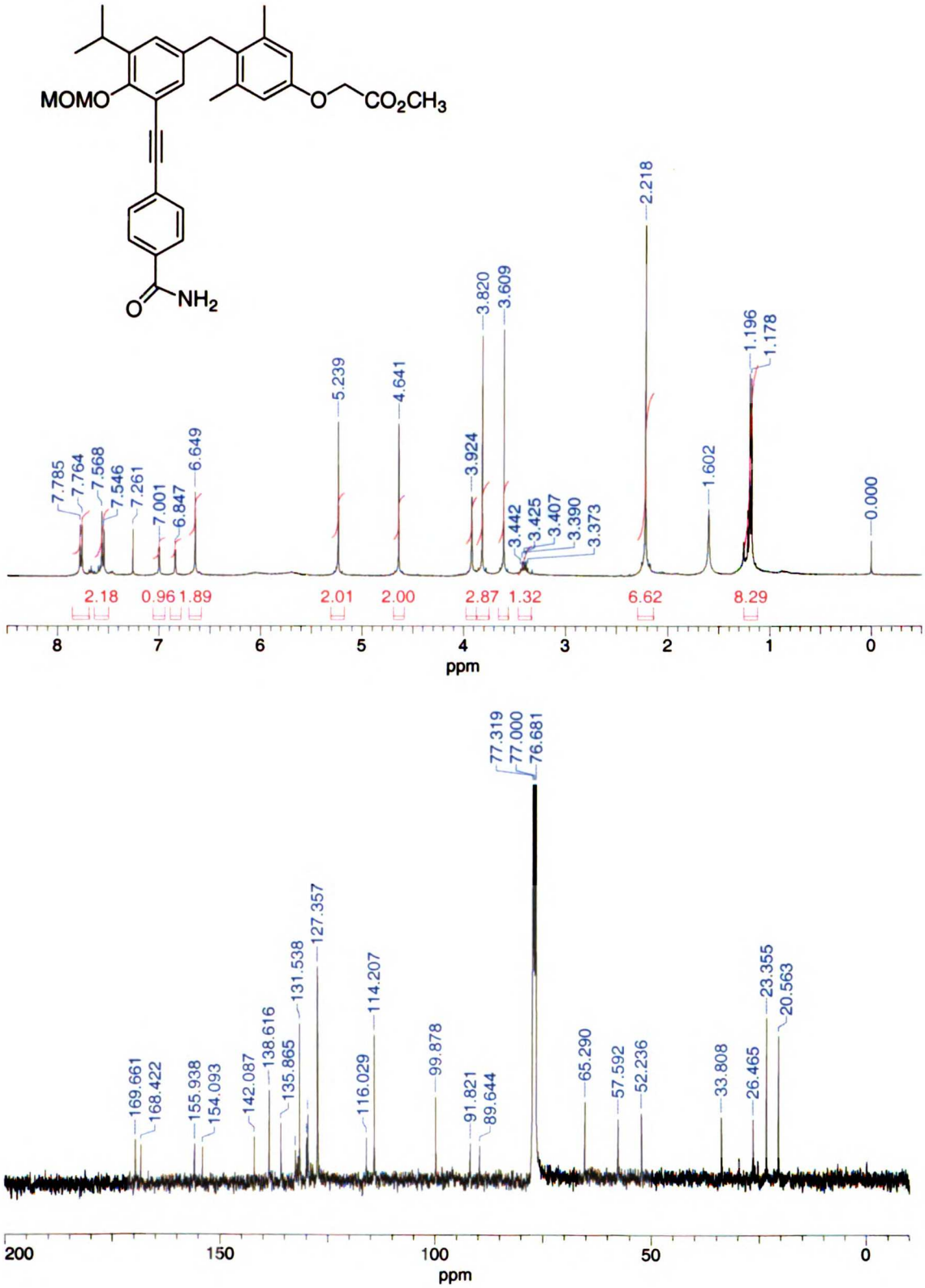

{4-[3-(4-Carbamoyl-phenylethynyl)-4-hydroxy-5-isopropyl-benzyl]-3,5-dimethylphenoxy}-acetic acid methyl ester

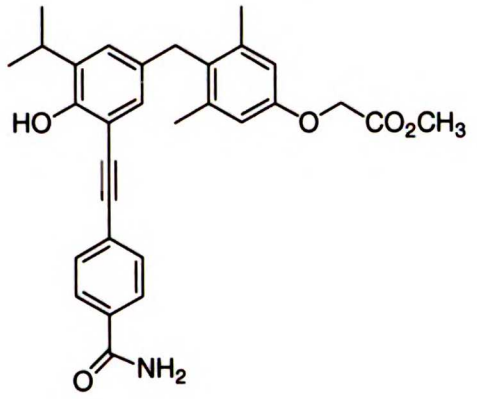

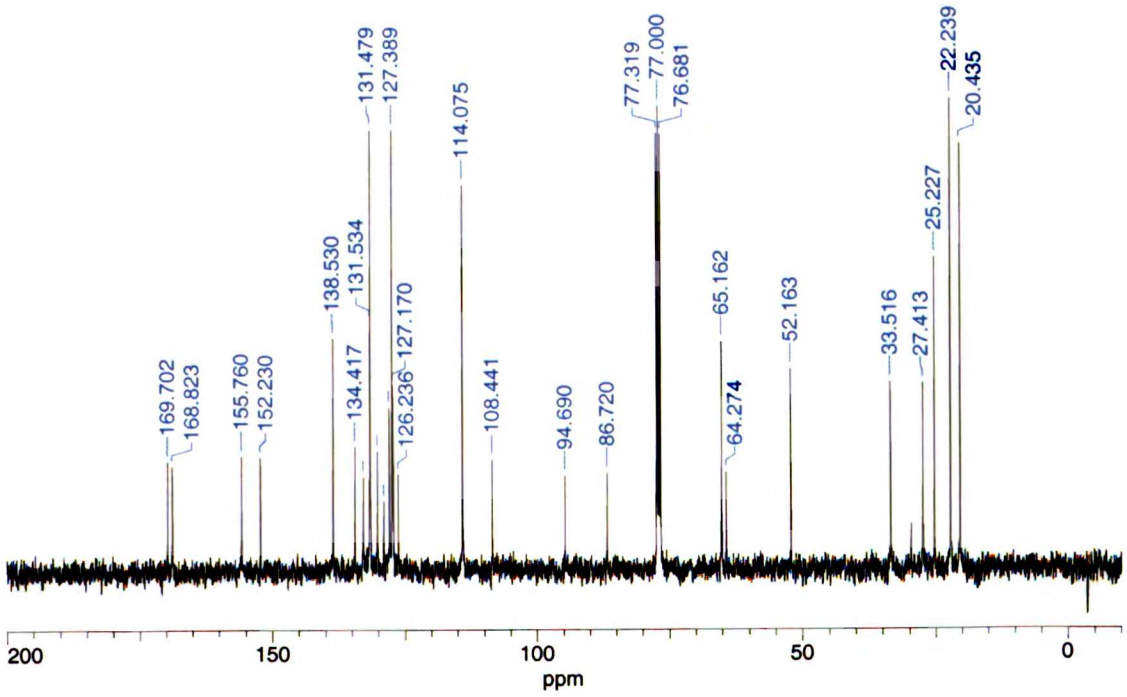

{4-[3-(4-Carbamoyl-phenylethynyl)-4-hydroxy-5-isopropyl-benzyl]-3,5-dimethyl-phenoxy}-acetic acid (18f, NH-15)

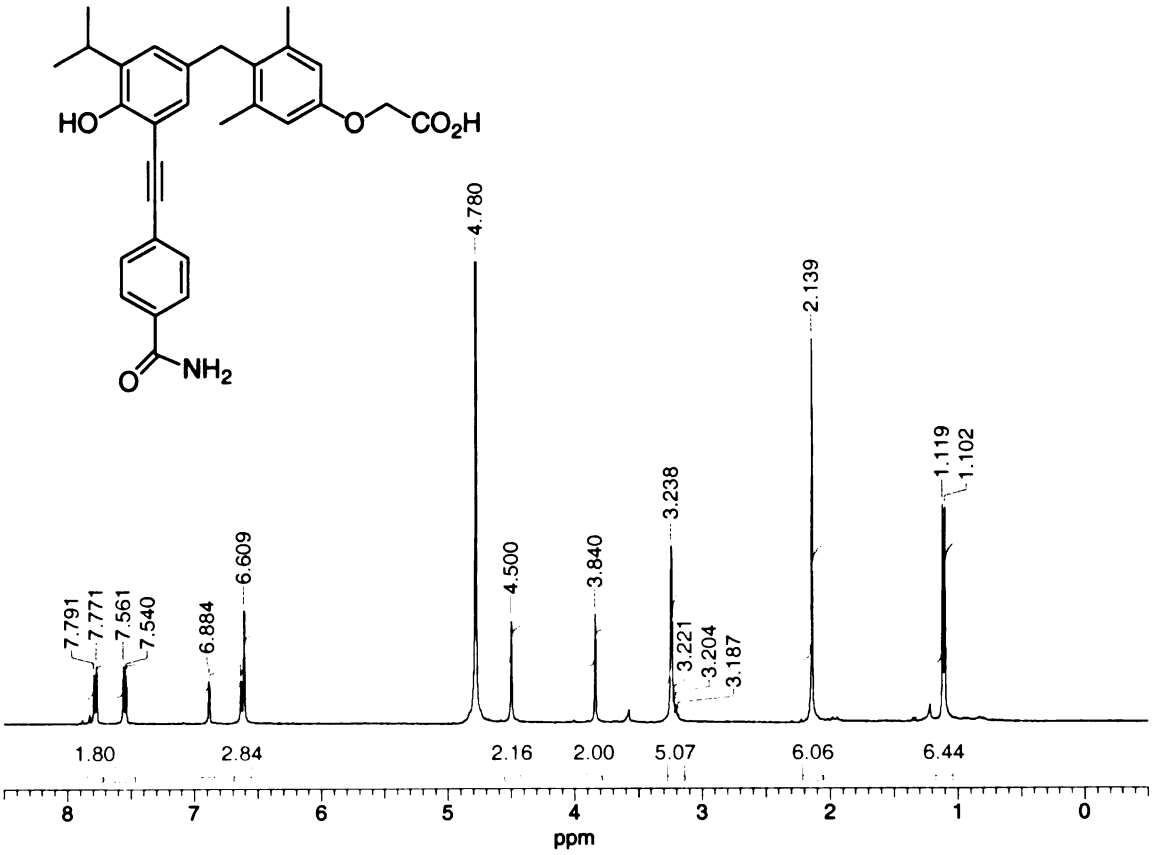

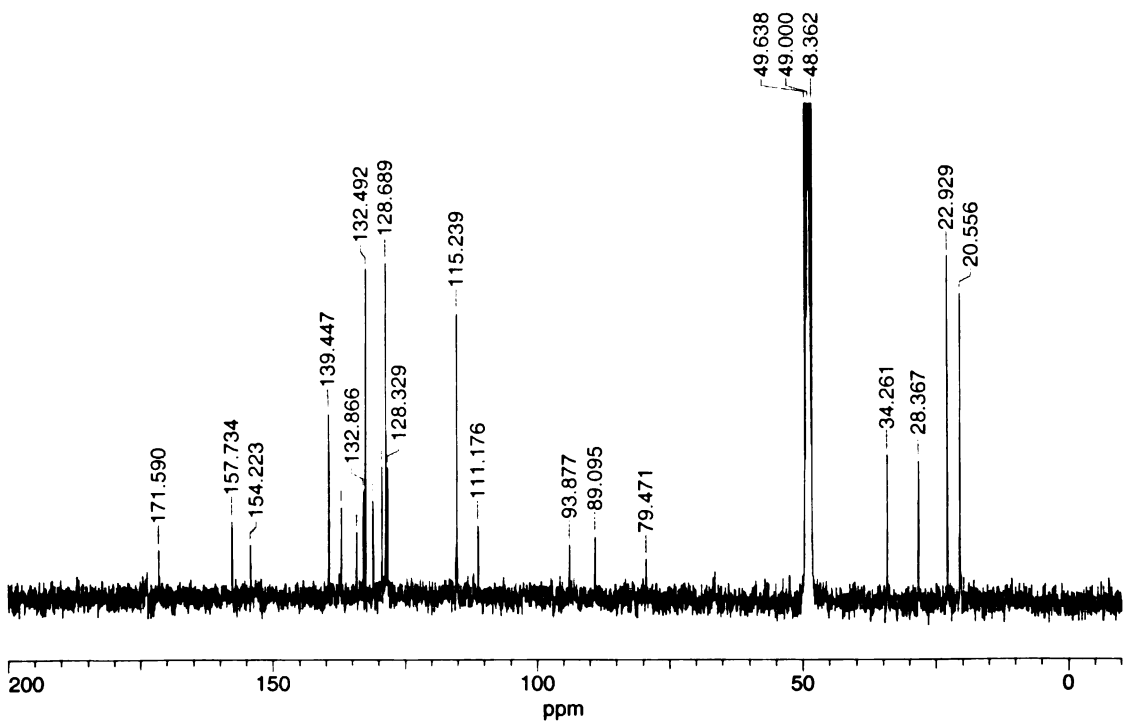

{4-[3-(4-Dimethylamino-phenylethynyl)-5-isopropyl-4-methoxymethoxy-benzyl]-3,5-dimethyl-phenoxy}-acetic acid methyl ester (17g)

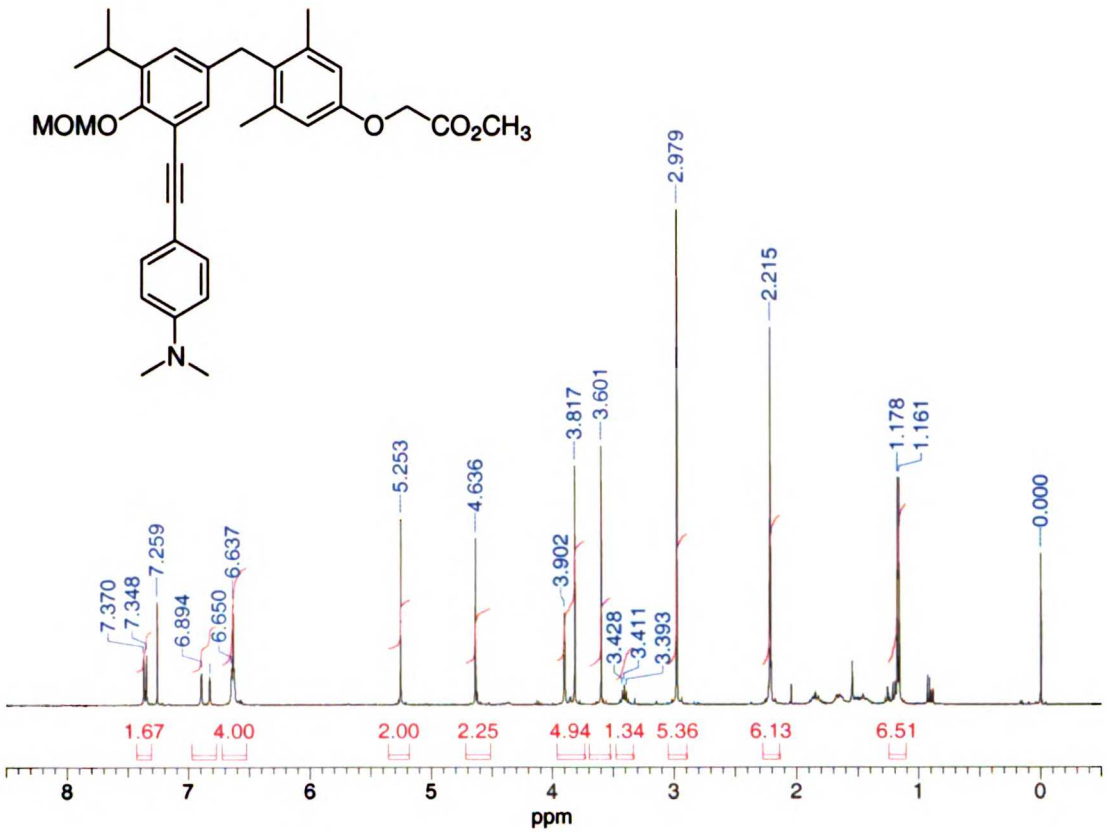

{4-[3-(4-Dimethylamino-phenylethynyl)-4-hydroxy-5-isopropyl-benzyl]-3,5-dimethyl-phenoxy}-acetic acid methyl ester

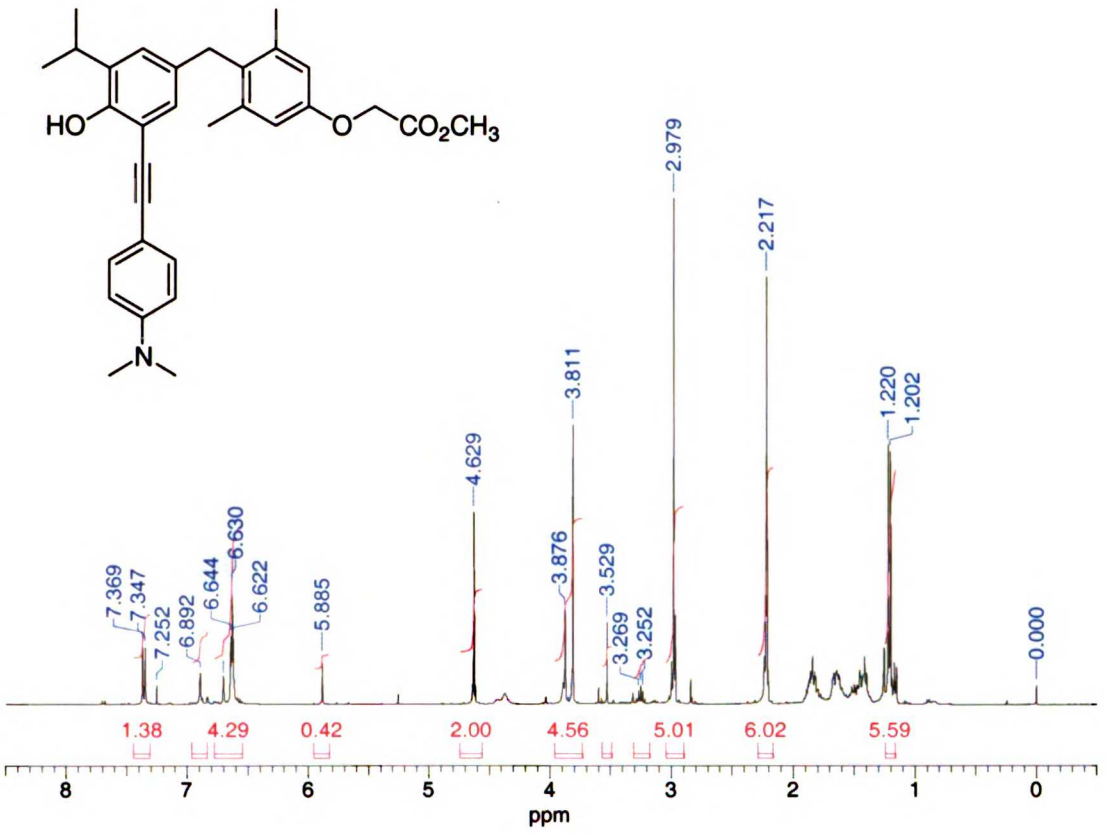

{4-[3-(4-Dimethylamino-phenylethynyl)-4-hydroxy-5-isopropyl-benzyl]-3,5-dimethyl-phenoxy}-acetic acid (18g, NH-24)

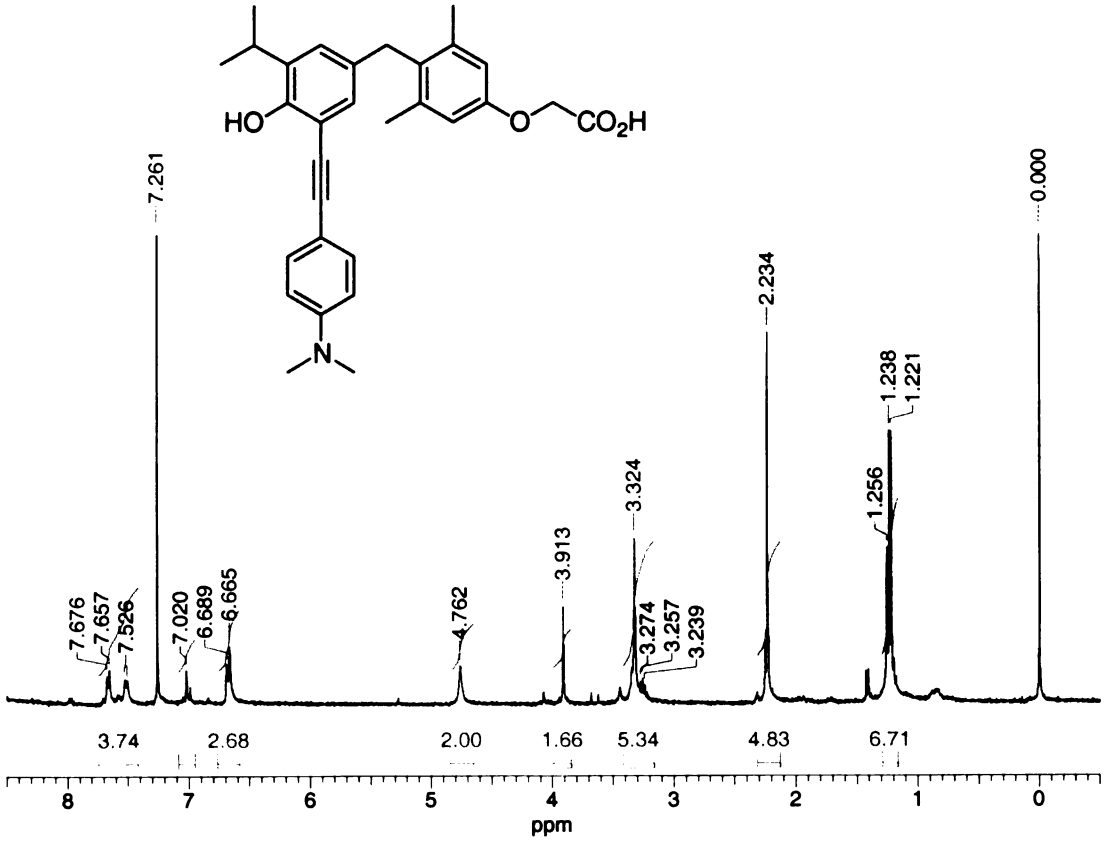

{4-[2-Hydroxy-3-isopropyl-5-(4-methoxycarbonylmethoxy-2,6-dimethyl-benzyl)-phenylethynyl-phenyl}-trimethyl-ammonium trifluoromethane sulfonate salt (NH-16)

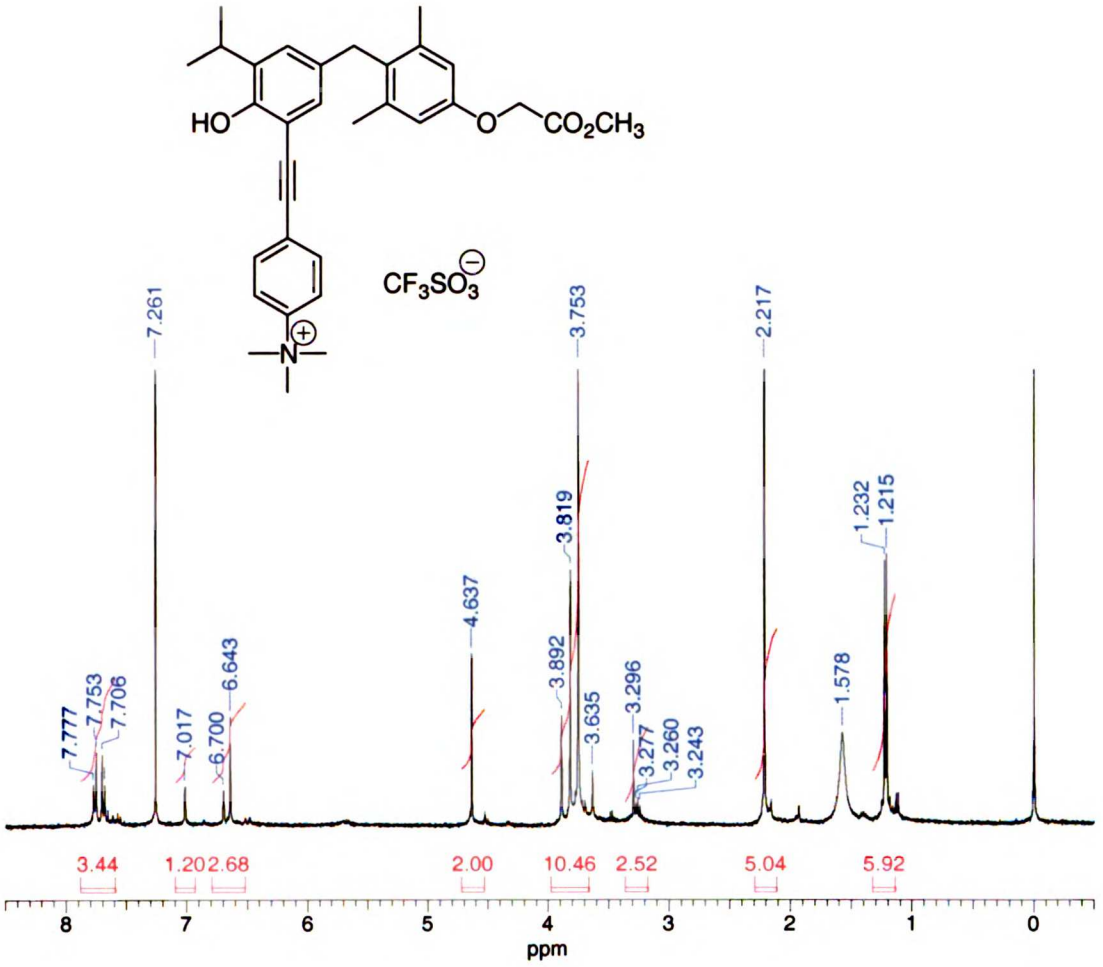

{4-[3-(4-Amino-phenylethynyl)4-hydroxy-5-isopropyl-benzyl]-3,5-dimethyl-phenoxy}-acetic acid methyl ester

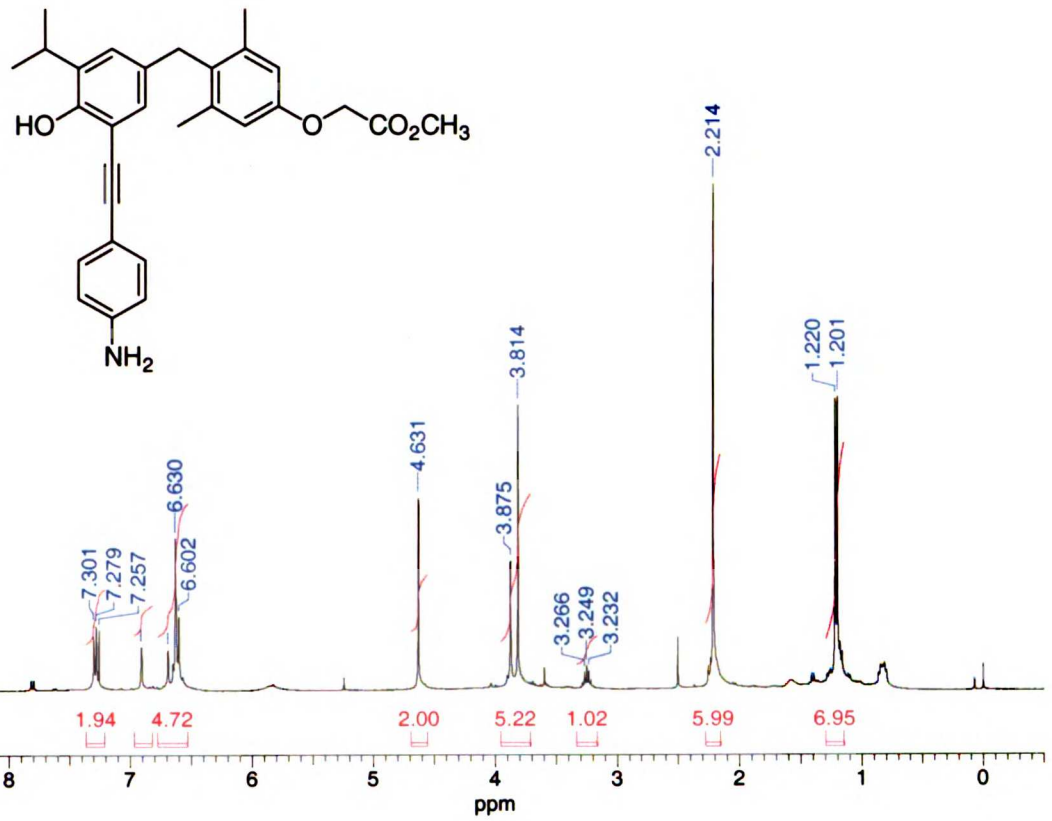

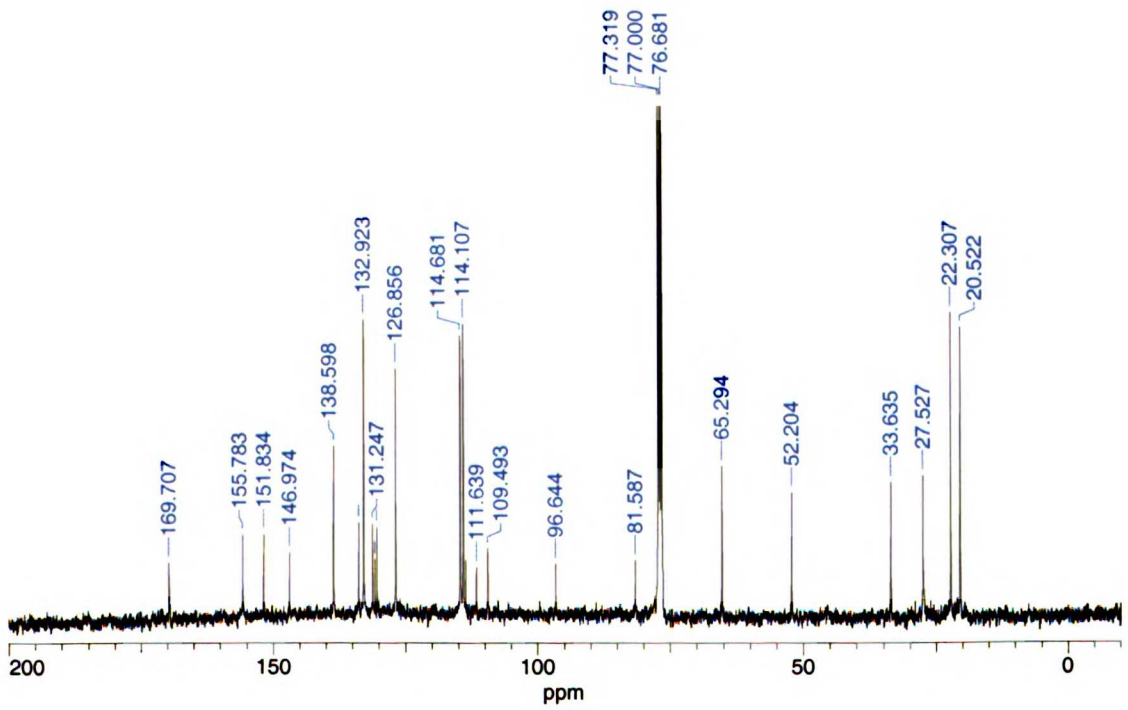

{4-[3-(4-Amino-phenylethynyl)4-hydroxy-5-isopropyl-benzyl]-3,5-dimethyl-phenoxy}-acetic acid (18l, NH-4)

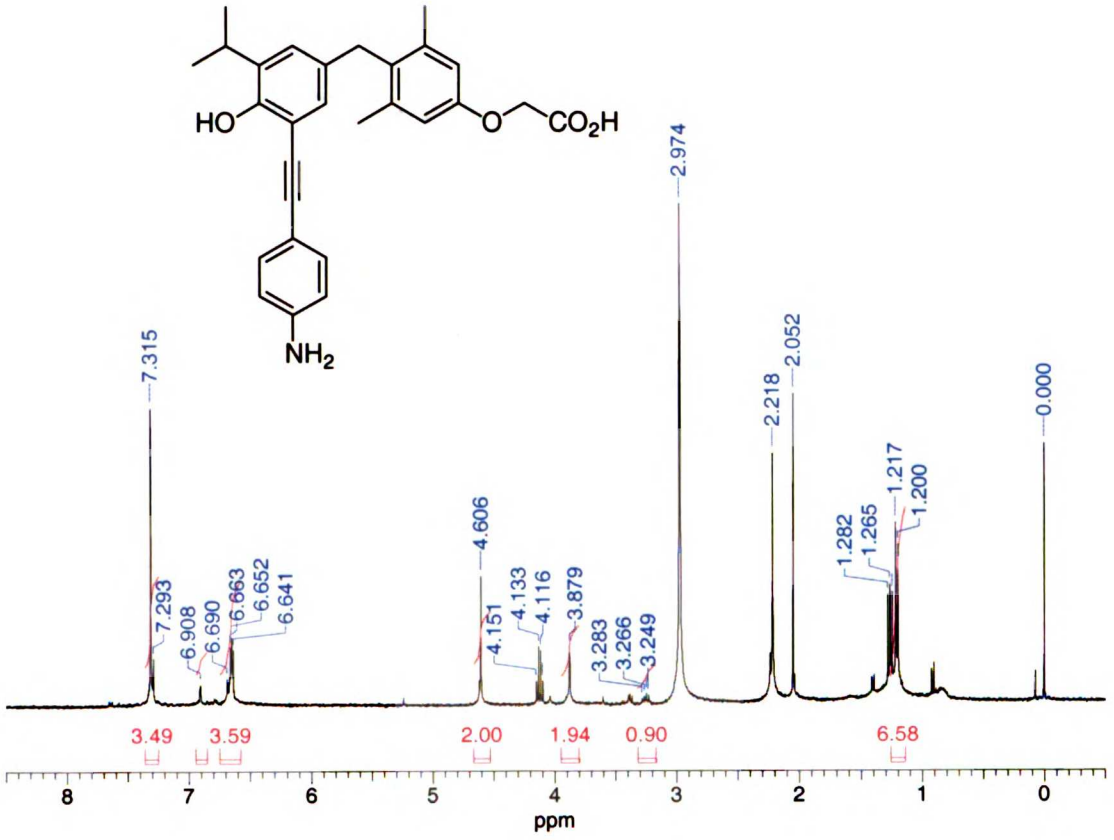

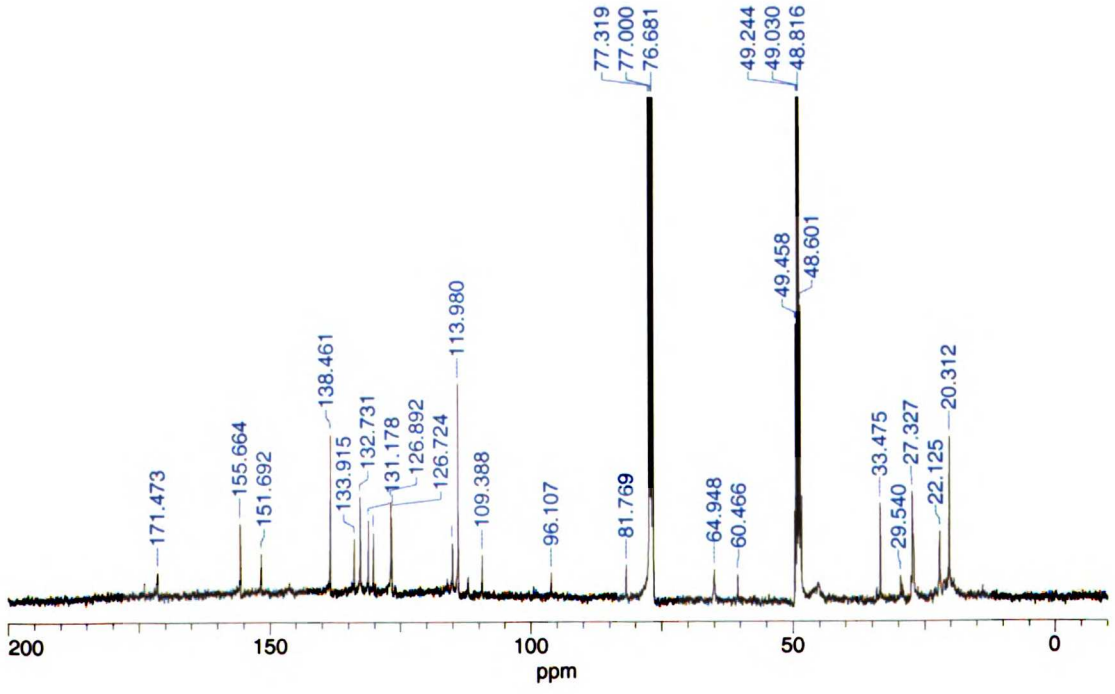

{4-[3-(4-Azido-phenylethynyl)-5-isopropyl-4-methoxymethoxy-benzyl]-3,5-dimethyl-phenoxy}-acetic acid methyl ester

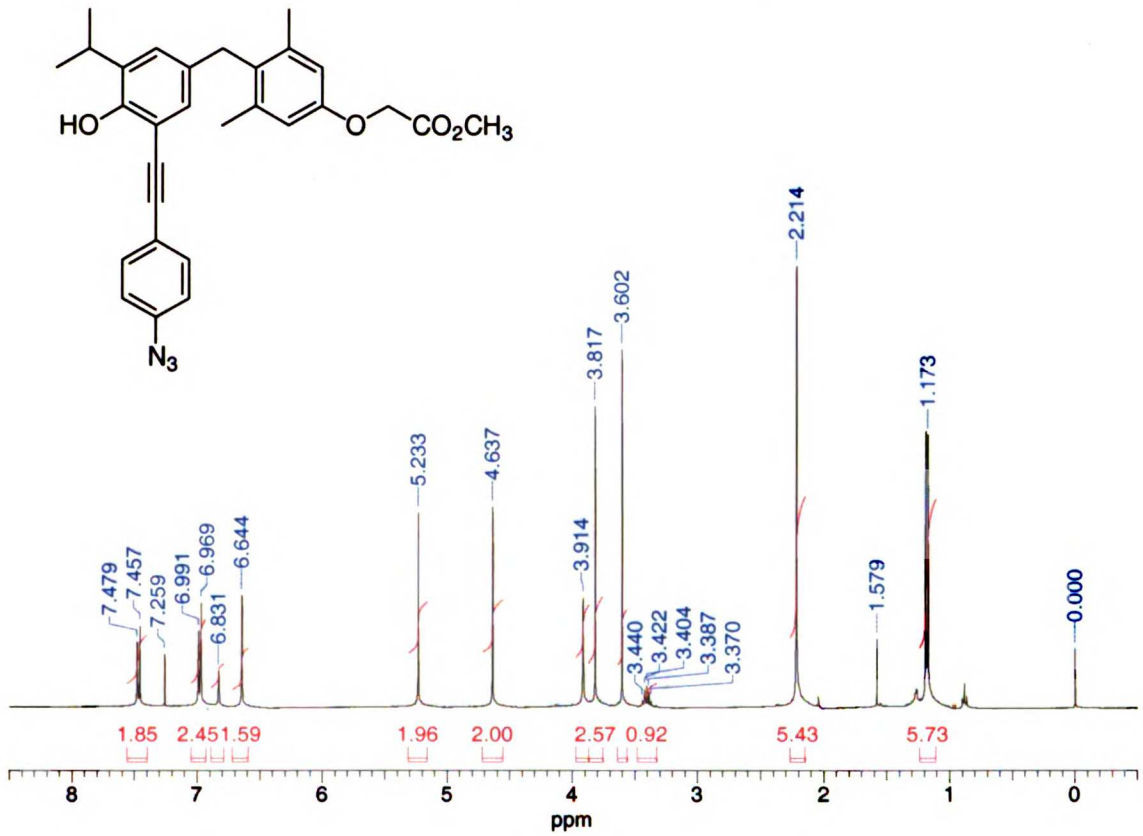

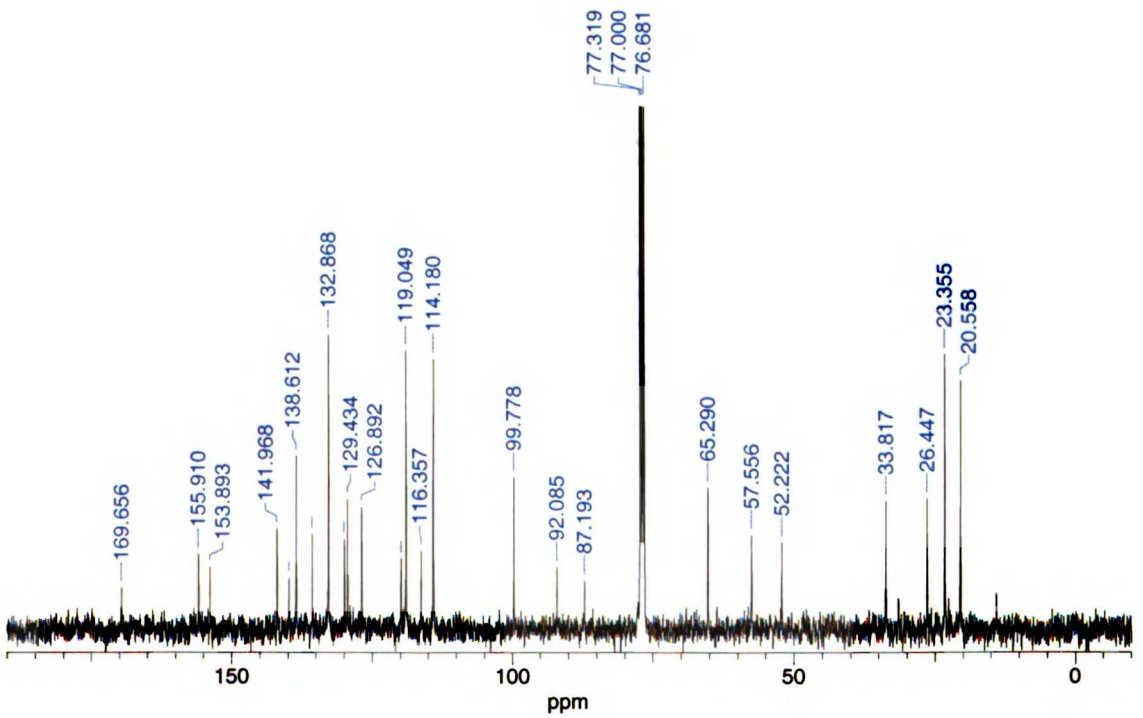

{4-[3-(4-Azido-phenylethynyl)-4-hydroxy-5-isopropyl-benzyl]-3,5-dimethyl-phenoxy}-acetic acid (NH-7)

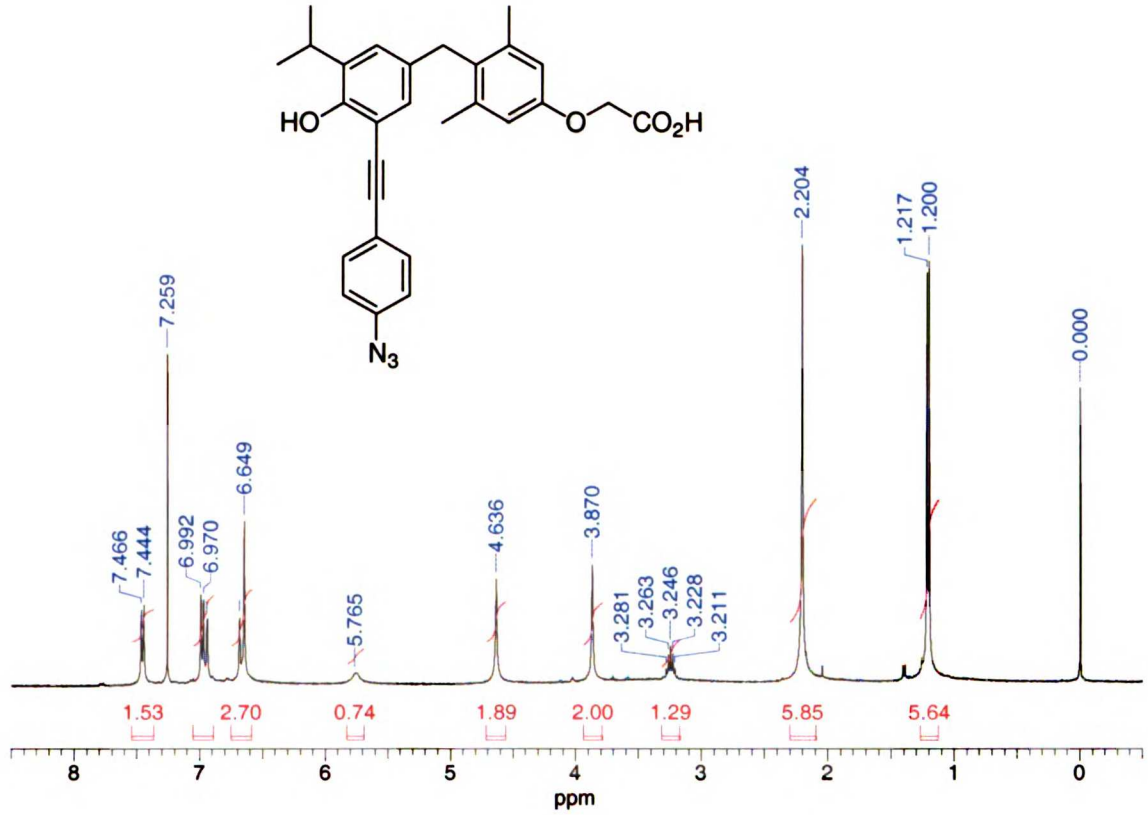

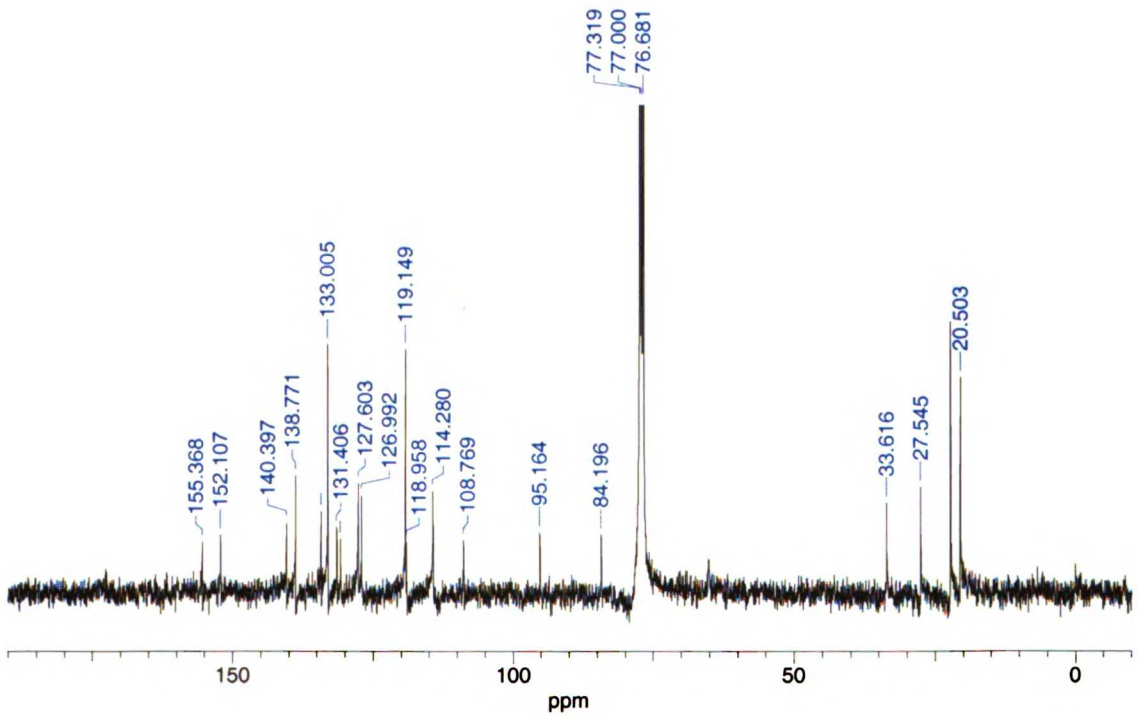

{4-[3-(4-Bromo-phenylethynyl)-5-isopropyl-benzyl]-3,5-dimethyl-phenoxy}-acetic acid methyl ester (17m)

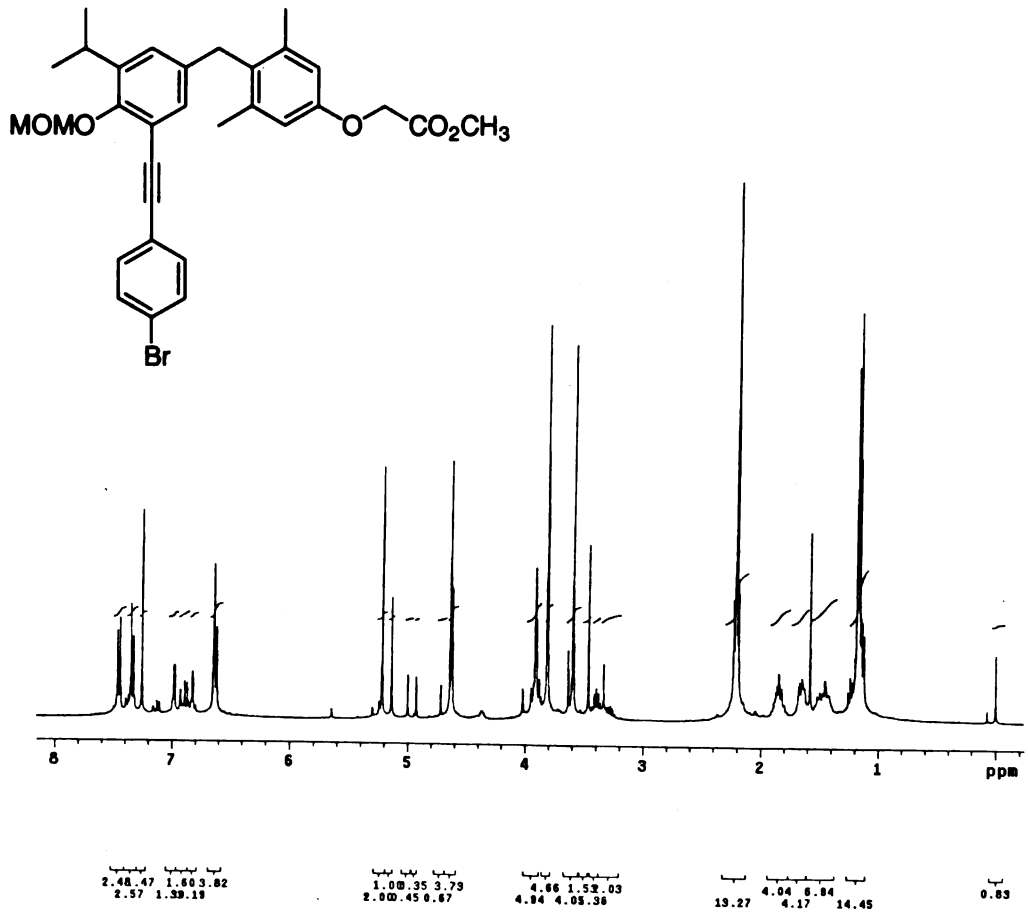

(4-{3-Isopropyl-4-methoxymethoxy-5-[4-(1-nitro-ethyl)-phenylethynyl]-benzyl}-3,5-dimethyl-phenoxy)-acetic acid methyl ester (23)

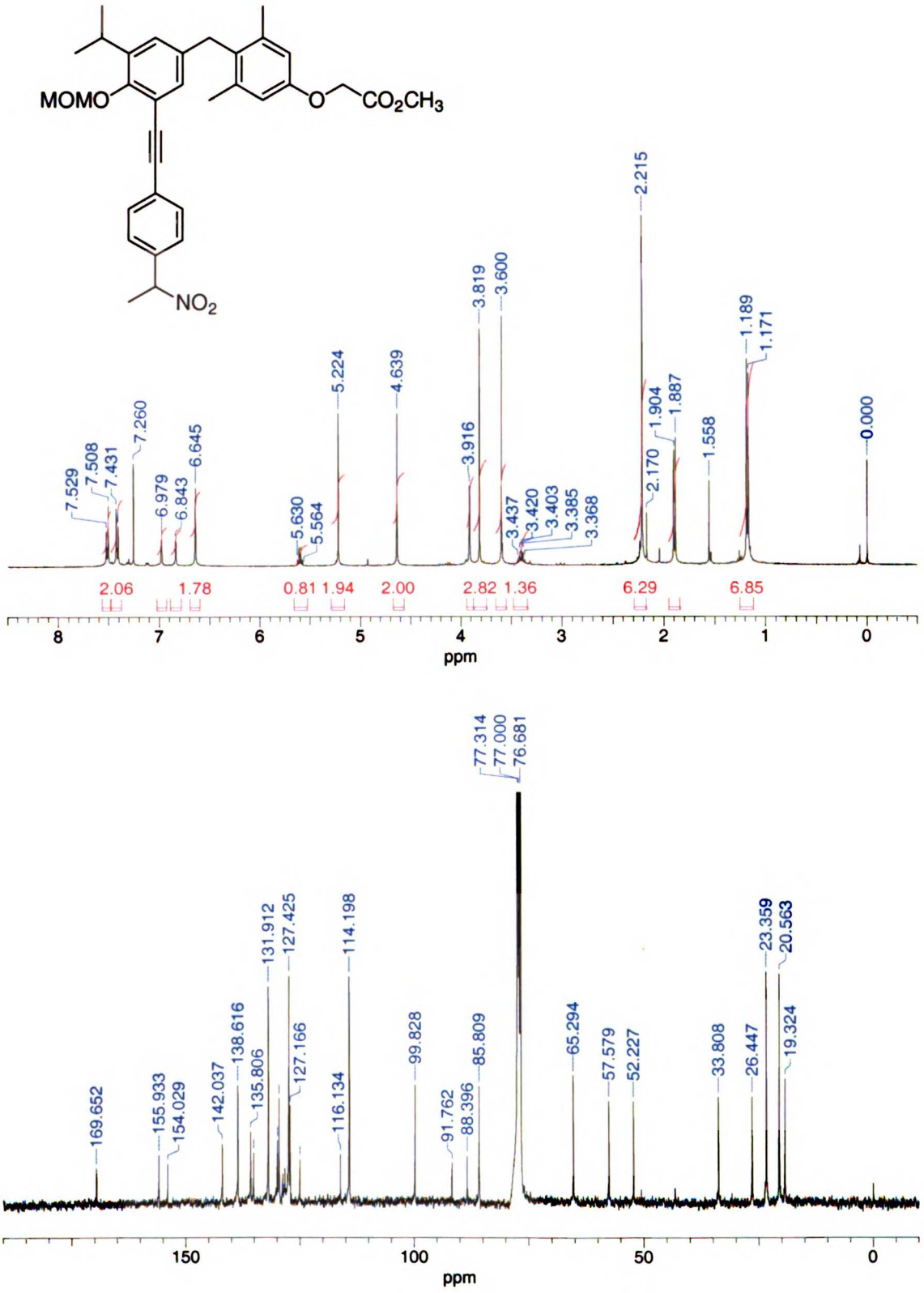

(4-{4-Hydroxy-3-isopropyl-5-[4-(1-nitro-ethyl)-phenylethynyl]-benzyl}-3,5-dimethyl-phenoxy)-acetic acid methyl ester

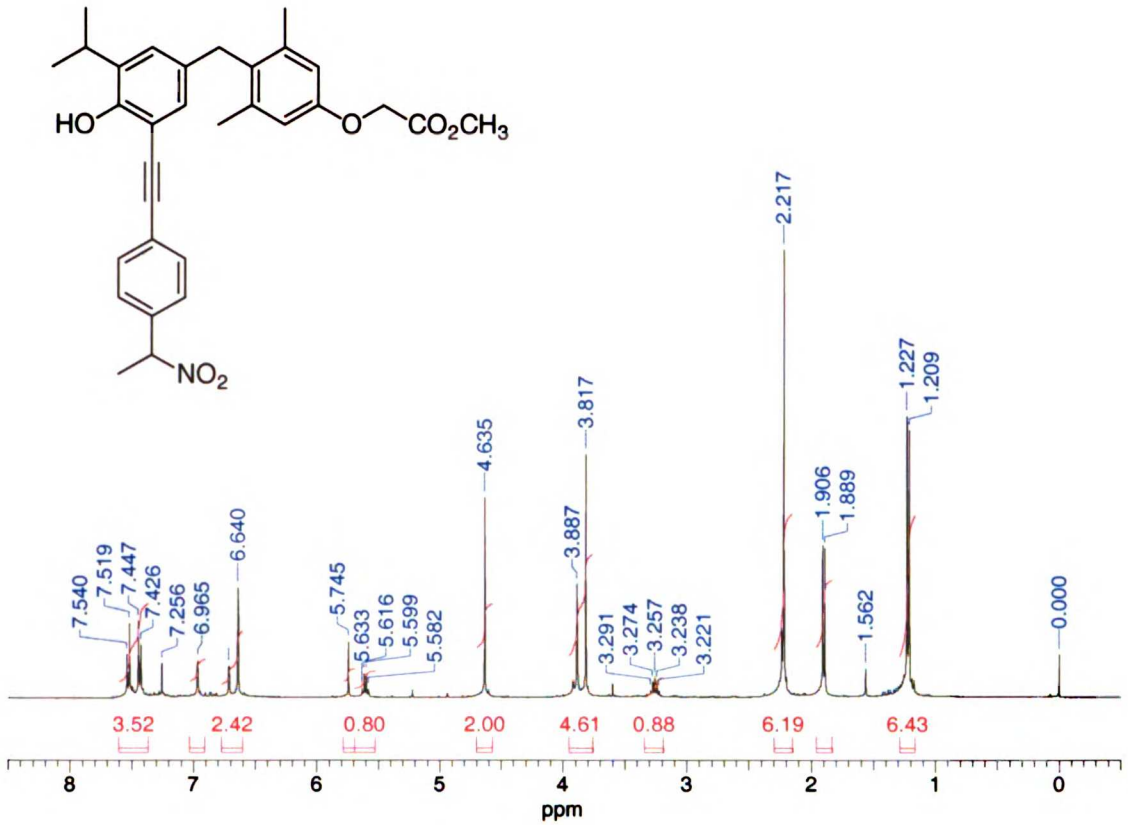

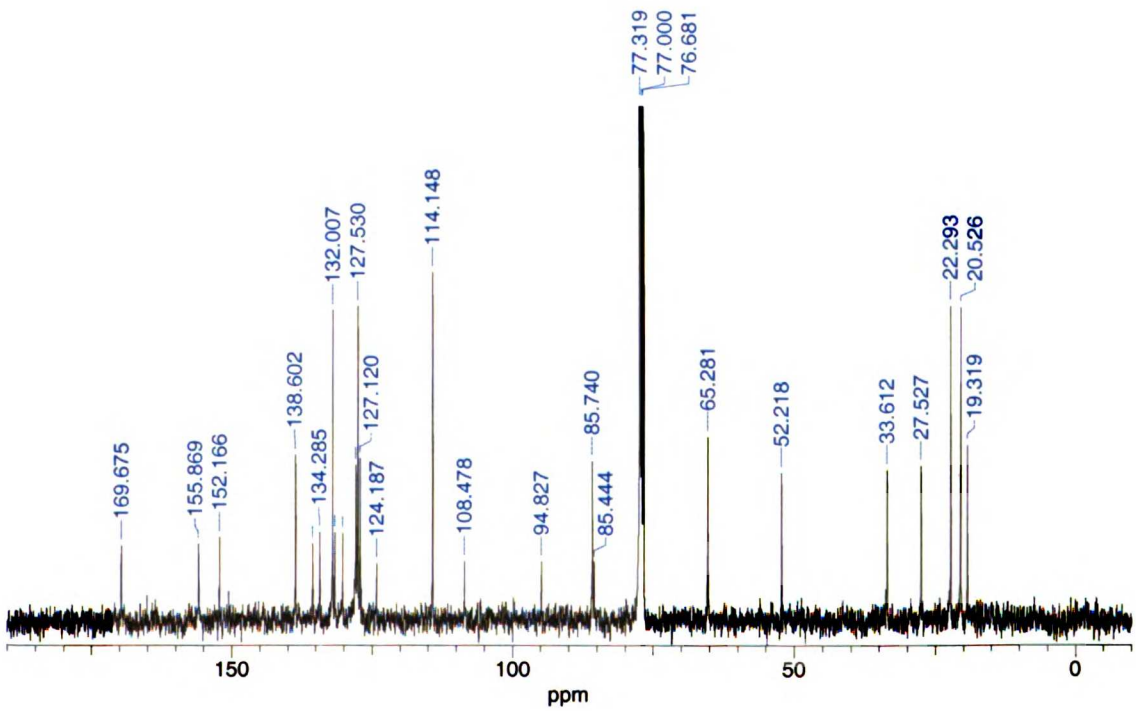

{4-[3-(4-Acetyl-phenylethynyl)-4-hydroxy-5-isopropyl-benzyl]3,5-dimethyl-phenoxy}-acetic acid (NH-9)

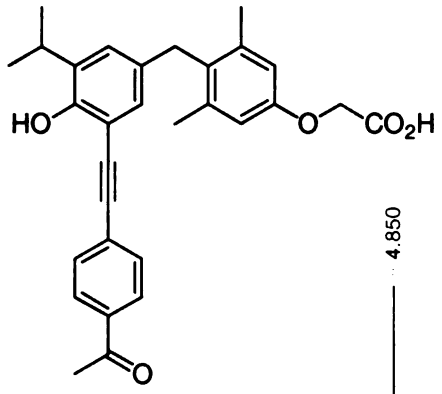

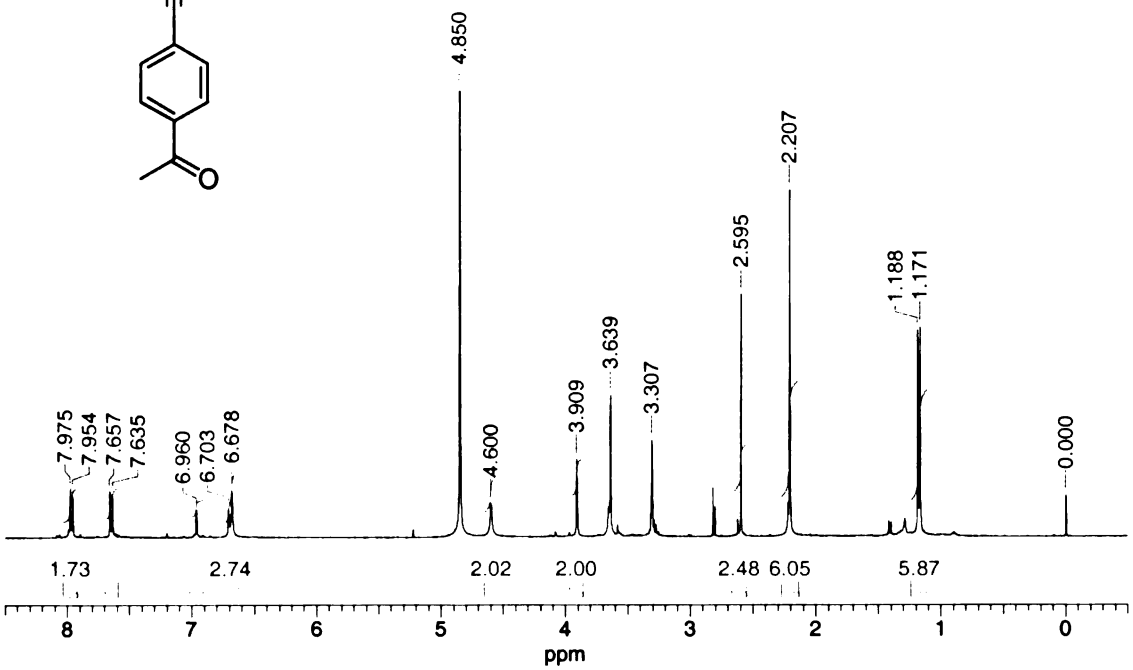

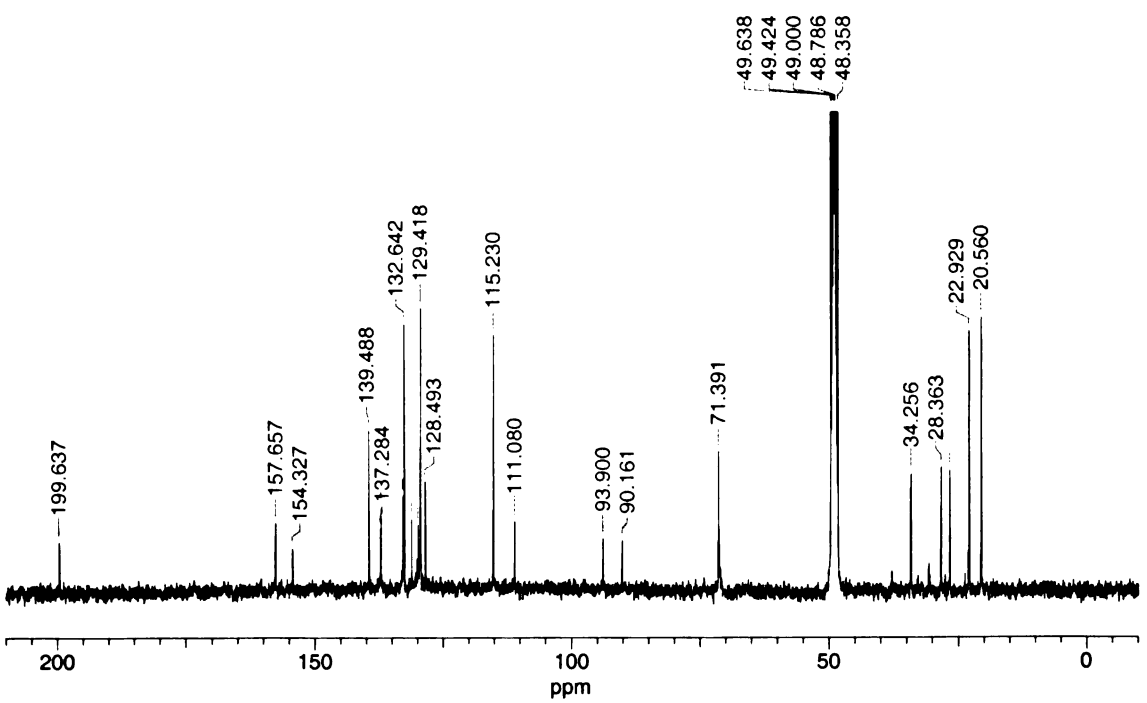

(4-{3-Isopropyl-4-methoxymethoxy-5-[4-(triisopropyl-silanyloxymethyl)-phenylethynyl]-benzyl}-3,5-dimethyl-phenoxy)-acetic acid methyl ester (17n)

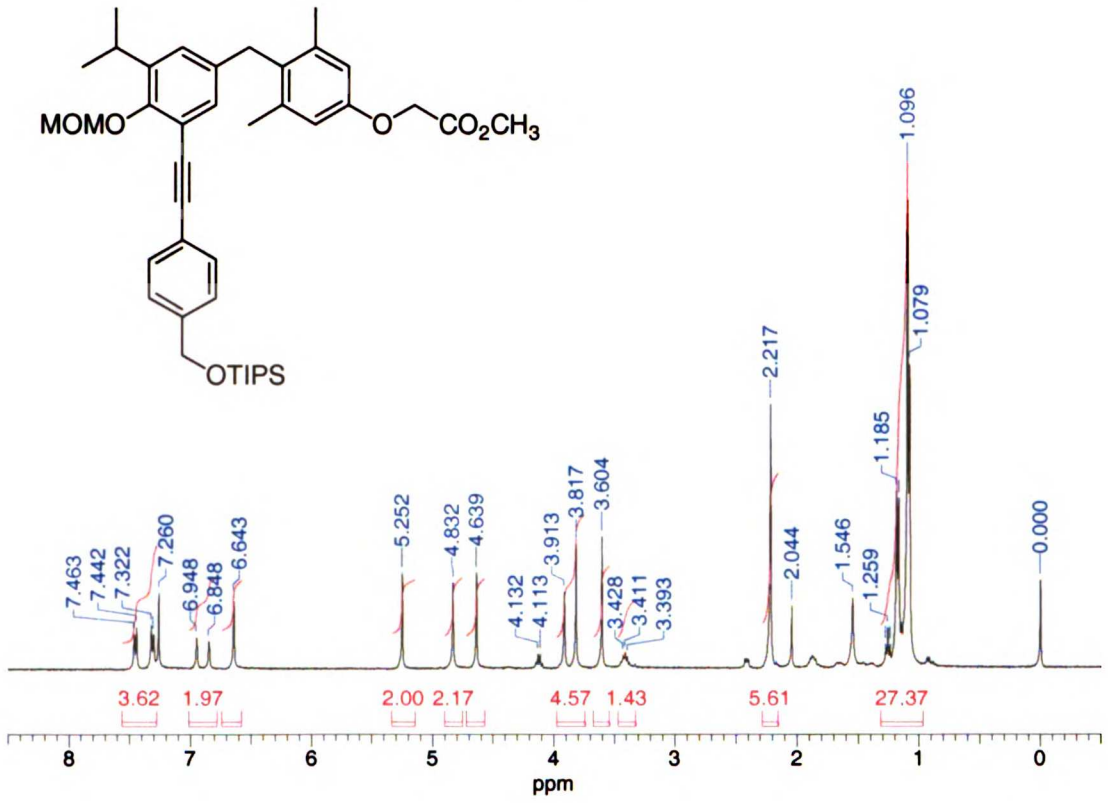

{4-[3-(4-Hydroxymethyl-phenylethynyl)-5-isopropyl-4-methoxymethoxy-benzyl]-3,5-dimethyl-phenoxy}-acetic acid methyl ester

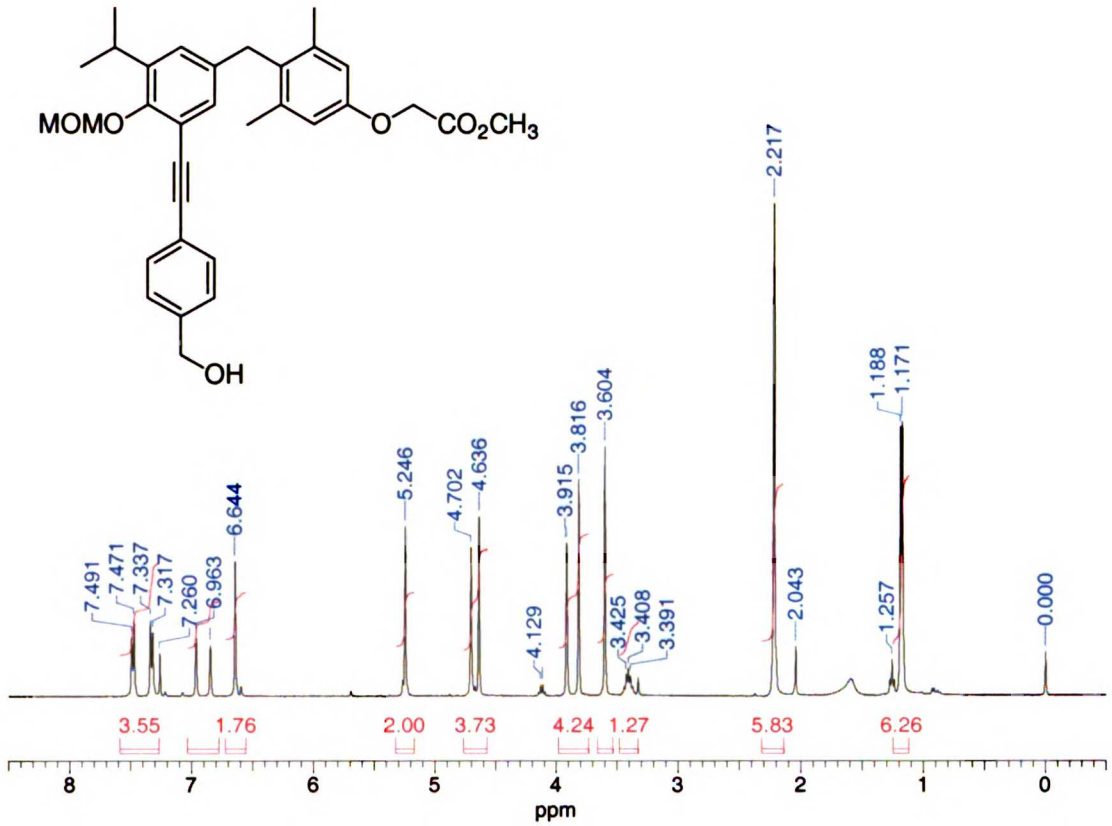

{4-[3-(4-Chloromethyl-phenylethynyl)-5-isopropyl-4-methoxymethoxy-benzyl]-3,5-dimethyl-phenoxy}-acetic acid methyl ester

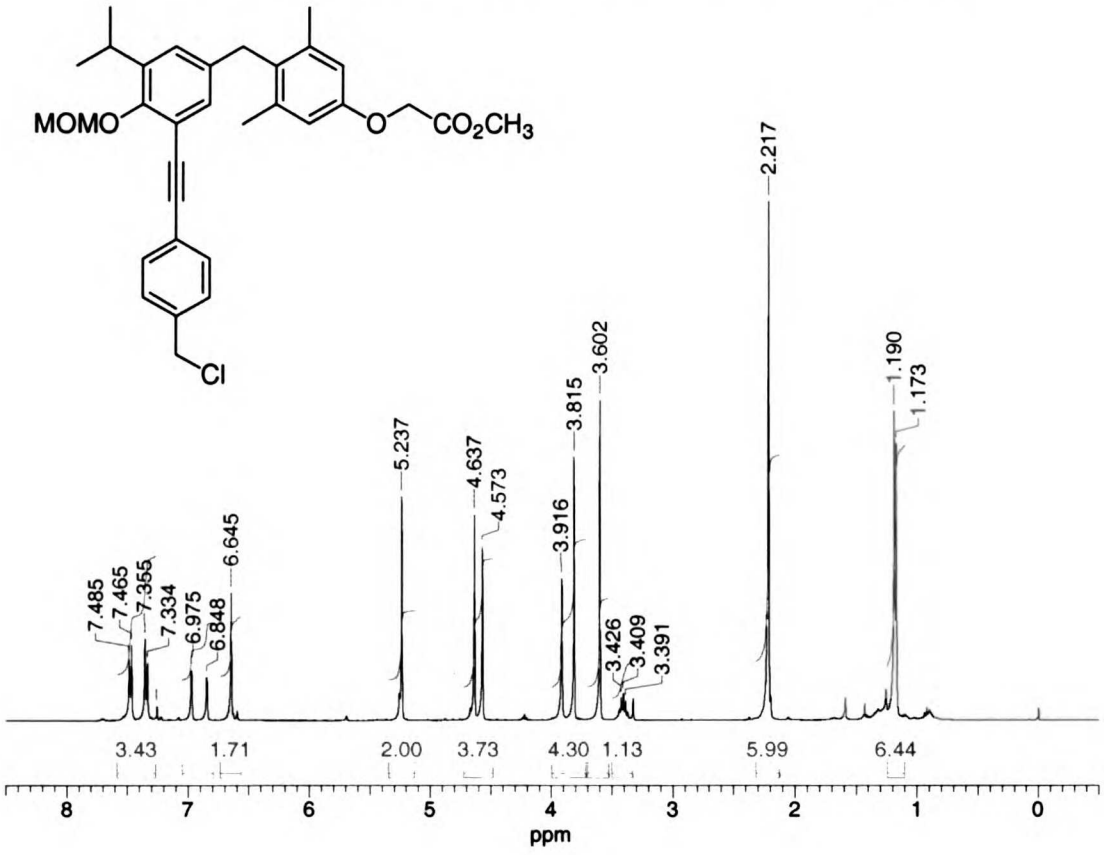

{4-[3-(4-Azidomethyl-phenylethynyl)-5-isopropyl-4-methoxymethoxy-benzyl]-3,5-dimethyl-phenoxy}-acetic acid methyl ester (24)

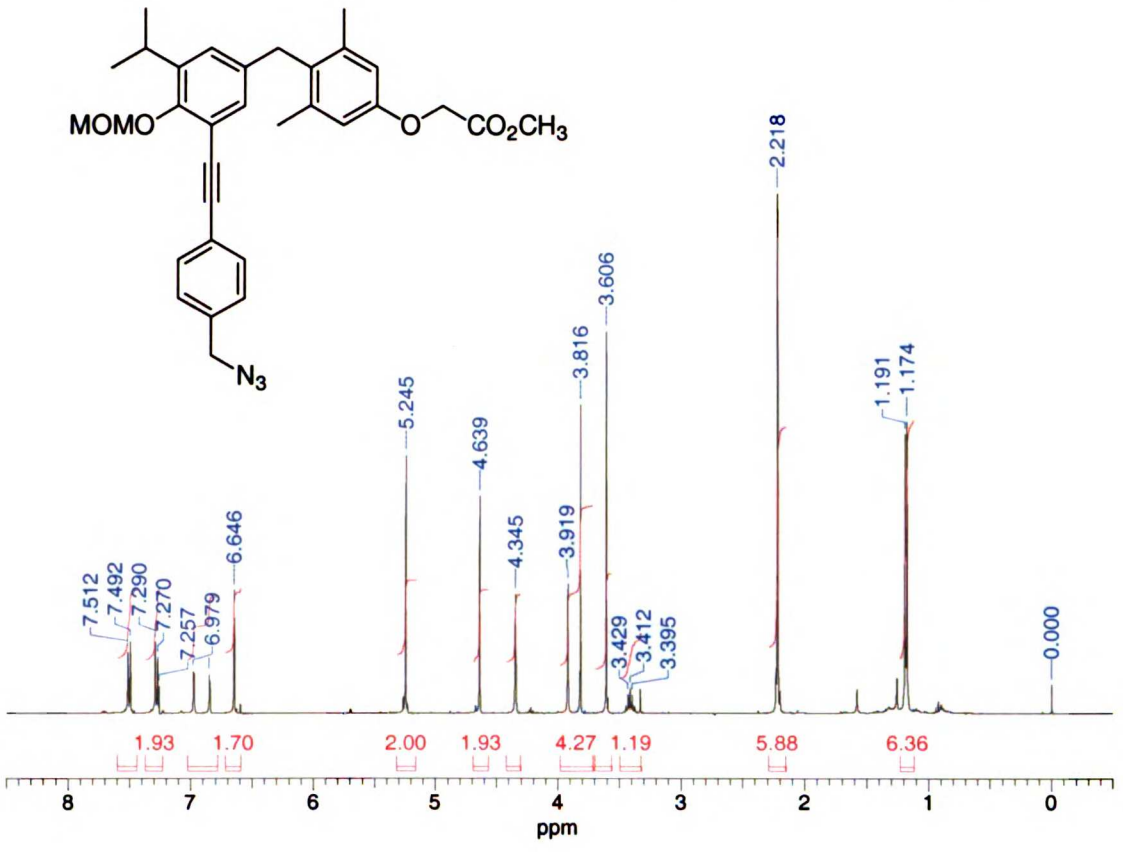

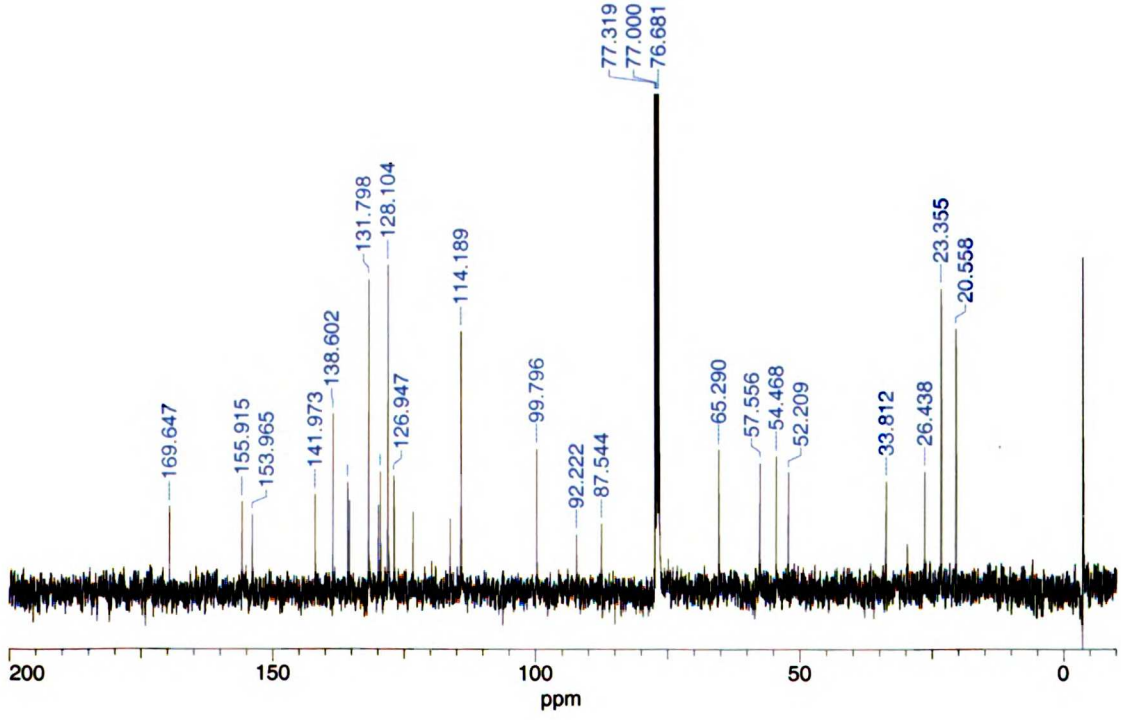

{4-[3-(4-Azidomethyl-phenylethynyl)-4-hydroxy-5-isopropyl-benzyl]-3,5-dimethyl-phenoxy}-acetic acid methyl ester

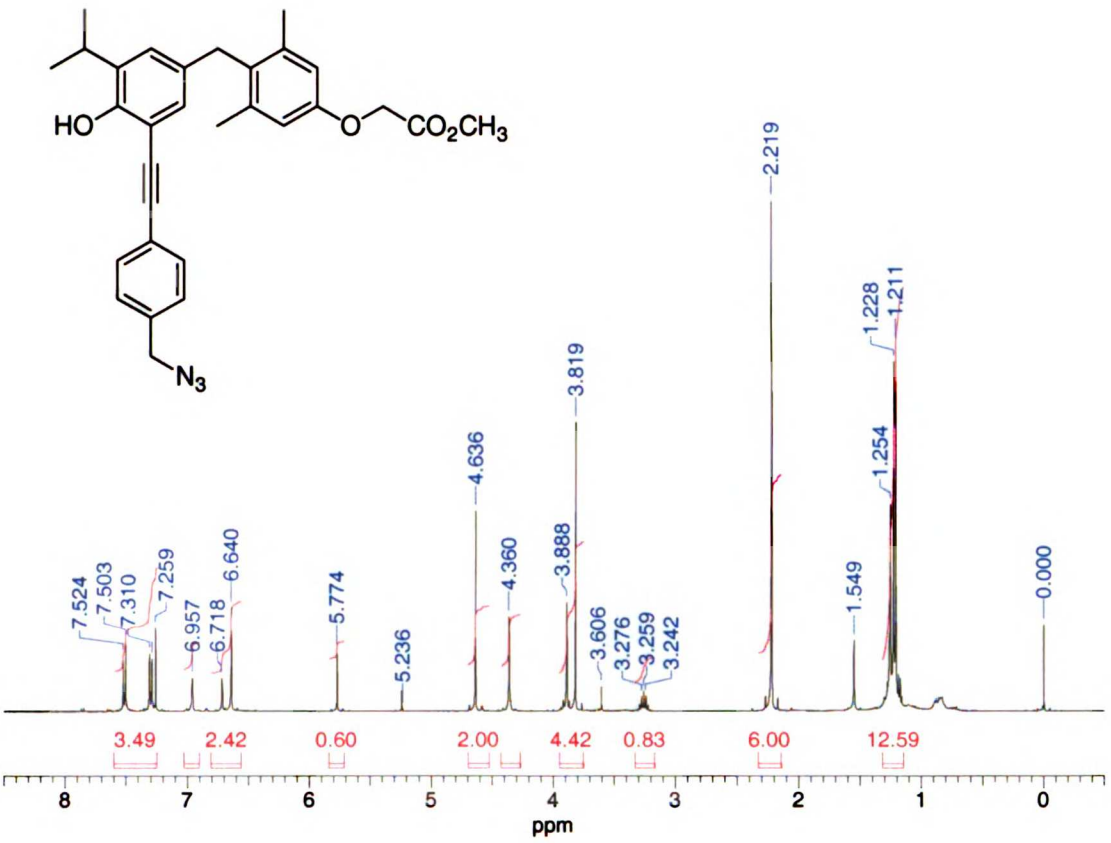

{4-[3-(4-Azidomethyl-phenylethynyl)-4-hydroxy-5-isopropyl-benzyl]-3,5-dimethyl-phenoxy}-acetic acid (NH-23)

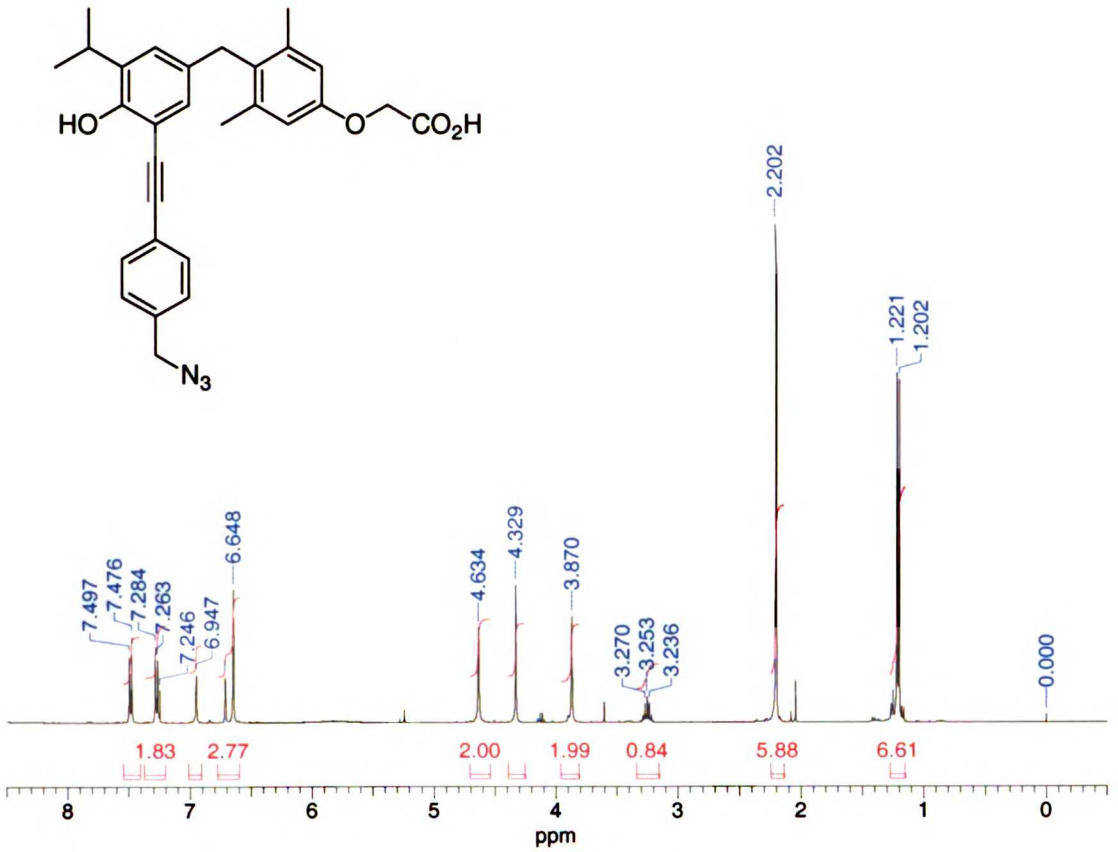

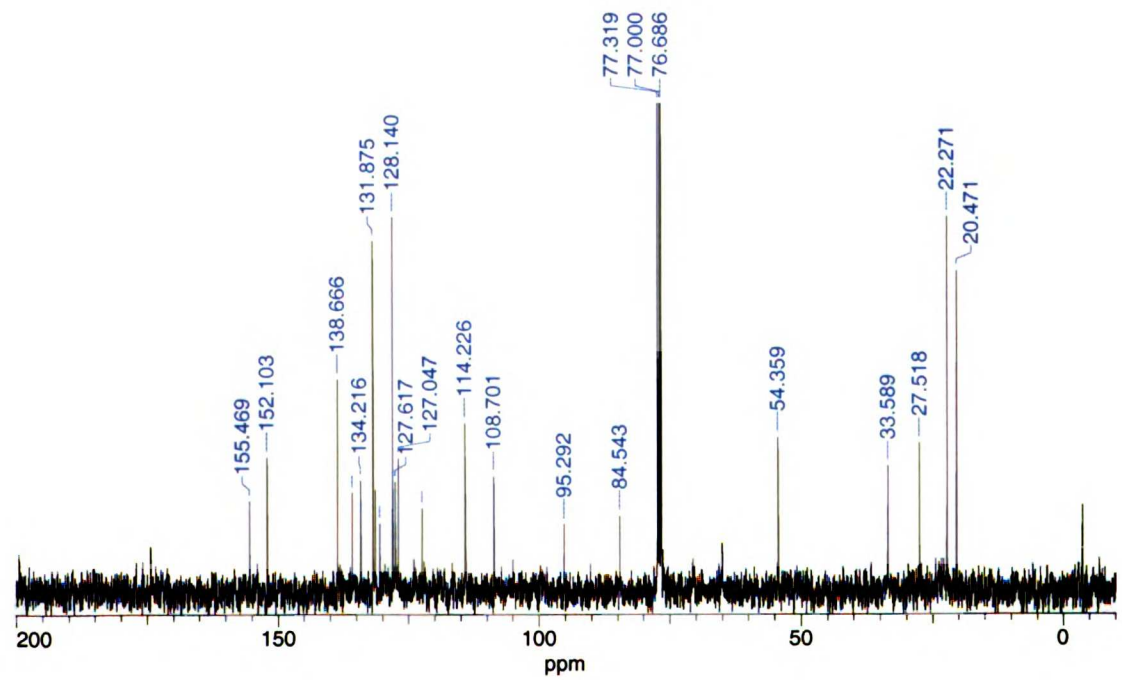

{4-[3-Isopropyl-4-methoxymethoxy-5-(3-trifluoromethyl-phenylethynyl)-benzyl]-3,5-dimethyl-phenoxy}-acetic acid methyl ester (17h)

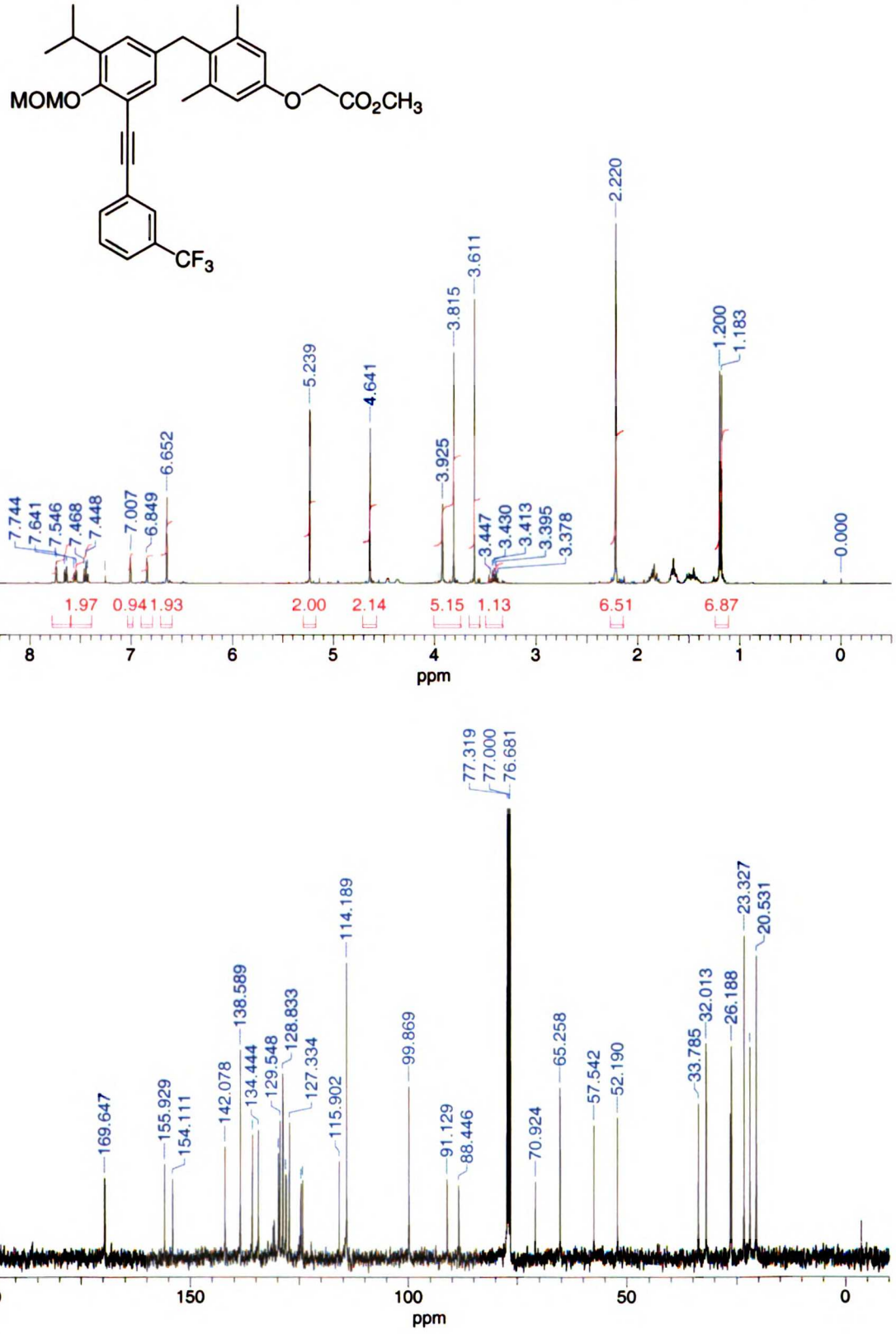

{4-[4-Hydroxy-3-isopropyl-5-(3-trifluoromethyl-phenylethynyl)-benzyl]-3,5-dimethyl-phenoxy}-acetic acid methyl ester

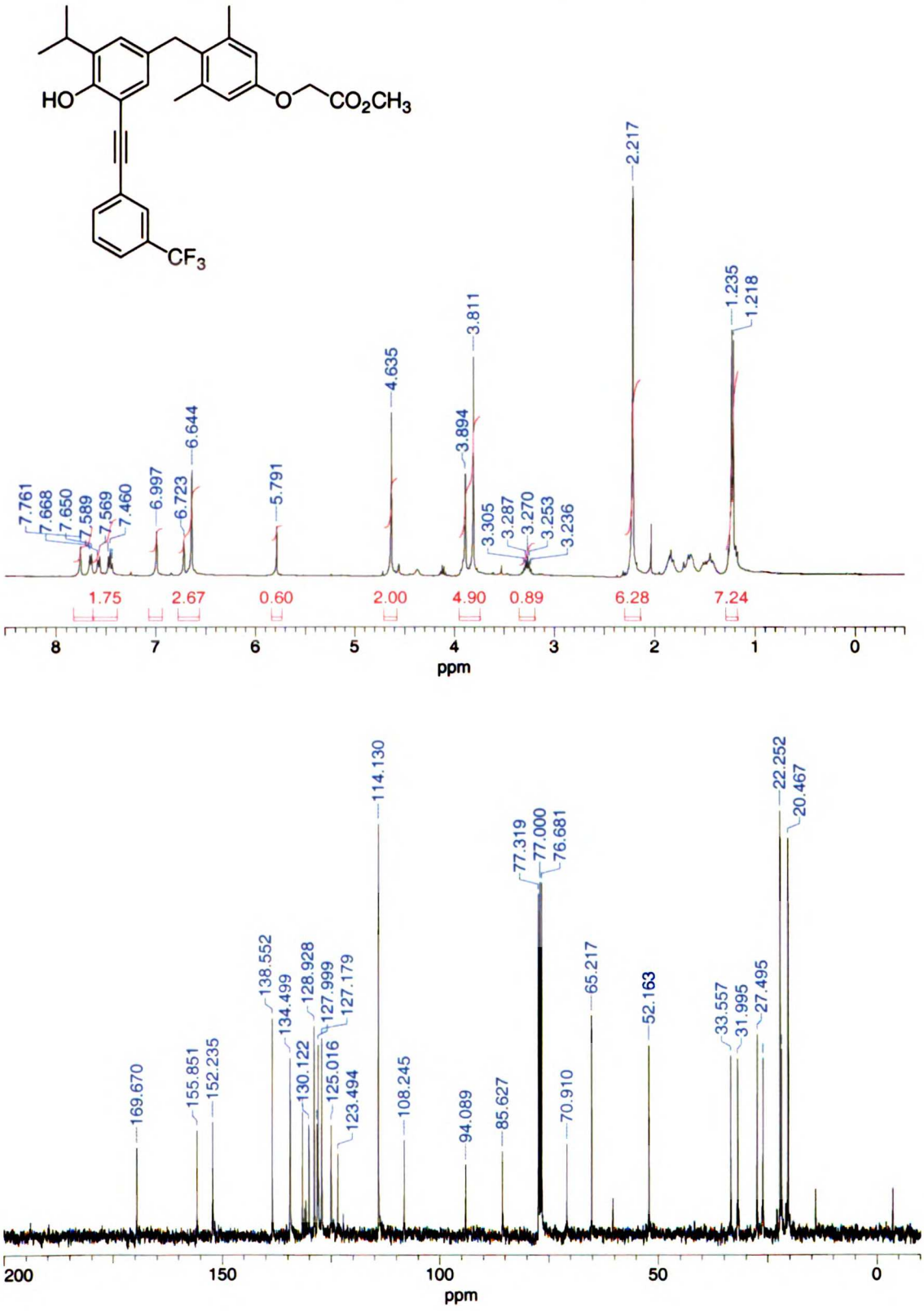

{4-[4-Hydroxy-3-isopropyl-5-(3-trifluoromethyl-phenylethynyl)-benzyl]-3,5-dimethyl-phenoxy}-acetic acid (18h, NH-17)

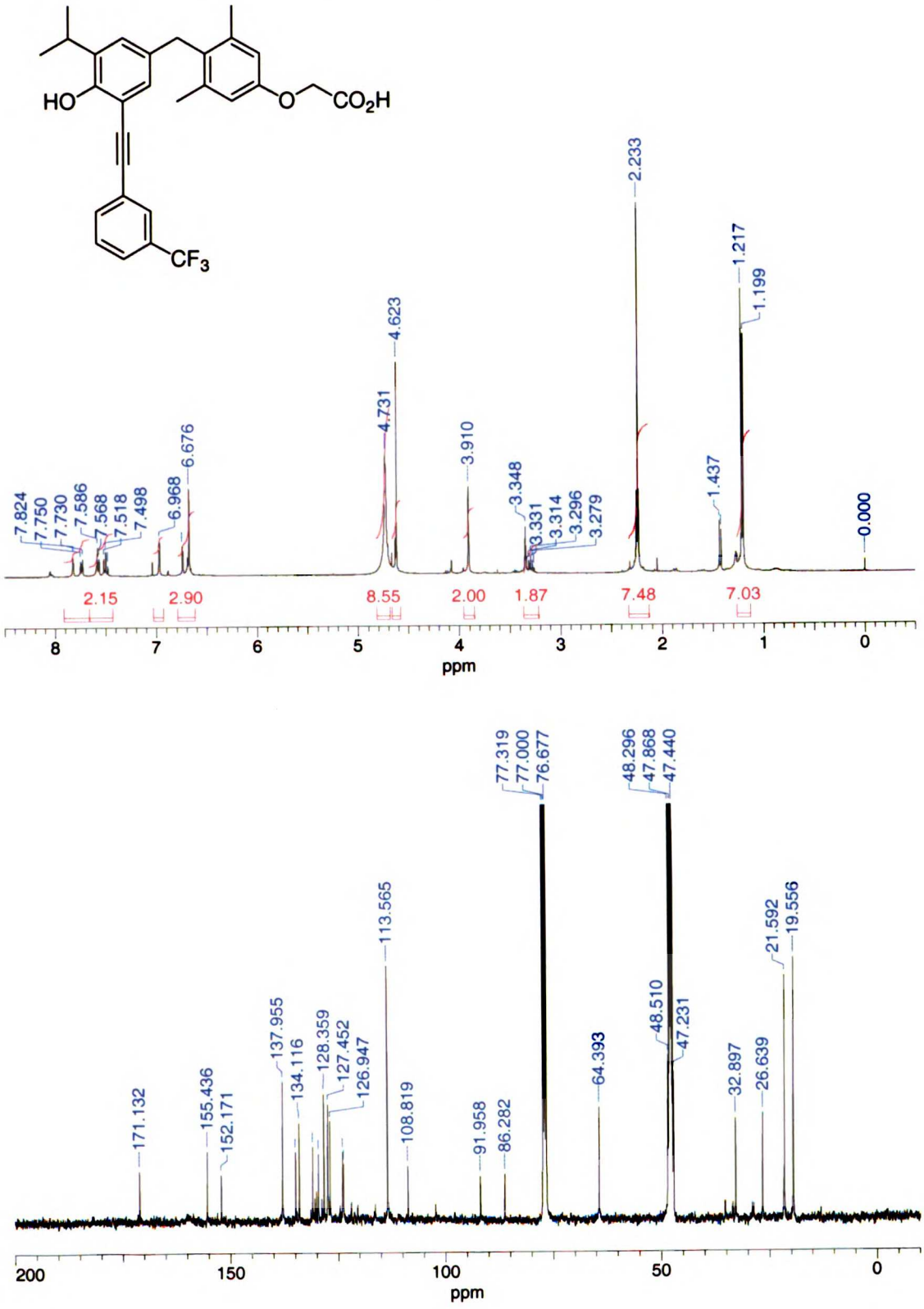

{4-[3-Isopropyl-4-methoxymethoxy-5-(2-trifluoromethyl-phenylethynyl)-benzyl]-3,5-dimethyl-phenoxy}-acetic acid methyl ester (17l)

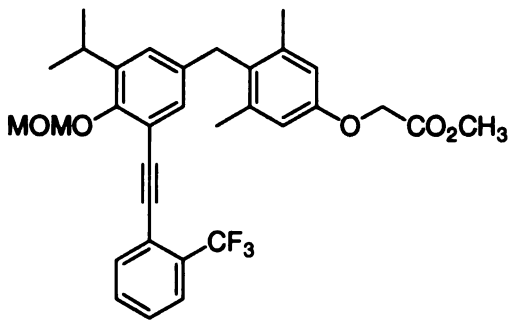

{4-[4-Hydroxy-3-isopropyl-5-(2-trifluoromethyl-phenylethynyl)-benzyl]-3,5-dimethyl-phenoxy}-acetic acid methyl ester

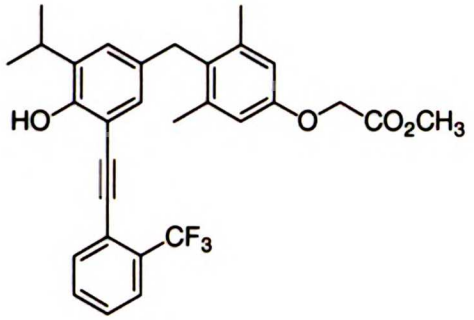

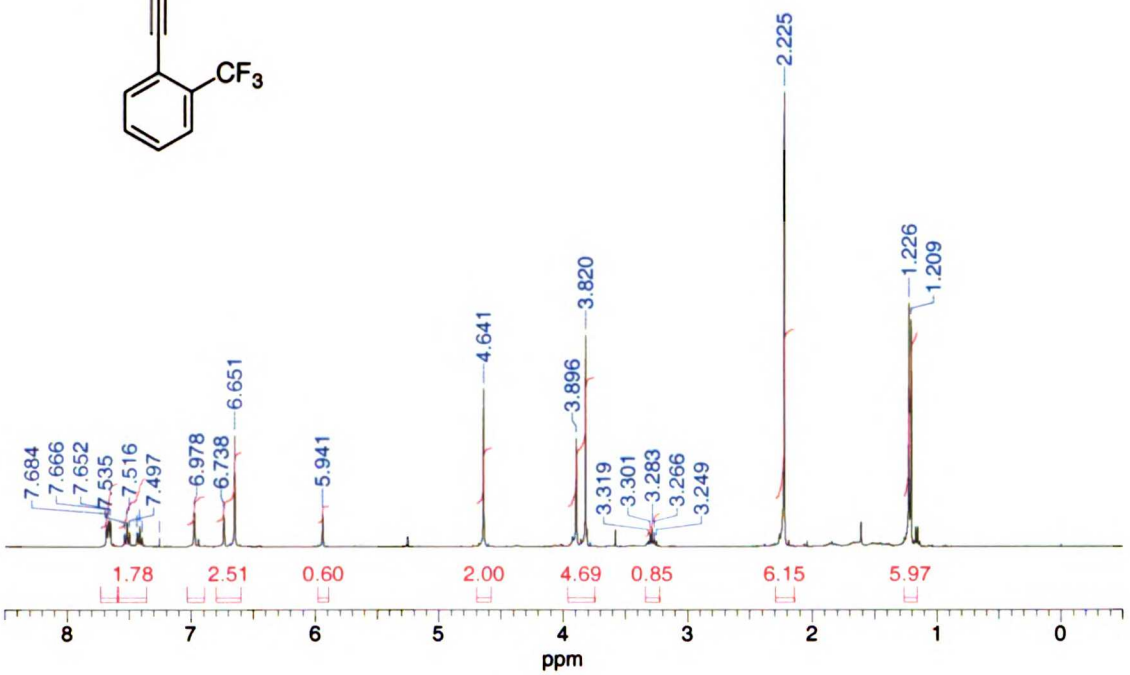

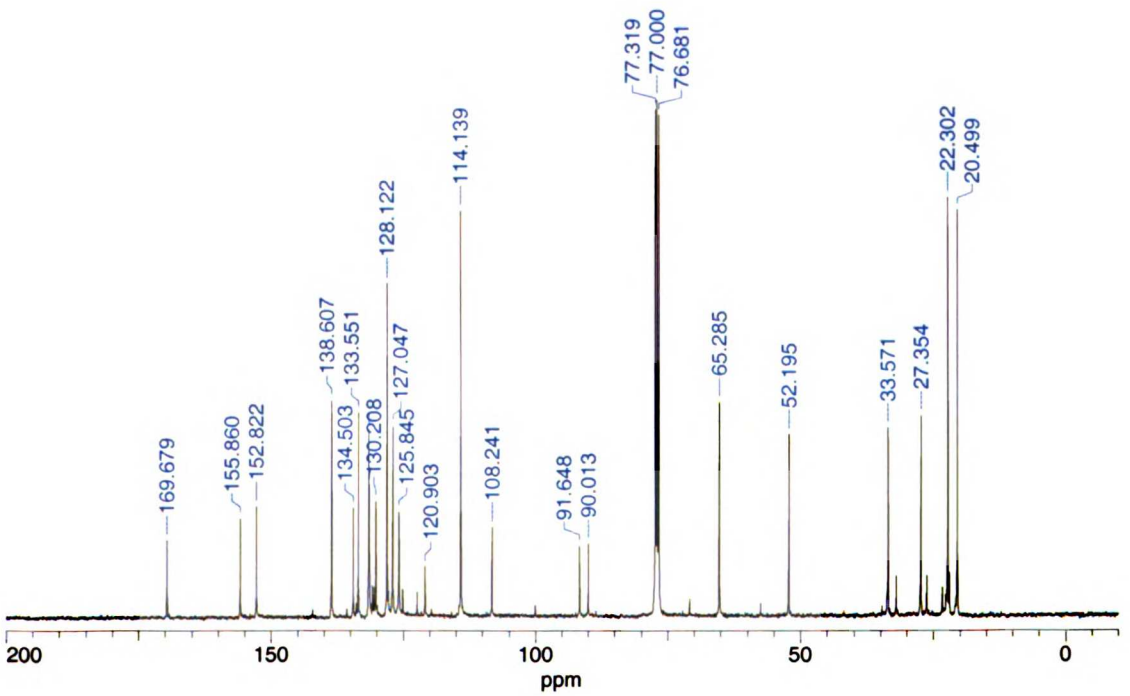

{4-[4-Hydroxy-3-isopropyl-5-(2-trifluoromethyl-phenylethynyl)-benzyl]-3,5-dimethyl-phenoxy}-acetic acid (18i, NH-18)

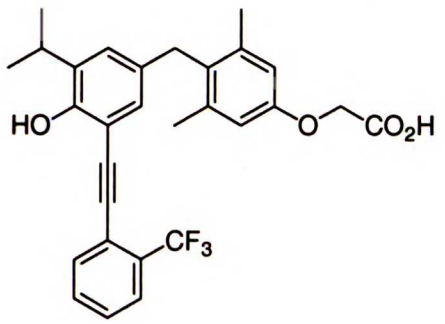

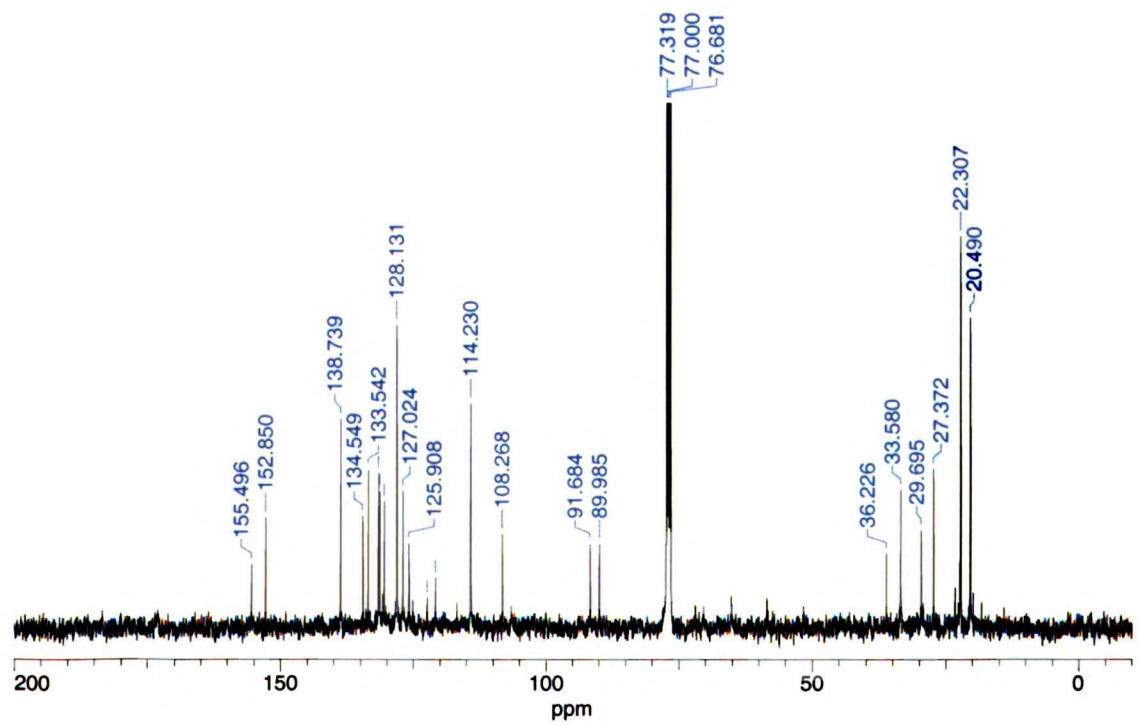

{4-[3-(3-Amino-phenylethynyl)-5-isopropyl-4-methoxymethoxy-benzyl]-3,5-dimethyl-phenoxy}-acetic acid methyl ester (17j)

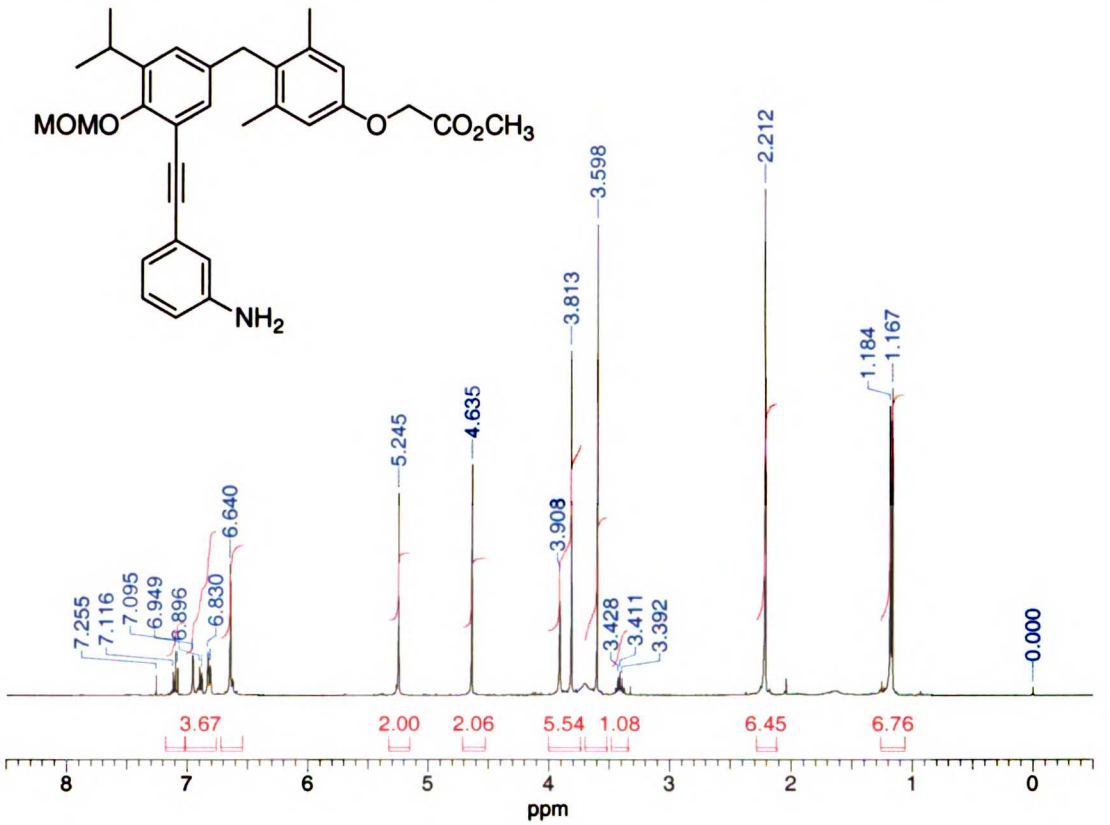

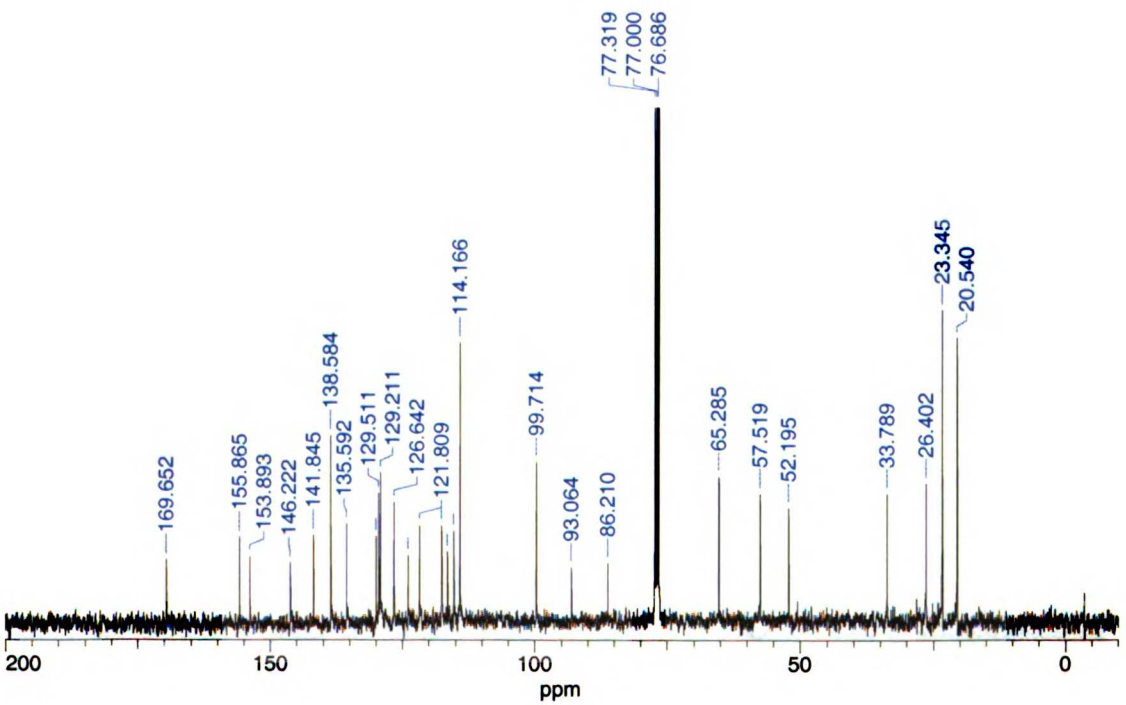

{4-[3-(3-Amino-phenylethynyl)-4-hydroxy-5-isopropyl-benzyl]-3,5-dimethyl-phenoxy}-acetic acid methyl ester (22)

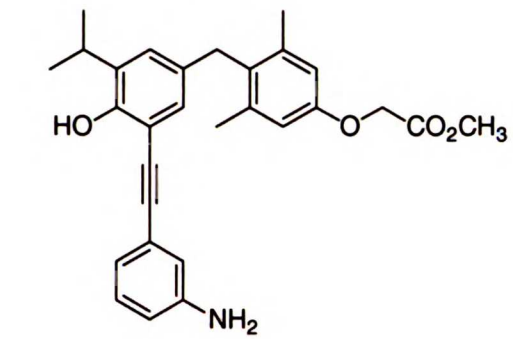

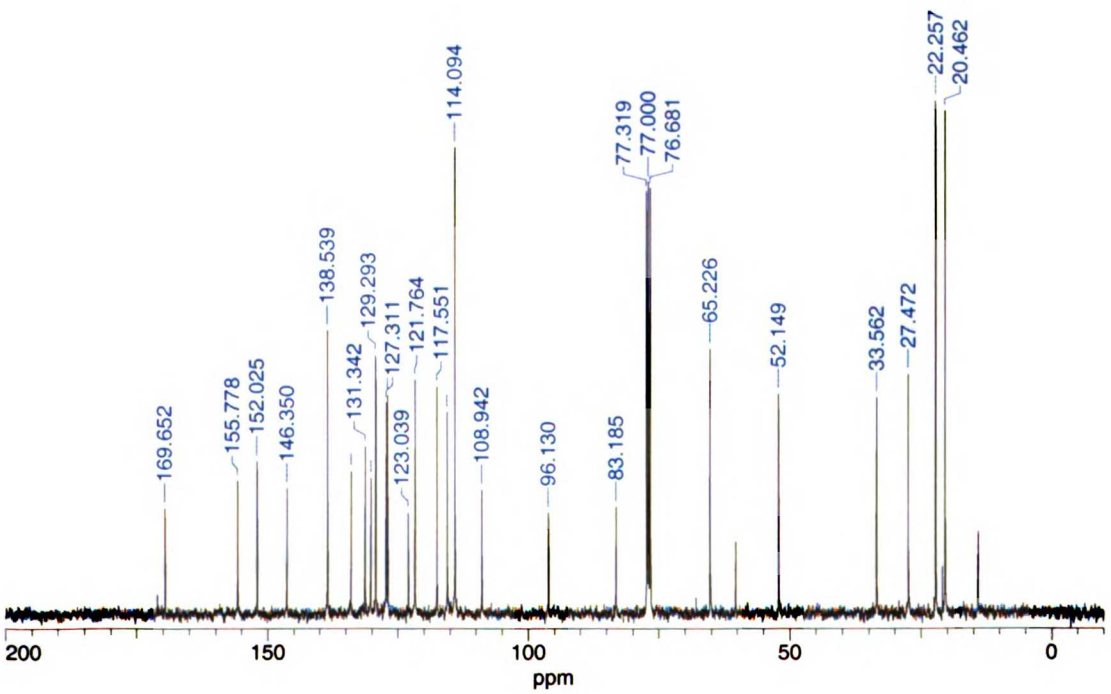

{4-[3-(3-Amino-phenylethynyl)-4-hydroxy-5-isopropyl-benzyl]-3,5-dimethyl-phenoxy}-acetic acid (18j, NH-21)

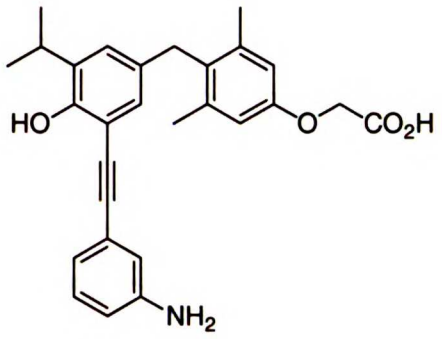

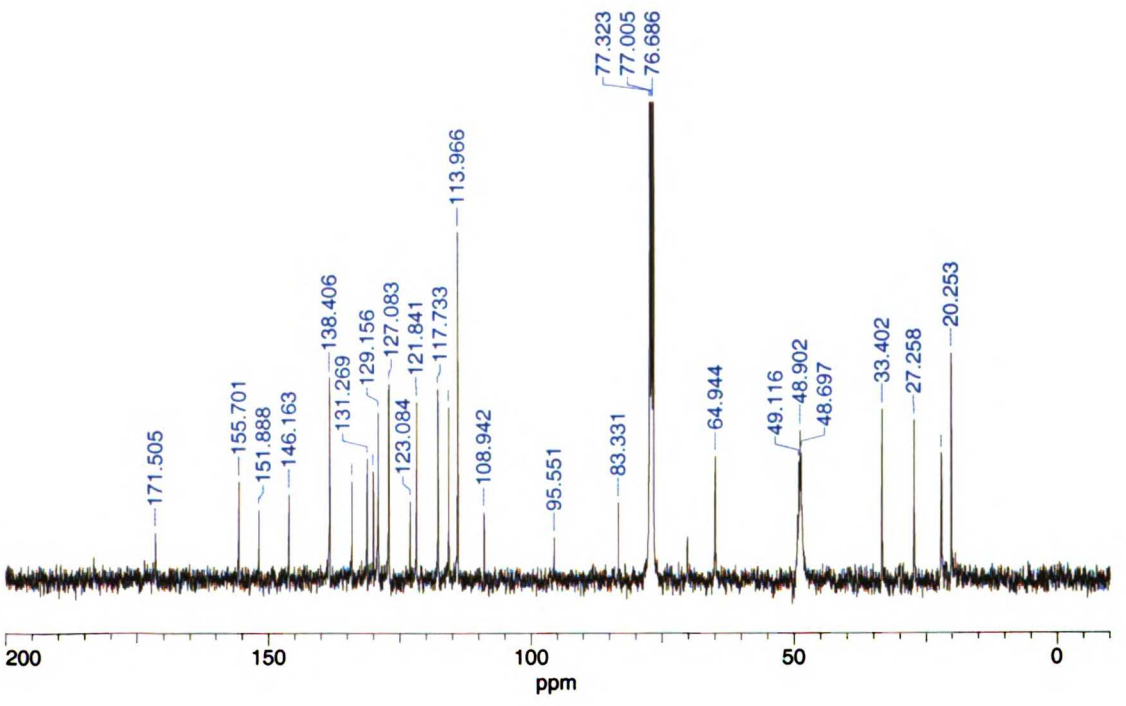

{4-[4-Hydroxy-3-isopropyl-5-(3-nitro-phenylethynyl)-benzyl]-3,5-dimethyl-phenoxy}-acetic acid methyl ester

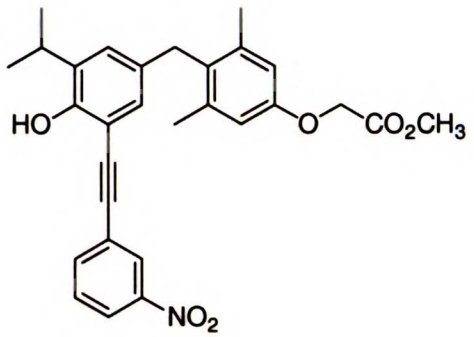

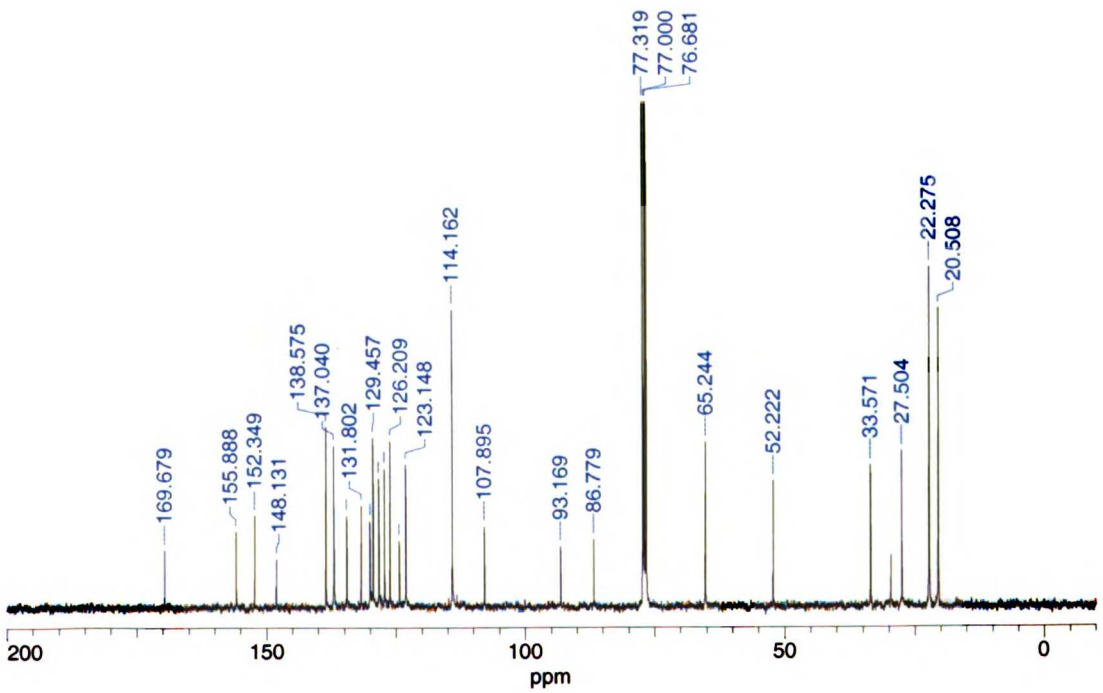

{4-[4-Hydroxy-3-isopropyl-5-(3-nitro-phenylethynyl)-benzyl]-3,5-dimethyl-phenoxy}-acetic acid (NH-19)

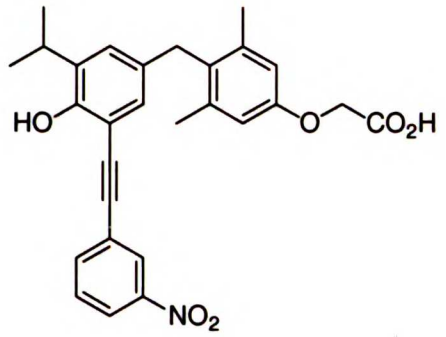

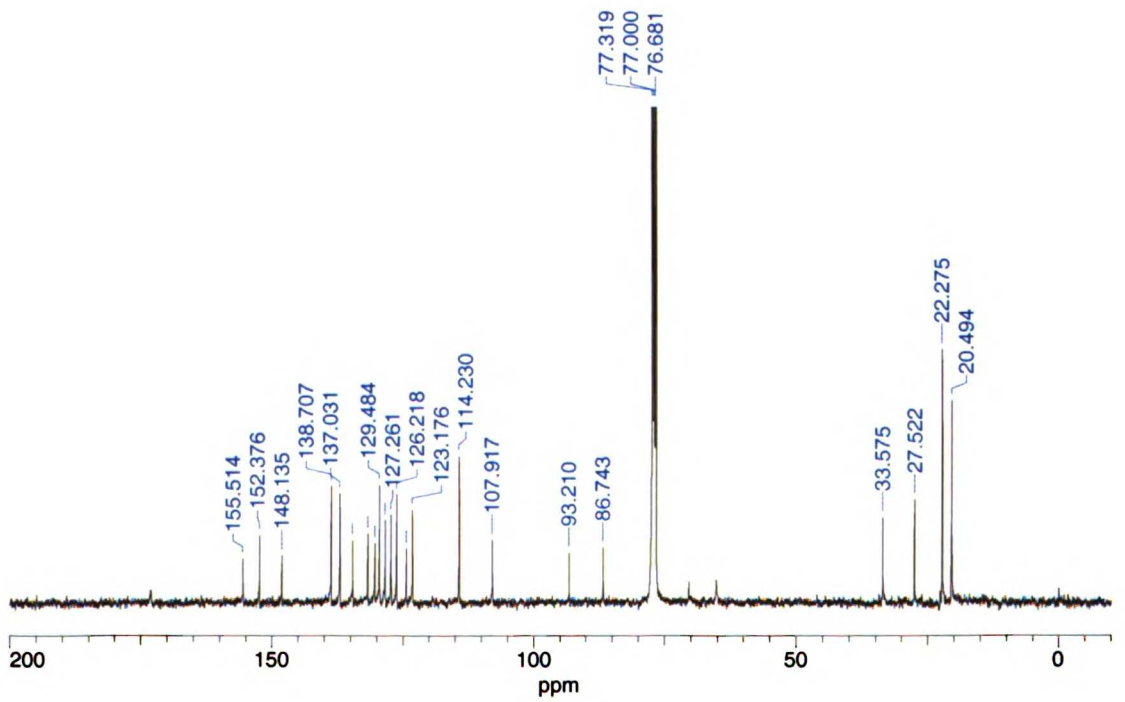

{4-[3-(2-Amino-phenylethynyl)-5-isopropyl-4-methoxymethoxy-benzyl]-3,5-dimethyl-phenoxy}-acetic acid methyl ester (17k)

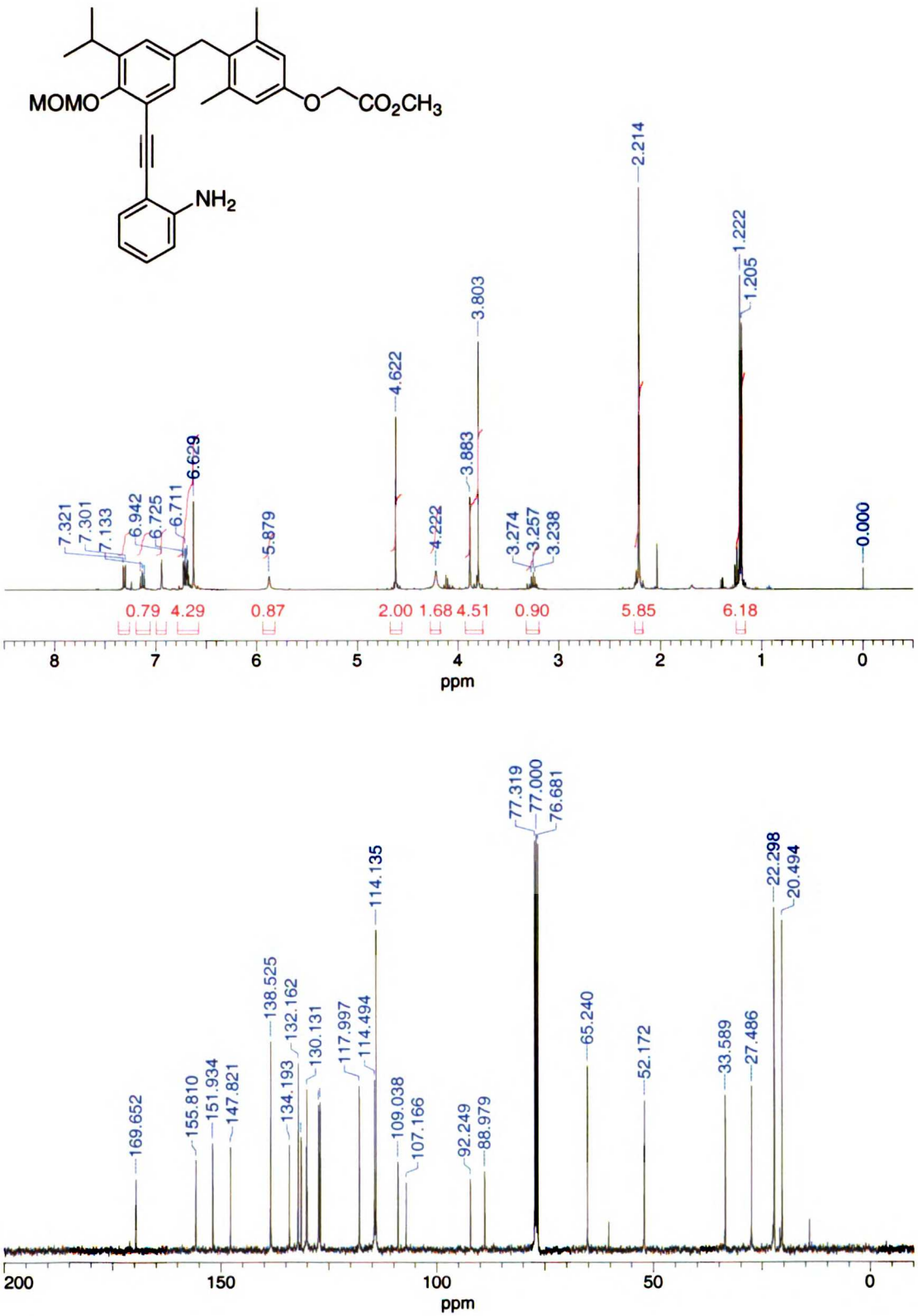

{4-[3-(2-Amino-phenylethynyl)-4-hydroxy-5-isopropyl-benzyl]-3,5-dimethyl-phenoxy}-acetic acid methyl ester (18k, NH-22)

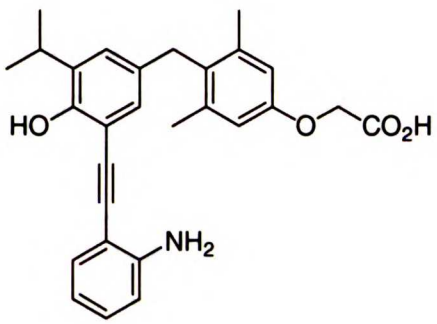

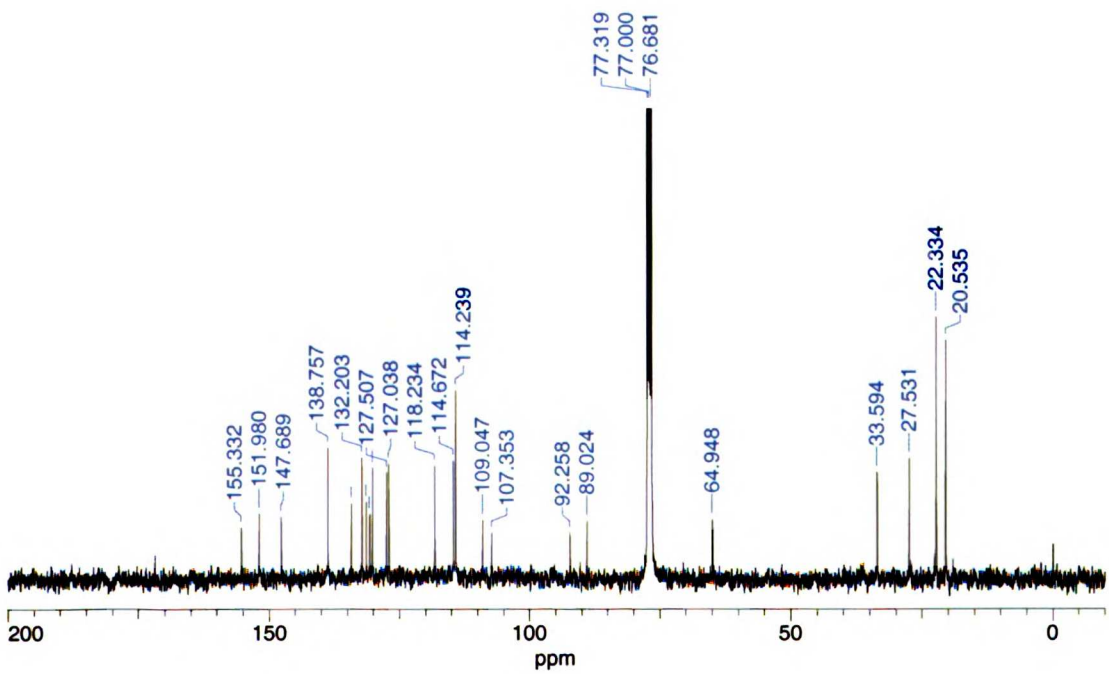

Triisopropyl-{4-[3-isopropyl-4-methoxymethoxy-5-(4-pentyl-phenyl-ethynyl)-benzyl]-3,5-dimethyl-phenoxy}-silane (19)

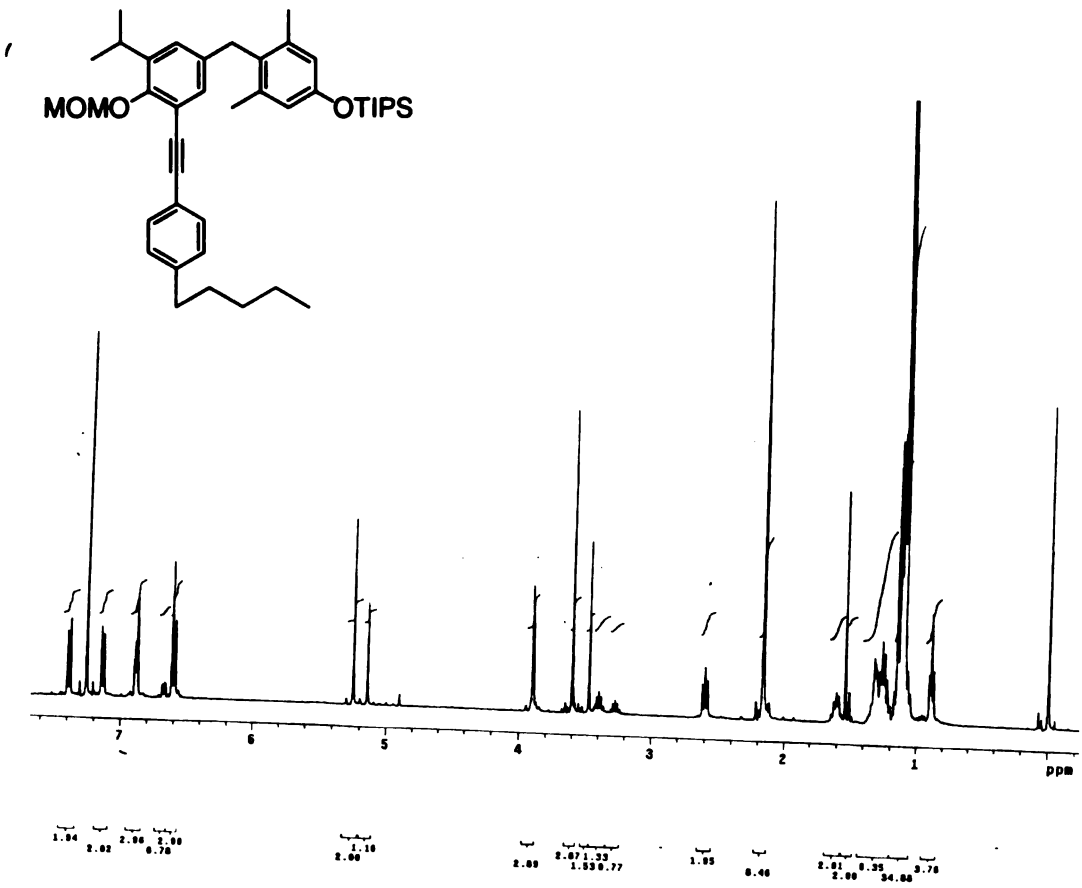

4-[3-Isopropyl-4-methoxymethoxy-5-(4-pentyl-phenylethynyl)-benzyl]-3,5-dimethyl phenol (20)

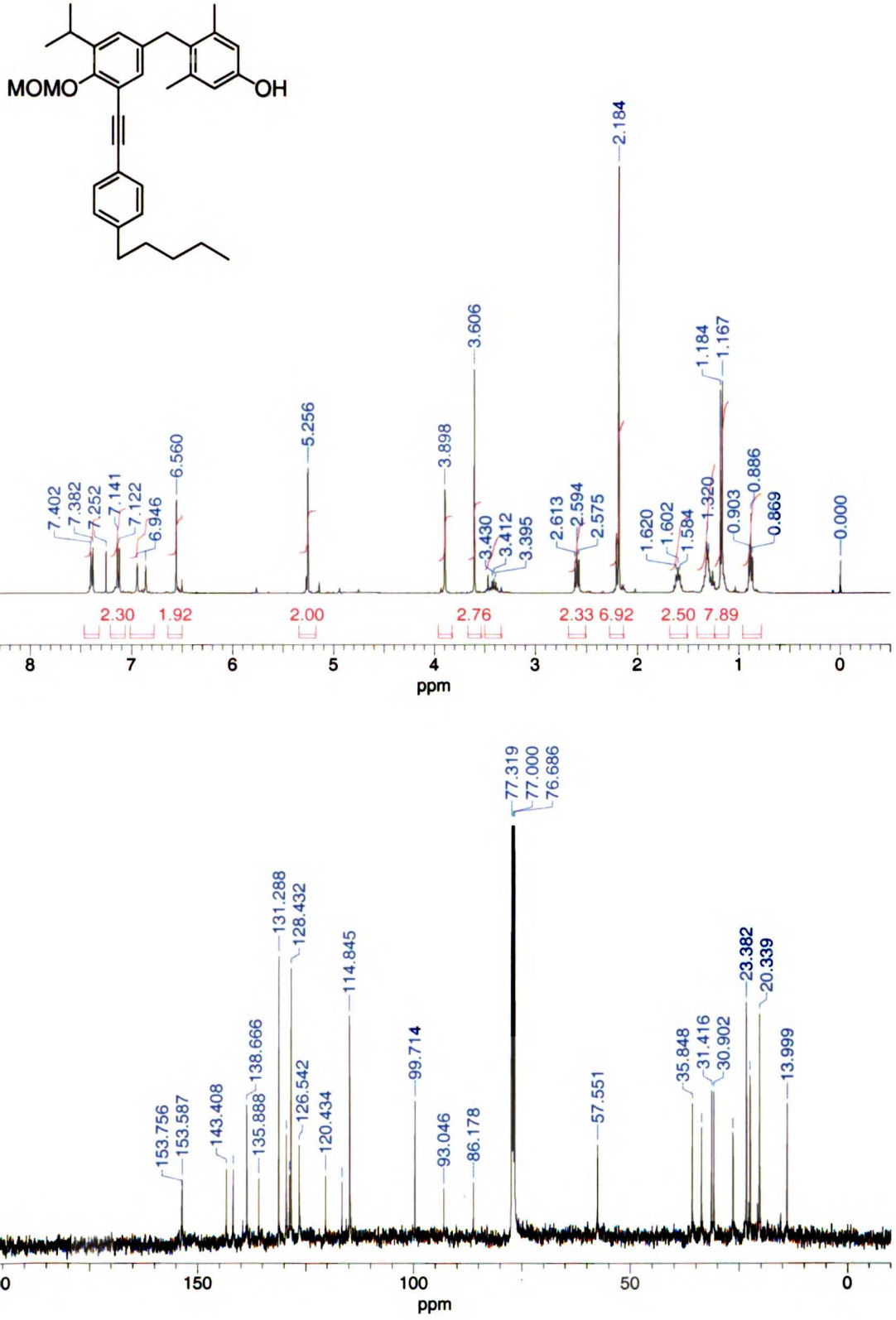

{4-[3-Isopropyl-4-methoxymethoxy-5-(4-pentyl-phenylethynyl)-benzyl]-3,5-dimethyl-phenoxy}-acetic acid *tert*-butyl ester (21)

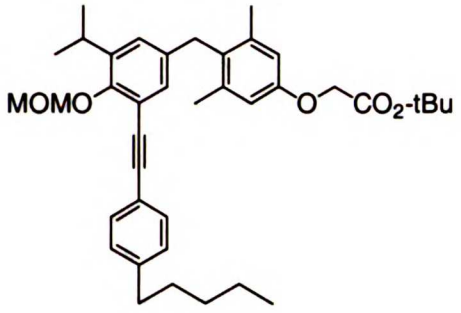

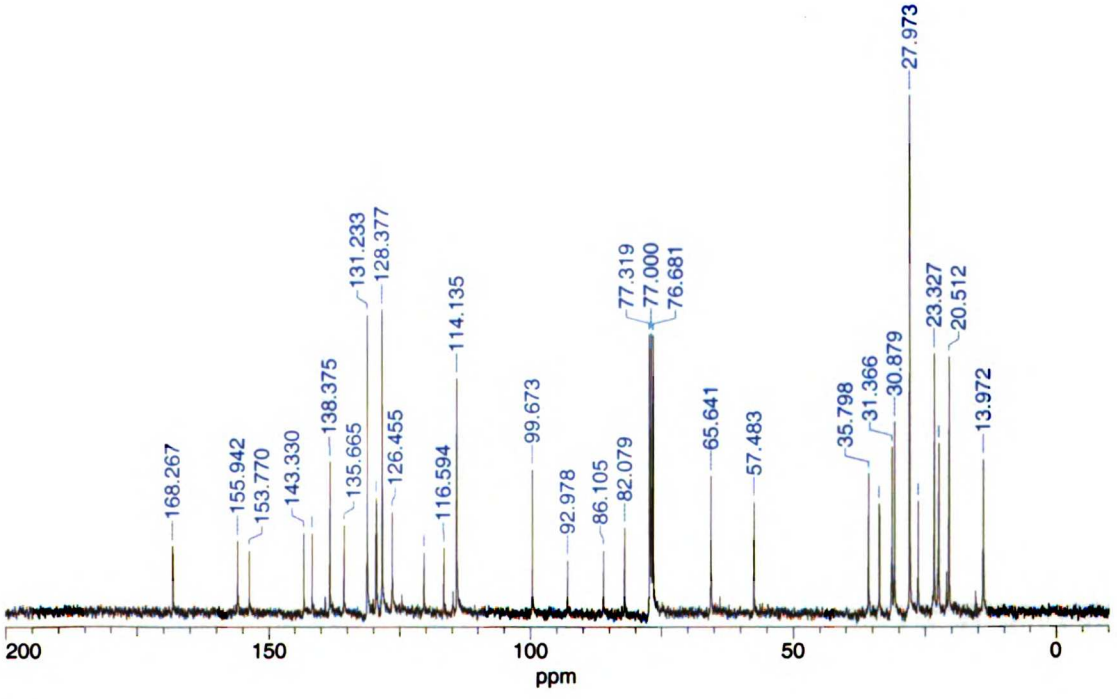

{4-[3-Isopropyl-4-hydroxy-5-(4-pentyl-phenylethynyl)-benzyl]-3,5-dimethyl-phenoxy}-acetic acid *tert*-butyl ester

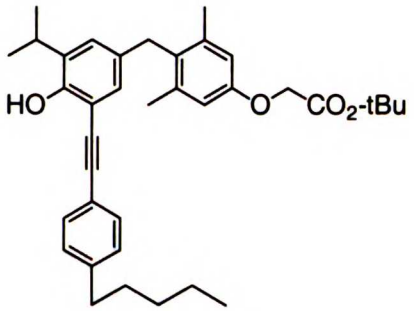

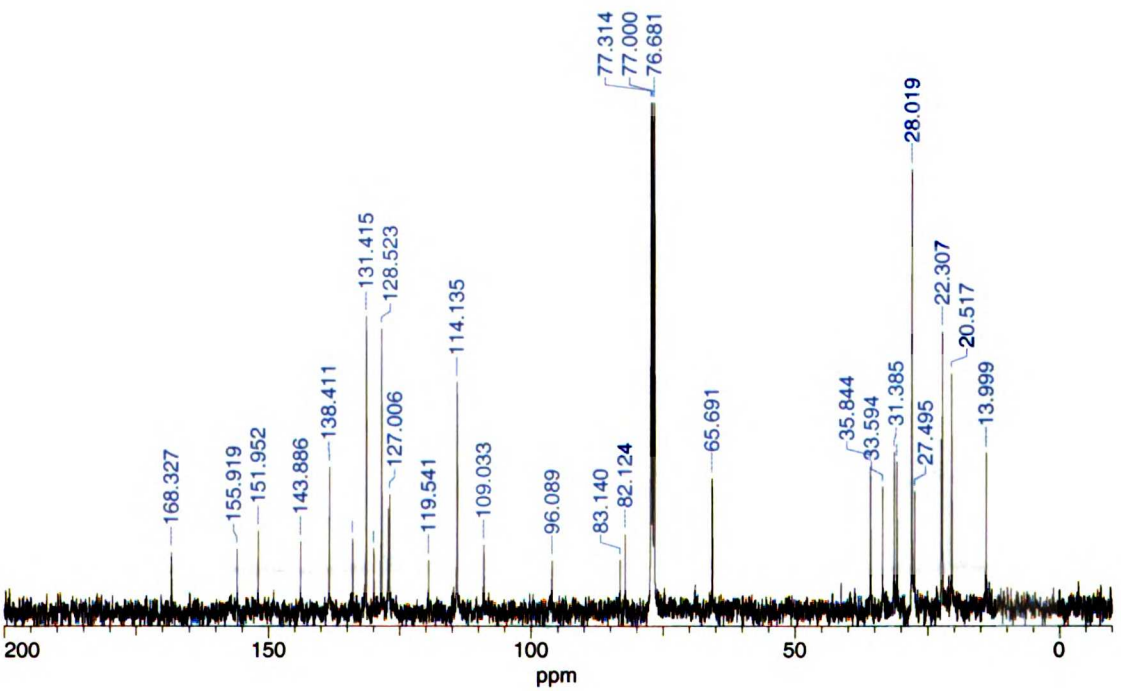

{4-[3-Isopropyl-4-hydroxy-5-(4-pentyl-phenylethynyl)-benzyl]-3,5-dimethyl-phenoxy}-acetic acid (NH-2)

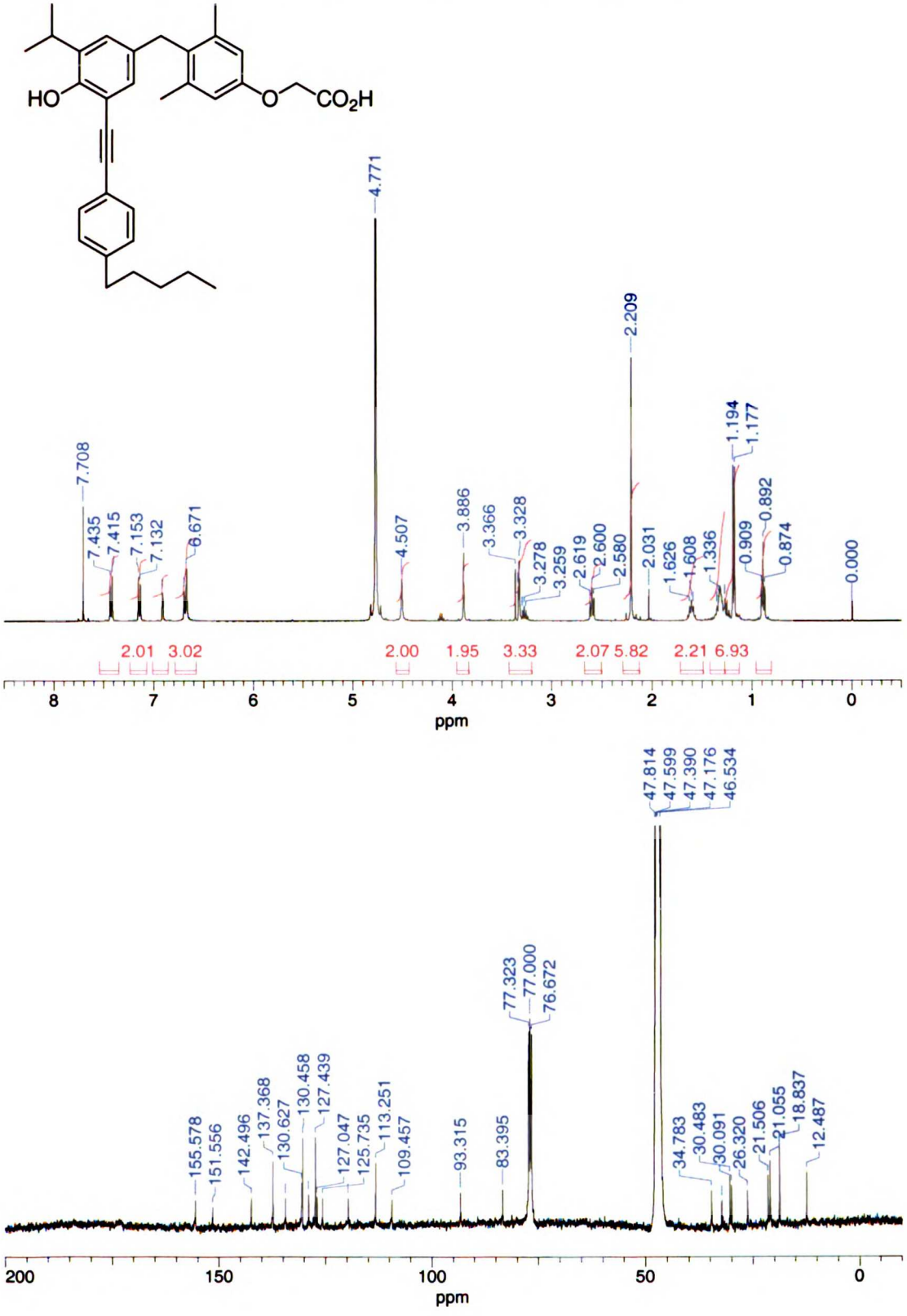

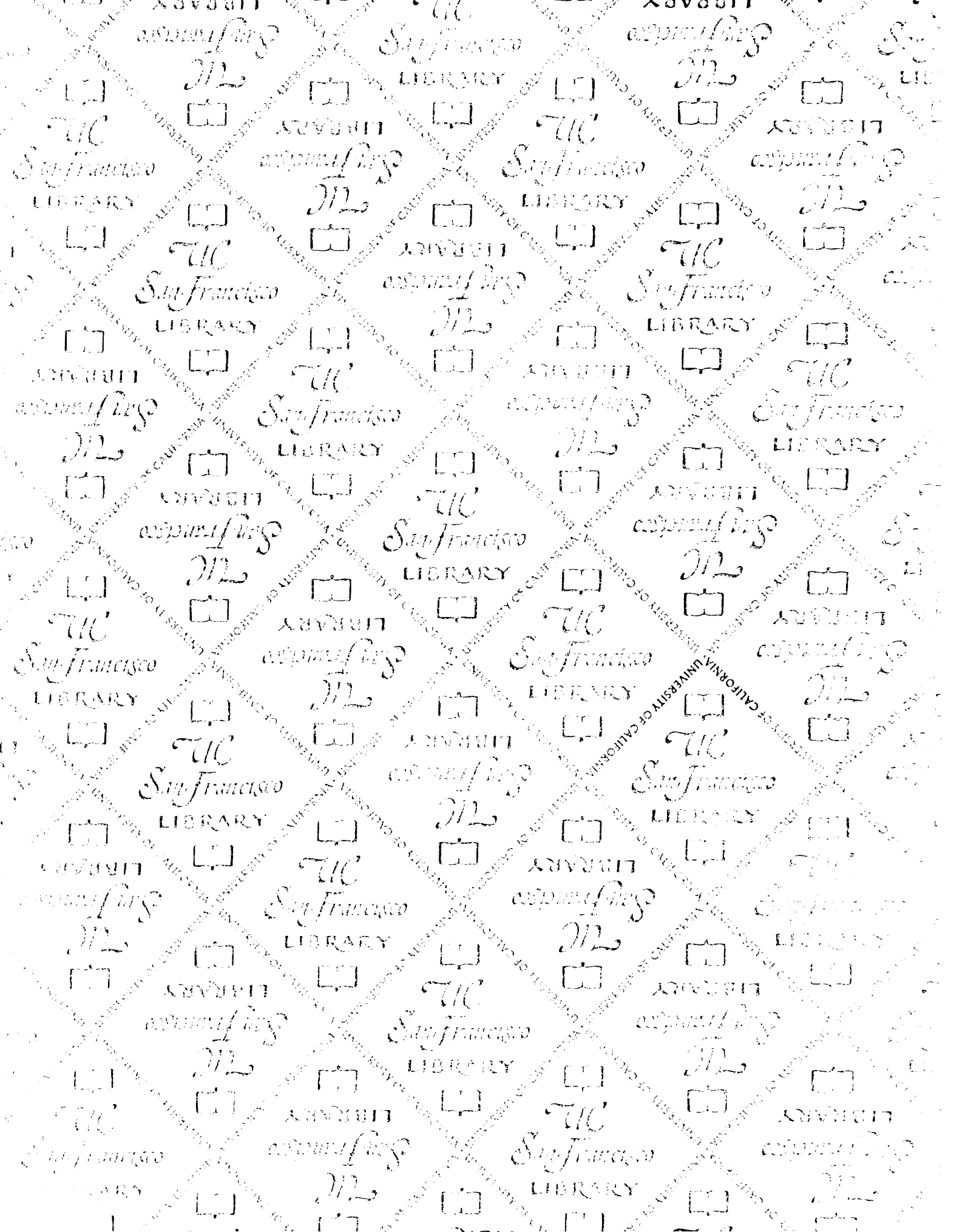
UC
San Francisco
LIBRARY
UNIVERSITY OF CALIFORNIA